Valorisation of Biomass-Derived Platform Molecules

A thesis submitted for the degree of Doctor of Philosophy

of The Australian National University

By

Brett Leslie Pollard

Research School of Chemistry

Canberra, Australia

September, 2023

Declaration

I declare that, to the best of my knowledge, the material presented in this thesis represents the result of original work carried out by the author during the period 2020-2023 and has not been presented for examination for any other degree. This thesis is less than 100,000 words in length. Established methodologies have been acknowledged, wherever possible, by citation of the original publications from which they derive.

Brett Pollard

September 2023

"We have a long way to go, and there is time ahead for thought.

It is something to have started."

\- J.R.R. Tolkien

Acknowledgements

Firstly, it is with pleasure that I thank Professors Luke Connal and Martin Banwell for their consistent support, guidance, and wisdom throughout my candidature, and for being a pleasure to work with. Between your distinctive approaches to research, I have undertaken a most unique candidature which I believe has given me a greater breadth of experience than I could have ever expected. I will be forever grateful.

I wish to thank all members of the Connal group, especially to Ashwani Kumar (who has been an entertaining and valued collaborator), Peidong Shen, Moki Thanusing, Sandra Jestin (who also proofread this thesis), Dhanya Veedu, Jekaterina Viktorova, Heather Graham, Lilian Boton, Md. Saifur Rahaman, Yumeng Liu and Lachlan Niven, as well as to our international visiting students Kalyanshi Ubnare, Shraddha Bhat, and Keshav Pareek. I also thank the members of the Banwell group, including Sebastian Young Ye, Hannah Bollard, Jiří Mikušek and Madushani Amarasiri. I further extend my gratitude to all those who have collaborated on the research described within this thesis. I give special mention to Isaac Christian Hampton, who tragically passed away during my candidature.

I must also thank my family for their support and confidence in me throughout my studies. I could not be the person I am today without the love you have all so generously provided. I also thank my partner Serena for being such an inspiration and for making Canberra feel like home. Finally, I thank my amazing friends, as well as the musicians I have had the privilege to perform with during my candidature, for providing me with the diversion required to maintain sanity in the pursuit of research.

Publications and Presentations

The following list details the publications, patents and presentations that have resulted from research performed during the candidature of the Doctor of Philosophy.

Published

- Banwell, M.G.; **Pollard, B**.; Liu, X.; Connal, L.A. Exploiting Nature's Most Abundant Polymers: Developing New Pathways for the Conversion of Cellulose, Hemicellulose, Lignin and Chitin into Platform Molecules (and Beyond). *Chem. Asian J*. **2021**, *16*, 604.
- Liu, X.[†]; **Pollard, B**.[†]; Banwell, M.G.; Yu, L-J.; Coote, M.L.; Gardiner, M.G.; van Vugt-Lussenburg, B.M.A.; van der Burg, B.; Grasset, F.L.; Campillo, E.; Sherwood, J.; Byrne, F.P.; Farmer, T.J. Simple and modestly scalable synthesis of *iso*-Cyrene from levoglucosenone and its comparison to the bio-derived and polar aprotic solvent Cyrene®. *Aust. J. Chem.* **2022**, *75*(5), 331-344.
- **Pollard, B**.; Liu, X.; Connal, L.A.; Banwell, M.G.; Gardiner, M.G. The synthesis and manipulation of certain Diels-Alder adducts of levoglucosenone and *iso*-levoglucosenone. *Aust. J. Chem,* **2023**, *76*(11), 797-811.
- **Pollard, B**.; Banwell, M.G.; Connal, L.A. Polymers from cellulosic waste: Direct polymerization of levoglucosenone using DBU as a catalyst. *ChemSusChem*, **2023**, e202301165.
- Shen, P.; Jiang, Z.; Viktorova, J.; **Pollard, B**.; Kumar, A.; Stachurski, Z.; Connal, L. A. Conductive and Self-Healing Carbon Nanotube–Polymer Composites for Mechanically Strong Smart Materials. *ACS Appl. Nano Mater*. **2023**, 6, 2, 986–994.
- Thanusing, M.K.; Shen, P.; **Pollard, B.L**.; Connal, L.A. Structure-property relationships in the rational design of water-harvesting hydrogels. *Mol. Syst. Des. Eng.* **2023**, *9*, 63-72.

(**[†]**authors contributed equally)

In Preparation

- **Pollard, B**.†; Kumar. A.†; Ubnare, K.; Bhat, S.R.; Pareek, K.; Niven, L.; Connal, L.A.; Fully Bio-Based & Compostable Dynamic Thermosets.
- Kumar, A.; **Pollard, B**.; Connal, L.A. Upcycling waste: Fully biomass-derived and backyard compostable imine thermosets.
- Shen, P.; **Pollard, B**.; Connal, L.A. Controlled aldehyde release by polycyclic aminals and investigation of dynamic aminal exchange.

  (†authors contributed equally)

Patents

- **Pollard, B**., Kumar, A., Connal, L.A. "Bio-Based Polymers" *Australia Provisional Patent Application Number 2022903603* (28th November 2022)

Presentations

- The 17th Pacific Polymer Conference, **Oral Seminar**, Fully Bio-Based & Compostable Coffee Thermosets (13th December 2022)
- CSIRO Ending Plastic Waste Symposium 2023, **Poster Presentation**, Fully Bio-Based & Compostable Coffee Thermosets (23rd May 2023)

Abstract

Conventional chemistry in the 20th and 21st centuries is hinged on the extraction and manipulation of non-renewable, fossil-derived chemical feedstocks. This thesis details new efforts to pivot towards the valorisation of sustainable biomass-derived platform molecules as a source of commodity chemicals. Primarily, the work involves the utilisation of levoglucosenone, a compound available in the kiloton scale from the pyrolysis of acid-treated cellulosic waste. In **Chapter 2**, the landscape of sustainable platform molecules is described, as well as the existing work performed on levoglucosenone, giving context to the experimental work reported herein. **Chapter 3** is an experimentally based article which provides a novel synthesis of *iso*-levoglucosenone, the pseudo-enantiomer of levoglucosenone, formed through a new and synthetically concise 1,3-carbonyl transposition. This approach was also compared to an alternate synthesis from D-glucose. This material was then hydrogenated to form a novel potential solvent (*iso*-Cyrene), the properties of which were compared to the levoglucosenone-derived solvent Cyrene®. **Chapter 4** provides novel transformations of levoglucosenone and *iso*-levoglucosenone-derived Diels-Alder adducts using several dienes, including the biomass-derived α-terpinene. The products of these cycloadditions were then subjected to reduction of the carbonyl to afford diastereomeric alcohols, which could then be transformed using Wagner-Meerwein rearrangements and intramolecular bromoetherifications. These fully characterised products give novel and distinct chemical structures. Finally, **Chapter 5** describes the most direct polymerisation of levoglucosenone reported to date, facilitated using a catalytic amount of nucleophilic base. This polymer was obtained in quantitative yields and with relatively high molecular weights. Further, the material was functionalised using a green Baeyer-Villiger oxidation to give an extremely hydrophilic and freely water-soluble polymer.

Abbreviations

The following abbreviations have been used throughout this thesis.

Å	Angstrom(s)
$[\alpha]_D$	optical rotation at the sodium D-line, *i.e.* λ = 589 nm (10^{-1}.deg.cm^2.g^{-1})
δ	chemical shift (parts per million)
Đ	polydispersity index
µg	microgram(s)
µL	microlitre(s)
µwave	microwave
λ	wavelength (nm)
ν_{max}	infrared absorption maxima (cm^{-1})
Ac	acetyl
AcGGM	*O*-acetylgalactoglucomannan
a.k.a	also known as
aq.	aqueous
atm	atmosphere(s)
BMDPM	biomass-derived platform molecule
br	broad
ca.	*circa* (around)
cat.	catalytic
cf.	*confer* (compare)
CLSC	closed loop supply chain
cm	centimetre(s)
conc.	concentrated
COSMO-RS	conductor-like screening model for real solvents
CPD	cyclopentadiene
CS	chitin synthase
d	doublet
DABCO	1,4-diazabicyclo[2.2.2]octane

DAST	diethylaminosulfur trifluoride
DBU	1,8-diazabicyclo[5.4.0]undec-7-ene
DMAc	*N,N*-dimethylacetamide
DMAP	4-(dimethylamino)pyridine
DMF	dimethylformamide
DMP	Dess-Martin periodinane
DSC	differential scanning calorimetry
ee	enantiomeric excess
EI	electron impact (mass spectrometry)
e.g.	*exempli gratia* (for example)
equiv.	equivalents
ESI	electrospray ionisation (mass spectrometry)
ESP	electrostatic surface potential
et al.	*et alia* (and others)
Et	ethyl
EtOAc	ethyl acetate
eV	electron volts
FT	Fourier transform
FT	Fischer-Tropsch
g	gram(s)
GC	gas chromatography
GC-O	gas chromatography-olfactometry
GPC	gel permeation chromatography
h	hour(s)
HMBC	heteronuclear multiple-bond correlation
HMF	hydroxymethylfurfural
HPLC	high performance liquid chromatography
HMQC	heteronuclear multiple-quantum coherence
HRMS	high-resolution mass spectrometry
hv	light

Hz	Hertz
i.e.	*id est* (that is)
IR	infrared
iso-LGO	*iso*-levoglucosenone
J	coupling constant (Hz)
L	litre(s)
l	path length (cm)
LA	levulinic acid
LD_{50}	median lethal dose
LGO	levoglucosenone
lit.	literature value
LOEC	lowest observed effect concentration
LRMS	low resolution mass spectrometry
m	multiplet
M	molar
MBH	Morita-Baylis-Hillman
m-CPBA	*meta*-chloroperbenzoic acid
Me	methyl
MeCN	acetonitrile
MHz	mega-Hertz
min	minute(s)
mL	millitre(s)
mol	mole(s)
m.p.	melting point (°C)
M_N	number average molecular weight
MS	mass spectrometry
MS	molecular sieves
M_W	weight average molecular weight
m/z	mass-to-charge ratio
NAG	*N*-acetyl-D-glucosamine

NBS	*N*-bromosuccinimide
NCCs	nitrogen-containing compounds
nm	nanometre(s)
NMO	*N*-methylmorpholine-*N*-oxide
NMP	*N*-methyl-2-pyrrolidone
NMR	nuclear magnetic resonance
PM	platform molecule
ppm	parts per million
q	quartet
quant.	quantitative
R	unspecified alkyl group
RC	Rauhut-Currier
ref.	reference
R_f	thin layer chromatography retention factor
ROMP	ring-opening metathesis polymerisation
s	singlet
SM	supplementary material
SI	supporting information
t	triplet
T_D	decomposition temperature
TGA	thermogravimetric analysis
THF	tetrahydrofuran
tlc	thin layer chromatography
TPA	terephthalic acid
TsCl	*p*-toluenesulfonyl chloride
UDP	uridine diphosphate
UV	ultraviolet (spectroscopy)
viz.	*videlicit* (namely)
vs.	versus
v/*v*	unit volume per unit volume (ratio)

v/*v*/*v*	unit volume per unit volume per unit volume (ratio)
wt %	weight percent
w/*w*	unit weight per unit weight (%)

Table of Contents

Chapter One - Introduction

The landscape of modern chemistry is underpinned by the once seemingly miraculous font of fossil fuels and their commodity chemical products. These fossil fuels, namely petroleum, natural gas, and coal, have been the primary geopolitical factor determining national prosperity in the 20th and now 21st century. As of 2022, approximately 93% of fossil fuel usage is combustion for energy production.[1] The balance of this fossil fuel consumption is the production of commodity chemicals: materials, solvents, lubricants, pharmaceuticals, and fine chemicals. Fossil fuels, a non-renewable source of hydrocarbons, have enabled for the logistics and considerable energy requirements critical to the expansion of modern society.

Despite their utility, fossil-derived hydrocarbons have fallen into common view as a major cause of concern for the wellbeing of the environment. The combustion of fossil fuels for energy production has resulted in rapid and alarming changes to the Earth's temperature and atmospheric composition in well-known phenomena referred to as the greenhouse effect, and, by extension, climate change (**Figure 1**).

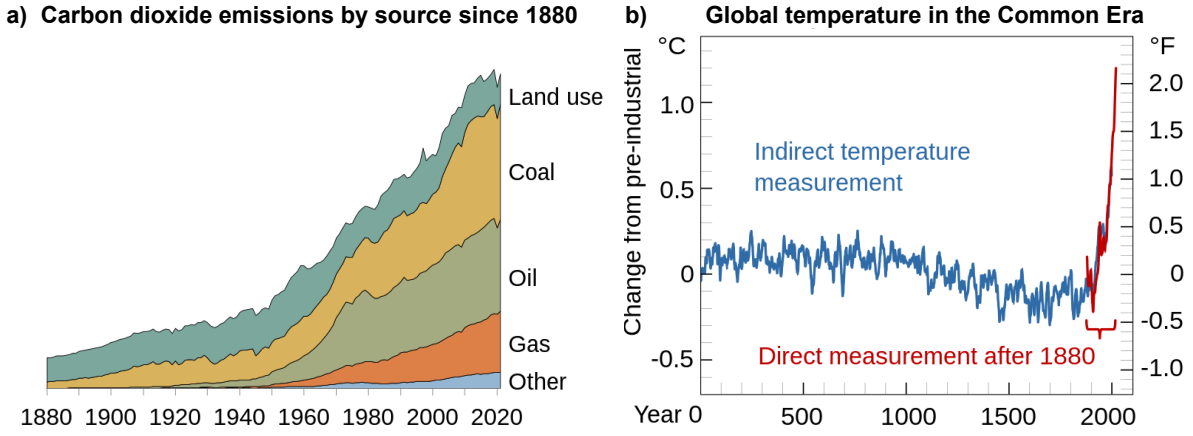

Figure 1: a) Carbon dioxide emissions emissions reported by emission source for the period 1880 – 2020, adapted from Friedlingstein *et al.*[2] b) global temperature as a function of time, with direct measurements reported after 1880, adapted from Neukom *et al.*[3]

This global climate change phenomenon has broad consequences including the increased incidence (and severity) of natural disasters, food and water shortages, as well as the forced displacement of peoples. Beyond this, the extraction and processing of coal, gas and oil has a significant impact on local ecosystems.[4,5] The availability and price of fossil-derived hydrocarbons is also massively subject to geopolitics,[6,7] the reverberations of which have tangible impacts on consumers and the wider economy.

Aside from energy production, the use of fossil-derived hydrocarbons as commodity chemicals is critical to modern chemistry, and, as a result, modern society. The uses of these commodity chemicals include: materials (*viz.* polymers derived from monomers), solvents, as well as fine and specialty chemicals such as pharmaceuticals, dyes, pesticides, and detergents.

Materials, namely polymers and plastics, comprise 80% of the chemical industry output,[8] with the largest volumes being ascribed to polyethylene (in its various forms), polyvinyl chloride, polypropylene and polystyrene.[9]

Such plastics are affordable, tough, lightweight, largely corrosion resistant and highly insulating, which has led to their widespread adoption and use globally. Since World War II, these polymers have been the primary instrument enabling the storage and transportation logistics required to feed the growing human population, as well as finding use in countless industrial and consumer applications.

Polymers are manufactured at a scale of over 400 Mt per year, and, unfortunately, around 80% of all plastic ever generated is accumulating in either landfill or the natural environment.[9] Further accentuating the bleak ultimate destination of plastics is the fact that none of the conventionally used plastics are biodegradable. Indeed, bio-based and biodegradable plastics represent around only 1% of their total annual production.[10]

Another significant proportion of the fossil-derived hydrocarbon industry output is solvents, which are themselves plagued with environmental and occupational health issues. Solvents are of great utility and find use in a swathe of major applications, *inter alia*, coatings (in paints and varnishes), in chemical production (as a reaction medium and for purification), in solvent extraction, cleaning, and in formulation (such as in lubricants, surfactants, dispersants and adhesives). In Europe, paints, coatings and the pharmaceutical industry represent over half of overall solvent usage, with the lion's share allotted to the former two.[11] Historically, solvents such as benzene, carbon disulfide and carbon tetrachloride (and, more recently under scrutiny, dichloromethane),[12] which are fossil-derived, have been associated with severe adverse health effects as well as issues with ozone depletion.[13] Other extremely common solvents such as tetrahydrofuran, *N,N*-dimethylformamide, 1,4-dioxane, hexanes, toluene and *N*-methyl-2-pyrrolidone bear their own health risks and their use is the subject of increasing debate.[14]

Developing less toxic and, ideally, bio-based sustainable solvents remains a research topic of considerable focus in modern chemistry. Water, the ideal green solvent, lends itself poorly to many applications given its polarity and protic nature, as well as high heat of vaporisation. Bio-derived ethanol and methanol also represent excellent solvents but bear limitations like those described for water. Numerous alternative green solvents have been described, most of which are oxohydrocarbons: alcohols and ketones, esters, carbonates and ethers, as well as some hydrocarbons and heteroatomic compounds.

A promising alternative to the environmentally and biologically problematic fossil-derived hydrocarbons is the valorisation of sustainable biopolymers and their degradation products, described as biomass-derived platform molecules (BMDPMs). The most abundant biopolymers, namely cellulose, hemicellulose, lignin and chitin, are produced at a staggering scale of 170 billion metric tons *per annum*.[15] These materials are synthesised through the process of photosynthesis, which fixes carbon dioxide and water into carbohydrates with the energy provided by sunlight, releasing oxygen in the process.[16] The functionalisation of these carbohydrates through biosynthetic pathways thereby provide all known forms of biomass.

A literature review published during the preparation of this thesis is presented in **Chapter 2** which covers the broad range of BMDPMs available to the early 21st century chemist, each of which may very well merit a thesis of study on their own. **Chapter 2** also describes prior work performed on the BMDPM levoglucosenone (**1**), which lays the foundation for the work described herein. This thesis focusses on the efforts of myself and collaborators in expanding upon and uncovering novel utilities for **1** as a promising BMDPM and is compiled from three research chapters presented in the form of articles, out of which one has been published, one has been accepted for publication, and the third has been submitted for publication.

Levoglucosenone (**1**), the central molecule in this work, is a BMDPM derived from the pyrolysis of acid-treated cellulose waste, with its preparation first reported in the early 1970's. Levoglucosenone is a homochiral, bicyclic derivative of glucose, and is a liquid at room temperature. The distinct chemical functionalities present in **1** enable its functionalisation and modification. The most significant of these are the reactive Michael acceptor as well as the 1,6-anhydro bridge which offers defined stereochemistry (**Scheme 1**). The production of **1** has been refined in recent history to the point where the Circa Group™ are able to produce LGO at the

kiloton scale from wood pulp treated with acidic conditions under temperatures 170 – 350 °C with *ca*. 40% yield.[17]

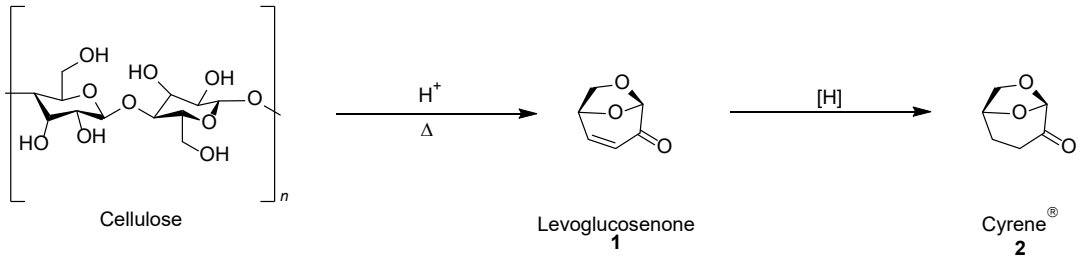

Scheme 1: Production of levoglucosenone (**1**) through the pyrolysis of acid-treated cellulose, conducted sustainably using waste streams of cellulose.

Given its scale of production and renewable origin, this homochiral compound has since been explored as a biomass-derived commodity chemical in a variety of applications. Perhaps the most direct of these, to date, is its use as a solvent. The reduction of levoglucosenone gives dihydro-levoglucosenone (**2**), which is marketed as Cyrene®, a solvent proffered as a safer and greener substitute for the widely used and petrochemically derived *N*-methylpyrrolidine (NMP).[18]Approximately 250,000 tons of NMP are produced annually[19] and the solvent finds applications in petrochemical processing, polymer chemistry, surface treatments and paint strippers, as well as in the pharmaceutical industry.[20] Despite its utility, NMP shows marked reproductive toxicity,[21] whereas the sustainable alternative Cyrene® has been assessed to be negative in mutagenicity testing and is also almost completely non-ecotoxic (LD_{50} > 2000 mg/L).[22,23]

In **Chapter 3**, our efforts to expand upon the scope of solvents derived from **1** are presented. Cyrene® is a homochiral solvent, a property which, to date, has not been effectively yoked (in, for example, fractional crystallisation). There exists the pseudo-enantiomer of **1** referred to as *iso*-levoglucosenone (**3**), the reduced product of which (referred to as *iso*-Cyrene) had been

previously prepared by two approaches.[24,25] However, these preparations were both limited to the sub-gram quantity, and so the properties of *iso*-Cyrene as a solvent were not assessed. Given the distinct homochirality of these two species, it was our expectation that *iso*-Cyrene could potentially act complementary to Cyrene® to serve as a chiral auxiliary and perhaps facilitate or enhance enantioselectivity. Further, the reactivity of *iso*-Cyrene was expected to be markedly different from Cyrene®, particularly with respect to the ability of the latter to form hydrates, as well its stability in the presence of base, characteristics well documented for Cyrene®.[26,27] In this work, we report a facile and concise synthesis for the 1,3-carbonyl transposition of **1** to *iso*-levoglucosenone (**3**) alongside a comparison to a previously reported and scalable preparation of *iso*-levoglucosenone from D-glucose.[28] Further, through characterisation, we determined that *iso*-Cyrene did, in fact, exhibit markedly different stabilities, and in many situations, superior chemical stability when compared to Cyrene®.

Aside from solvents, **1** has also been extensively explored as a precursor to monomers for the preparation of polymeric materials.[29-37] Within the Australian National University Research School of Chemistry, previous work published dealt with the Diels-Alder adducts formed by the reaction of LGO (**1**) and *iso*-LGO (**3**) with 1,3-cyclopentadiene (**Scheme 2**). The products of these, as well as some of their products formed through reduction of the ketone to corresponding diastereomeric alcohols, were then subjected to ring-opening metathesis polymerisation (ROMP) so as to generate polymers:[38]

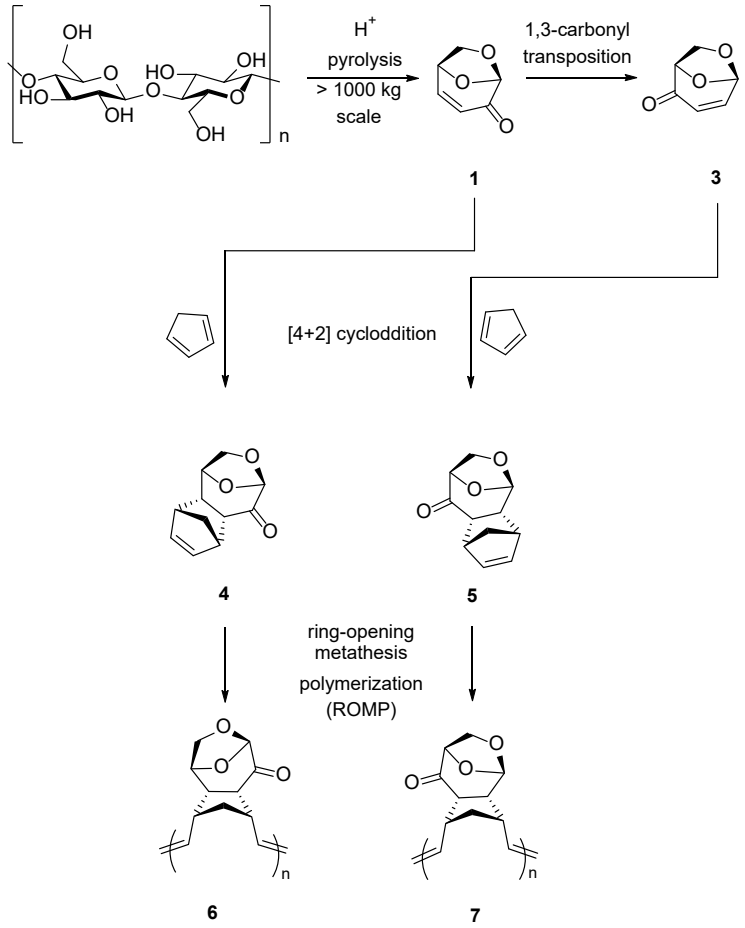

Scheme 2: Functionalisation of LGO (**1**) and *iso*-LGO (**3**) to Diels-Alder adducts, and, then, their resulting polymers obtained through ring opening metathesis polymerisation.[38]

The defined stereochemistry of **1** has led to its use in total synthesis, and in synthetic manipulations, including the complex structure tetrodotoxin, *inter alia*.[39] In **Chapter 4** of this thesis, an article accepted for publication is presented which details efforts to further functionalise these Diels-Alder adducts and explore their diverse chemistries. Beyond finding use as monomers, these materials provide novel caged and heterocyclic scaffolds through their Wagner-Meerwein type transformations and rearrangements.

An obvious drawback of using the Diels-Alder adducts presented in **Chapter 4** for polymer synthesis is the requirement for incorporating fossil-derived dienes. While we address this using

the sustainable diene of α-terpinene (itself prepared through the acid-catalysed rearrangement of α-pinene), the direct utilisation of **1** as a monomer without additional synthetic steps was a highly desirable research target.

In **Chapter 5**, we report for the first time, a method for the direct use of levoglucosenone as a monomer through the harnessing of its reactive Michael acceptor in a Rauhut-Currier style polymerisation using the nucleophilic base 1,8-diazabicyclo(5.4.0)undec-7-ene (DBU). We further report a green functionalisation of this material into a hydrophilic and highly water-soluble polymer derivative. To date, this represents the most atom efficient and direct route to the preparation of high molecular weight polymers from **1** directly and provides a novel scaffold for functional polymer synthesis.

Levoglucosenone is but one of a great number of BMDPMs which are accessible on a practical scale and which also possess avenues for valorisation. The expansion, development and further valorisation of BMDPMs is, in the author's opinion, one of the most practical solutions to producing essential commodity chemicals while mitigating the environmental impact their production causes. This thesis presents efforts to further this field of study and to valorise the use of one of many promising BMDPMs for real world applications.

References

1. See https://www.eia.gov/todayinenergy/detail.php?id=35672 (accessed 3/8/2023).
2. Friedlingstein, P.; O'Sullivan, M.; Jones, M. W.; Andrew, R. M.; Gregor, L.; Hauck, J.; Le Quéré, C.; Luijkx, I. T.; Olsen, A.; Peters, G. P.; et al. Global Carbon Budget 2022. *Earth System Science Data* **2022**, *14*(11), 4811-4900. License: https://creativecommons.org/licenses/by/4.0/
3. Neukom, R.; Barboza, L. A.; Erb, M. P.; Shi, F.; Emile-Geay, J.; Evans, M. N.; Franke, J.; Kaufman, D. S.; Lücke, L.; Rehfeld, K.; et al. Consistent multi-decadal variability in global temperature reconstructions and simulations over the Common Era. *Nature Geoscience* **2019**, *12*(8), 643-649.
4. Harfoot, M. B. J.; Tittensor, D. P.; Knight, S.; Arnell, A. P.; Blyth, S.; Brooks, S.; Butchart, S. H. M.; Hutton, J.; Jones, M. I.; Kapos, V.; et al. Present and future biodiversity risks from fossil fuel exploitation. *Conservation Letters* **2018**, *11*(4), e12448.
5. Shamoon, A.; Haleem, A.; Bahl, S.; Javaid, M.; Bala Garg, S.; Chandmal Sharma, R.; Garg, J. Environmental impact of energy production and extraction of materials - a review. *Materials Today: Proceedings,* **2022**, *57*, 936-941.
6. Alam, M. M.; Aktar, M. A.; Idris, N. D. M.; Al-Amin, A. Q. World energy economics and geopolitics amid COVID-19 and post-COVID-19 policy direction. *World Development Sustainability,* **2023**, *2*, 100048.
7. Bricout, A.; Slade, R.; Staffell, I.; Halttunen, K. From the geopolitics of oil and gas to the geopolitics of the energy transition: Is there a role for European supermajors? *Energy Research & Social Science* **2022**, *88*, 102634.
8. Singh, K. *Chemistry in Daily Life*; Pretence Hall of India, 2012.
9. Geyer, R.; Jambeck, J. R.; Law, K. L. Production, use, and fate of all plastics ever made. *Science Advances* **2017**, *3*(7), e1700782.
10. Döhler, N.; Wellenreuther, C.; Wolf, A. Market dynamics of biodegradable bio-based plastics: Projections and linkages to European policies. *EFB Bioeconomy Journal* **2022**, *2*, 100028.
11. See https://www.esig.org/ (accessed 4/8/2023).
12. Jordan, A.; Stoy, P.; Sneddon, H. F. Chlorinated Solvents: Their Advantages, Disadvantages, and Alternatives in Organic and Medicinal Chemistry. *Chemical Reviews* **2021**, *121*(3), 1582-1622.
13. Winterton, N. The green solvent: a critical perspective. *Clean Technologies and Environmental Policy* **2021**, *23*(9), 2499-2522.

14. Alder, C. M.; Hayler, J. D.; Henderson, R. K.; Redman, A. M.; Shukla, L.; Shuster, L. E.; Sneddon, H. F. Updating and further expanding GSK's solvent sustainability guide. *Green Chemistry,* **2016**, *18* (13), 3879-3890.

15. Banwell, M. G.; Pollard, B.; Liu, X.; Connal, L. A. Exploiting Nature's Most Abundant Polymers: Developing New Pathways for the Conversion of Cellulose, Hemicellulose, Lignin and Chitin into Platform Molecules (and Beyond). *Chemistry: An Asian Journal,* **2021**, *16*(6), 604-620.

16. Singhal, G. S., Renger, G., Sopory, S.K., Irrgang, K.-D., Govindjee. *Concepts in Photobiology. Photosynthesis and Photomorphogenesis*; Kluwer Academic Publishers, **1999**.

17. See https://www.circagroup.com.au/the-company (accessed 2/8/2023).

18. Sherwood, J.; De bruyn, M.; Constantinou, A.; Moity, L.; McElroy, C. R.; Farmer, T. J.; Duncan, T.; Raverty, W.; Hunt, A. J.; Clark, J. H. Dihydrolevoglucosenone (Cyrene) as a bio-based alternative for dipolar aprotic solvents. *Chemical Communications,* **2014**, *50*(68), 9650-9652.

19. Harreus, A. L.; Backes, R.; Eichler, J. O.; Feuerhake, R.; Jäkel, C.; Mahn, U.; Pinkos, R.; Vogelsang, R. 2-Pyrrolidone, *Ullmann's Encyclopedia of Industrial Chemistry*, **2011**.

20. Hunt, A.; Dale, N. Economic valuation in 1-Methyl-2-pyrrolidone (NMP) regulation. **2018**. DOI: 10.1787/ef67fa08-en.

21. Sitarek, K.; Stetkiewicz, J. Assessment of reproductive toxicity and gonadotoxic potential of N-methyl-2-pyrrolidone in male rats. *International Journal of Occupational Medicine and Environmental Health,* **2008**, *21*(1), 73-80.

22. Camp, J. E.; Nyamini, S. B.; Scott, F. J. Cyrene™ is a green alternative to DMSO as a solvent for antibacterial drug discovery against ESKAPE pathogens. *RSC Medicinal Chemistry,* **2020**, *11*(1), 111-117.

23. Jordan, A.; Hall, C. G. J.; Thorp, L. R.; Sneddon, H. F. Replacement of Less-Preferred Dipolar Aprotic and Ethereal Solvents in Synthetic Organic Chemistry with More Sustainable Alternatives. *Chemical Reviews,* **2022**, *122*(6), 6749-6794.

24. Ledingham, E. T.; Greatrex, B. W. Diastereoselective Weitz-Scheffer epoxidation of levoglucosenone for the synthesis of isolevoglucosenone and derivatives. *Tetrahedron,* **2018**, *74*(42), 6107-6115.

25. J. Pecka, J. S., jr and M. Černý. *Preparation and the properties of 2,3-, 2,4-, and 3,4-dideoxy derivatives of 1,6-anhydro-β-D-glycero-hexopyranosuloses and corresponding alcohols*. *Collection of Czechoslovak Chemical Communications,* **1974**, *39*(5), 1192-1209.

26. De bruyn, M.; Budarin, V. L.; Misefari, A.; Shimizu, S.; Fish, H.; Cockett, M.; Hunt, A. J.; Hofstetter, H.; Weckhuysen, B. M.; Clark, J. H.; et al. Geminal Diol of Dihydrolevoglucosenone as a Switchable Hydrotrope: A Continuum of Green Nanostructured Solvents. *ACS Sustainable Chemistry & Engineering,* **2019**, *7*(8), 7878-7883.

27. Hughes, L.; McElroy, C. R.; Whitwood, A. C.; Hunt, A. J. Development of pharmaceutically relevant bio-based intermediates though aldol condensation and Claisen–Schmidt reactions of dihydrolevoglucosenone (Cyrene®). *Green Chemistry,* **2018**, *20*(19), 4423-4427.

28. Horton, D.; Roski, J. P.; Norris, P. Cycloaddition of Cyclopentadiene to 3-Deoxy-1,2:5,6-di-O-isopropylidene-α-d-erythro-hex-3-enofuranose. Synthesis and Representative Chemistry of 1,6-Anhydro-2,3-dideoxy-β-d-glycero-hex-2-enopyran-4-ulose ("Isolevoglucosenone"). *The Journal of Organic Chemistry,* **1996**, *61*(11), 3783-3793.

29. Diot-Néant, F.; Mouterde, L.; Fadlallah, S.; Miller, S. A.; Allais, F. Sustainable Synthesis and Polycondensation of Levoglucosenone-Cyrene-Based Bicyclic Diol Monomer: Access to Renewable Polyesters. *Chemistry Sustainable Chemistry,* **2020**, *13*(10), 2613-2620.

30. Fadlallah, S.; Peru, A. A. M.; Flourat, A.; Allais, F. A straightforward access to functionalizable polymers through ring-opening metathesis polymerization of levoglucosenone-derived monomers. *European Polymer Journal,* **2020**, *138*, 109980.

31. Diot-Néant, F.; Mouterde, L. M. M.; Couvreur, J.; Brunois, F.; Miller, S. A.; Allais, F. Green synthesis of 2-deoxy-D-ribonolactone from cellulose-derived levoglucosenone (LGO): A promising monomer for novel bio-based polyesters. *European Polymer Journal,* **2021**, *159*, 110745.

32. Kayishaer, A.; Fadlallah, S.; Mouterde, L. M. M.; Peru, A. A. M.; Werghi, Y.; Brunois, F.; Carboué, Q.; Lopez, M.; Allais, F. Unprecedented Biodegradable Cellulose-Derived Polyesters with Pendant Citronellol Moieties: From Monomer Synthesis to Enzymatic Degradation, *Molecules*, **2021**, *26*.

33. Fadlallah, S.; Flourat, A. L.; Mouterde, L. M. M.; Annatelli, M.; Peru, A. A. M.; Gallos, A.; Arico, F.; Allais, F. Sustainable Hyperbranched Functional Materials via Green Polymerization of Readily Accessible Levoglucosenone-Derived Monomers. *Macromolecular Rapid Communications,* **2021**, *42* (19), e2100284.

34. Debsharma, T.; Schmidt, B.; Laschewsky, A.; Schlaad, H. Ring-Opening Metathesis Polymerization of Unsaturated Carbohydrate Derivatives: Levoglucosenyl Alkyl Ethers. *Macromolecules,* **2021**, *54*(6), 2720-2728.

35. Fadlallah, S.; Kayishaer, A.; Annatelli, M.; Mouterde, L. M. M.; Peru, A. A. M.; Aricò, F.; Allais, F. Fully renewable photocrosslinkable polycarbonates from cellulose-derived monomers. *Green Chemistry,* **2022**, *24*(7), 2871-2881.

36. Fadlallah, S.; Carboué, Q.; Mouterde, L. M. M.; Kayishaer, A.; Werghi, Y.; Peru, A. A. M.; Lopez, M.; Allais, F. Synthesis and Enzymatic Degradation of Sustainable Levoglucosenone-Derived Copolyesters with Renewable Citronellol Side Chains, *Polymers*, **2022,** *14*.

37. Warne, C. M.; Fadlallah, S.; Whitwood, A. C.; Sherwood, J.; Mouterde, L. M. M.; Allais, F.; Guebitz, G. M.; McElroy, C. R.; Pellis, A. Levoglucosenone-derived synthesis of bio-based solvents and polyesters. *Green Chemistry Letters and Reviews,* **2023**, *16*(1), 2154573.

38. Banwell, M. G.; Liu, X.; Connal, L. A.; Gardiner, M. G. Synthesis of Functionally and Stereochemically Diverse Polymers via Ring-Opening Metathesis Polymerization of Derivatives of the Biomass-Derived Platform Molecule Levoglucosenone Produced at Industrial Scale. *Macromolecules,* **2020**, *53*(13), 5308-5314.

39. Camp, J. E.; Greatrex, B. W. Levoglucosenone: Bio-Based Platform for Drug Discovery. *Frontiers in Chemistry,* **2022**, *10*.

Chapter Two – Literature Review

Foreword

This review, published in Chemistry: An Asian Journal, provides a comprehensive overview of the use of biopolymers and their degradation products as biomass-derived platform molecules in chemistry and industry. This review was written during the first six months of my candidature, during which time laboratory access was rendered impossible due to the global pandemic. Fortunately, it provided a significant opportunity for reviewing the available literature and preparing a manuscript of considerable utility throughout the course of my studies, particularly with respect to understanding the landscape of biomass-derived platform molecules and their valorisation.

Australian National University

Statement of Contribution

This thesis is submitted as a Thesis by Compilation in accordance with https://policies.anu.edu.au/ppl/document/ANUP_003405

I declare that the research presented in this Thesis represents original work that I carried out during my candidature at the Australian National University, except for contributions to multi-author papers incorporated in the Thesis where my contributions are specified in this Statement of Contribution.

Title: Exploiting Nature's Most Abundant Polymers: Developing New Pathways for the Conversion of Cellulose, Hemicellulose, Lignin and Chitin into Platform Molecules (and Beyond)

Authors: Martin G. Banwell, Brett Pollard, Xin Liu, Luke A. Connal

Publication outlet: *Chem. Asian J.* **2021**, *16*, 604.

Current status of paper: Published

Contribution to paper: This is a review article and the candidate prepared a preliminary outline, and thereafter the body of the paper was written by Professor Martin Banwell and edited by the candidate.

Senior author or collaborating authors endorsement: M. G. Banwell

BRETT L POLLARD		21/8/2023
Candidate – Print Name	Signature	Date
Endorsed		
Luke Connal		21/8/23
Primary Supervisor – Print Name	Signature	Date
Mark Humphrey	Mark Humphrey	22/8/23
Delegated Authority – Print Name	Signature	Date

Exploiting Nature's Most Abundant Polymers:

Developing New Pathways for the Conversion of Cellulose, Hemicellulose, Lignin and Chitin into Platform Molecules (and Beyond)

M. G. Banwell, **B. Pollard**, X. Liu, L. A. Connal, *Chem. Asian J.* **2021**, 16, 604 - 620.

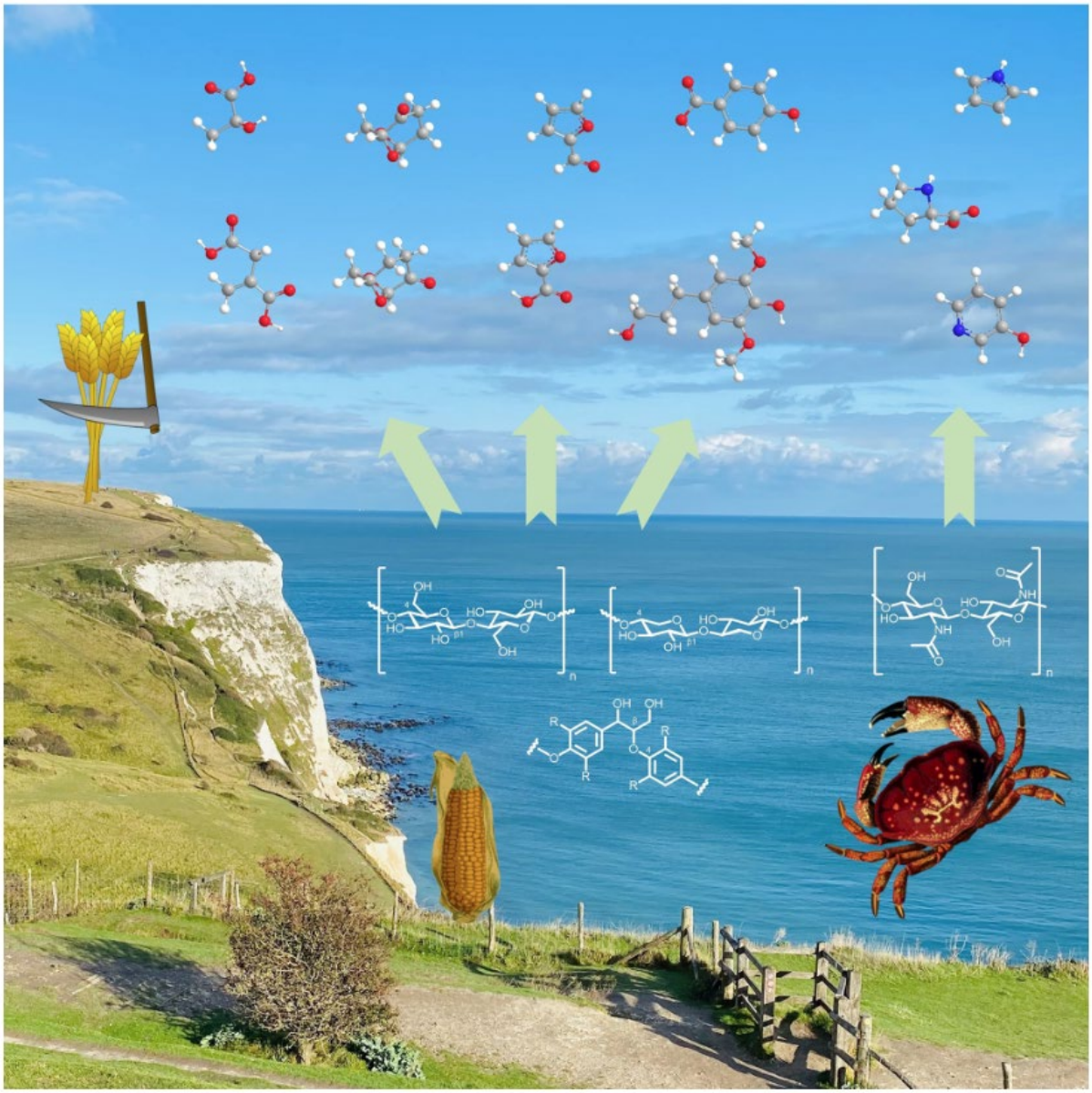

Introduction

Weaning the world off its unsustainable dependence on petrochemicals is a global concern[1] that is driven by both environmental and economic considerations.[2] While extreme dependence only emerged in the 19th century, the earliest conspicuous exploitation of petrochemicals dates back to (at least) the ancient Babylonians, Chinese and Egyptians, the last of whom who used bitumen (pitch) for embalming and even in the construction of the pyramids.[3] However, the first examples of chemicals being derived from fossil hydrocarbons at industrial scale is much more recent and probably includes the production of carbon black. This started in the 1870's and involved the partial combustion of natural gas and so allowing for the generation of synthetic rubber.[4] Some fifty years later the Standard Oil Company in the US began producing propylene both for use as a fuel and as a raw material in the petrochemical supply chain. Nowadays, about 7% of the world's fossil-derived hydrocarbons are used in the production of commodity petrochemicals with the balance being consumed, in large part, for energy production.[5] The unfortunate environmental impacts of this situation are clear and have prompted major drives towards the development of more sustainable and benign methods for, *inter alia*, the production of commodity chemicals. Many such efforts involve the valorisation of various forms of biomass,[6-30] particularly the most abundant ones, these being the biopolymers cellulose, hemicellulose, lignan and chitin. This article attempts to provide an overview of such efforts that revolve around the development of biorefineries.[20-30] Exemplifications of some of these activities are provided through descriptions of research currently underway in the authors' laboratories.

In focusing on the title biopolymers it should be noted that other forms of biomass, such as proteins and lipids (notably triglycerides and terpenes),[9,31-33] have also been exploited as sustainably available raw materials for the production of both commodity and fine chemicals as well as, in certain cases, fuels. However, the scales at which these are available do not match, at least at the present time, those derivable from the title biopolymers. Of course other activities such as approaching sustainability through enhanced recycling,[34-36] especially by applying the closed loop supply chain (CLSC) concept,[37] are also being embraced but details of such extensive efforts are beyond the scope of this article.

In considering the broad spectrum of biomass that might be exploited in biorefineries it must be remembered that all of these materials have a common and fundamental origin, namely their generation through photosynthesis (**Scheme 1**) and wherein carbon dioxide and water are converted, in the presence of sunlight and natural sensitisers (e.g. chlorophyll), into C_5- and C_6-carbohydates (mostly xylose and glucose, respectively) together with oxygen.[38] Downstream processes, including polymerisation, the shikimic acid pathway and the incorporation of ammonia derived from nitrogen fixation, then provide all known forms of biomass.

As a consequence of such biosynthetic events, 170 billion metric tons of biomass are produced each year, 75% of which can be classified as carbohydrate-based, but only a small fraction (<5%) of such material is used for either food or non-food purposes.[6,13] Global biomass production appears roughly evenly split between the terrestrial and marine environments. Lignocellulose, the most abundant form of biomass, is a robust, non-edible material that provides, *inter alia*, structural integrity to plants. As the name suggests, lignocellulose is a composite material with 10-20 (dry) wt % of it being lignin, 20-40 wt % hemicellulose and 30-50 wt % cellulose. The precise proportions of these components vary considerably between

species. In the marine environment, cellulose is also one of the basic structural units of algae, tunicates (sea squirts) and certain bacteria.

$$5/6\ CO_2 + 5/6\ H_2O \xrightarrow{\text{photosynthesis}} C_5H_{10}O_5/C_6H_{12}O_6 + 5/6\ O_2$$

Scheme 1: Photosynthesis: the fountain-head for all biomass production.

The delignification (fractionation) of lignocellulose so as to deliver the constituent polymers is normally achieved using chemical and mechanical methods (or combinations thereof) with common sources of the raw material including corn stover and cobs, various crop straws, saw dusts, sugarcane bagasse, rice hulls, certain fruit peels and the shells of various nuts.[6-19,39, 40] The conversion of such materials into a pulp consisting of almost pure cellulose fibres, as required, for example, in the production of paper, is normally achieved by the kraft process (kraft being the German word for strength) and wherein the substrate is first subject to high temperature treatment with caustic soda and sodium sulfide. Various steps involving phase separations and other processes then follow and these eventually provide cellulose and lignin (the hemicellulose associated with the substrate is degraded into low-molecular weight and water soluble components). The process has been optimised for the economical delivery of high purity cellulose and this is achieved, in the kraft variant, through selective degradation and condensation reactions of the lignins present in the lignocellulose. This and other drawbacks to this still dominant mode of cellulose production have prompted the search for more environmentally benign processes, including enzymatic and microbiological ones.[16,10] However, detailed discussions of such important efforts are not provided herein.

The exploitation of the four title polymers in establishing bio-based chemical supply chains is now detailed on a more-or-less individual basis although the reader must bear in mind that the first three are all key components of lignocellulose. As such they cannot be discussed in

completely compartmentalised ways and so where a commentary on their interconnectedness is required we have attempted to provide this.

Cellulose and its Uses as an Intact Polymer

Cellulose (**1**) (**Figure 1**) is a linear polymer comprising between several hundred to ten-thousand β-1,4-linked *D*-glucopyranose units that each adopt a $^4C_1$ conformation in which all of the associated ring substituents are in equatorial orientations and thus contributing to the rigidity/strength of the polymer backbone. The isomeric and more flexible polysaccharide amylose (**2**), a key component of starch, is comprised of α-1,4-linked *D*-glucopyranose residues. Commercially available cellulose may contain small amounts (usually less that 1%) of arabinoxylans arising from the hemicellulose contained within the precursor lignocellulose.[41]

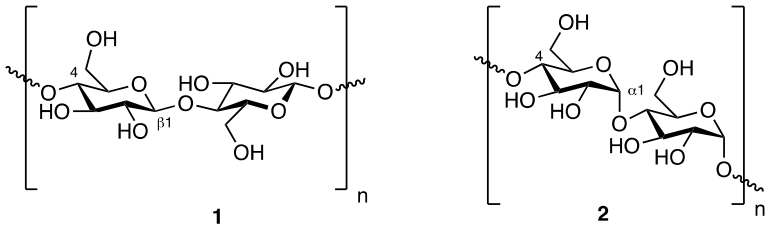

Figure 1: The structures of cellulose (**1**) and amylose (**2**)

Cellulosic fibres have been used for producing textiles and cordage (ropes) for thousands of years and, in more industrial times, for producing cellophane films (after mercerisation of cotton, for example, using caustic soda), explosives, hygiene and absorbent products as well as dietary supplements. It is also used in cement, automotive bodies and automotive interiors. Emerging uses include those involved with water and air filtration, with various medical products, in materials science, in electronics and in a range of catalytic processes.[42,43] In nanocrystalline form, cellulose is finding applications in an increasingly wide range of settings including as functional paper, as an anti-bacterial coating, in tissue scaffolds, in drug delivery

(as a excipient) and in electrochemically controlled separation.[44-47] Perhaps the earliest reported method for the chemical manipulation of cellulose involved its nitration using nitric acid in conjunction with (typically) sulfuric acid. This conversion was first reported in 1865 and the nitrocellulose thus formed, and commonly known as gun cotton, is a mild explosive used in propellants as well as leather finishing. Celluloids are produced by mixing nitrocellulose with the terpene camphor and represent the first synthetic plastic materials, serving as substitutes for ivory, tortoiseshell and horn in the production of toiletry items (e.g. combs), billiard balls and fountain pen casings. Famously, of course, it was used in the making of movie film although its highly combustible nature (as projectionists of the time will testify!) meant that it fell into disfavour after some decades. As a result, today the primary use of celluloids is in the production of table tennis (ping pong) balls where it is considered to be a material without equal. Readily produced cellulose acetate, on the other hand, continues to be a high-volume commodity material now used in making photographic films, tapes, labels, textiles and apparel as well as in producing cigarette filters.[48] Xanthates obtained by treating cellulose with carbon disulfide in the presence of sodium hydroxide afford a highly processible material which, after removal of the xanthate groups, provides the widely utilised polymer known as viscose or Rayon®. This was the first man-made (semi-synthetic) fibre and serves as a substitute for silk (and is thus sometimes called imitation silk or wood silk). It continues to be used extensively, notably in sportswear, because of its breathability although its decomposition into toxic small molecules has been cited as a source of concern.[49] Interestingly, certain xanthate esters derived from cellulose have been used in aminolysis reactions to immobilise proteins.[50] Cellulose fatty acid esters are hydrophobic materials that continue to be investigated as biopolymers that might serve as completely processable substitutes for petroleum-derived polymer films. While the

cost-effective manufacture of such esters remains a challenge they are considered particularly attractive candidates for use in food packaging.[51-54] The etherification of cellulose by various means has produced a plethora of derivatives that have been exploited as, *inter alia*, thermoplastics, water binders, flow-control agents, and film formers. Such products are also used in food, cosmetics, pharmaceuticals, oil recovery, ceramics, and textiles. The proto-typical ether is methyl cellulose and this is used, for example, as an emulsifier and thickener in foods, as a bulk-forming laxative as well as in cosmetic products.[55]

Cellulose Breakdown Products (Platform Molecules)

The most important and obvious small-molecule breakdown product derived from cellulose is glucose and this conversion (saccharification) can be achieved using either chemical or enzymatic methods, the most common involving acid hydrolysis. Typically, this is a process requiring high temperatures and pressures. Apart from its applications in the food industry, the glucose so formed is also converted through fermentation using, for example, baker's yeast into ethanol (**Scheme 2**) that is itself employed as a fuel additive/biofuel.[6-19,56, 57] The original modes of generation of ethanol by such means (**path a**), and from sucrose in particular, lead to the so-called "fuel vs food debate"[58] and has resulted in new generation biofuel production processes that exploit non-edible forms of biomass and rely on the production and transformation of syngas (producer gas), this being comprised primarily of hydrogen and carbon monoxide together with some carbon dioxide. The Fischer-Tropsch (FT) process is employed in the closing stages of the biomass $\rightarrow$ syngas $\rightarrow$ ethanol sequence.[59,60,155] Biobutanol is also produced by related biocatalytic pathways and given its superior calorific content and physical properties it seems poised to assume a significant role as a renewable form of liquid fuel.[25 61] Bacteria that

exploit the Wood–Ljungdahl biochemical pathway have also been used to convert syngas into bio-alcohols for use as fuels (**path b**).[26]

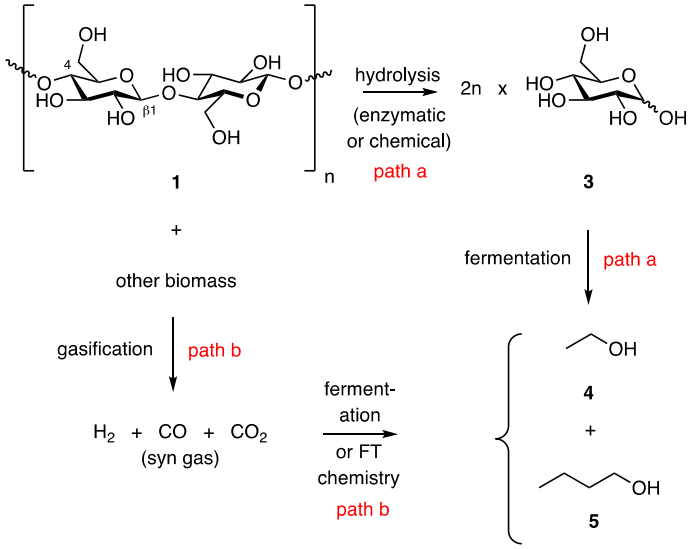

Scheme 2: The cellulose (**1**) to glucose (**3**) to ethanol (**4**) production stream (path a) and a more modern variant (path b) that also provides butanol (**5**)

The dehydration of bioethanol and biobutanol to produce ethene and butenes, respectively, provide downstream products that also have considerable value but from a fine chemical perspective, essentially all of the functional and structural value of the precursor glucose is lost in such conversions. Accordingly, there is a considerable interest in both biocatalytic and chemical pathways that convert glucose into still functionally-rich products (platform molecules or PMs). In the former category, the most notable (fermentation) products are (**Figure 2**) lactic acid (**6**), succinic acid (**7**), 3-hydroxypropinoic acid (**8**), itaconic acid (**9**) and glutamic acid (**10**). However, a key challenge associated with forming such glucose metabolites at scale is establishing an economically-viable means of isolating the pure material. For example, it is estimated that 50% of the cost of lactic acid production is associated with its isolation from the fermentation broth.[6-30]

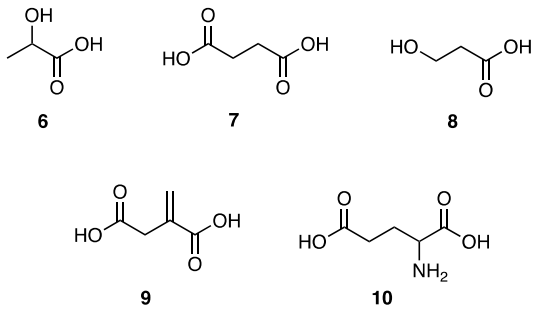

Figure 2: Key products, **6**-**10**, obtained through the biotransformation of glucose (**3**)

Each of the biotransformation products **6**-**10** can be manipulated by various means to give what might be termed secondary or second-order platform molecules/compounds (2°-PMs).[24] So, for example, reduction of lactic acid (**6**) affords 1,2-propanediol (**11**) (**Figure 3**), oxidation delivers pyruvic acid (**12**), dehydration gives acrylic acid (**13**), cyclodehydration affords lactide (**14**) and esterification gives products such as ethyl lactate (**15**).[6-30,64] Of course, each of the remaining metabolites **7**-**10** has a corresponding set of simple derivatives that further expands the suite of available biomass-derived small molecules,[6-30] a number of which serve as precursors to various important polymers. For example, poly(lactic acid) is a high-volume and biodegradable plastic derived from compound **6**.[65]

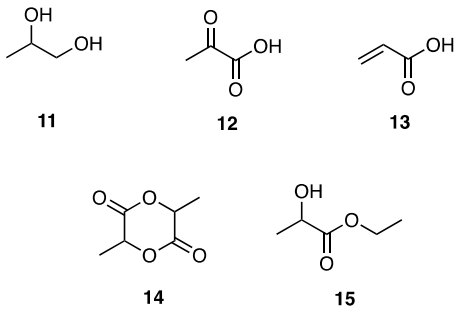

Figure 3: Second-order platform molecules, **11**-**15**, obtained from conventional chemical transformations of lactic acid (**6**)

Other valuable and initial/primary platform molecules (1°-PMs) are derived from the chemical manipulation of hexoses, especially glucose. So, for example, hydrogenation of glucose over various metal catalysts produces sorbitol (**16**) (**Figure 4**), an important precursor to ascorbic acid (vitamin C), at quantities approaching one million tons per year. Depending on the precise conditions involved, catalytic oxidation of glucose using air or hydrogen peroxide in aqueous solution and in the presence of metal species such as Pt-Bi/C affords gluconic acid (**17**), glucaric acid (**18**) and/or 2-ketogluconic acid (**19**).[6-19] However, the equivalent biological oxidation reactions remain the primary modes of production of the last three compounds. Telescoped processes that allow for the "one-pot" conversion of cellulose, via glucose, into final products **16**-**19** have been investigated in recent times.[6-30] Once again, each of the 1°-PMs **16**-**19** can be manipulated by a wide variety of chemical or biochemical means and so affording an impressive collection of 2°-PMs.[6-30]

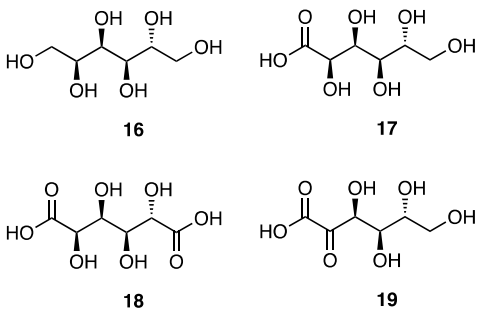

Figure 4: 1°-PMs **16**-**19** arising from the catalytic reduction (with H_2) or oxidation (with O_2 or H_2O_2) of glucose (**3**).

Some of the earliest reported and in many ways most useful biomass-derived 1°-PMs are generated through treatment of glucose with mineral and other acids. In particular, 5-hydroxymethylfurfural or HMF (**20**) and levulinic acid or LA (**21**) (**Figure 5**) are produced by

by such means and attempts to optimise the formation of these compounds by using, for example, novel Lewis acids for their formation continue to be investigated as do the mechanistic pathways by which they are formed. In the last respect, it is clear the HMF is a precursor to LA, the latter often being isolated by steam distillation.[66-68] 5-Chloromethylfurfural (structure not shown) is readily produced through microwave heating of various sugars and polysaccharides in the presence of concentrated aqueous hydrochloric acid.[69]

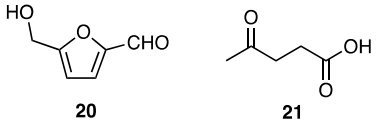

20 **21**

Figure 5: The 1°-PMs HMF (**20**) and LA (**21**) arising from the mineral acid-catalysed dehydration of glucose (**3**)

HMF (**20**), a solid, has found extensive use both as a precursor to monomers that are themselves subject to polymerisation and as a starting material in the synthesis of pharmaceuticals, insecticides, flavour enhancers, crown ethers and possible biofuels.[66-68] LA (**21**), also a solid, has attracted attention as a potential anti-freeze agent and as a precursor to biofuels. It is used industrially in the manufacture of resins, plasticisers, textiles and animal feed. Furan-2,5-dicarboxylic acid, another HMF derivative that is also obtained through oxidative dehydration of glucose, is being pursued as a renewably generated source of and substitute for terephthalic acid (TPA) in the production of polyesters and related systems incorporating aromatic residues.[70-72]

In the early 1970's pyrolysis of acid-treated and carbohydrate-containing biomass was shown to produce levoglucosenone (LGO) (**22**) (**Figure 6**), a homochiral compound that was identified as such at that time. Various refinements of this process in the interim have culminated in Circa Group's thermal method (conducted in the temperature range 170 to 350 °C) for treating wood

pulp under acid conditions and so affording LGO in *ca*. 40% at multi-kilogram scales.[73-76] A recent DFT-based theoretical study of the LGO-forming process suggests a dioxyallyl cation intermediate is likely to be involved[77] while other research has demonstrated that by controlling the water content of the "reaction mixture" then LGO formation can be favoured over HMF (**20**) and furfural co-production.[75]

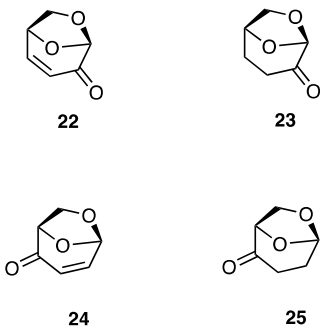

Figure 6: The 1°-PM LGO (**22**) and its derivatives Cyrene® (**23**), *iso*-LGO (**24**) and *iso*-Cyrene (**25**)

Catalytic hydrogenation of LGO leads to its dihydro-analogue **23** that is now marketed under the tradename Cyrene®, by Circa Group, as an industrial replacement for the dipolar aprotic and "environmentally suspect" solvents *N*-methyl-2-pyrrolidone (NMP) and DMF.[75,49] It is interesting to note that while Cyrene® is finding a number of important applications, its homochiral features do not appear to have been exploited thus far. In an effort to redress this matter we have sought to use this new solvent as a means of resolving racemates through fractional crystallisation but with no success to date.

Another aspect of LGO chemistry that we have pursued involves its conversion, through the application of 1,3-carbonyl transposition protocols, into the pseudo-enantiomeric *iso*-levoglucosenone (*iso*-LGO) (**24**) (**Figure 6**). Various means for effecting this conversion have

been realised[78, 79] and the most efficient that we have found to date involves a three-step process that starts with the facile addition of water to LGO in a hetero-Michael fashion and thus allowing for the formation of compound **24** in multi-gram quantities. The reduction of *iso*-LGO to *iso*-Cyrene (**25**) is readily achieved under conventional conditions and so facilitating our ongoing investigation of the physico-chemical properties of the latter.[78,79]

The ready availability of both LGO (**22**) and pseudo-enantiomer **24** have prompted us to pursue various ways in which they might be exploited. In one such effort (**Scheme 3**), concerned with the identification of new scaffolds for drug discovery,[80] we converted each of these into the corresponding α-iodinated enones **26** and **27**, respectively, using a simple protocol originally developed by Johnson and co-workers. These halogenated products could be cross-coupled, using a palladium-catalysed Ullmann reaction, with brominated nitropyridines such as **28** and **29** to afford the α-pyridinylated enones **30** and **31**, respectively, and each of these was subjected to reductive cyclisation using molecular hydrogen in the presence of a suitable catalyst. By such means the corresponding azaindoles such as **32** and **33** were formed. While azaindoles more generally are considered privileged structures in medicinal chemistry, congeners such as **32** and **33** proved inactive in a range of microbiological and cytotoxicity screens conducted by colleagues at the University of Queensland.[80] In contrast, on subjecting various of the precursor α-pyridinylated enones, notably **30** and **31**, to the same assays these were shown to be active at sub-micro-molar levels (**Scheme 3**).

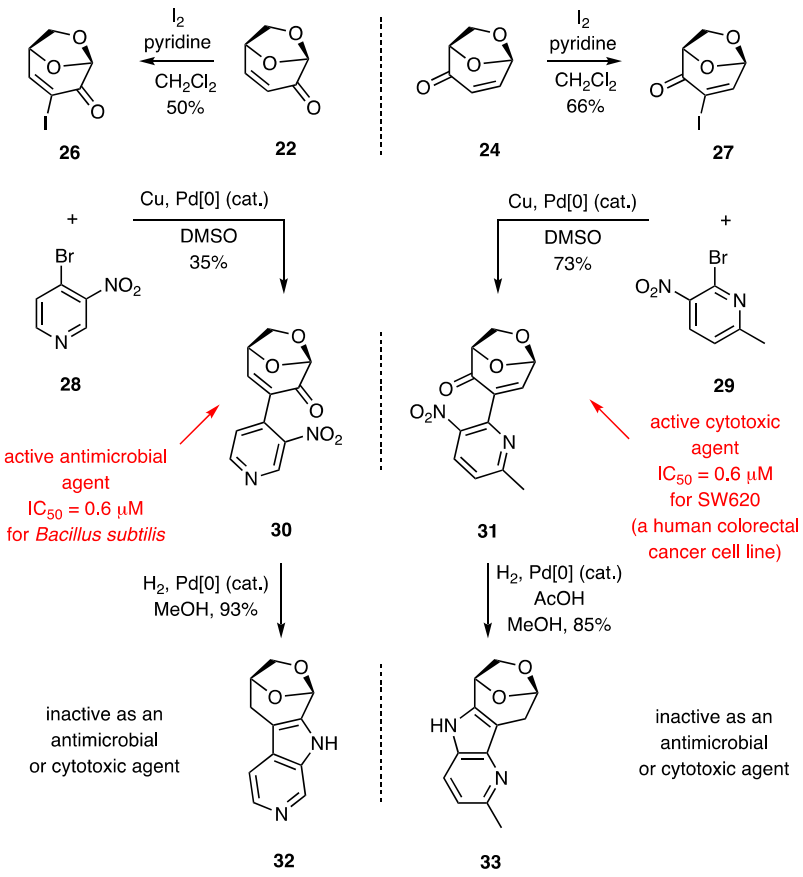

Scheme 3: Investigating LGO (**22**) and *iso*-LGO (**24**) as scaffolds for drug development.

The possibility that compounds such as **30** and **31** might exert these effects by conjugating with nucleophilic sites on the amino acid residues of target proteins is supported by the observation that *S*-cysteine (**34**) (**Scheme 4**) engages in hetero-Michael addition reactions with compound **35** to give a mixture of the diastereoisomeric adducts **36** and **37**.[80]

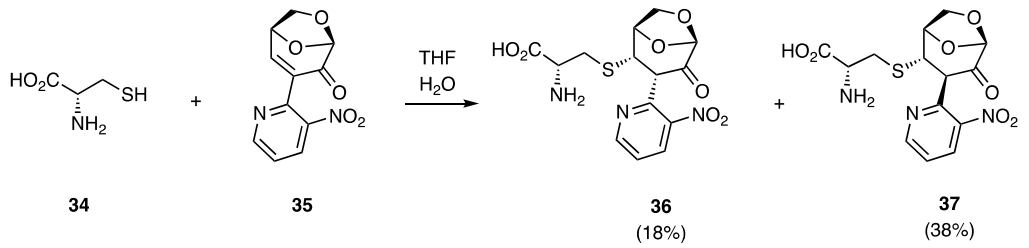

Scheme 4: The conjugate addition of *S*-cysteine (**34**) to the α-pyridinylated enone **35** and leading to adducts **36** and **37**.

In a quite distinct synthetic application of LGO (**22**) and *iso*-LGO (**24**), these were each reacted (**Scheme 5**) with cyclopentadiene (CPD) to give the known Diels-Alder adducts **38** and **39**, respectively, and these, in turn, subjected to a ring-opening metathesis polymerisation (ROMP) using the Grubbs' III catalyst to give polymers **40** and **41**. Co-polymers and block co-polymers such as **42** could also be formed by analogous means.[81,82]

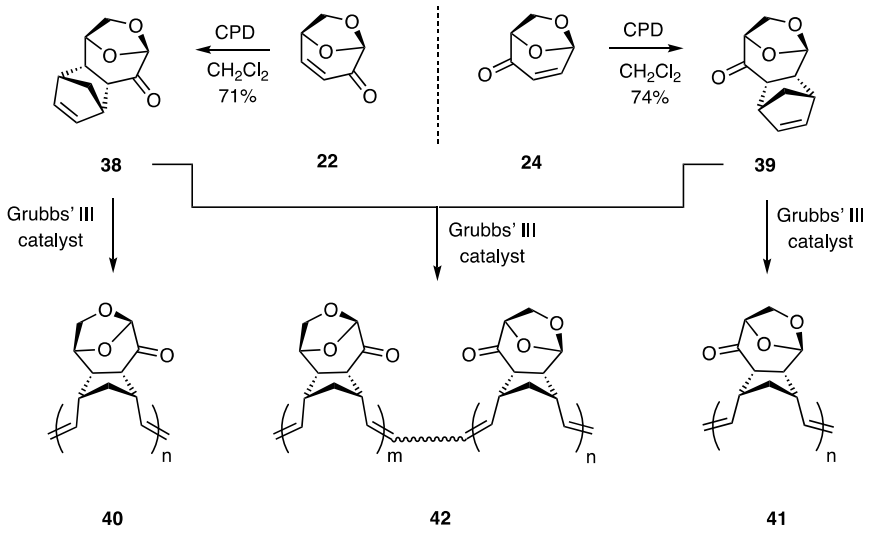

Scheme 5: The synthesis of polymers and block copolymers from LGO (**22**) and *iso*-LGO (**24**)

Sodium borohydride-mediated reduction of the ketone carbonyl residue within the Diels-Alder adduct **22** provides the corresponding and epimeric alcohols **43** and **44** (**Figure 7**) that can be functionalised in various simple ways to give a significant suite of derivatives, e.g. **45**-**52**. All of these norborene-containing monomers also engage in ROMP reactions with the Grubbs' III catalyst to give the corresponding polymers. It can reasonably be assumed that an equivalent set of manipulations of adduct **39** would deliver the corresponding and pseudo-enantiomeric monomers and that these too would form, via ROMP, the corresponding polymers.

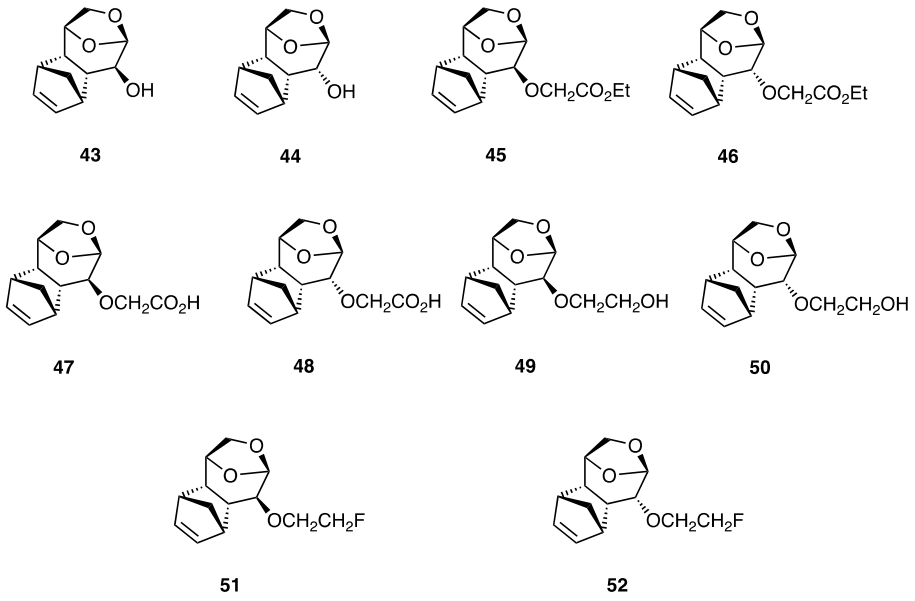

43 **44** **45** **46**

47 **48** **49** **50**

51 **52**

Figure 7: The stereochemically and functionally diverse monomers for ring-opening metathesis polymerisation (ROMP) obtained from Diels-Alder adduct **38**

The polymers we have obtained thus far from all of the above-mentioned norbornene-containing monomers show low dispersities and have a range of interesting properties including, in certain instances, particularly good thermal stabilities. As such and given the wide range of other monomers likely to be available through related manipulations of LGO and *iso*-LGO, as well as the possibility of deploying these in both homo- and co-polymerisations, a very

large library of new polymers should now be available for development. Of course, it remains to be seen if the functional and structural diversity available by the pathways described here can provide a means for "dialling up" polymers with the required/necessary properties. Using combinatorial protocols for exploring this new part of chemical space could provide the most effective approach for establishing if this is indeed the case. Another critical feature of polymers such as **41**-**42** that needs to be examined is how environmentally persistent or otherwise they might be. Certainly, the presence of an internal acetal residue within all of them should facilitate biodegradation processes but the incorporation of additional functionalities is likely to be important in this regard.[81]

While the LGO- or *iso*-LGO-derived portion of the monomers described above are sustainably derived molecular fragments, the corresponding CPD-derived portion is not (CPD is a petroleum product). As such, none of the polymers we have produced thus far can legitimately be described as "full-blooded" biopolymers, these being systems of great interest at the present time. Other groups have recently reported[83] producing LGO-derived polymers that have entirely sustainable pedigrees and we are attempting to identify modifications to the chemistry shown in **Scheme 5** such that the products so formed can be similarly described.

Regardless of precisely how the chemistries shown in **Schemes 3** and **5** might evolve it seems reasonable to state, as we have done previously, that "this work further highlights the extraordinary utility of LGO as an abundant chemical building block." Its deceptively simple structure belies the remarkable range of chemical transformations that it can participate in. Of particular note, from our point of view, is the ease with which it can now be converted into its pseudo-enantiomer, *iso*-levoglucosenone and so providing another suite of fascinating derivatives.[49]

Hemicellulose and its Uses as an Intact Polymer

Unlike the situation with cellulose, the precise composition of hemicellulose is highly variable and depends on the sources from which it is extracted. *O*-Acetyl-4-*O*-methylglucoronoxylan is the predominant form of hemicellulose found in hardwoods and the backbone, **53**, of this is comprised of 1,4-β-linked D-xylose residues (**Figure 8**). As such it is analogous to cellulose but with D-xylopyranose units (**54**) replacing D-glucose. This backbone incorporates 4-*O*-methyl-D-glucuronic acid and/or acetate side-chain residues at particular positions of the monomeric subunit. In broad terms, about one in ten of the backbone xylose units bears a glucoronic residue at C-2 while seven in ten are acetylated at C-2 or C-3 and these appendages impart a strength to the biopolymer that creates significant challenges in its valorisation. The major hemicellulose component in switchgrass (*Panicum virgatum*) is known as arabinoxylan and is named as such because the backbone unit **53** now incorporates α-(1 → 2)- and α-(1 → 3)-linked arabinose side-chain units.[84-86]

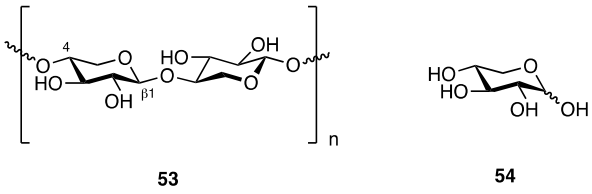

53 **54**

Figure 8: The structure, **53**, of the backbone of the hemicelluloses found in hardwoods and switch grass and the corresponding monomer xylose (**54**)

In contrast, hemicellulose derived from softwoods often incorporates, within the backbone, randomly distributed D-glucose and D-mannose repeating units together with branching D-galactose residues (attached at either backbone hexose residue). Furthermore, up to one in five of the hydroxyl groups associated with the D-mannose units is acetylated. This biopolymer is named *O*-acetylgalactoglucomannan (AcGGM). Hemicelluloses can also be obtained from the

soft tissues of certain sugar beet and fruit pulps. These include mannan, arabinan, galactan, arabinogalactan and rhamnogalactan.[84-86]

Hemicelluloses have found a significant number of industrial applications, including as components of hydrogels, as additives in papermaking, in cosmetics and in pharmaceuticals. Like with cellulose, chemical modifications of hemicelluloses, through derivatisation of the associated hydroxyl residues, have been investigated extensively and as a means for rendering them more hydrophobic and, thereby, potentially more useful. Films made from acetylated hemicellulose have been used as near oxygen-impervious and biodegradable food packaging. As is the case with cellulose, esterification of hemicellulose using fatty acids provides materials suitable for coating paper/board. Various etherification processes also provide hemicellulose derivatives that offer utility as coatings and/or packaging materials. Hemicellulose analogues of Rayon® have been examined as wound dressings, especially in burns units, on the basis that, like Rayon®, these provide a suitable microenvironment for the regeneration of skin. Since xylan can be degraded by microflora in the human gut, appropriately constituted hemicelluloses have also been investigated as drug delivery agents, including in the form of capsules.[84-86]

Hemicellulose Breakdown Products (Platform Molecules)

Hemicellulose has been investigated as a source of both biofuels and platform molecules in much the same way that has been described above for cellulose. From a chemical point-of-view, the most notable difference between these two forms of biopolymer is that the former frequently embodies five-carbon sugars and so the suite of breakdown products that can be obtained from hemicellulose is a distinctive one. From a biofuels perspective, there is less difference between these two forms of biomass and so the following discussion is confined to

descriptions of the production of platform molecules from various forms of hemicellulose. Recent reports indicate that furfural (**55**) (**Figure 9**) is generated from hemicellulosic-derived biomass at the rate of about 300,000 tons/year.[155] This involves the hydrolysis, normally effected with mineral acid, of the relevant xylan into the constituent pentoses (xylose and arabinose) that upon further acid treatment (and now involving dehydration) affords furfural. Chemical manipulations of this 1°-PM lead, through reductive and related processes, to the 2°-PMs including furfuryl alcohol (**56**), 2-methylfuran (**57**), 2-methyltetrahydrofuran (**58**) and tetrahydrofuran (**59**) itself.[87,155] Oxidation, on the other hand, affords furoic (**60**) and succinic acids (**61**), the latter also being available from D-glucose.[87]

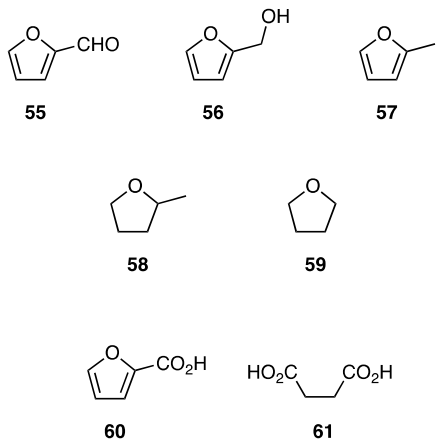

Figure 9: The 1°-PM furfural (**55**) obtained from acid-treated, biomass-derived pentoses and the derived 2°-PMs **56**-**61**.

The reduction of *D*-xylose (**54**) obtained from hardwood hemicellulose hydrolysate is accomplished at industrial scale using a nickel catalyst at elevated temperatures and pressures to provide xylitol (**62**) (**Figure 10**),[11] a naturally occurring polyol that is 20% sweeter than sucrose but has a 60% lower calorific content. Furthermore, mammalian metabolism of xylitol does not require insulin and so it is considered an important sugar substitute for diabetics.[155] A number of efforts to improve the production of xylitol from biomass have focused on either direct conversion using acid in combination with ruthenium catalysed reductions or enzymatic

cleavage of xylans to afford xylose under milder and more efficient conditions. The reduction of *L*-arabinose, another pentose available in quantity from certain hemicelluloses, affords *L*-arabinitol (a.k.a. *L*-arabitol or *L*-lyxitol) (**63**), a compound of interest as a food additive that reduces fat deposits in the human intestine and that is also used as a drug excipient.[6-19]

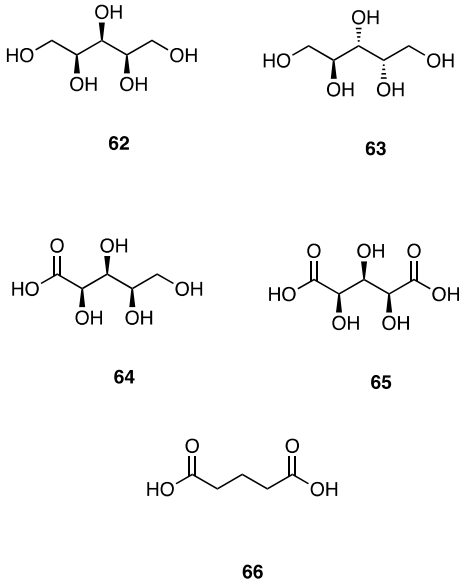

Figure 10: 1°-PMs **62**-**66** available through the chemical manipulation of biomass-based pentoses

The oxidation of *D*-xylose (**54**) so as to form the 1°-PM xylonic acid (**64**) (**Figure 10**) and, in some instances, the two-fold oxidation product xylaric acid (**65**), has not been well studied but can be accomplished by various chemical and biological methods.[6-19] It has been suggested that compound **65** may serve, through three-fold deoxygenation, as a precursor to glutaric acid (**66**) for which there is great demand industrially as a precursor to various polymers.[88,89]

A particularly intriguing recent development is the single-step conversion of various non-food forms of biomass into isoprene (**67**) (the product has been named Bioisopropene®) (**Figure 11**) using microbial fermentation techniques. The company behind this process is Genencor and it

has partnered with the Goodyear Tire and Rubber Company so as to produce tyres using this sustainably produced monomer for rubber production. This metabolite may also serve as a precursor to various biofuels.[88,89,90,155] While it is not entirely clear if this material is being produced from five- and/or six-carbon sugars, from an atom-economical point-of-view the former source would be the preferable one. The sesquiterpene farnesene (structure not shown) can be produced at volume by related means.[88]

67

Figure 11: The structure of isopropene (**67**) that can now be produced through microbial fermentation of biomass

Lignin

Among the three components of lignocellulosic biomass, the aromatic biopolymer lignin is the structurally most complex and, as a consequence, also the most intractable in terms of its valorisation.[91-114] As testimony to this situation, the lignin waste deriving from pulp and paper manufacture is frequently used as a low grade-fuel for powering the production plant although its exploitation in the production of syngas is now receiving increasing attention. Nevertheless, there is intense current interest in obtaining higher value products from lignin and a multitude of means for doing so is being developed and informed by an increasingly sophisticated knowledge of the various lignin structures.[91-114]

The precise composition of lignin is highly variable and a function of the species of producing plant as well as the environmental and seasonal conditions it is or has been exposed to. Softwoods tend to contain the highest proportions of lignin (21-29 wt %) with hardwoods coming next (18-25 wt %) and followed by herbaceous plants (15-24 wt %).[91-114]

In broad terms, lignin is comprised of cross-linked phenolic polymers with the key monomeric precursors (monolignols) involved in the so-called phenylpropanoid biosynthetic pathway being the cinnamyl alcohols **68**, **69** and **70** (**Figure 12**). These are themselves biosynthesised from phenylalanine and/or tyrosine. There is also emerging evidence that certain flavonoids, hydroxystilbenes and hydroxycinnamic amides can serve as monomers and become fully embedded in the lignin polymer.[100] The polymerisation processes involved are undoubtedly free-radical in nature and likely initiated by enzymes such as laccases and peroxidases.

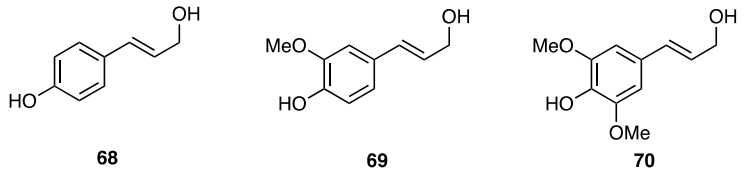

Figure 12: The primary monolignols **68**-**69** involved in the formation of lignin

Some of the key ways in which such phenylpropanoid residues are incorporated into the polymeric lignin framework are shown in **Figure 13**. A knowledge of these has informed studies of model compounds undertaken in efforts to define conditions for the controlled depolymerisation of lignins.[106,115-119] So, for example, Hartwig and co-workers have devised hydrogenolytic methods for the cleavage of biaryl ethers (see **73**), and so affording the corresponding mixtures of aryls and phenols,[116,118] while Ford *et al* have reported[115] related means for cleaving dihydrobenzofurans (see **74**). On the other hand, the Bolm Group has investigated the base-catalysed cleavage of models for the β-O-4 linkage (see **71**).[117]

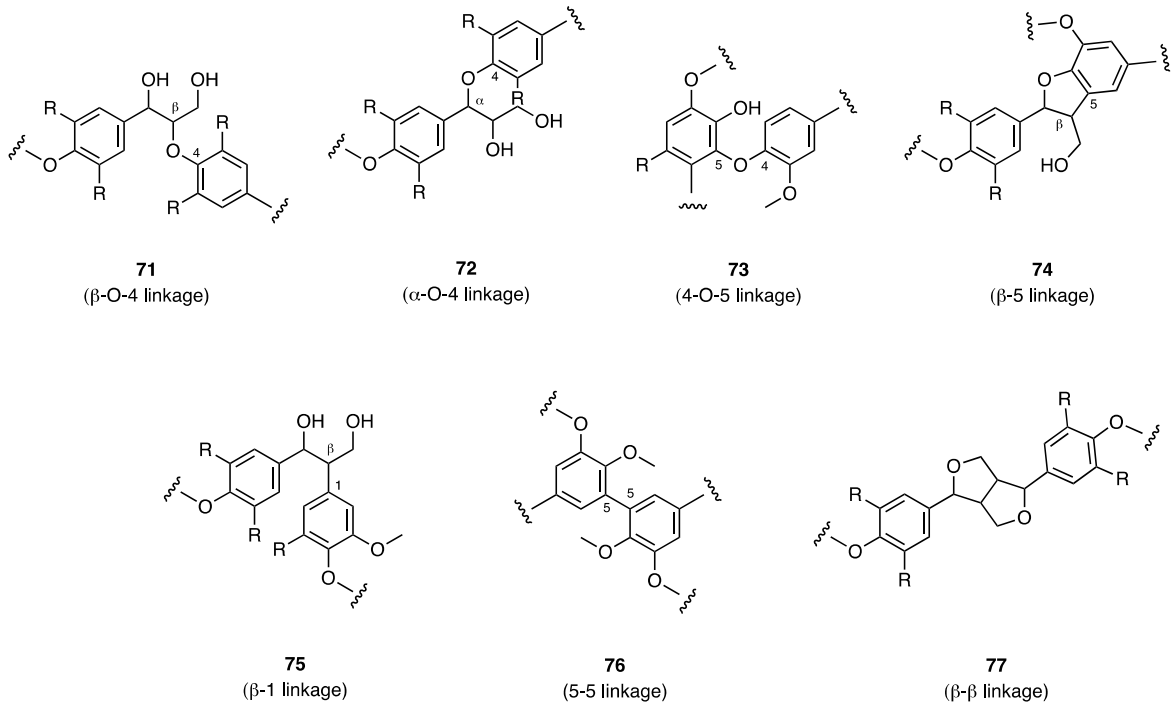

Figure 13: Key linkages, **71**-**77**, associated the incorporation phenylpropanoid residues within lignin polymers

In terms of the manipulation (valorisation) of lignin, which can, as highlighted above, take many structural forms, a wide range of techniques has been investigated. Since conventional deligninification processes that deliver cellulose significantly degrade the lignin and so potentially devaluing it, a so-called "lignin-first" approach to deriving useful chemicals from it has attracted attention.[103] This can take various forms including "organosolv" fractionation wherein organic solvents such as methanol, ethanol, butanol, acetone, formic acid, acetic acid or even ionic liquids are used.[94,98,101,102,112] Such fractionations are often conducted in conjunction with hydrogenolytic techniques, selective precipitations and/or membrane separations, and so providing low molecular weight aromatics that are free of sulfur-based contaminants (as encountered in materials arising from the kraft process). Catalytic oxidative and pyrolytic depolymerisation processes have also attracted attention, as have various enzymatic techniques.

The so-called reductive catalytic fractionation or RCF/lignin-first approach,[108,120] which takes various forms, can exploit formic acid as a source of hydrogen as well as simple alcohols as capping agents to shutdown (re)polymerisation processes which introduce "second order" complexity, is considered to have particular promise. It is thought likely to contribute to second and perhaps even third generation biorefineries. Electrocatalytic, photocatalytic and microwave techniques for processing lignin are also garnering attention.[93,105,114]

The lignins derived from existing industrial processes are described as technical forms and include kraft lignins, soda lignin, organosolv lignin and lignosulfonates with the last types, in particular, finding applications as binding agents and emulsifiers, as a rheology modifier, and in polymer formulations. This last application often entails the conversation of the hydroxyl groups associated with the lignin into "macromonomer"-derived polymers incorporating, for example, ester, urethane and epoxide residues.[92,95,101,102] Composite materials involving lignin as one component are also attracting increasing attention.[91-114]

The plethora of techniques available for the depolymerisation of lignin coupled with the structural complexities of this biopolymer has provided a correspondingly large suite of aromatic-containing 1°-PMs including compounds **78**-**88** (**Figure 14**).[91-114] Vanillin (**84**) is a particularly notable such product that can be obtained in good yield and at significant volume through the oxidation, under alkaline conditions, of kraft lignin. As a consequence vanillin-derived polymers are now attracting increasing attention.[92] Despite such successes it remains the case that lignin valorisation is less well developed than the equivalent processes associated with the exploitation of cellulose and hemicellulose. That said, the emerging concepts/techniques of biocatalytic and chemocatalytic funnelling appear to offer some

prospects for the reliable/predictable generation of useful building blocks from complex lignin precursors.[95,108]

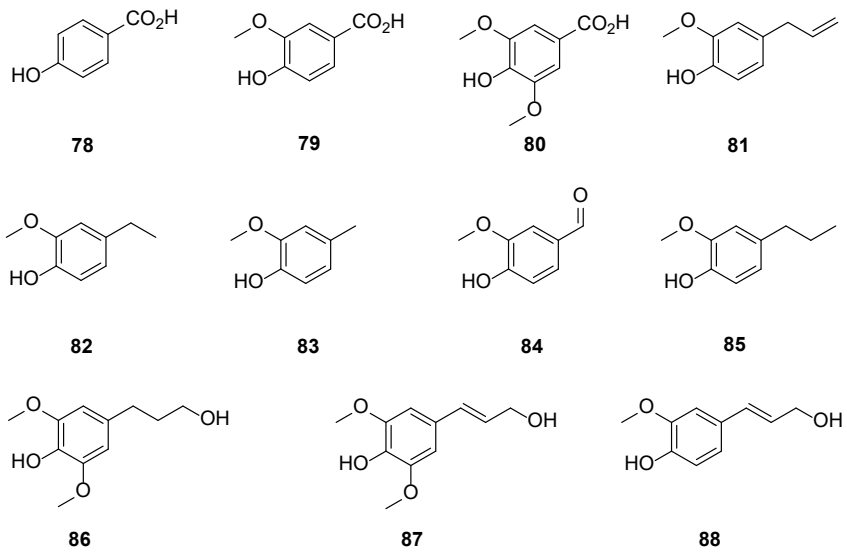

Figure 14: Some representative examples, **78**-**88**, of aromatic compounds derived from the valorisation of lignin

Lignans, norlignans and neolignans are low molecular weight phytochemicals (conventional natural products) and biogenetically related to lignins because they too are derived from precursors such as the monolignols **68**-**69**.[121] The resulting phenolic dimers take different forms depending upon the manner in which the phenylpropyl subunits are linked to one another. Prominent examples of such compounds are steganone (**89**) and podophylotoxin (**90**) (**Figure 15**) that have attracted attention because they display significant cytotoxic effects against certain cancer cell lines. While the traditional focus on lignans and their congeners has been examining their potential as leads for drug discovery purposes,[122-125] they also have considerable potential as neutraceuticals/functional foods. This is because certain edible plants or parts of plants are prolific producers of some lignans. So, for example, the bis-glycosylated

lignan **91**, known as secoisolariciresinaol diglucoside (SDG), together with matairesinol (**92**) are notable components of oil seeds such flaxseed (linseed).[126] 1°-PM **91**, which is an anti-oxidant phytoestrogen, can be extracted from, for example, flaxseed hulls using microwave techniques at up to 40 mg/g.[127] Such compounds can be manipulated in various ways[128,129] so to generate a range of 2°-PMs.

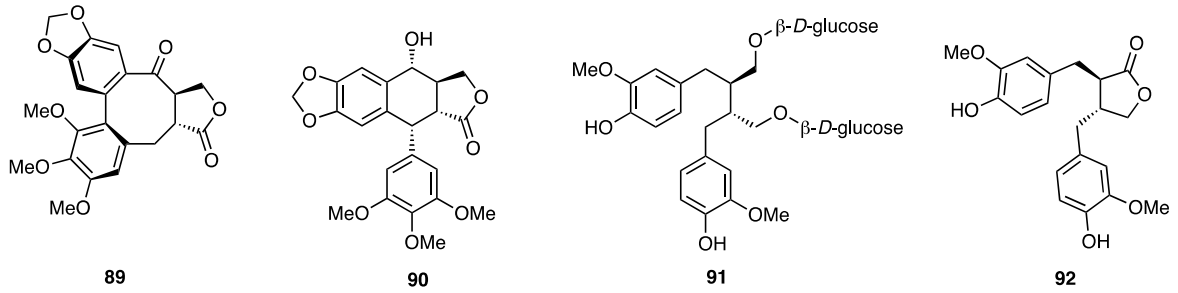

89 **90** **91** **92**

Figure 15: The lignans steganone (**89**), podophylotoxin (**90**), SDG (**91**) and matairesinol (**92**)

Given the foregoing, it would appear that the development of lignans as a source of what might be described as boutique platform (aromatic) molecules would appear to be a promising area of research.

Chitin

Chitin (**93**) (**Figure 16**) is a polymer comprised of β-1,4-linked *N*-acetyl-*D*-glucosamine (NAG, **94**) residues and found in the exoskeleta (shells) of shrimps, crabs, crayfish and insects as well as in the cell walls of both brown and green algae. Shrimp and crab shells are high-volume and distinctly underutilised by-products of the food processing industry. Chitin is a major source of biologically fixed nitrogen and thus quite distinct from lignocellulosic biomass.[130-132] Indeed, it has been estimated that chitin is produced at an annual rate of 10^{11} tonnes through a multistep

biosynthetic pathway, a key component of which is the action of chitin synthase (CS) on uridine diphosphate (UDP)-*N*-acetyl-*D*-glucosamine and so resulting in polymer chain assembly.[133]

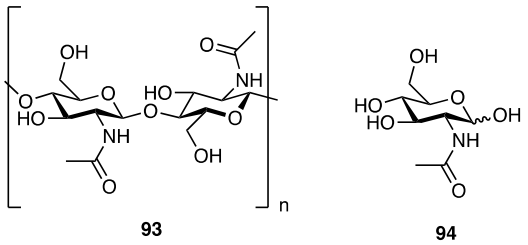

Figure 16: The structure of the nitrogen-containing biopolymer chitin (**93**) and the associated monomer *N*-acetyl-*D*-glucosamine (**94**).

The extraction of chitin, which occurs as crystalline microfibrils in nature, from the source material (e.g. shrimp and crab shells) is time consuming and involves treatments with hydrochloric acid and sodium hydroxide so as to remove calcium carbonate and protein, respectively. Vigorous treatment with sodium hydroxide (at 120 °C for 1-3 h) effects cleavage of the acetyl groups and so forming the polymer chitosan incorporating free 1°-amine residues.[134] Deacetylation can also be accomplished enzymatically.[135] Chitin-based materials, which are considered biocompatible and can be fabricated in various ways, have been employed in a multitude of medical and other settings. For example, they have been used in tissue engineering, wound healing, drug delivery, surgical dressings, as anti-bacterial agents, in anti-aging cosmetics, as adjuvants in vaccines, as anti-cancer agents and for the production of ionic liquids.[130-132]

In contrast to the rather extensive studies of the production of 1°-PMs from the components of lignocellulosic biomass, much less work has been directed toward the analogous conversion (depolymerisation) of chitin. That said, the treatment of chitin with concentrated hydrochloric acid affords, after both depolymerisation and deacetylation, glucosamine, a compound seeing increasing use for the treatment and prevention of osteoarthritis.[134] Chitinases, amongst other

enzymes, have been used for the degradation of the polymer and so producing, as the major product, the dimer of *N*-acetyl-*D*-glucosamine (**94**), *viz*. $(GlcNAc)_2$, although oligomers up to $(GlcNAc)_6$ are also observed.[135] Mechanochemical means can be used to effect, in a catalytic manner, the depolymerisation of chitin with retention of the *N*-acetyl group.[136] Recently, the conversion of pre-treated chitin, using metabolically engineered *E. coli*, into tyrosine and L-DOPA has been reported.[137]

The pyrolysis of chitin has been reported under various conditions although many such studies, particularly earlier ones, have been confined to GC/MS analyses of the products so formed. More recently, we[138,139] and others[140-145] have been focused on studying the formation of isolable and fully characterisable pyrolysis products (*viz*. 1°-PMs) derived from this biopolymer, an activity that has been described as creating a shell biorefinery.[140-145] In our investigation of such matters we were inspired by the large scale, pyrolytic conversion of acid-treated cellulose into levoglucosenone (LGO) as described above and wondered what would happen if chitin was subjected to an analogous depolymerisation process.

To such ends, commercially available chitin or *N*-acetyl-*D*-glucosamine was pre-treated under a range of different conditions with various mineral or organic acids then dried and subjected to pyrolysis at temperatures ranging between 150 and 350 °C. In order to ensure at least some measure of effective heat transfer the treated substrate was intimately mixed with chromatography grade sand and this mixture then pyrolysed, at reduced pressure and under nitrogen, in a simple home-built apparatus. As a result products **95**-**108** (**Figure 17**),[138,139] that include hetero- and carbo-cyclic ones, were obtained in various combinations and the structures of the majority of these established by single-crystal X-ray analysis. Acetamide (**95**) was invariably obtained under all conditions investigated and often in *ca*. 90% yield. In contrast, the remaining products were obtained at <1% yield.

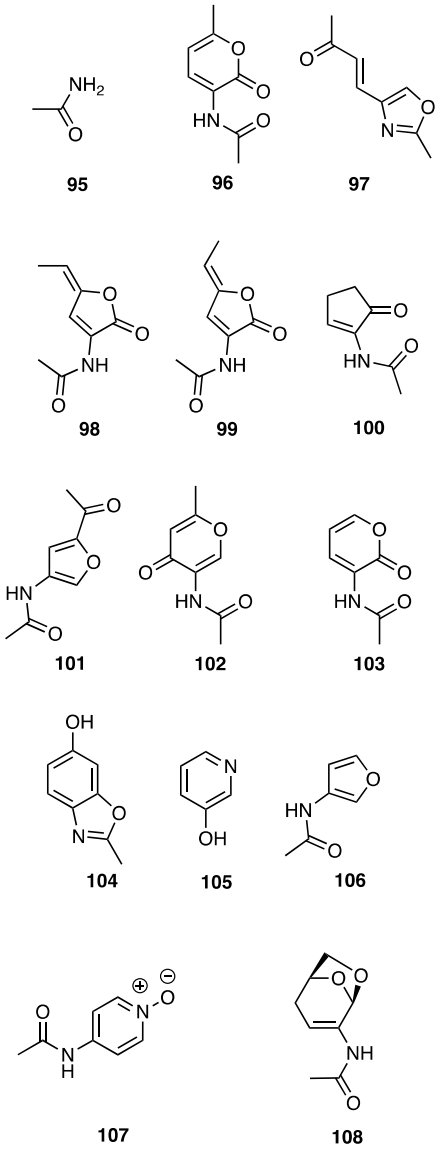

Figure 17: The structures of the small molecule products, **95-108**, obtained through pyrolysis of acid-treated chitin or *N*-acetyl-*D*-glucosamine.

Mechanisms for the formation of all of products **96-108** have been proposed and, in certain cases, supported by high-level computational studies.[138,139] As shown in **Scheme 6**, for example, it is assumed that cleavage of the chitin polymer in the presence of acid delivers the cyclic oxonium ion **109** that is intercepted by the proximate acetamide residue to give the isomeric species **110** that can itself be captured by water and rearrange to give the open-chain

oxonium ion **111**. A 5-*endo*-trig cyclisation reaction then follows with the resulting bicyclic product **112** undergoing a 1,4-hydride shift with accompanying loss of water to give diol **113**. This, in turn, could undergo a cyclo-dehydration reaction and so providing the cyclic ether **114**, fragmentation of which provides the unsaturated lactone **115**. Dehydration of this last species and subsequent migration of the terminal alkene so-formed would then deliver the observed and isomeric products **98** and **99**.

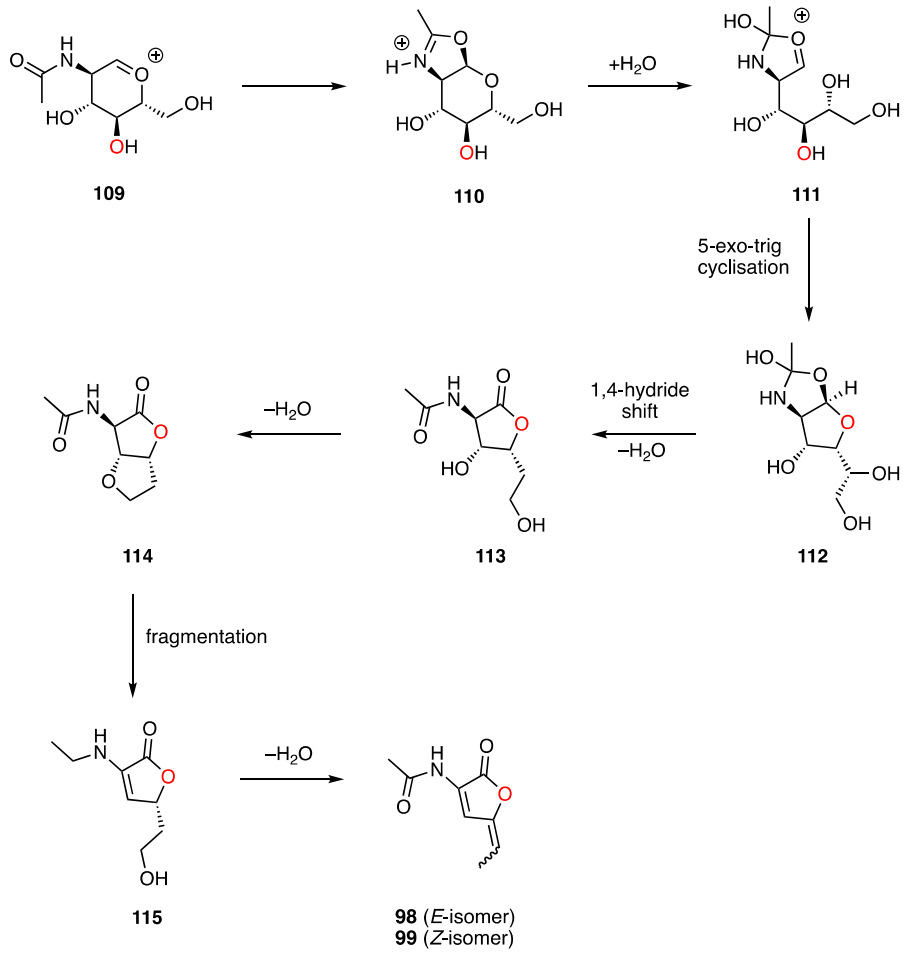

Scheme 6: A possible mechanism for the formation of compounds **98** and **99** from chitin under pyrolytic conditions (300 °C, 1 h).

1°-PMs **107** and **108** are notable in that the first is the only one we have obtained so far that contains two nitrogens while the second retains stereochemical features of the source

biopolymer. Several of the other pyrolysis products, including lactones **98** and **99**, can be characterised as dehydro-α-amino acid derivatives, a class of compound that holds considerable interest in a range of settings.[146]

The utility of certain of products **95**-**108** has already been demonstrated. So, for example, compound **101**, which has been reported previously by others[140-145] and recently shown to be available in good yield by treating NAG (**94**) with $AlCl_3$•$6H_2O$ in DMF at 120 °C,[147] has been exploited as a starting material in the laboratory-scale chemical synthesis of several simple natural products.[148]

Multiple additional opportunities exist for exploiting the various 1°-PMs obtained through the shell biorefinery. So, for example, the Diels-Alder adduct presumably available through reaction of the potential dienophile **97** with CPD could be engaged in ROMPs to give nitrogen-containing polymers. Similarly, the *s*-cissoid dienes **96**, **101**, **103** and **106** might be able to participate in Diels-Alder reactions with LGO and so-forming functionally intriguing adducts, the entire atom-componentry of which is bio-mass derived.

The fundamental challenge associated with realising possibilities such as those mentioned immediately above is the need to generate such pyrolysis products in a selective and higher-yielding manner and at multi-kilogram to tonne scale. This will require an extensive and multi-faceted research program involving both chemical and chemical engineering techniques. Since NAG (**94**) is a 1°-PM derived from chitin, an interim approach could be the exploration of the solution-phase modifications of this monomeric system in the hope that selective transformations (involving successive dehydration reactions) of it could be realised. The recent work of Fukuoka demonstrates the potential of this approach.[147] In another pathway to nitrogen-containing compounds (NCCs), Nan and co-workers have recently reported a catalytic protocol

whereby furfural (**55**) can be converted into pyrrole (**116**) (**Figure 18**) although ammonia is required for this purpose.[149] Nevertheless, this work provides a connection between lignocellulosic biomass and nitrogen heterocycles which are of great value in both chemical synthesis and medicinal chemistry. In the same report,[149] the conversion of pyrrole into (±)-proline (**117**) is described and so representing the reverse of one industrial route to the former compound and wherein proline-rich keratins (as encountered, for example, in sheep's wool) are treated with barium hydroxide.[150] The Nan group has also reported[151] the direct production of pyrrole and acetic acid from chitin and waste shrimp shells.

116 117

Figure 18: The structures of pyrrole (**116**) and (±)-proline (**117**)

Future Prospects

Over the last 150 years fossil hydrocarbons have been a dominant source of compounds [platform molecules (PMs)] for use as starting materials in chemical synthesis. However, with the inevitable depletion of the reserves of these petrochemicals and the rapidly increasing awareness of the impact that their use has on the environment, there is now a profound need to develop sustainable means and processes for producing PMs. The sheer volume of research published over the last two decades or so detailing efforts to implement this pivotal switch (as well as changing corporate[152] and societal[1] postures on the subject) suggests that a positive tipping point is approaching. Many opportunities would appear to be emerging as a result. The broad distribution and ready accessibility of biomass means that biorefineries can be set up

almost anywhere, at relatively modest expense and close to the user/customer. This situation stands in stark contrast to the enormous expenses associated with locating and tapping petrochemical deposits as well as the transport costs (and attendant risks) associated with moving the raw and refined materials across often vast distances. The creation of biorefineries should also democratise the commodity chemicals and fuel supply chains and so reducing the geopolitical tensions that seem to attend the exploitation of petrochemicals.

The burgeoning push to establish biorefineries, especially integrated ones,[13] is likely to create exciting opportunities in chemical synthesis. Customised processes for the conversion of biomass into new PMs, which may be enzymatic and/or chemically-based, will continue to add to the repertoire of sustainably accessible (and logically accessed)[153, 154] small molecules available to the chemist and so creating new starting points for chemical synthesis.[72] This, in turn, is likely to create new products including, for example, bio-derived polymers, with a multitude of potential applications. In considering such possibilities, one rather prominent "gap" in the suite of biomass-derived 1°-PMs currently available is the very limited number of these that preserve the chirality inherent in the starting materials, *viz*. the cellulose, hemicellulose, lignin or chitin. Levoglucosenone (**22**) is a notable exception and the enthusiasm with which this compound has been explored as a starting point for chemical synthesis[73-75] suggests a likely high demand for new homochiral and biomass-derived PMs.

References

1. See https://unfccc.int/process-and-meetings/the-paris-agreement/the-paris-agreement (accessed 14/09/2020).
2. Olson, C.; Lenzmann, F. The social and economic consequences of the fossil fuel supply chain. *MRS Energy & Sustainability,* **2016**, *3*(1), 6.
3. Harrell, J.; Lewan, M. Sources of mummy bitumen in ancient Egypt and Palestine. *Archaeometry,* **2002**, *44*, 285-293.
4. See https://www.asahicarbon.co.jp/global_site/product/cb/manufacturing.html (accessed 13/9/2020).
5. See https://www.eia.gov/todayinenergy/detail.php?id=35672 (accessed 3/8/2023).
6. Corma, A.; Iborra, S.; Velty, A. Chemical Routes for the Transformation of Biomass into Chemicals. *Chemical Reviews,* **2007**, *107*(6), 2411-2502.
7. Fuels from Biomass. In *Biorefineries: For Biomass Upgrading Facilities*, Demirbas, A. Ed.; Springer London, **2010**, 33-73.
8. Sanderson, K. Lignocellulose: A chewy problem. *Nature,* **2011**, *474*(7352), S12-S14.
9. Tuck, C. O.; Pérez, E.; Horváth, I. T.; Sheldon, R. A.; Poliakoff, M. Valorization of biomass: deriving more value from waste. *Science,* **2012**, *337*(6095), 695-699.
10. Franssen, M. C. R.; Steunenberg, P.; Scott, E. L.; Zuilhof, H.; Sanders, J. P. M. Immobilised enzymes in biorenewables production. *Chemical Society Reviews,* **2013**, *42*(15), 6491-6533.
11. Besson, M.; Gallezot, P.; Pinel, C. Conversion of Biomass into Chemicals over Metal Catalysts. *Chemical Reviews,* **2014**, *114*(3), 1827-1870.
12. Straathof, A. J. Transformation of biomass into commodity chemicals using enzymes or cells. *Chemical Reviews,* **2014**, *114*(3), 1871-1908.
13. Sheldon, R. A. Green and sustainable manufacture of chemicals from biomass: state of the art. *Green Chemistry,* **2014**, *16*(3), 950-963.
14. Chen, X.; Yan, N. Novel Catalytic Systems to Convert Chitin and Lignin into Valuable Chemicals. *Catalysis Surveys from Asia,* **2014**, *18*(4), 164-176.
15. Singhvi, M. S.; Chaudhari, S.; Gokhale, D. V. Lignocellulose processing: a current challenge. *RSC Advances,* **2014**, *4*(16), 8271-8277.
16. Sheldon, R. A. Green chemistry, catalysis and valorization of waste biomass. *Journal of Molecular Catalysis,* **2016**, *422*, 3-12.
17. Fang, R.; Dhakshinamoorthy, A.; Li, Y.; Garcia, H. Metal organic frameworks for biomass conversion. *Chemical Society Reviews,* **2020**, *49*(11), 3638-3687.
18. Costa, J. R.; Tonon, R. V.; Cabral, L.; Gottschalk, L.; Pastrana, L.; Pintado, M. E. Valorization of Agricultural Lignocellulosic Plant Byproducts through Enzymatic and Enzyme-Assisted

Extraction of High-Value-Added Compounds: A Review. *ACS Sustainable Chemistry & Engineering,* **2020**, *8*(35), 13112-13125.

19. Ventura, M.; Marinas, A.; Domine, M. E. Catalytic Processes for Biomass-Derived Platform Molecules Valorisation. *Topics in Catalysis,* **2020**, *63*(9), 846-865.
20. A. Aden, J. B., J. Holladay, J. White. Top Value Added Chemicals from Biomass. Volume II – Results of Screening for Potential Candidates from Biorefinery Lignin. Laboratory, P. N. N., Ed.; Pacific Northwest National Laboratory: National Renewable Energy Laboratory, **2007**, 1-76.
21. Bozell, J. J.; Petersen, G. R. Technology development for the production of biobased products from biorefinery carbohydrates—the US Department of Energy's "Top 10" revisited. *Green Chemistry,* **2010**, *12*(4), 539-554.
22. Cherubini, F. The biorefinery concept: Using biomass instead of oil for producing energy and chemicals. *Energy Conversion and Management,* **2010**, *51*, 1412-1421.
23. Farmer, T. J.; Mascal, M. Platform Molecules. In *Introduction to Chemicals from Biomass*, 2015; 89-155.
24. Bomtempo, J.-V.; Chaves Alves, F.; de Almeida Oroski, F. Developing new platform chemicals: what is required for a new bio-based molecule to become a platform chemical in the bioeconomy? *Faraday Discussions,* **2017**, *202*, 213-225.
25. Wagemann, K.; Tippkötter, N. Biorefineries: A Short Introduction, *Advances in Biochemical Engineering and Biotechnology,* **2019**, *166*, 1-11.
26. J. R. Phillips, R. L. Huhnke, H. K. Atiyeh, Syngas Fermentation: A Microbial Conversion Process of Gaseous Substrates to Various Products, *Fermentation*, **2017**, *3*, 28.
27. Aristizábal-Marulanda, V.; Cardona Alzate, C. A. Methods for designing and assessing biorefineries: Review. *Biofuels, Bioproducts and Biorefining,* **2019**, *13*(3), 789-808.
28. Liu, Z.; Wang, K.; Chen, Y.; Tan, T.; Nielsen, J. Third-generation biorefineries as the means to produce fuels and chemicals from CO2. *Nature Catalysis,* **2020**, *3*(3), 274-288.
29. Bugg, T. D. H.; Williamson, J. J.; Rashid, G. M. M. Bacterial enzymes for lignin depolymerisation: new biocatalysts for generation of renewable chemicals from biomass, **2020**, 1879-0402.

30. Gérardy, R.; Debecker, D. A.-O.; Estager, J.; Luis, P.; Monbaliu, J. A.-O. Continuous Flow Upgrading of Selected C(2)-C(6) Platform Chemicals Derived from Biomass, *Current Opinion in Chemical Biology,* **2020**, *55*, 26-33.
31. Scott, E.; Peter F Fau - Sanders, J.; Sanders, J. Biomass in the manufacture of industrial products--the use of proteins and amino acids, *Applied Microbiology Biotechnology*, **2007**, *75(*4*)*, 751-762.
32. W. Wu, R. W. D. One-pot bioconversion of algae biomass into terpenes for advanced biofuels and bioproducts, *Algal Research,* **2016**, *17*, 316-320.
33. De Schouwer, F.; Claes, L.; Vandekerkhove, A.; Verduyckt, J.; De Vos, D. E. Protein-Rich Biomass Waste as a Resource for Future Biorefineries: State of the Art, Challenges, and Opportunities. *Chemistry Sustainable Chemistry* **2019**, *12*(7), 1272-1303.
34. See http://web.missouri.edu/ikerdj/papers/Nebraska-recycling.htm (accessed 15/9/2020).
35. See https://circulareconomy.europa.eu/platform/en /knowledge/el-dorado-chemical-recycling-state-play-and-policy-challenges (accessed 29/9/2020).
36. Tullo, A. *Chemical Engineering News* **2020**, *98*(29), 26-31.
37. Zhou, J.; Xia, W.; Wang, K.; Li, H.; Zhang, Q. Fuzzy Bi-Objective Closed-Loop Supply Chain Network Design Problem with Multiple Recovery Options, *Sustainability*, **2020**, 12.
38. Govindjee, J. W. The Photosynthetic Process. In: Singhal, G.S., Renger, G., Sopory, S.J., Irrgang, K.D., Govindjee (eds) Concepts in Photobiology. Springer, Dordrecht, **1999**.
39. Gierer, J. Chemistry of delignification. *Wood Science and Technology* **1985**, *19*(4), 289-312.
40. O. Sánchez, R. Sierra and C. J. Alméciga-Díaz, Delignification Process of Agro-Industrial Wastes an Alternative to Obtain Fermentable Carbohydrates for Producing Fuel. In *Alternative Fuel*, Maximino, M. Ed.; IntechOpen, **2011**, Ch. 6.
41. Heinze, T. Cellulose: Structure and Properties. In *Cellulose Chemistry and Properties: Fibers, Nanocelluloses and Advanced Materials*, Rojas, O. J. Ed.; Springer International Publishing, 2016; 1-52.
42. Yao, Y.; Wang, H.; An Overview on Chemical Modification of Cellulose, *Materials Reports,* **2018**, *32*, 3478-3488.
43. Abushammala, H.; Mao, J. A Review of the Surface Modification of Cellulose and Nanocellulose Using Aliphatic and Aromatic Mono- and Di-Isocyanates. In *Molecules*, **2019**, *24*.
44. Thomas, B.; Raj, M. C.; B, A. K.; H, R. M.; Joy, J.; Moores, A. A.-O. X.; Drisko, G. A.-O.; Sanchez, C. A.-O. Nanocellulose, a Versatile Green Platform: From Biosources to Materials and Their Applications, **2018**, *Chemical Reviews, 118(*24*)*.
45. Klemm, D.; Cranston, E. D.; Fischer, D.; Gama, M.; Kedzior, S. A.; Kralisch, D.; Kramer, F.; Kondo, T.; Lindström, T.; Nietzsche, S.; et al. Nanocellulose as a natural source for groundbreaking applications in materials science: Today's state. *Materials Today* **2018**, *21*(7),

720-748.46. Aguiar, J.; Bondancia, T.; Claro, P.; Mattoso, L.; Farinas, C.; Marconcini, J. M. Enzymatic Deconstruction of Sugarcane Bagasse and Straw to Obtain Cellulose Nanomaterials. *ACS Sustainable Chemistry & Engineering* **2020**, DOI: 10.1021/acssuschemeng.9b06806.

47. Dufresne, A.; Preparation and Properties of Cellulose Nanomaterials. *Paper and Biomaterials,* **2020**, *5*(3), 1-13.
48. See https://www.marketsandmarkets.com/Market-Reports/cellulose-acetate-market-1193.html (accessed 19/9/2020).
49. See https://www.sustainabilityconsult.com/news/404-research-shows-versatility-of-bio-based-platform-chemical-as-building-block-for-drug-discovery (accessed 20/9/2020).
50. Yamazaki, H.; Boyd, C. S. Activation of Rayon/Polyester Cloth for Protein Immobilization. In *Immobilization of Enzymes and Cells*, Bickerstaff, G. F. Ed.; Humana Press, **1997**, 77-81.
51. I. Sebti, F. H.-P. a. V. C. *Journal of Agricultural and Food Chemistry,* **2002**, *20*, 4290-4294.
52. Crépy, L.; Chaveriat L Fau - Banoub, J.; Banoub J Fau - Martin, P.; Martin P Fau - Joly, N.; Joly, N. Synthesis of cellulose fatty esters as plastics-influence of the degree of substitution and the fatty chain length on mechanical properties, *Chemistry Sustainable Chemistry,* **2009**, *2(2)*, 165-170.
53. T. Kulomaa, J. M., P. Karhunen, M. Heikkilä, J. Fiskari and I. Kilpeläinen. *RSC Advances,* **2015**, *5*, 80702-80708.
54. Willberg-Keyriläinen, P.; Vartiainen, J.; Harlin, A.; Ropponen, J. The effect of side-chain length of cellulose fatty acid esters on their thermal, barrier and mechanical properties. *Cellulose,* **2017**, *24*(2), 505-517.
55. Heinze, T.; El Seoud, O. A.; Koschella, A. Etherification of Cellulose. In *Cellulose Derivatives: Synthesis, Structure, and Properties*, Heinze, T., El Seoud, O. A., Koschella, A. Eds.; Springer International Publishing, **2018**, 429-477.
56. Mika, L. A.-O.; Cséfalvay, E.; Németh, Á. Catalytic Conversion of Carbohydrates to Initial Platform Chemicals: Chemistry and Sustainability, *Chemistry Reviews,* **2018**, *118(2)*, 505-613.
57. K. Guo, Q. G., J. Xu, W. Tan. *Journal of Bioresources and Bioproducts,* **2019**, *4*, 202-213.
58. See https://sciencemeetsfood.org/food-vs-fuel/ (accessed 21/9/2020).
59. Daniell, J.; Köpke, M.; Simpson, S. D. Commercial Biomass Syngas Fermentation. In *Energies*, **2012**, *5*, 5372-5417.
60. Gruber, H.; Groß, P.; Rauch, R.; Reichhold, A.; Zweiler, R.; Aichernig, C.; Müller, S.; Ataimisch, N.; Hofbauer, H. Fischer-Tropsch products from biomass-derived syngas and renewable hydrogen. *Biomass Conversion and Biorefinery,* **2021**, *11*(6), 2281-2292.
61. Xu, G. C.; Ding, J. C.; Han, R. Z.; Dong, J. J.; Ni, Y. Enhancing cellulose accessibility of corn stover by deep eutectic solvent pretreatment for butanol fermentation. *Bioresources Technology,* **2016**, *203*, 364-369.

62. Pham, T. T.; Chen, X.; Söhnel, T.; Yan, N.; Sperry, J. Haber-independent, diversity-oriented synthesis of nitrogen compounds from biorenewable chitin. *Green Chemistry* **2020**, *22* (6), 1978-1984.

63. Salleh, M. S. M.; Ibrahim, M. A.-O.; Roslan, A. M.; Abd-Aziz, S. Improved Biobutanol Production in 2-L Simultaneous Saccharification and Fermentation with Delayed Yeast Extract Feeding and in-situ Recovery, *Science Reports,* **2019**, *9(*1*)*, 7443.

64. Mäki-Arvela, P.; Simakova Il Fau - Salmi, T.; Salmi T Fau - Murzin, D. Y.; Murzin, D. Y. Production of lactic acid/lactates from biomass and their catalytic transformations to commodities, *Chemical Reviews*, **2014***, 114(*3*)*, 1909-1971.

65. Singhvi, M.; Gokhale, D. Biomass to biodegradable polymer (PLA). *RSC Advances,* **2013**, *3*(33), 13558-13568.

66. van Putten, R. J.; van der Waal Jc Fau - de Jong, E.; de Jong E Fau - Rasrendra, C. B.; Rasrendra Cb Fau - Heeres, H. J.; Heeres Hj Fau - de Vries, J. G.; de Vries, J. G. Hydroxymethylfurfural, a versatile platform chemical made from renewable resources, *Chemical Reviews*, **2013**, *113(*3*)*, 1499-1597.

67. Xia, H.; Xu, S.; Hu, H.; An, J.; Li, C. Efficient conversion of 5-hydroxymethylfurfural to high-value chemicals by chemo- and bio-catalysis. *RSC Advances,* **2018**, *8*(54), 30875-30886.

68. Pfersich, J.; Arauzo, P. J.; Lucian, M.; Modugno, P.; Titirici, M.-M.; Fiori, L.; Kruse, A. Hydrothermal Conversion of Spent Sugar Beets into High-Value Platform Molecules. In *Molecules*, **2020**, *25*.

69. S. W. Breeden, J. H. C., T. J. Farmer, D. J. Macquarrie, J. S. Meimoun, Y. Nonne and J. E. S. J. Reid. **2013**, *15*, 72-75.

70. Williams, C. L.; Chang, C.-C.; Do, P.; Nikbin, N.; Caratzoulas, S.; Vlachos, D. G.; Lobo, R. F.; Fan, W.; Dauenhauer, P. J. Cycloaddition of Biomass-Derived Furans for Catalytic Production of Renewable p-Xylene. *ACS Catalysis,* **2012**, *2*(6), 935-939.

71. Pacheco, J. J.; Davis, M. E. Synthesis of terephthalic acid via Diels-Alder reactions with ethylene and oxidized variants of 5-hydroxymethylfurfural. *Proceedings of the National Academy of Sciences,* **2014**, *111*(23), 8363-8367.

72. Volanti, M.; Cespi, D.; Passarini, F.; Neri, E.; Cavani, F.; Mizsey, P.; Fozer, D. Terephthalic acid from renewable sources: early-stage sustainability analysis of a bio-PET precursor. *Green Chemistry,* **2019**, *21*(4), 885-896.

73. Kudo, S.; Goto, N.; Sperry, J.; Norinaga, K.; Hayashi, J.-i. Production of Levoglucosenone and Dihydrolevoglucosenone by Catalytic Reforming of Volatiles from Cellulose Pyrolysis Using Supported Ionic Liquid Phase. *ACS Sustainable Chemistry & Engineering,* **2017**, *5*(1), 1132-1140.

74. Comba, M. B.; Tsai, Y.-h.; Sarotti, A. M.; Mangione, M. I.; Suárez, A. G.; Spanevello, R. A. Levoglucosenone and Its New Applications: Valorization of Cellulose Residues. *European Journal of Organic Chemistry,* **2018**, *2018*(5), 590-604.

75. Camp, J. E. Bio-available Solvent Cyrene: Synthesis, Derivatization, and Applications. *Chemistry Sustainable Chemistry,* **2018**, *11*(18), 3048-3055.

76. See https://www.circagroup.com.au/the-company (accessed 2/8/2023).

77. Greatrex, B. A.-O.; Meisner, J. A.-O.; Glover, S. A.; Raverty, W. Support for a Dioxyallyl Cation in the Mechanism Leading to (-)-Levoglucosenone, *Journal of Organic Chemistry,* **2017**, *82(*23*)*, 12294-12299.

78. Ma, X.; Anderson, N.; White, L. V.; Bae, S.; Raverty, W.; Willis, A. C.; Banwell, M. G. The Conversion of Levoglucosenone into Isolevoglucosenone. *Australian Journal of Chemistry,* **2015**, *68* (4), 593-599.

79. Ma, X.; Liu, X.; Yates, P.; Raverty, W.; Banwell, M. G.; Ma, C.; Willis, A. C.; Carr, P. D. Manipulating the enone moiety of levoglucosenone: 1,3-Transposition reactions including ones leading to isolevoglucosenone, *Tetrahedron,* **2018**, *74* (38), 5000-5011.

80. Liu, X.; Carr, P.; Gardiner, M. G.; Banwell, M. G.; Elbanna, A. H.; Khalil, Z. G.; Capon, R. J. Levoglucosenone and Its Pseudoenantiomer iso-Levoglucosenone as Scaffolds for Drug Discovery and Development. *ACS Omega,* **2020**, *5*(23), 13926-13939.

81. Banwell, M. G.; Liu, X.; Connal, L. A.; Gardiner, M. G. Synthesis of Functionally and Stereochemically Diverse Polymers via Ring-Opening Metathesis Polymerization of Derivatives of the Biomass-Derived Platform Molecule Levoglucosenone Produced at Industrial Scale. *Macromolecules,* **2020**, *53*(13), 5308-5314.

82. Fadlallah, S.; Peru, A. A. M.; Flourat, A.; Allais, F. A straightforward access to functionalizable polymers through ring-opening metathesis polymerization of levoglucosenone-derived monomers. *European Polymer Journal,* **2020**, *138*, 109980.

83. T. Debsharma, F. N. B., A. Laschewsky, H. Schlaad. *Angewandte Chemie International Edition*, **2019**, *131*, 6790-6793.

84. Farhat, W.; Venditti, R. A.; Hubbe, M.; Taha, M.; Becquart, F.; Ayoub, A. A Review of Water-Resistant Hemicellulose-Based Materials: Processing and Applications. *Chemistry Sustainable Chemistry*, **2017**, *10(2)*, 305-323.

85. Fu, G.-Q.; Hu, Y.-J.; Bian, J.; Li, M.-F.; Peng, F.; Sun, R.-C. Isolation, Purification, and Potential Applications of Xylan. In *Production of Materials from Sustainable Biomass Resources*, Fang, Z., Smith, J. R. L., Tian, X.-F. Eds.; Springer Singapore, **2019**, 3-35.

86. Cartaxo da Costa Urtiga, S.; Rodrigues Marcelino, H.; Sócrates Tabosa do Egito, E.; Eleamen Oliveira, E. Xylan in drug delivery: A review of its engineered structures and biomedical applications. *European Journal of Pharmaceutics and Biopharmaceutics*, **2020**, *151*, 199-208.

87. Li, X.; Jia, P.; Wang, T. Furfural: A Promising Platform Compound for Sustainable Production of C4 and C5 Chemicals. *ACS Catalysis* **2016**, *6* (11), 7621-7640.

88. See http://www.genencor.com/uploads/tx_tcdaniscofiles/GENC10053_BioIsoprene_ Backgrounderprt.pdf (accessed 21/10/2020).

89. Kuznetsov, A.; Kumar, G.; Ardagh, M. A.; Tsapatsis, M.; Zhang, Q.; Dauenhauer, P. J. On the Economics and Process Design of Renewable Butadiene from Biomass-Derived Furfural. *ACS Sustainable Chemistry & Engineering,* **2020**, *8*(8), 3273-3282.

90. Climent, M. J.; Corma, A.; Iborra, S. Conversion of biomass platform molecules into fuel additives and liquid hydrocarbon fuels. *Green Chemistry,* **2014**, *16*(2), 516-547.

91. Zakzeski, J.; Bruijnincx, P. C. A.; Jongerius, A. L.; Weckhuysen, B. M. The Catalytic Valorization of Lignin for the Production of Renewable Chemicals. *Chemical Reviews,* **2010**, *110*(6), 3552-3599.

92. Upton, B. M.; Kasko, A. M. Strategies for the Conversion of Lignin to High-Value Polymeric Materials: Review and Perspective. *Chemical Reviews,* **2016**, *116*(4), 2275-2306.

93. Liu, W. C., Q. Xia, B. Guo, Q. Wang, S. Liu, Y. Liu, J. Li,; Yu, H. *Chemistry Sustainable Chemistry,* **2017**, *10*, 1692-1700.

94. Gordobil, O.; Herrera, R.; Yahyaoui, M.; İlk, S.; Kaya, M.; Labidi, J. Potential use of kraft and organosolv lignins as a natural additive for healthcare products. *RSC Advances,* **2018**, *8*(43), 24525-24533.

95. Schutyser, W.; Renders, T.; Van den Bosch, S.; Koelewijn, S. F.; Beckham, G. T.; Sels, B. F. Chemicals from lignin: an interplay of lignocellulose fractionation, depolymerisation, and upgrading. *Chemical Society Reviews.* **2018**, *47*(3), 852-908.

96. Sun, Z.; Fridrich, B.; de Santi, A.; Elangovan, S.; Barta, K.; Bright Side of Lignin Depolymerization: Toward New Platform Chemicals, *Chemical Reviews.* **2018**, *118*(2), 614-678.

97. Zhang, G. G.; Zhou, X. X.; Liang, K.; Guo, B. C.; Li, X. L.; Wang, Z.; Zhang, L. Q. Mechanically Robust and Recyclable EPDM Rubber Composites by a Green Cross-Linking Strategy. *ACS Sustainable Chemistry & Engineering.* **2019**, *7*(13), 11712-11720

98. C. Cheng, J. T., J. A. Barrett, D. Shen, M. M. Abu-Omar and P. C. Ford. *ACS Sustainable Chemistry & Engineering,* **2020**, *8*, 1023-1030.

99. Fang, Z.; Weisenberger, M. C.; Meier, M. S. Utilization of Lignin-Derived Small Molecules: Epoxy Polymers from Lignin Oxidation Products. *ACS Applied Bio Materials,* **2020**, *3*(2), 881-890.

100. del Río, J. C.; Rencoret, J.; Gutiérrez, A.; Elder, T.; Kim, H.; Ralph, J. Lignin Monomers from beyond the Canonical Monolignol Biosynthetic Pathway: Another Brick in the Wall. *ACS Sustainable Chemistry & Engineering,* **2020**, *8*(13), 4997-5012.

101. Giannì, P.; Lange, H.; Crestini, C. Functionalized Organosolv Lignins Suitable for Modifications of Hard Surfaces. *ACS Sustainable Chemistry & Engineering,* **2020**, *8*(20), 7628-7638.

102. Trubetskaya, A.; Lange, H.; Wittgens, B.; Brunsvik, A.; Crestini, C.; Rova, U.; Christakopoulos, P.; Leahy, J. J.; Matsakas, L. Structural and Thermal Characterization of Novel Organosolv Lignins from Wood and Herbaceous Sources. In *Processes*, **2020**, Vol. 8.

103. Korányi, T. I.; Fridrich, B.; Pineda, A.; Barta, K. Development of 'Lignin-First' Approaches for the Valorization of Lignocellulosic Biomass. In *Molecules*, **2020**, Vol. 25.

104. Gigli, M.; Crestini, C. Fractionation of industrial lignins: opportunities and challenges. *Green Chemistry,* **2020**, *22*(15), 4722-4746.

105. Garedew, M.; Lin, F.; Song, B.; DeWinter, T. M.; Jackson, J. E.; Saffron, C. M.; Lam, C. H.; Anastas, P. T. Greener Routes to Biomass Waste Valorization: Lignin Transformation Through Electrocatalysis for Renewable Chemicals and Fuels Production. *Chemistry Sustainable Chemistry,* **2020**, *13*(17), 4214-4237.

106. Lahive, C. W.; Kamer, P. C. J.; Lancefield, C. S.; Deuss, P. J. An Introduction to Model Compounds of Lignin Linking Motifs; Synthesis and Selection Considerations for Reactivity Studies. *Chemistry Sustainable Chemistry,* **2020**, *13*(17), 4238-4265.

107. Xu, J.; Li, C.; Dai, L.; Xu, C.; Zhong, Y.; Yu, F.; Si, C. Biomass Fractionation and Lignin Fractionation towards Lignin Valorization. *Chemistry Sustainable Chemistry,* **2020**, *13*(17), 4284-4295.

108. Liu, X.; Bouxin, F. P.; Fan, J.; Budarin, V. L.; Hu, C.; Clark, J. H. Recent Advances in the Catalytic Depolymerization of Lignin towards Phenolic Chemicals: A Review. *Chemistry Sustainable Chemistry,* **2020**, *13*(17), 4296-4317.

109. Shen, X.; Xin, Y.; Liu, H.; Han, B. Product-oriented Direct Cleavage of Chemical Linkages in Lignin. *Chemistry Sustainable Chemistry,* **2020**, *13*(17), 4367-4381.

110. Abdelaziz, O. Y.; Hulteberg, C. P. Lignin Depolymerization under Continuous-Flow Conditions: Highlights of Recent Developments. *Chemistry Sustainable Chemistry,* **2020**, *13*(17), 4382-4384.

111. Sun, R.-C. Lignin Source and Structural Characterization. *Chemistry Sustainable Chemistry,* **2020**, *13*(17), 4385-4393.

112. Tanis, S. B. K. a. M. H. *Biomass Conversion and Biorefinery,* **2020**.

113. Zhao, C.; Hu, Z.; Shi, L.; Wang, C.; Yue, F.; Li, S.; Zhang, H.; Lu, F. Profiling of the formation of lignin-derived monomers and dimers from Eucalyptus alkali lignin. *Green Chemistry,* **2020**, *22*(21), 7366-7375.

114. Yang, C.; Kärkäs, M. A.-O.; Magallanes, G. A.-O.; Chan, K.; Stephenson, C. A.-O. Organocatalytic Approach to Photochemical Lignin Fragmentation. *Organic Letters,* **2020**, *22*(20), 8082-8085.

115. Macala, G. S.; Matson Td Fau - Johnson, C. L.; Johnson Cl Fau - Lewis, R. S.; Lewis Rs Fau - Iretskii, A. V.; Iretskii Av Fau - Ford, P. C.; Ford, P. C. Hydrogen transfer from supercritical methanol over a solid base catalyst: a model for lignin depolymerization. *Chemistry Sustainable Chemistry,* **2009**, *2*(3), 215-217.

116. Gao, F.; Webb, J. D.; Hartwig, J. F. Chemo- and Regioselective Hydrogenolysis of Diaryl Ether C−O Bonds by a Robust Heterogeneous Ni/C Catalyst: Applications to the Cleavage of Complex Lignin-Related Fragments. *Angewandte Chemie International Edition,* **2016**, *55*(4), 1474-1478.

117. Dabral, S.; Mottweiler, J.; Rinesch, T.; Bolm, C. Base-catalysed cleavage of lignin β-O-4 model compounds in dimethyl carbonate. *Green Chemistry,* **2015**, *17*(11), 4908-4912.

118. F. Gao, J. D. W., H. Sorek, D. E. Wemmer and J. F. Hartwig. *ACS Catalysis* **2016**, *6*, 7385-7392.

119. Y. Li, S. D. K., B. Demir, H. Kim, J. Luterbacher, J. A. Dumesic, S. S. Stahl, J. Ralph. *Chemistry Sustainable Chemistry,* **2020**, *13*, 4487-4494.

120. Espro, C.; Gumina, B.; Szumelda, T.; Paone, E.; Mauriello, F. Catalytic Transfer Hydrogenolysis as an Effective Tool for the Reductive Upgrading of Cellulose, Hemicellulose, Lignin, and Their Derived Molecules. In *Catalysts*, **2018**, Vol. 8.

121. Suzuki, S.; Umezawa, T. Biosynthesis of lignans and norlignans. *Journal of Wood Science,* **2007**, *53*(4), 273-284.

122. Teponno, R. B.; Kusari, S.; Spiteller, M. Recent advances in research on lignans and neolignans. *Natural Product Reports,* **2016**, *33*(9), 1044-1092.

123. Buckler, J. N.; Banwell, M. G.; Kordbacheh, F.; Parish, C. R.; Santiago, F. S.; Khachigian, L. M. Developing Neolignans as Proangiogenic Agents: Stereoselective Total Syntheses and Preliminary Biological Evaluations of the Four Guaiacylglycerol 8-O-4′-Coniferyl Ethers. *ACS Omega,* **2017**, *2*(10), 7375-7388.

124. Barker, D. Lignans. In *Molecules*, **2019**, *24*(7), 1424.

125. Frezza, C.; Venditti, A.; Toniolo, C.; De Vita, D.; Franceschin, M.; Ventrone, A.; Tomassini, L.; Foddai, S.; Guiso, M.; Nicoletti, M.; et al. Nor-Lignans: Occurrence in Plants and Biological Activities—A Review. *Molecules*, **2020**, *25*(1), 197.

126. Touré, A.; Xueming, X. Flaxseed Lignans: Source, Biosynthesis, Metabolism, Antioxidant Activity, Bio-Active Components, and Health Benefits. *Comprehensive Reviews in Food Science and Food Safety,* **2010**, *9*(3), 261-269.

127. Orsat, S. M. N. a. V. *Food Analytical Methods,* **2012**, *5*, 551-563.

128. Hosseinian, F. S.; Muir, A. D.; Westcott, N. D.; Krol, E. S. AAPH-mediated antioxidant reactions of secoisolariciresinol and SDG. *Organic & Biomolecular Chemistry,* **2007**, *5*(4), 644-654.

129. P. Lan, M. D., Y. Teng, M. G. Banwell, H. Nie, M. J. T. Reaney and Y. Wang. *Journal of Agricultural and Food Chemistry,* **2019**, *67*, 14152-14159.

130. Belalia, R.; Grelier, S.; Benaissa, M.; Coma, V. New bioactive biomaterials based on quaternized chitosan, *Journal of Agricultural and Food Chemistry,* **2008**, *56*(5), 1582-1588.

131. Elieh-Ali-Komi, D.; Hamblin, M. R. Chitin and Chitosan: Production and Application of Versatile Biomedical Nanomaterials. *International Journal of Advanced Research,* **2016**, *4*(3), 411-427.

132. Komabayashi, M.; Nokami, T.; Jopp, S. From Chitin to CHILs: First Glucosamine based Ionic Liquids. *Asian Journal of Organic Chemistry,* **2020**, *9*(12), 2092-2094.

133. Finney, A. R. Y. a. N. S. *Journal of Organic Chemistry,* **2005**, *70*, 1269-1275.

134. Einbu, A.; Vårum, K. M. Depolymerization and de-N-acetylation of chitin oligomers in hydrochloric acid. *Biomacromolecules,* **2007**, *8*(1), 309-314.

135. Ramos, R. A. A. M. V. S. a. V. *Enzymatic Depolymerization of Chitins and Chitosans*; Humana Press Inc., **1999**.

136. Yabushita, M.; Kobayashi, H.; Kuroki, K.; Ito, S.; Fukuoka, A. Catalytic Depolymerization of Chitin with Retention of N-Acetyl Group. *Chemistry Sustainable Chemistry,* **2015**, *8*(22), 3760-3763.

137. Ma, X.; Gözaydın, G.; Yang, H.; Ning, W.; Han, X.; Poon, N. Y.; Liang, H.; Yan, N.; Zhou, K. Upcycling chitin-containing waste into organonitrogen chemicals via an integrated process. *P Proceedings of the National Academy of Sciences of the United States of America,* **2020**, *117*(14), 7719-7728.

138. Nikahd, M.; Mikusek, J.; Banwell, M. G.; Yu, L.-J.; Coote, M. L.; Gardiner, M. G. Further, Small-Molecule Pyrolysis Products Derived from Chitin. *Australian Journal of Chemistry,* **2020**, *73*(12), 1187-1196.

139. Nikahd, M.; Mikusek, J.; Yu, L.-J.; Coote, M. L.; Banwell, M. G.; Ma, C.; Gardiner, M. G. Exploiting Chitin as a Source of Biologically Fixed Nitrogen: Formation and Full Characterization of Small-Molecule Hetero- and Carbocyclic Pyrolysis Products. *The Journal of Organic Chemistry* **2020**, *85* (7), 4583-4593.
140. Yan, N.; Chen, X. Sustainability: Don't waste seafood waste. *Nature,* **2015**, *524*(7564), 155-157.
141. Chen, X.; Yang, H.; Yan, N. Shell Biorefinery: Dream or Reality? *Chemistry – A European Journal,* **2016**, *22*(38), 13402-13421.
142. C. Liu, H. Z., R. Xiao and S. Wu. *Carbohydrate Polymers,* **2017**, *156*, 118-124.
143. Hülsey, M. J. Shell biorefinery: A comprehensive introduction. *Green Energy & Environment,* **2018**, *3*(4), 318-327.
144. Yang, H.; Gözaydın, G.; Nasaruddin, R. R.; Har, J. R. G.; Chen, X.; Wang, X.; Yan, N. Toward the Shell Biorefinery: Processing Crustacean Shell Waste Using Hot Water and Carbonic Acid. *ACS Sustainable Chemistry & Engineering,* **2019**, *7* (5), 5532-5542.
145. Dai, J.; Li, F.; Fu, X. Towards Shell Biorefinery: Advances in Chemical-Catalytic Conversion of Chitin Biomass to Organonitrogen Chemicals. *Chemistry Sustainable Chemistry,* **2020**, *13*(24), 6498-6508.
146. Bogart, J. W.; Bowers, A. A. Dehydroamino acids: chemical multi-tools for late-stage diversification. *Organic & Biomolecular Chemistry,* **2019**, *17* (15), 3653-3669.
147. Padovan, D.; Kobayashi, H.; Fukuoka, A. Facile Preparation of 3-Acetamido-5-acetylfuran from N-Acetyl-d-glucosamine by using Commercially Available Aluminum Salts. *Chemistry Sustainable Chemistry,* **2020**, *13*(14), 3594-3598.
148. T. T. Pham, X. C., N.; Yan, J. A. S. *Monatshefte für Chemie*, **2018**, *149*, 857-861.
149. Song, S.; Fung Kin Yuen, V.; Di, L.; Sun, Q.; Zhou, K.; Yan, N. Integrating Biomass into the Organonitrogen Chemical Supply Chain: Production of Pyrrole and d-Proline from Furfural. *Angewandte Chemie International Edition,* **2020**, *59*(45), 19846-19850.
150. See https://www.drugfuture.com/chemdata/1H-Pyrrole.html (accessed 30/9/2020).
151. Gao, X.; Chen, X.; Zhang, J.; Guo, W.; Jin, F.; Yan, N. Transformation of Chitin and Waste Shrimp Shells into Acetic Acid and Pyrrole. *ACS Sustainable Chemistry & Engineering,* **2016**, *4*(7), 3912-3920.
152. See https://www.bp.com/en/global/corporate/sustainability.html (accessed 27/9/2020).
153. Shanks, B. H.; Keeling, P. L. Bioprivileged molecules: creating value from biomass. *Green Chemistry,* **2017**, *19*(14), 3177-3185.

154. Broadbelt, B. H. S. a. L. J. *Chemistry Sustainable Chemistry,* **2019**, *12*, 2970-2975

155. Takkellapati, S.; Li, T.; Gonzalez, M. A. An Overview of Biorefinery Derived Platform Chemicals from a Cellulose and Hemicellulose Biorefinery. *Clean Technologies and Environmental Policy,* **2018**, *20*(7), 1615-1630.

Chapter Three

Simple and Modestly Scalable Synthesis of *iso*-Cyrene from Levoglucosenone and Its Comparison to the Bio-Based and Polar Aprotic Solvent Cyrene®

Xin Liu, Brett Pollard, Martin G. Banwell, Li-Juan Yu, Michelle L. Coote, Michael G. Gardiner, Barbara M. A. van Vugt-Lussenburg, Bart van der Burg, Fabien L. Grasset, Elisabeth Campillo, James Sherwood, Fergal Byrne and Thomas J. Farmer

Aust. J. Chem. **2022**, ***75***(*5*), 331-344

Australian National University

Statement of Contribution

This thesis is submitted as a Thesis by Compilation in accordance with https://policies.anu.edu.au/ppl/document/ANUP_003405

I declare that the research presented in this Thesis represents original work that I carried out during my candidature at the Australian National University, except for contributions to multi-author papers incorporated in the Thesis where my contributions are specified in this Statement of Contribution.

Title: Simple and modestly scalable synthesis of *iso*-Cyrene from levoglucosenone and its comparison to the bio-derived and polar aprotic solvent Cyrene®

Authors: Xin Liu, Brett Pollard, Martin G. Banwell, Li-Juan Yu, Michelle L. Coote, Michael G. Gardiner, Barbara M.A. van Vugt-Lussenburg, Bart van der Burg, Fabien L. Grasset, Elisabeth Campillo, James Sherwood, Fergal P. Byrne, Thomas J. Farmer.

Publication outlet: Australian Journal of Chemistry, **2022**, *75*(5), 331-344.

Current status of paper: Published

Contribution to paper: This is a full paper and the candidate carried out half of the experimental work reported within it. In addition, the candidate collated and formatted all of the spectral data presented in the Supporting Information document. The candidate also wrote the entirety of the Experimental Section and conducted relevant literature surveys. A preliminary outline was generated by the candidate and thereafter the body of the paper was written by Professor Martin Banwell and edited by the candidate.

Senior author or collaborating authors endorsement: M. G. Banwell

BRETT L POLLARD		21/8/2023
Candidate – Print Name	Signature	Date

Endorsed

Luke Connal		21/8/23
Primary Supervisor – Print Name	Signature	Date
Mark Humphrey	Mark Humphrey	22 August 2023
Delegated Authority – Print Name	Signature	Date

Foreword

The focus of this thesis is the valorisation of biomass-derived platform molecules, principally, levoglucosenone (**1**). In this chapter, I focus on expanding the utility of levoglucosenone derivatives as renewable, non-toxic solvents. Levoglucosenone, which is the precursor to the green solvent Cyrene® (**2**), has been converted, at multi-gram scale, into its pseudo-enantiomer (*iso*-LGO, **3**) and then reduced to *iso*-Cyrene (**4**). A less effective synthesis of this last compound from D-glucose is also described. Various physicochemical as well as certain toxicological properties of compound **4** are reported and compared to those established for the now commercially available Cyrene® (**2**). Such studies reveal that there are significant enough differences in the properties of the sustainably-derived Cyrene® (**2**) and isomer **4** (*iso*-Cyrene) to suggest they will exert complementary effects as solvents in a range of settings. This chapter was published in the July 2022 edition of the Australian Journal of Chemistry, of which I am equal first author. My contribution to the manuscript includes the design of synthetic protocols, purifications, characterisation of resulting materials, data analysis, as well as preparing and revising the manuscript and figures (overall 50%). The published version of the manuscript is presented here. Xin Liu contributed to the synthesis and characterisation of materials, Martin G. Banwell contributed to the synthetic protocol design, data analysis and project design, as well as preparing and revising the manuscript and figures. Li-Juan Yu and Michelle L. Coote performed computational studies and data analysis. Michael G. Gardiner contributed through spectroscopic analysis. Barbara M. A. van Vugt-Lussenburg and Bart van der Burg contributed biological testing. James Sherwood, Fergal P. Byrne and Thomas J. Farmer further contributed to characterisation of the product.

Introduction

Organic solvents represent a major proportion of the chemicals currently derived from the petroleum industry. In order to achieve more sustainable manufacturing regimes, there is an increasing interest in identifying and establishing routes to bio-derived solvents.[1] Arguably, the most recent and notable development in this area has been the high- volume, pyrolytic conversion of acid-treated cellulose into the small molecule levoglucosenone (**1**) (**Fig. 1**) and its reduction to dihydro-derivative **2**.[2–4] The latter compound is now marketed as Cyrene®,[5] a bio-derived solvent that displays a range of useful properties and such that it is touted as a replacement for the widely-deployed and petroleum- derived *N*-methylpyrrolidine (NMP). This is because, *inter alia*, NMP displays reproductive toxicity[2] while Cyrene® has tested negative for such properties as well as mutagenicities and is, additionally, almost completely non-ecotoxic (LD50 > 2000 mg/L).[6]

Our ongoing interest in exploring and expanding the chemical utility of LGO (**1**),[7,8] which can now be regarded as an abundant fine chemical, promoted us to refine our earlier route from this compound to its pseudo-enantiomer *iso*-LGO (**3**) so as to produce the latter compound on a multi-gram scale and then reduce this to form *iso*-Cyrene (**4**). Such an outcome would allow for the evaluation of the solvent properties of ketone **4**, a compound that has received little attention experimentally. Indeed, it only appears to have been prepared on two previous occasions,[9,10] the first being in the 1970s[9a] and whereby a *β*,D-*arabino*-hexopyranose derivative was converted into compound **4** over multiple steps. The second synthesis was reported[10] in 2018 and involved the reduction of *iso*-LGO (**3**) that had been generated by a protocol closely related to the one we described[8] in 2018. In each case *iso*-Cyrene was obtained in sub-gram quantities.

While, in various respects, the solvent properties of Cyrene® and *iso*-Cyrene are expected to be similar,[3] the pseudo-enantiomeric relationship between them might ultimately be the most significant difference that allows their complementary use in facilitating/enhancing enantioselection in certain organic transformations or in the fractional crystallisation (resolution) of racemic compounds. In a related vein, it could also serve as a chiral auxiliary and (perhaps) act in a complementary fashion to Cyrene®.[11] The presence of the internal and inductively electron-withdrawing acetal residue adjacent to the ketone carbonyl within Cyrene® as well as possibilities for intramolecular hydrogen bonding[9a] creates a capacity to form the corresponding hydrate,[9a,12] a feature that has been used to 'tune' its solvent properties.[12] Given the more remote relationship between the equivalent residues within *iso*-Cyrene (**4**), hydrate formation should be a less significant process in this case,[9] a feature that may prove advantageous in some instances. Such considerations provided the motivation for the study detailed herein.

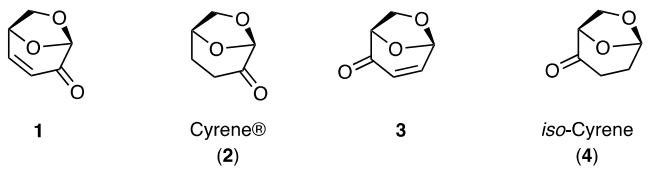

Figure 1: The structures of the bio-derived platform molecule levoglucosenone (**1**), its dihydro-derivative Cyrene® (**2**) and their isomeric congeners **3** and **4**.

Results and Discussions

Synthetic Studies

The synthetic sequence used to accumulate *iso*-Cyrene at a 10 g scale from LGO (**1**) is shown in **Scheme 1** and was informed by our earlier studies. In particular, the necessary 1,3-carbonyl transposition still exploited the operationally simple and triethylamine-catalysed conjugate

addition of water to LGO and thereby forming the previously reported[8,13,14] hydroxyketone **5**, which was obtained in 72% yield as a clear, colourless oil. The high α-face diastereoselectivity of this process is as expected and largely determined by the steric demands of the 1,6-anhydro-type bridge occupying the β-face of 2*H*-pyran-3(6*H*)-one core of the substrate. Accompanying product **5** were small amounts (0.5%) of the chromatographically separable and previously reported[15] dimeric compound **6**, the structure of which was confirmed by single crystal X-ray analysis (see the Experimental and Supplementary Material for details). Compound **6** is presumed to arise through the participation of the starting enone **1** in a triethylamine-catalysed intermolecular Rauhut–Currier or vinylogous Morita–Baylis–Hillman reaction.[16] Reductive amination of ketone **5** was accomplished using dimethylamine and hydrogen in the presence of 10% Pd on C and afforded a 1:3 mixture of the epimeric forms of amine **7**. A range of reagents was explored for the purposes of converting the hydroxyl group in this last compound into the β-amino-ketone **8** but the only effective oxidant, among dozens tested, proved to be the Swern reagent.[17] As a consequence, when the relevant conditions were employed, a mixture of the target ketone **8**, the oxidation/elimination product *iso*-LGO (**3**) and the sulfide **9** was obtained. We assume that the last product, which could be isolated in pure form and 13% yield by conventional chromatographic techniques, arises through initial (and diastereofacially selective) conjugate addition of dimethyl sulfide (the by-product of the Swern oxidation)[17]

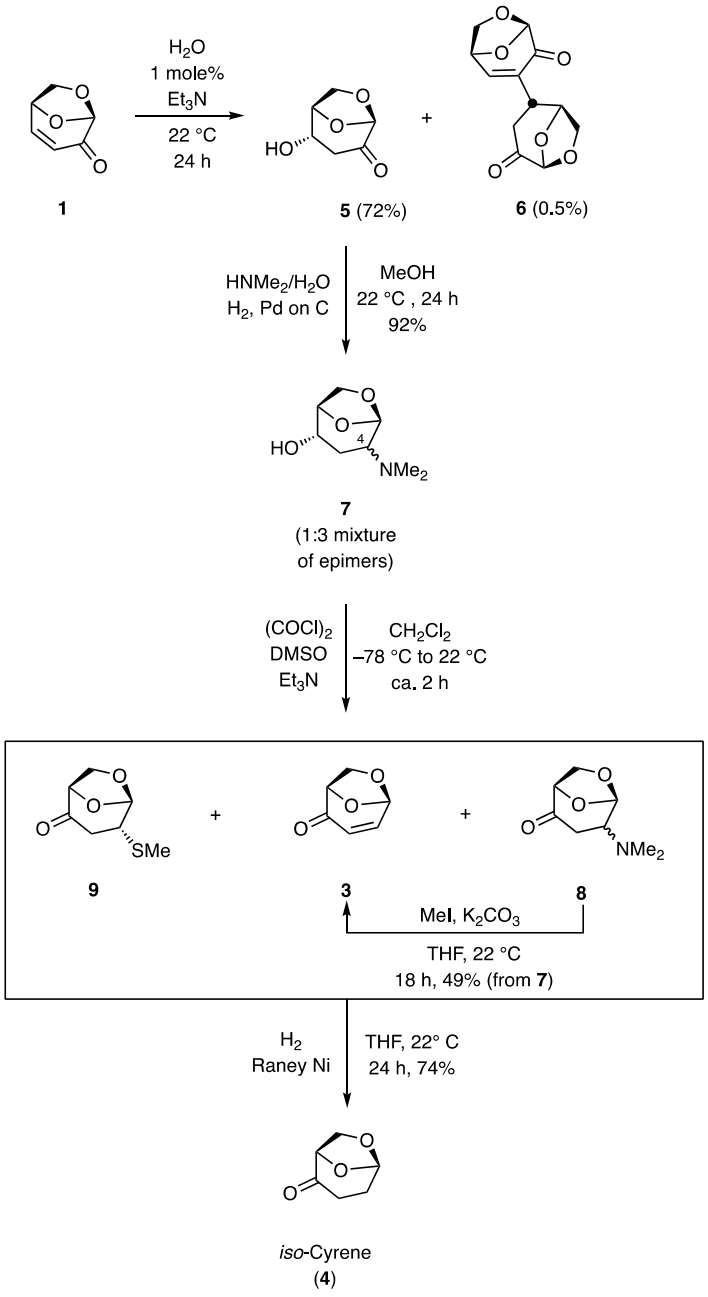

Scheme 1: Synthetic sequence leading from LGO (**1**) to *iso*-Cyrene (**4**).

to *iso*-LGO (**3**) with the resulting trialklylsulfonium ion then undergoing demethylation, perhaps through nucleophilic attack by triethylamine,[18] to give the compound **9**. The conversion of product **7** into *iso*-LGO (**3**) was best achieved by treating the crude mixture from the oxidation reaction with methyl iodide and potassium carbonate in THF at ambient temperatures and so affording, after flash chromatography, the latter in 49% yield (albeit still containing

traces of sulfide **9**). The conversion of *iso*-LGO into its dihydro- congener was first attempted by using the same conditions as employed in the conversion 1 → 2,[14] *viz*. by using hydrogen in the presence 10% Pd on C. However, this reduction proved sluggish at ambient temperatures with complete conversion requiring many days. This situation may be attributed to catalyst poisoning by sulfur residues present in the substrate. In contrast, when Raney nickel (W2) was employed in the presence of hydrogen at 22°C then *iso*-Cyrene was obtained in 74% yield after 24 h. GC/MS analysis of this material indicated that it still contained ca. 5% of compound **9** and this is despite the capacity of Raney nickel to effect desulfurisation reactions.

In order to accumulate the ca. 10 g sample of *iso*-Cyrene (**4**) deemed necessary for a meaningful evaluation of its physical and biological properties, it was most convenient to repeat the reaction sequence shown above (and detailed in the Experimental) multiple times. This approach highlights the most obviously restrictive feature associated with the approach, namely the need to apply Swern oxidation conditions to amino-alcohol **7** and thus affording a mixture of amino-ketone **8**, iso-LGO (**3**) and sulfide **9**.

Given the difficulties just described, we also examined the route from D-glucose (**10**) to *iso*-LGO (**3**) reported by Horton and co-workers in 1996[19] (**Scheme 2**). In this approach the starting hexose **10** was converted into the bis-acetonide **11** (74%) with the most effective catalyst system for this purpose being a combination of phosphoric acid (H3PO4) and zinc chloride ($ZnCl_2$) – using either sulfuric acid or this in combination with $CuSO_4$ led to the co-production of tar-like by-products. The structure of compound **11** was confirmed by single-crystal X-ray analysis (see Experimental and Supplementary Material for details) and the associated free 2°-alcohol was esterified using *p*-toluenesulfonyl chloride in pyridine to afford the crystalline sulfonate **12** (83%) and the structure of this also confirmed by single-crystal X-ray analysis (See

Experimental and Supplementary Material for details).[20] Reaction of ester **12** with potassium tert-butoxide in THF at 0°C for 2 h effected the anticipated elimination reaction in a regio-selective manner to afford the dihydrofuran **13** albeit in quite variable yield because it sometimes proved difficult to drive the reaction to completion and, exacerbating matters, to separate the product from the starting material. Treatment of enol ether **13** with aluminium chloride ($AlCl_3$) under the rather specific conditions defined by Horton[19] resulted in cleavage of the associated acetonide residues and thereby affording *iso*-LGO (**3**) albeit in highly variable and normally low yield (ca. 30% at best in our hands). A plausible mechanistic pathway for this last (and crucial) step has been proposed by Horton.[19] All the spectral data acquired on the samples of compound **3** prepared by this route matched those reported[19] as well as those derived from the material generated using the protocols shown in **Scheme 1**. Raney-nickel catalysed hydrogenation of *iso*-LGO (**3**) generated by the route shown in **Scheme 2** proceeded as before and thus affording *iso*-Cyrene (**4**) in 74% yield.

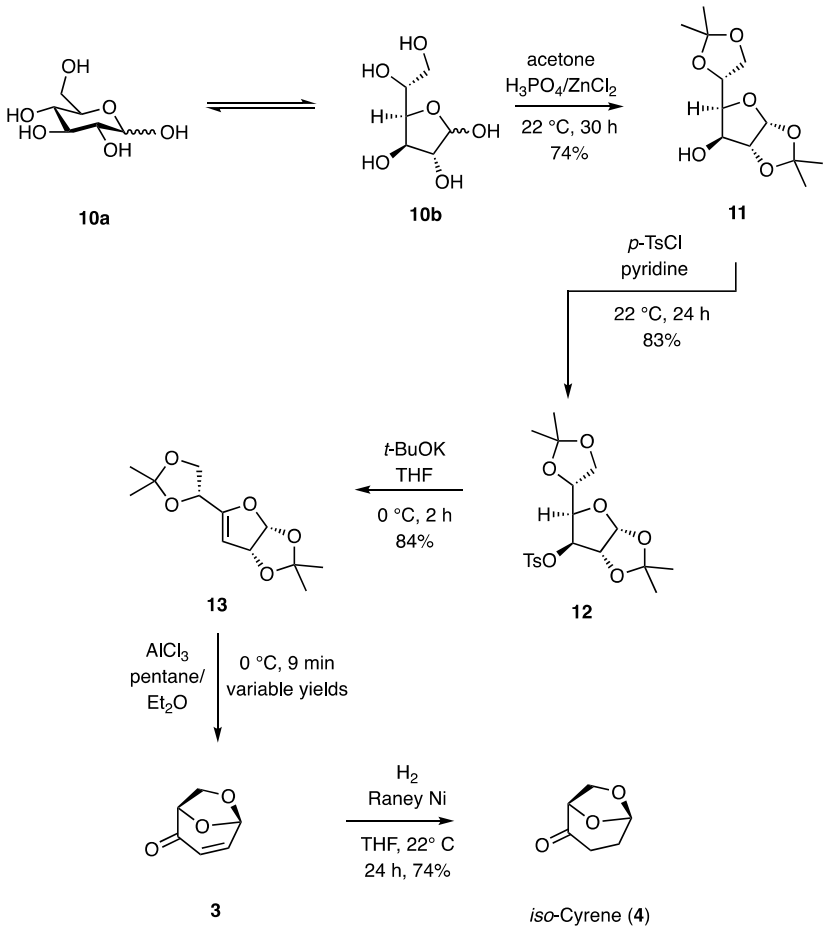

Scheme 2: The synthesis of *iso*-Cyrene (**4**) from D-glucose (**10**)

While the samples of compound **4** produced by this second route were uncontaminated by thio-ether **9**, the reaction sequence was less attractive than the first in a number of respects. In particular, it lacked many of the atom-economical features of the first route, it was operationally more tedious to prosecute the third and fourth steps, *viz.* the sequence **12** → **13** → **3**, proved capricious and low-yielding, at least in our hands. On balance, then, at the present time we favour the route shown in Scheme 1 for the purposes of generating serviceable quantities of *iso*-LGO (**3**) and, thence, *iso*-Cyrene (**4**). The multi-gram accumulation of *iso*-Cyrene (**4**) by the route shown in **Scheme 1** allowed for evaluations of various of its spectroscopic, physical, chemical and biological properties. Details are presented in the following sections.

Spectroscopic Studies

A comparison of the ^{1}H NMR spectroscopic data recorded on Cyrene® (**2**) with those acquired for *iso*-Cyrene (**4**) is provided in **Table 1**. This reveals that the dioxymethine proton associated with the former compound resonates at significantly higher field (δ_H 5.01) than its counterpart (δ_H 5.73) in isomer **4**. This difference can be attributed to the acetal proton of the former compound sitting within the shielding zone of the adjacent ketone carbonyl residue and so serving to emphasise the proximity and, therefore, the interactions between these two residues. The chemical shift differences between the resonances due to the remaining protons are much less pronounced.

Table 1: The ^{1}H NMR spectral data recorded for compounds **2** and **4**[a]

Compound	**δ_H, proton count, multiplicity, couplings**						
Cyrene® (**2**)	5.01, 1H s	4.64, 1H s	3.98, 1H d, *J* 7.7[b]	3.88, 1H m	2.58, 1H m	2.35-2.16 2H, cm[c]	1.96 1H m
iso-Cyrene (**4**)	5.73, 1H, broad s	4.50, 1H, d, *J* 5.6	3.97, 1H, d, *J* 8.0	3.87, 1H, dd *J* 8.0, 6.0	2.47, 2H *J* 7.6	2.21-2.11 1H, cm[c]	2.04 1H m

[a] Spectra recorded in $CDCl_3$ at 400 MHz; [b]coupling constants presented in Hz; [c] cm = complex multiplet

An analogous comparison of the chemical shifts of the resonances due to the constituent carbons observed in the ^{13}C NMR spectrum of compound **4** with those recorded for congeners **1-3** is presented in **Table 2** and reveals that it (*iso*-Cyrene) shows the most deshielded signal for the associated ketone carbonyl resonance.

Table 2: The ^{13}C NMR chemical shift data recorded for compounds **1**-**4**[a]

Compound	δ_C					
LGO (**1**)	188.9	148.4	126.6	101.5	71.3	66.5
iso-LGO (**3**)	194.5	147.3	127.1	96.1	79.6	62.7
Cyrene® (**2**)	200.4	101.4	73.1	68.1	30.8	29.8
iso-Cyrene (**4**)	205.6	100.9	79.3	67.2	31.5	30.7

[a] All spectra recorded in $CDCl_3$ at 100 MHz

In the infra-red spectrum of Cyrene® two carbonyl absorption bands are observed at 1724 and 1741 cm^{-1} while a single one (at 1733 cm^{-1}) is observed in the corresponding spectrum of *iso*-Cyrene. This difference reinforces the distinct relationship between the ketone carbonyl groups in each compound and the proximate (in the case of Cyrene®) or remote (in the case of *iso*-Cyrene) internal acetal. Specifically, the 'splitting" of the carbonyl absorption band in Cyrene® can be attributed to the distinct dipole-dipole interactions between the ketone carbonyl and the conformationally locked, axially- and equatorially-oriented C–O bonds of the adjacent internal acetal moiety.[21] The specific rotation $\{[\alpha]_D\}$ reported[9a] for compound **2**[9a] is –246 (c = 0.4, $CHCl_3$) while that recorded, during the course of this work, for congener **4** is of the same sign but significantly smaller in magnitude [–79.1 (c = 0.91, $CHCl_3$)].

The 70 eV electron-impact mass spectrum of *iso*-Cyrene (**4**) revealed a weak molecular ion (10% of base peak) at *m/z* 128 and a cluster of major fragment ions at *m/z* 86 (81%), 85 (base peak) and 84 (80%). The formation of the latter species probably arises through the fragmentation pathway shown in **Scheme 3** and wherein the molecular ion **14** (*m/z* = 128) undergoes heterolytic fission of the C1-C2 bond with the resulting radical cation losing the

elements of ketene (MW = 42) to afford the 1,3-dioxole **15** (*m/z* = 86) that itself losses a hydrogen atom and so producing the 2-methylene-1,3-dioxolane cation **16** (*m/z* = 85). Finally,loss of a second hydrogen would deliver the 2-methylene-1,3-dioxole radical cation **17** (*m/z* = 84).

Scheme 3: Possible fragmentation pathways operating during the EI-induced mass spectral analysis of *iso*-Cyrene (**4**).

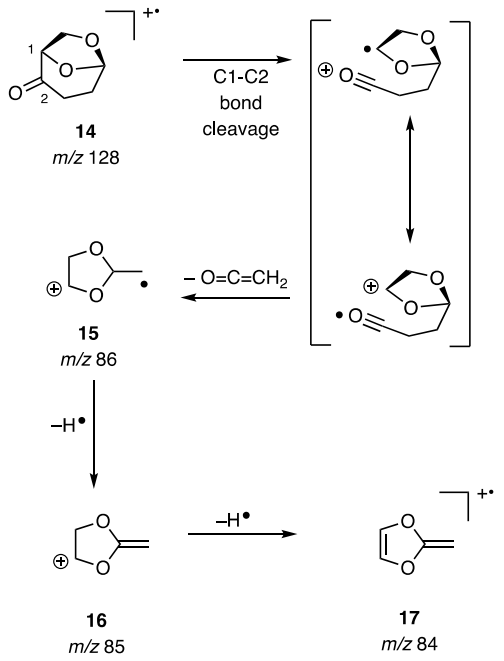

Key Physical Properties of *iso*-Cyrene

The experimentally determined density of *iso*-Cyrene at 22 °C was 1.29 g/mL (± *ca*. 3%), a value that compares with 1.25 g/mL reported[5] for Cyrene®. Attempts to establish the boiling point of *iso*-Cyrene were conducted at *ca*. 743 mm Hg (Canberra altitude is *ca*. 600 m) using DSC techniques. This led to the identification, as shown in **Figure S4** of the SI, of a transition point at *ca.* 117 °C that we take to signify the onset of a decomposition event, the details of which remain to be established. In keeping with such observations, prolonged heating of solutions of the compound in $(CD_3)_2SO$ led to the formation of a dark-yellow coloration while

analogous heating of neat material resulted in it developing a distinct brown colour. More specifically, while heating a $(CD_3)_2SO$ solution of compound **4** at 120 °C for 1 h did not lead to any noticeable change in the ^1H NMR spectrum of the material, after 18 h no resonances due to *iso*-Cyrene could be detected. An experimentally determined boiling point of 220 °C (presumably recorded at 760 mm Hg) has been reported for Cyrene® while the theoretically predicted (ex. CAS) boiling point for *iso*-Cyrene (**4**) is 227.3 (± 25 °C) at 760 mm Hg.

In keeping with expectations, *iso*-Cyrene proved to be entirely miscible, at 22 °C, with equal volumes of cyclohexane, diethyl ether, THF, dichloromethane, ethyl acetate, DMSO, DMF, Cyrene® and NMP. In contrast, it did not mix with water and ^1H NMR titration experiments indicated that, unlike its isomer **2**,[12b] *iso*-Cyrene (**4**) does not form a hydrate even when diluted in a 1:10 *v/v* ratio and allowed to stand at ambient temperatures for > 72 h.

Preliminary Studies on the Chemical Reactivity of *iso*-Cyrene

The differences between the chemical behaviours of the LGO (**1**)/Cyrene® (**2**) pair and their isomeric counterparts **3** and **4**, respectively, are quite conspicuous. For example, unlike LGO (**1**), *iso*-LGO (**3**) does not undergo ready conjugate addition of the elements of water (cf. conversion **1** → **5** in **Scheme 1**) and nor does it readily form dimers (cf. conversion **1** → **6** in **Scheme 1**). Similarly, unlike Cyrene® (**2**),[22] isomer **4** does not undergo ready self- or trans-aldol-type reactions in the presence of, for example, the base K_3PO_4. In terms of its acid-stability, it has been stated[5] that Cyrene® can be "heated with trifluoracetic acid at 60 °C for 18 h without apparent change". Likewise, when *iso*-Cyrene (**4**) is treated under the same conditions, no chemical change, as assessed by ^1H NMR spectroscopic analysis, is observed. In contrast, treatment of compound **4** with 2 M aqueous HCl at ambient temperatures for several hours resulted in notable decomposition and the appearance, in the ^1H NMR spectrum of the

product mixture, of a resonance attributable to an aldehyde. Analogous treatment of congener **2** only appeared to effect addition of water to the carbonyl moiety and so delivering the corresponding and previously reported[12b] geminal diol (see SI for relevant ^{1}H NMR spectroscopic analyses).

Computational Studies

In an effort to quantify the difference in polarity between congeners **2** and **4**, the dipole moment of each was calculated using density functional theory (see Experimental and SI for details). The outcomes of these calculations, together with those obtained on the unsaturated precursors **1** and **3**, are shown in **Table 3**. Thus, Cyrene® (**2**) has a significantly higher dipole moment than *iso*-Cyrene (**4**) but both are lower than those of their corresponding unsaturated counterparts. These variations seem intuitively reasonable and consistent with the aligned (in the case of **2**) or opposing (in the case of **4**) acetal and ketone carbonyl residues in these systems. Of course, the introduction of the conjugated C-C double bond into these systems, as manifest in compounds **1** and **3**, increases the dipole moment of each. This increase in polarity is also clear in the electrostatic potential surfaces of compounds **1**-**4**, as determined in the gas phase at the M06-2X/6-31+G(d,p) level of theory, which are shown in **Figure 2**.

Table 3: The Calculated Dipole Moments of Compounds **1-4**

Compound #	**1**	**2**	**3**	**4**
Structure[a]	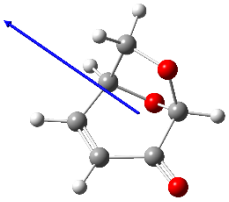	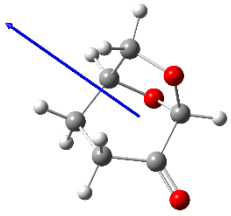	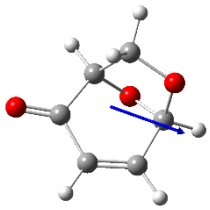	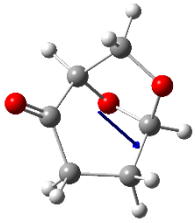
Dipole Moment (Debye)[b]	4.69	4.40	2.09	1.79

[a] Structures shown were produced using GaussView 6

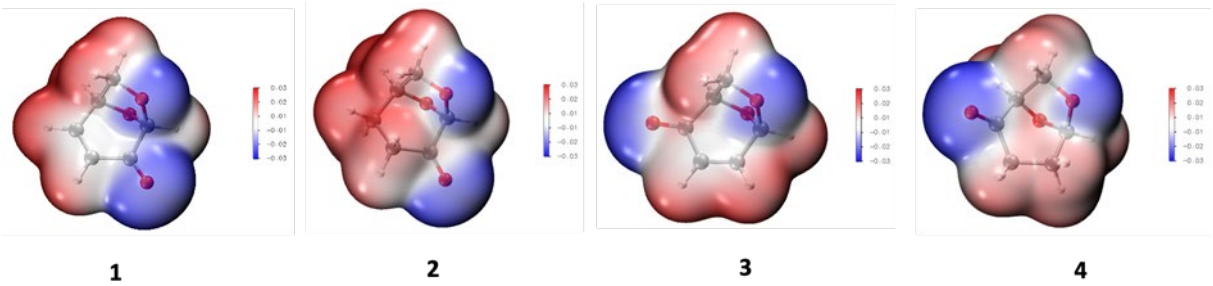

Figure 2: Electrostatic potential surfaces (ESPs) of compounds **1-4**, as calculated at the M062X/6-31+G(d,p) level of theory (in the gas phase).

COSMO-RS calculations[23] were also used to understand the solvation properties of Cyrene® and *iso*-Cyrene (and compared to NMP for reference). The molecular size and surface charges of *iso*-Cyrene are very similar to Cyrene® (as determined with COSMO-RS at the B88-VWN-PB86/TZVP level of theory, see SI, **Figure S5**). This suggests *iso*-Cyrene could take the place of Cyrene® in solvent substitutions despite its smaller dipole moment, which is particularly useful where miscibility and reactivity with water is undesirable. *iso*-Cyrene and Cyrene® are calculated not to interact as strongly with positive charges as NMP and other conventional dipolar aprotic solvents. This may limit applications requiring the stabilisation of charges or the solubility of salts.

Biological Properties

In vitro toxicological profiling

Cyrene® (**2**) is widely reported to offer reduced toxicity in comparison to common *N*-containing polar aprotic solvents such as NMP, *N,N*-dimethylformamide (DMF) and *N,N*-dimethylacetamide (DMAc).[2,6] Toxicological evaluations of emerging new solvents that conform to regulatory guidelines and involve conventional animal tests remain a challenge since large quantities of ultra-pure sample are required. They are also time-consuming and costly. As such, the rapid *in vitro* assessment of neoteric solvents is an ideal alternative for initial assessments of toxicity and thus reducing the risk of "regrettable substitutions".[24] Accordingly, *iso*-Cyrene (**4**) was analysed using a panel of eleven CALUX® *in vitro* reporter gene assays, covering different toxicological endpoints. These CALUX assays specifically detect the ability of a test compound to modulate a certain nuclear receptor (ERα, AR, TRβ, PPARγ, PXR and AhR CALUX) or a cell signaling pathway (AP-1, ESRE, Nrf2 and p53 CALUX). The assays have been used successfully in several large screening programs, such as the EU Framework program (FP) projects ReProTect, ChemScreen and EU-ToxRisk.[25-31] Additionally, they have been applied to safety assessments of bio-based solvents[32] and bio-based plasticisers.[33] The assays selected for the present study cover a broad range of toxicological endpoints, including endocrine activity (ERα, AR, TRβ), xenobiotic sensing (PXR, AhR), oxidative stress (Nrf2), protein unfolding (ESRE) and DNA damage/genotoxicity (AP-1, p53).

The lowest effective concentrations (LOECs) in LogM observed for Cyrene® (**2**) and *iso*-Cyrene (**4**) in all eleven *in vitro* assays are shown in **Table 4**. Both compounds have remarkably similar profiles, indicating that these regioisomers differ little in their *in vitro* activity. Cyrene® (**2**) has previously been shown to be non-mutagenic and non-ecotoxic.[6] The present study reveals that Cyrene® (**2**) shows slight cytotoxicity and activates two cellular stress pathways (AP-1: cell cycle control and Nrf2: oxidative stress) but such activation takes place at concentrations 2-6 orders of magnitude higher than the LOECs of the assays' reference compounds (top row) and indicating a low potency. Since the *in vitro* profile of *iso*-Cyrene (**4**) on the eleven CALUX assays was virtually identical, there is no indication that it has a less favourable toxicological profile.

Table 4: *In vitro* CALUX reporter gene assay results for Cyrene® (**2**) and *iso*-Cyrene (**4**)[a]

Compound	Cytotox 20%	ERα	AR-anti	TRβ-anti	PPARγ	PXR	AhR	AP-1	ESRE	Nrf2	p53
Assay references	–6.6	–12.2	–7.7	–6.9	–7.7	–7.1	–12.3	–9.5	–7.5	–5.4	–9.0
Cyrene™ (**2**)	–3.2	>	>	>	>	>	>	–3.3	>	–3.5	>
iso-Cyrene (**4**)	–3.1	>	>	>	>	>	>	–2.0	>	–3.5	>

[a]*In vitro* results are presented as lowest observed effect concentrations (LOECs) in LogM; '>': no activity detected up to the highest tested concentration. 'N/A': not analysed; Top row: LOECs of each assay's positive control reference compound. Cells are color-coded based on the LOECs: green = LOEC > [max analysed]; light orange = LOEC >-4; orange = LOEC <-5;

Gas chromatographic-olfactometry (GC-O) analysis

Pure Cyrene® (**2**) was evaluated by perfumers and flavorists and described as having bacon, smoked and vanilla notes. In contrast, olfactory evaluation of *iso*-Cyrene (**4**) performed by trained panelists revealed only sulfury and unpleasant olfactive notes and these are attributed to the introduction of contaminants during the Swern oxidation step associated with the synthetic sequence outlined in **Scheme 1**. Accordingly, gas chromatographic-olfactometry

(GC-O) analysis[34] (**Figure 3**) was then performed to specifically assess the odour of the compounds (**Table 5**). By such means, Cyrene® (**2**) eluting between 5.54 and 5.80 min proved to smell exactly as expected with a better appreciation of the vanilla note on the GC-O. On the other hand, no odour was detected between 4.95 and 5.10 min of retention time which correspond to the elution of the peak of the *iso*-Cyrene (**4**). Sulfury notes were detected on compounds barely responsive to FID.

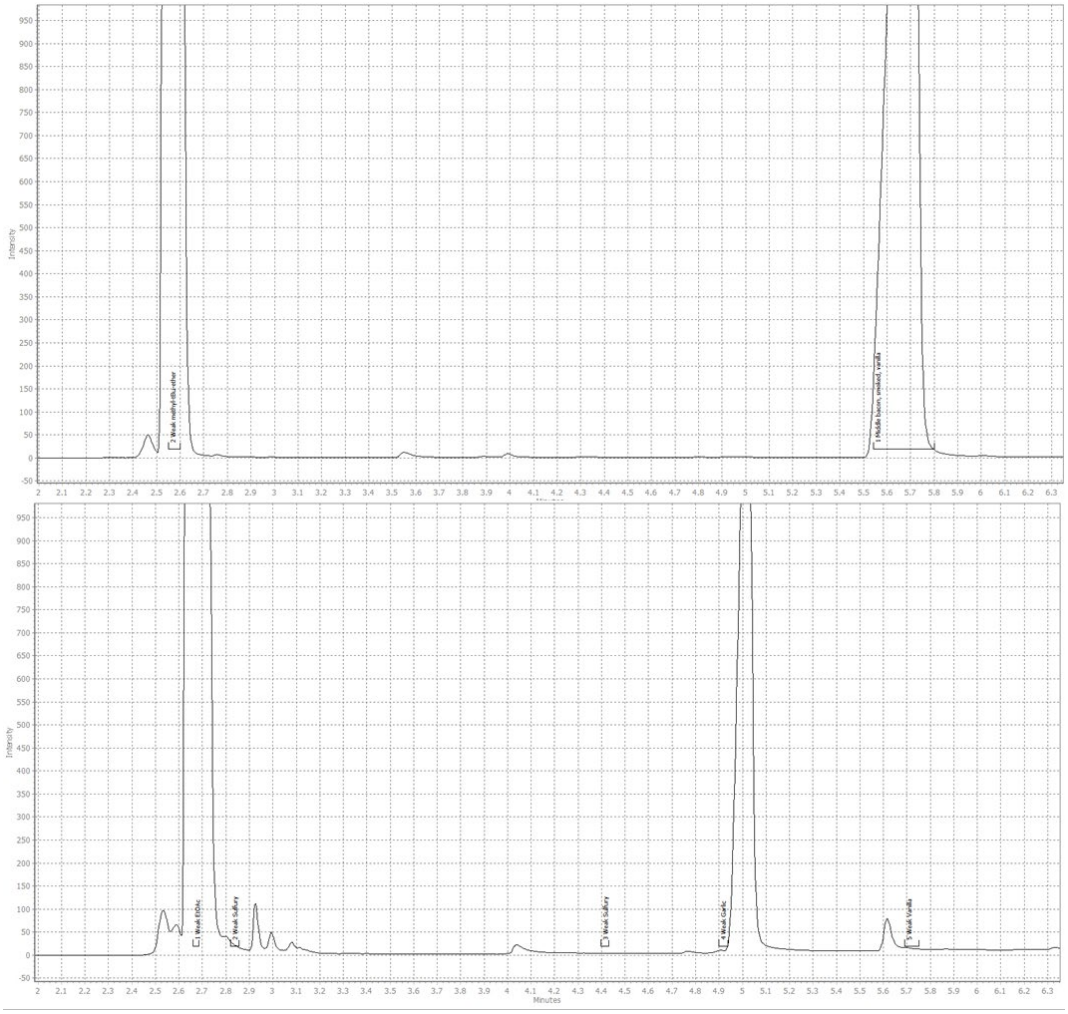

Figure 3: GC-O analysis of Cyrene® (**2**) (top) and *iso*-Cyrene (**4**) (bottom). Markers were placed during the analysis when an odor was detected. The earlier eluting and major peak in each chromatogram is due to the diluting solvent, this being either methyl tert-butyl ether (top) or ethyl acetate (bottom).

Table 5: Retention time and odour description obtained during GC-O analysis of a sample of Cyrene® (**2**) and of *iso*-Cyrene (**4**).

Sample	Retention time (min)	Odor	Intensity
Cyrene®	2.54-2.60	methyl *tert*-butyl ether (dilution solvent)	Weak
	5.54-5.80	bacon, smoked, vanilla	Medium
***iso*-Cyrene**	2.65-2.69	ethyl acetate (dilution solvent)	Weak
	2.81-2.85	sulfury	Weak
	4.39-4.42	sulfury	Weak
	4.90-4.92	garlic	Weak
	5.68-5.73	vanilla	Weak

Conclusions

These studies reported here reveal that there are significant enough differences in the properties of the sustainably-derived Cyrene® (**2**) and isomer **4** (*iso*-Cyrene) to suggest they will exert complementary effects as solvents in a range of settings. These differences are due, in large part, to the relative positioning of the ketone and acetal residues within the associated bicyclic frameworks. In compound **2** the adjacent location of these functionalities increases the electrophilicity of the carbonyl moiety and the acidity of the hydrogens associated with the α-methylene unit. Likewise, the acid-stability of the acetal group is increased by the presence of

the neighbouring and electron-withdrawing ketone residue. In compound **4** there is significantly less interaction between the equivalent residues and such that they behave much like "normal" (isolated) ketone and acetal groups. As a consequence, Cyrene® (**2**) is likely to be somewhat less acid sensitive than isomer **4** (*iso*-Cyrene) while the latter is less base sensitive. These same structural differences also dictate (and explain) the differing miscibilities of the compounds with water. As detailed above, *in vitro* testing suggests compounds **2** and **4** have similar and favourable toxicological properties. That said, the lack of an odour associated with *iso*-Cyrene (**4**) may confer some advantages in terms of its exploitation as solvent although doing so would require the development of superior means of preparing it. Regardless of how this might be achieved, this work reinforces the significant value of LGO (**1**) as a bio-derived platform molecule.[35]

Experimental

General Experimental Procedures

Unless otherwise specified, proton (^{1}H) and carbon (^{13}C) NMR spectra were recorded at 18 °C in base-filtered $CDCl_3$ on a Varian spectrometer operating at 400 MHz for proton and 100 MHz for carbon nuclei. For ^{1}H NMR spectra, signals arising from the residual protio-forms of the solvent were used as the internal standards. ^{1}H NMR data are recorded as follows: chemical shift (δ multiplicity, coupling constant(s) *J* (Hz), relative integral] where multiplicity is defined as: s = singlet; d = doublet; t = triplet; q = quartet; m = multiplet or combinations of the above. The signal due to residual $CHCl_3$ appearing at δ_H 7.26 and the central resonance of the $CDCl_3$ "triplet" appearing at δ_C 77.2 were used to reference ^{1}H and ^{13}C NMR spectra, respectively. Infrared spectra (δ_{max}) were recorded on a Perkin-Elmer 1800 Series FTIR Spectrometer. Samples were analysed as thin films on KBr plates. Low-resolution ESI mass spectra were

recorded on a Micromass LC-ZMD single quadrupole liquid chromatograph-mass spectrometer while high-resolution measurements were conducted on an LCT Premier time-of-flight instrument. Low- and high-resolution EI mass spectra were recorded on an Autospec Premier Micromass magnetic-sector machine. Optical rotations were recorded in $CHCl_3$ at 20 °C on a Perkin Elmer Model 343 Polarimeter. Melting points were measured on an Optimelt automated melting point system and are uncorrected. Analytical thin layer chromatography (TLC) was performed on aluminium-backed 0.2 mm thick silica gel 60 F_{254} plates as supplied by Merck. Eluted plates were visualised using a 254 nm UV lamp and/or by treatment with a suitable dip followed by heating. These dips included phosphomolybdic acid : ceric sulfate : sulfuric acid (conc.) : water (37.5 g : 7.5 g : 37.5 g : 720 mL) or potassium permanganate : potassium carbonate : 5% sodium hydroxide aqueous solution : water (3 g : 20 g: 5 mL : 300 mL). Flash chromatographic separations were carried out following protocols defined by Still *et al*.[36] with silica gel 60 (40-63 μm) as the stationary phase and using the AR- or HPLC-grade solvents indicated. Starting materials and reagents were generally available from the Sigma-Aldrich, Merck, TCI, Strem or Lancaster Chemical Companies and were used as supplied. Drying agents and other inorganic salts were purchased from the AJAX, BDH or Unilab Chemical Companies. Tetrahydrofuran (THF), methanol and dichloromethane were dried using a Glass Contour solvent purification system that is based upon a technology originally described by Grubbs *et al*.[37] Where necessary, reactions were performed under an inert atmosphere.

Specific Synthetic Transformations

(1*R*,2*S*,5*R*)-2-Hydroxy-6,8-dioxabicyclo[3.2.1]octan-4-one (5) and Dimer 6. A magnetically stirred solution of levoglucosenone (**1**) (5.94 g, 47.1 mmol) in water (470 mL) maintained at 22 °C was treated with triethylamine (4.70 mL, 3.72 mmol). After 1 h the reaction mixture was concentrated under reduced pressure and the ensuing residue subjected to flash chromatography

(silica, 1:10 *v/v* ethyl acetate/40-60 petroleum ether → ethyl acetate gradient elution) and so affording two fractions, A and B.

Concentration of fraction A (R_f = 0.3) gave a solid that on recrystallisation (CH_2Cl_2) afforded dimer **6**[15] (64 mg, 0.5%) as white, crystalline solid, m.p. = 163-165 °C (lit.[15a] m.p. = 170-172 °C), $[\alpha]_D$ = –444 (*c* 0.49, acetone) {lit.[15a] $[\alpha]_D$ = –482 (*c* 0.3, acetone)}. ^{1}H NMR (400 MHz, $CDCl_3$) δ 7.11 (d, *J* = 6.0 Hz, 1H), 5.43 (s, 1H), 5.14 (s, 1H), 5.09 (m, 1H), 4.55 (m, 1H), 4.18 (d, *J* = 8.4 Hz, 1H), 4.06 (m, 1H), 3.91 (m, 1H), 3.73 (d, *J* = 6.8 Hz, 1H), 3.46 (d, *J* = 8.4 Hz, 1H), 3.00 (dd, *J* = 17.6 and 8.4 Hz, 1H), 2.25 (d, *J* = 17.6 Hz, 1H); ^{13}C{^{1}H} NMR (100 MHz, $CDCl_3$) δ 200.2, 188.3, 143.9, 137.2, 101.8, 101.1, 75.1, 72.4, 68.3, 66.5, 38.6, 35.1; IR ν_{max} 2971, 2902, 1729, 1686, 1120, 1097, 981, 968, 906, 896, 867, 844, 819, 670 cm^{-1}; MS (EI, 70 eV) *m/z* 252 ($M^{+\bullet}$, <1%), 224 (<1), 149 (78), 105 (100), 91 (77), 79 (60); HRMS (EI, 70 eV) calcd for $C_{12}H_{12}O_6$ ($M^{+\bullet}$) 252.0628, found 253.0623.

Concentration of fraction B (R_f = 0.2) gave compound **5**[8] (4.88 g, 72%) as a clear, light-yellow oil that was identical, in all respects, with material obtained earlier.[8]

(1*R*,2*S*,4*S*,5*R*)-4-(Dimethylamino)-6,8-dioxabicyclo[3.2.1]octan-2-ol (4*S*-7) and (1*R*,2*S*, 4*R*,5*R*)-4-(Dimethylamino)-6,8-dioxabicyclo[3.2.1]octan-2-ol (4*R*-7). A magnetically stirred solution of compound **5** (4.00 g, 27.8 mmol), prepared as described immediately above, and dimethylamine (10 mL of a 40% aqueous solution, 83.0 mmol) in methanol (140 mL) maintained at 22 °C was treated with 10% palladium on carbon (200 mg). The resulting mixture was placed under a balloon of hydrogen and after 24 h the reaction mixture was filtered through a pad of diatomaceous earth and the filtrate concentrated under reduced pressure. The resulting oil was dissolved into dichloromethane (200 mL) then dried (Na_2SO_4) and filtered before being concentrated under reduced pressure to give compound **7** (4.40 g, 92%) as a clear, yellow oil

and *ca*. 3:1 mixture of epimers. ^{1}H NMR (400 MHz, $CDCl_3$) δ 5.61 (s, 0.75H), 5.57 (s, 0.25H), 4.48 (broad s, 1H), 3.92-3.76 (complex m, 3H), 2.75 (m, 1H), 2.38 (s, 6H), 1.98 (m, 1H), 1.98-1.90 (complex m, 1H), 1.87-1.80 (complex m, 1H); ^{13}C NMR (100 MHz, $CDCl_3$) δ 101.0 (major isomer), 100.7 (minor isomer), 78.4, 67.8, 67.3, 66.6, 66.4, 63.7, 61.4, 44.1, 42.0, 27.5, 25.8; IR ν_{max} 3368, 2953, 2892, 2827, 2783, 1458, 1131, 1037, 1002, 901, 861, 781, 688, 483 cm^{-1}; MS (ESI, +ve) *m/z* 222 (100%), 174 [$(M+H)^+$, 90]; HRMS calcd for $C_8H_{16}NO_3$ [$(M+H)^+$] 174.1130, found 174.1127.

(1*R*,5*R*)-6,8-Dioxabicyclo[3.2.1]oct-3-en-2-one (3), (1R,5R)-4-(Dimethylamino)-6,8-dioxabicyclo[3.2.1]octan-2-one (8) and (1*R*,4*R*,5*R*)-4-(Methylthio)-6,8-dioxabicyclo[3.2.1]-octan-2-one (9). A solution of DMSO (1.88 g, 24 mmol) in dichloromethane (20 mL) was added, dropwise *via* syringe, to a magnetically stirred solution of oxalyl chloride (1.52 g, 12 mmol) in dichloromethane (30 mL) maintained at –70 °C. The ensuing mixture was allowed warm to –58 °C then re-cooled to –70 °C over a 0.25 h period. Thereafter, a solution of amino-alcohol **7** (1.73 g, 10 mmol) in dichloromethane (30 mL) was added to the reaction mixture over 10 min. After a further 0.75 h, triethylamine (5.58 mL, 40 mmol) was added to the reaction mixture over 5 min. After this time, the reaction mixture was allowed to slowly warm to –5 °C and then filtered through a pad of diatomaceous earth contained in a sintered glass funnel. The filtrate was concentrated under reduced pressure to afford a malodorous, light-yellow oil comprised of a mixture of compounds **3**, **8** and **9**.

In order to obtain a sample of the last compound for the purposes of spectroscopic characterisation, this oil was subjected to flash chromatography (silica, 1:10 *v/v* ethyl acetate/petroleum ether elution) and so affording, after concentration of the relevant fractions

(R_f = 0.2), compound **9** (226 mg, 13%) as a foul-smelling, yellow oil, $[\alpha]_D$ = –23.6 (*c* = 0.06, $CHCl_3$). ^{1}H NMR (400 MHz, $CDCl_3$) δ 5.69 (s, 1H), 4.54 (d, *J* = 5.4 Hz, 1H), 3.96 (d, *J* = 8.1 Hz, 1H), 3.86 (dd, *J* = 8.1 and 5.4 Hz, 1H), 3.02 (m, 1H), 2.85 (m, 1H), 2.52 (dd, *J* = 17.5 and 4.8 Hz, 1H), 2.18 (s, 3H); ^{13}C NMR (100 MHz, $CDCl_3$) δ 204.7, 103.8, 79.2, 67.1, 45.4, 39.0, 13.9; IR ν_{max} 2963, 2896, 1732, 1668, 1406, 1173, 1114, 1010, 894, 793, 754 cm^{-1}; MS (ESI, +ve) 229 [(M+MeOH+Na)$^+$, 100%]; MS (EI, +ve) *m/z* 174 ($M^{+\bullet}$, 50%), 74 (100); HRMS calcd for $C_7H_{10}O_3S$ ($M^{+\bullet}$) 174.0351, found 174.0347.

The high polarity of the presumed primary oxidation product **8** as well as its seeming propensity to engage in (possibly) Schiff-base-type condensation and other reactions thwarted efforts to obtain it in pure form.

Conversion of Amino-ketone 8 into *iso*-LGO (3). A magnetically stirred solution of the crude product obtained, as described immediately above, from the Swern oxidation of amine **7** in THF (50 mL) and maintained at 22 °C was treated with methyl iodide (1.2 mL, 20 mmol) and potassium carbonate (2.70 g, 20 mmol). After 18 h the reaction mixture was filtered through a pad of diatomaceous earth and the filtrate concentrated under reduced pressure. The residue so obtained was subjected to flash chromatography (silica, 1:10 *v/v* ethyl acetate/petroleum ether elution) and concentration of the relevant fractions (R_f = 0.2) gave compound **3**[8a] (617 mg, 49%) as a clear, yellow oil. This material was identical, in all respects, with that obtained earlier.[8a]

(1*R*,5*R*)-6,8-Dioxabicyclo[3.2.1]octan-2-one (*iso*-Cyrene, 4). A magnetically stirred mixture of *iso*-LGO (**3**) (2.56 g, 20 mmol) and W2 Raney Ni (*ca*. 200 mg) in THF (100 mL) maintained at 22 °C was placed under a balloon of hydrogen. After 24 h an externally applied magnet was used to retain the solid catalyst within the reaction flask while the supernatant liquid was

decanted into another vessel. The retained solids were washed with ethyl acetate (2 × 30 mL) (CAUTION: the washed solid should be treated with water so as to prevent combustion). The combined organic phases were concentrated under reduced pressure to give a clear, colourless oil that was subjected to flash column chromatography (silica, 1:10 *v/v* ethyl acetate/ petroleum ether elution). Concentration of the relevant fractions (R_f = 0.1) gave an oil that was subject to distillation at reduced pressure and thus affording *iso*-Cyrene (**4**)[9,10] (1.89 g, 74%) as a clear, colourless oil of undefined boiling point, $[\alpha]_D$ = –79.1 (*c* = 0.91, $CHCl_3$) {lit.[9a] $[\alpha]_D$ = –83 (*c* = 0.8, $CHCl_3$)}. ^{1}H NMR (400 MHz, $CDCl_3$) δ see **Table 1**; ^{13}C NMR (100 MHz, $CDCl_3$) δ see **Table 2**; IR ν_{max} 2963, 1733, 1118, 1008, 1017, 995, 871 cm^{-1}; MS (EI, +ve) *m/z* 128 ($M^{+\bullet}$, 10%), 86 (81), 85 (100), 84 (80); HRMS calcd for $C_6H_8O_3$ ($M^{+\bullet}$) 128.0473, found 128.0473.

(3a*R*,5*S*,6*S*,6a*R*)-5-((*R*)-2,2-Dimethyl-1,3-dioxolan-4-yl)-2,2-dimethyltetrahydrofuro[2,3-*d*][1,3]dioxol-6-ol (11): Phosphoric acid (1.0 mL of an 85% solution in water) was added, dropwise, to magnetically stirred, anhydrous acetone (300 mL) and the resulting solution was treated with a well-dried and finely powdered mixture of D-glucose (**10**) (30.0 g) and anhydrous zinc chloride (26.0 g). Stirring was continued for 30 h at 22 °C before the reaction mixture was cooled in an ice-bath then basified (to pH 8) through the portion-wise addition of sodium hydroxide (1 M aqueous solution) while ensuring the temperature of the reaction mixture did not exceed 15 °C. The precipitated mass, comprising sodium sulfate, zinc chloride and unreacted D-glucose (**10**), was removed by filtration and the solids thus retained washed with acetone. The combined filtrates were concentrated under reduced pressure and the solid residue recrystallised (*n*-hexane) to give, after hot filtration then cooling, bis-acetonide **11**[38] (32.0 g, 74%) as a white, crystalline solid, m.p. = 104-105 °C (lit.[38] m.p. = 111-112 °C), $[\alpha]_D$ = –5.88 (*c* 0.17, acetone). ^{1}H NMR (400 MHz, $CDCl_3$) δ 5.95 (d, *J* = 3.6 Hz, 1H), 4.54 (d, *J* = 3.6 Hz,

1H), 4.38-4.30 (complex m, 2H), 4.17 (dd, *J* = 8.8 and 6.4 Hz, 1H), 4.07 (dd, *J* = 7.6 and 2.8 Hz, 1H), 3.97 (dd, *J* = 8.8 and 5.2 Hz, 1H), 1.50 (s, 3H), 1.44 (s, 3H), 1.36 (s, 3H), 1.32 (s, 3H); ^{13}C NMR (100 MHz, $CDCl_3$) δ 111.8, 109.7, 85.1, 81.1, 75.3, 73.5, 67.7, 26.9, 26.8, 26.2, 25.1.

(3a*R*,5*R*,6*S*,6a*R*)-5-((*R*)-2,2-Dimethyl-1,3- dioxolan-4-yl)-2,2-dimethyltetrahydrofuro[2,3-*d*]- [1,3]dioxol-6-yl 4-methylbenzenesulfonate (12) A solution of compound **11** (11.8 g, 45.3 mmol) and *p*-toluenesulfonyl chloride (17.3 g, 90.7 mmol) in pyridine (20 mL) was allowed to stand at 22°C for 24 h, then poured with stirring into ice-water (150 mL) and the resulting solid filtered off, washed several times with water, and then dried and recrystallised (methanol) to give compound **12**[39] (16.2 g, 86%) as a white crystalline solid, m.p. = 119–120°C (lit.[39a] m.p. = 119–120°C), [α]D = −51.7 (*c.* 0.2, acetone). 1H NMR (400 MHz, CDCl3) *δ* 7.84 (d, *J* = 8.4 Hz, 2H), 7.33 (d, *J* = 8.4 Hz, 2H), 5.92 (d, *J* = 3.6 Hz, 1H), 4.83 (d, *J* = 3.6 Hz, 1H), 4.79 (broad s, 1H), 4.08–3.95 (complex m, 3H), 3.90 (m, 1H), 2.45 (s, 3H), 1.48 (s, 3H), 1.31 (s, 3H), 1.20 (s, 3H), 1.15 (s, 3H); 13C NMR (100 MHz, CDCl3) *δ* 145.2, 132.8, 129.8, 128.6, 112.7, 109.2, 105.3, 83.5, 82.2, 80.0, 71.9, 67.3, 26.8, 26.4, 25.1, 21.8.

(3a*R*,6a*R*)-5-((*R*)-2,2-Dimethyl-1,3-dioxolan-4-yl)-2,2-dimethyl-3a,6a-dihydrofuro[2,3-*d*] -[1,3]dioxole (13): The conditions reported by Horton[19] and by Norris[40] for forming alkene **13** from tosylate **12** (7.3 g, 17.6 mmol) (by treating the latter with *t*-BuOK in THF) were employed on multiple occasions in the present study and in each instance a waxy-yellow solid was obtained after work-up. NMR spectroscopic analysis of this material suggested it contained varying mixtures of the starting ester (**12**) and the target alkene **13**[19,40] alongside other, unidentified components. All attempts to purify product **13** by chromatographic means failed. Accordingly, the waxy-solid obtained after work-up was subjected to treatment with aluminium chloride as detailed immediately below.

***iso*-LGO (3)**. Following the procedure of Horton,[19] anhydrous aluminium chloride (390 mg, 2.95 mmol) was added to a vigorously stirred mixture of dry diethyl ether (30 mL) and pentane (22 mL) that had been cooled to 0 °C under an argon atmosphere. A solution of the waxy-solid (1.43 g, 5.90 mmol) obtained from the preceding step (see immediately above) in diethyl ether (6 mL) was then added dropwise over a 2 min. period and the resulting mixture was stirred for an additional 7 min at 0 °C and then quickly transferred to a flash chromatography column (25 mm i.d.) containing a 4 cm deep pad of silica gel. The reaction mixture was rapidly forced through the apparatus using compressed air and the pad was then washed with diethyl ether/pentane (1:1 *v/v* mixture) until no more UV-active material could be detected (by TLC) in the column eluent (ca. 300 mL required). The combined filtrates were concentrated under reduced pressure to afford a brown syrup that was subjected to flash chromatography (silica, 5:1 *v/v* pentane/diethyl ether elution) to give, after concentration of the relevant fractions (*R*f = 0.2), compound **3**[8a] (60 mg, 8%) as a pale-yellow syrup. ^{1}H and ^{13}C NMR spectroscopic analyses of this material revealed that it was contaminated with a tosyl-containing species.

Crystallographic Studies

Crystallographic Data

Compound **6**. $C_{12}H_{12}O_6$, M = 252.22, T = 150 K, monoclinic, space group $P2_1$, Z = 4, a = 6.60390(10) Å, b = 18.9253(2) Å, c = 9.27500(10) Å; β = 107.663(2); V = 1104.55(3) Å^3, D_x = 1.517 Mg m^{-3}, 4431 unique data ($2\theta_{max}$ = 147.642°), R = 0.0579 [for 4385 reflections with $I > 2.0\sigma(I)$]; Rw = 0.0237 (all data), S = 1.055.

Compound **11**. $C_{12}H_{20}O_6$, M = 260.28, T = 150 K, monoclinic, space group C2, Z = 8, a = 20.7196(6) Å, b = 5.5609(2) Å, c = 24.6708(8) Å; β = 110.883(4); V = 2655.83(16) Å^3, D_x =

1.302 Mg m^{-3}, 4465 unique data ($2\theta_{max}$ = 133.172°), R = 0.0465 [for 4224 reflections with $I > 2.0\sigma(I)$]; Rw = 0.1218 (all data), S = 1.076.

Compound **12**. $C_{19}H_{26}O_8S$, M = 414.46, T = 150 K, orthorhombic, space group $P2_12_12_1$, Z = 4, a = 9.79882(18) Å, b = 10.1911(3) Å, c = 21.2482(5) Å; V = 2121.86(9) Å^3, D_x = 1.297 Mg m^{-3}, 3883 unique data ($2\theta_{max}$ = 136.494°), R = 0.0325 [for 3539 reflections with $I > 2.0\sigma(I)$]; Rw = 0.0833 (all data), S = 1.040.[20]

Structure Determinations

Data for compounds **6**, **11** and **12** were collected on a Rigaku Super Nova X-ray diffractometer employing CuKα radiation and a graphite monochromator (λ = 1.54184 Å). Using OLEX2,[41] the structures were solved by direct methods with the ShelXT[42] program and refined, using least squares minimisation, with the ShelXL[43] package. Atomic coordinates, bond lengths and angles, and displacement parameters have been deposited at the Cambridge Crystallographic Data Centre (CCDC nos. 2079098 and 2092948). These data can be obtained free-of-charge via www.ccdc.cam.ac.uk/data_request/cif, by emailing data_request@ccdc. cam.ac.uk, or by contacting The Cambridge Crystallographic Data Centre, 12 Union Road, Cambridge CB2 1EZ, UK; fax: +44 1223 336033.

Determination of Certain Physical Properties of *iso*-Cyrene

Miscibility and Degree of Hydration

For miscibility studies, equivalent volumes (ca. 5-10 μL) of *iso*-Cyrene and the relevant "co-solvent" were loaded into melting point tubes *via* micropipette. The loaded tubes were quickly inverted several times and then allowed to stand at 22 °C for 0.5 h. After this time the tubes were loaded into a melting point apparatus incorporating a magnifying aperture and the contents

of the tube inspected for the presence or absence of an interface between phases. Only in the case of the water/*iso*-Cyrene mixture was such an interface observed.

For the degree of hydration study, and following protocols used by Camp *et al*,[12b] an aliquot of *iso*-Cyrene was allowed to stand as a mixture with ten *v/v* equivalents of D_2O at ambient temperatures prior to analysis, at regular intervals up to 72 h, by ^1H NMR spectroscopy. No evidence for the formation of a hydrate analogous to that observed for Cyrene® was observed at any stage.

Density

Using micro-pipetting techniques, a defined volume (~20 μL) of *iso*-Cyrene was placed in a tared melting point tube and its weight determined, at 22 °C, using a micro-balance. Triplicate experiments gave an average density of 1.29 g/mL (±3%). This compares with a value of 1.25 g/mL reported[5] for Cyrene® at 20 °C.

Attempted boiling point determination

Attempts to determine the boiling point of *iso*-Cyrene (**4**) at ca. 743 mm Hg were undertaken using a TA Instruments Q20 DSC apparatus. A representative trace arising from this type of analysis is shown in Supplementary Fig. S4. The inflection point observed at ~117 °C is attributed to decomposition rather than to the boiling of the sample. A boiling point of 116–116.5 °C (at ~7.5 mm Hg) has been reported[5] for Cyrene®.

Chemical reactivity studies

To assess the stability of *iso*-Cyrene in the presence of base, an equivalent mass of tribasic potassium phosphate was intimately mixed with *iso*-Cyrene at *ca*. 22 °C, before being allowed

to stand for 18 h. The liquid was then decanted, dissolved in deuterated chloroform and analysed by proton NMR spectroscopy. This revealed that *iso*-Cyrene remained unaffected after exposure to such conditions.

To assess the stability of *iso*-Cyrene in the presence of acid, equal volumes (ca. 10 μL) of each of trifluoroacetic acid, D_2O and *iso*-Cyrene were intimately mixed then heated at 60 °C (oil bath) for 18 h. The resulting mixture was dissolved in $CDCl_3$ and analysed by ^1H NMR spectroscopy. This revealed that *iso*-Cyrene had not reacted under these conditions. In contrast, treatment of *iso*-Cyrene with a two-fold excess (*v/v*) of 2 M aqueous HCl at 60 °C for 1 h resulted in significant discoloration. Accordingly, the cooled reaction mixture was diluted with $(CD_3)_2SO$ and the ^1H NMR spectrum of the resulting solution was recorded (see below). This revealed significant decomposition had taken place. An analogous experiment involving Cyrene® did not result in any discoloration and analysis of the corresponding ^1H NMR spectrum (see below) suggested only formation of Cyrene® hydrate had occurred.

Theoretical studies

All calculations were performed at the M062X/6-31+G(d,p) level of theory using Gaussian G16c01.[44] Dipole moments and electrostatic potential maps were calculated in the gas phase, while SMD solvent corrections in cyclohexane were used to generate the van der Waals and solvent accessible surfaces. Electrostatic potential maps were generated with the Multiwfn program,[45] while GaussView 6[46] was used to plot the dipole moments and solute–solvent cavities. Molecular conformations of molecules were calculated with COSMOconfX (version 4.0; COSMOlogic GmbH & Co. KG, Leverkusen, Germany, 2015) while COSMOthermX (version C30_1705; COSMOlogic GmbH & Co. KG, 2017, TZVP basis set level) was used to

provide molecular surface charges, σ-profiles, and σ-potentials. COSMO-RS calculations are courtesy of, and authorised for the purposes of, Circa Group Pty Ltd.

Biological studies

CALUX reporter gene assay methodology

The *in vitro* assessment consisted of the analysis of the solvents against a panel of eleven CALUX® *in vitro* reporter gene assays, covering different toxicological endpoints [agonism on the estrogen (ERα), peroxisome proliferator activated (PPARγ), pregnane-X (PXR) and aryl hydrocarbon (AhR) receptors, antagonism on the androgen (AR) and thyroid (TRβ) receptors, activation of oxidative stress (Nrf2), unfolded protein response (ESRE), DNA damage (p53) and cell cycle control (AP-1) pathways, and cytotoxicity]. The assays are based on the human osteosarcoma cell line U-2 OS (ATCC HTB-96). Each cell line is stably transfected with a reporter gene plasmid containing luciferase under control of the responsive elements of a specific receptor (e.g. estrogen receptor) or cell signalling pathway (e.g. Nrf2). Activation of the transfected pathway or receptor by a test chemical results in luciferase production, which can be measured as light production by adding the substrate luciferin. Since most nuclear hormone receptors are not endogenously expressed in U-2 OS cells, these receptors were co-transfected when applicable (ERα, AR, TRβ, PXR, AhR, PPARγ). CALUX cells were routinely subcultured every 3–4 days in a growth medium consisting of DMEM (Gibco) supplemented with 7.5% fetal calf serum, 1× non-essential amino acids (Gibco) and 10 U mL^{-1} penicillin and 10 μg mL^{-1} streptomycin. Cells were maintained at 37°C under a 5% CO_2 atmosphere. All CALUX assays were performed as described in detail in the publicly available DBALM protocol 197.[47] The assay medium used consisted of DMEM without phenol-red indicator (Gibco) supplemented with 5% DCC- stripped fetal calf serum, 1× non-essential amino acids

(Gibco) and 10 U mL^{-1} penicillin and 10 µg mL^{-1} streptomycin. For seeding, a cell suspension in assay medium was made of 1 × 105 cells mL^{-1}, and the white 384-well plates were seeded with 30 µL per well cell suspension. After 24 h, cells were exposed to a dilution series of the test compound in DMSO (1% *v/v*) using a liquid handling robot (ex. Hamilton) coupled to an incubator (Cytomat). The final concentrations of the substances in the wells were 1×10^{-2} to 3×10^{-8} M in 0.5 log unit increments. All samples were tested in triplicate. After 24 h exposure the medium was removed and 10 µL per well Triton-lysis buffer was added. The luciferase signal was then measured in a luminometer (Infinite Pro reader coupled to a Connect stacker, both ex. TECAN Group Ltd). Molecular conformations of molecules were calculated with COSMOconfX (version 4.0; COSMOlogic GmbH & Co. KG, Leverkusen, Germany, 2015) while COSMOthermX (version C30_1705; COSMOlogic GmbH & Co. KG, 2017, TZVP basis set level) was used to provide molecular surface charges, σ-profiles, and σ-potentials. COSMO-RS calculations are courtesy of, and authorised for the purposes of, Circa Group Pty Ltd.

GC-O studies: The GC-Olfaction (GC-O) analyses was performed twice by two trained panelists using a Shimadzu GC-2010 Plus instrument equipped with a DB-1MS column (30 m × 0.32 mm × 0.25 µm), a FID detector and a Phaser sniffing port (ex. GL Sciences) and so allowing simultaneous olfactive evaluation and FID peak observation. The split ratio was 4:1 and an AOC-20i auto injector was used. The injection volume was 0.5 µL. Data analysis software including an olfactory voicegram interface kit (ex. GL Sciences) was used. A sample of Cyrene® (**2**) (18 mg, 0.14 mmol) was diluted in MTBE (0.72 g) and injected into the GC-O instrument. The odor of the Cyrene® peak corresponded to the odor of the pure liquid which is described as 'bacon, smoked, vanilla'. The vanilla note is more appreciable on the GC-O. A sample of *iso*-Cyrene (**4**) (36 mg, 0.28 mmol) was diluted in ethyl acetate (1.27 g) and injected into GC-O system. No odour was detected for the *iso*-Cyrene peak.

Plots derived from the single-crystal X-ray analyses of compounds 6, 11 and 12

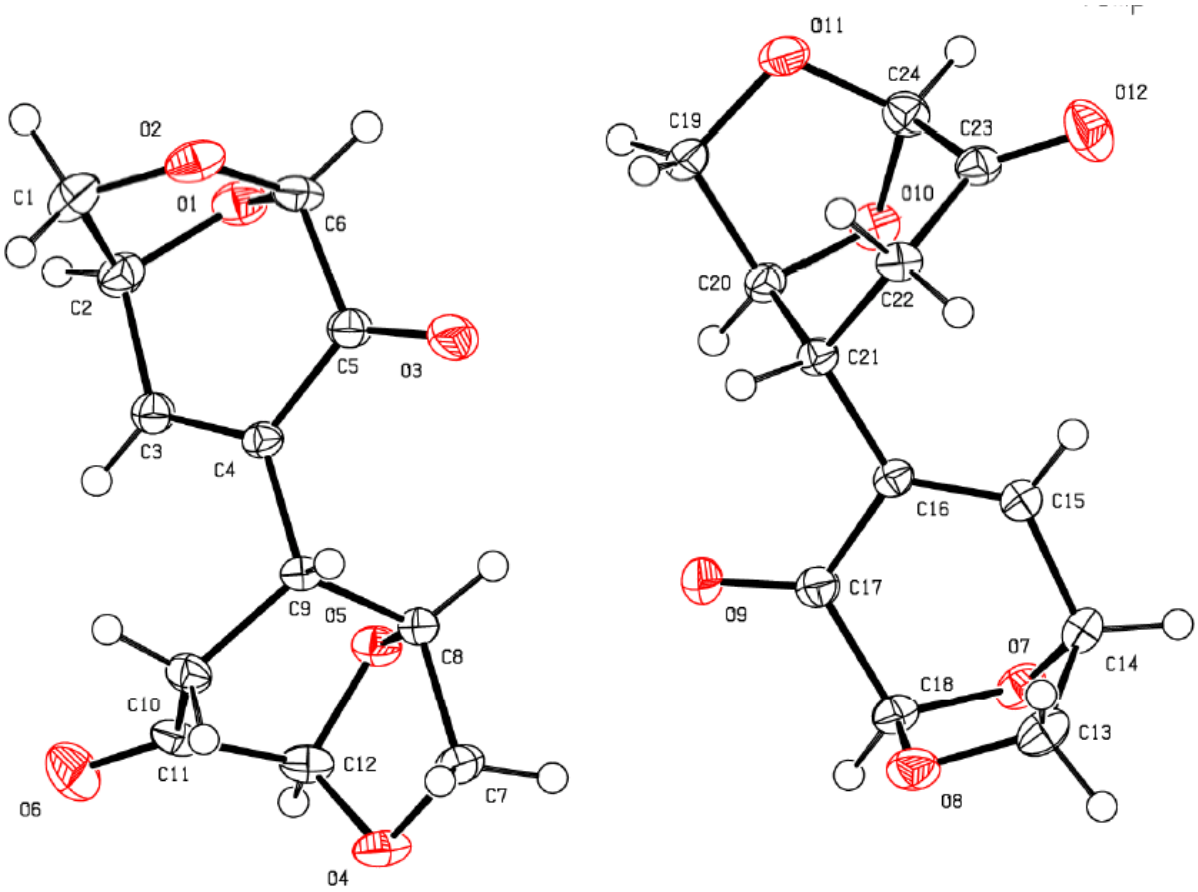

Figure S1: Molecular structure of compound **6** (CCDC 2079098) and showing the relative orientations of the molecules within the unit cell. Atomic displacement parameters shown at 50% probability level (crystal grown from dichloromethane).

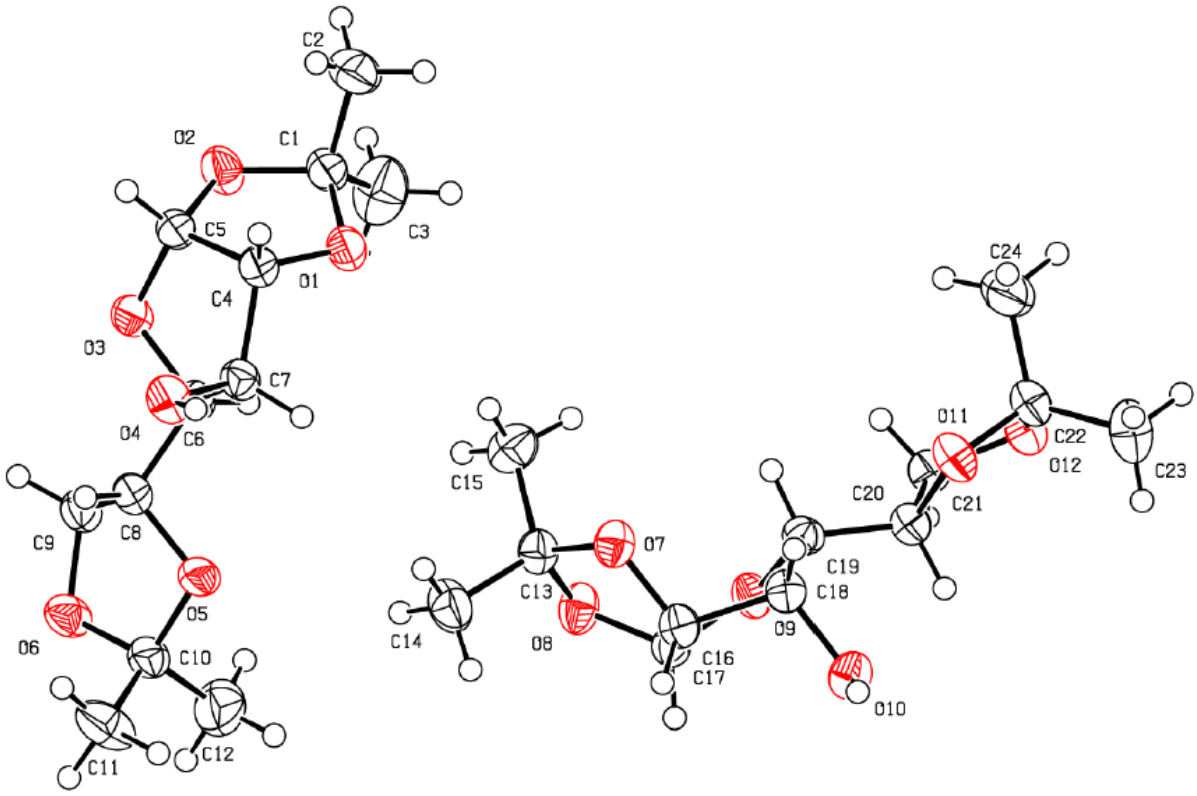

Figure S2: Molecular structure of compound **11** (CCDC 2112086). Atomic displacement parameters shown at 50% probability level (crystal obtained by recrystallisation from hexane).

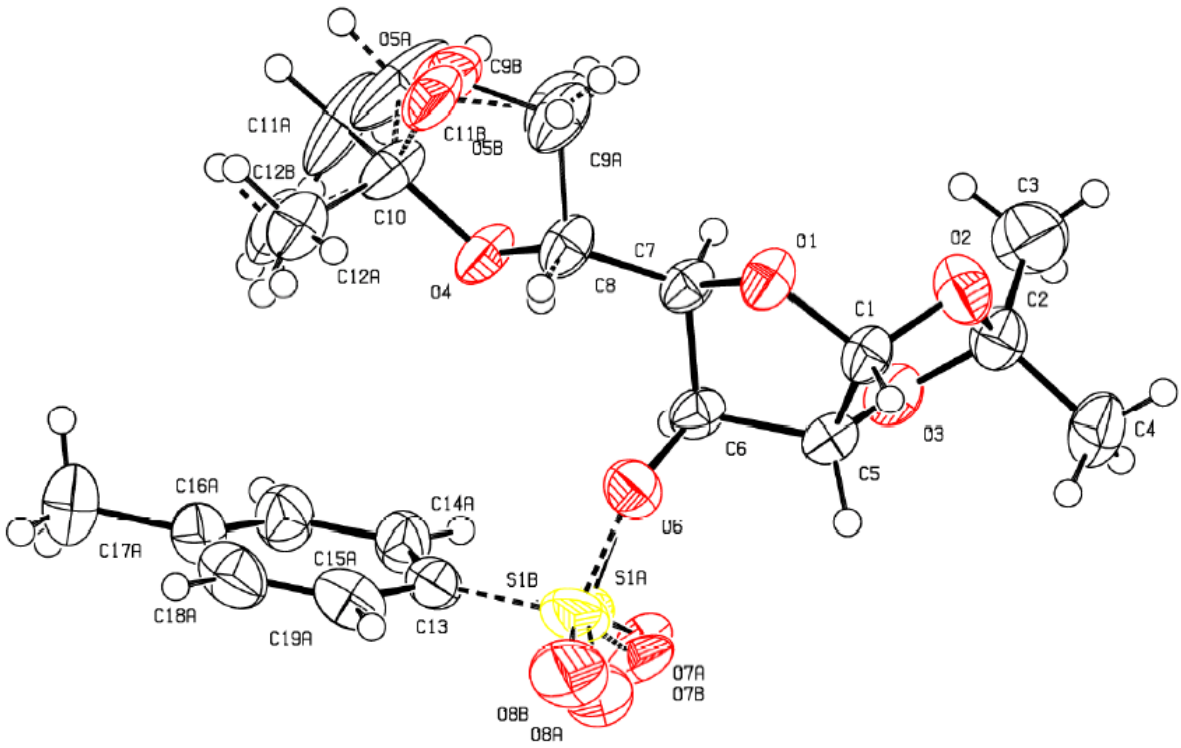

Figure S3: Molecular structure of compound **12** (CCDC 2092948) and showing the relative orientations of the molecules within the unit cell. Atomic displacement parameters shown at 50% probability level (crystal obtained by recrystallisation from ethanol).

Trace arising from the DSC analysis of *iso*-Cyrene (4)

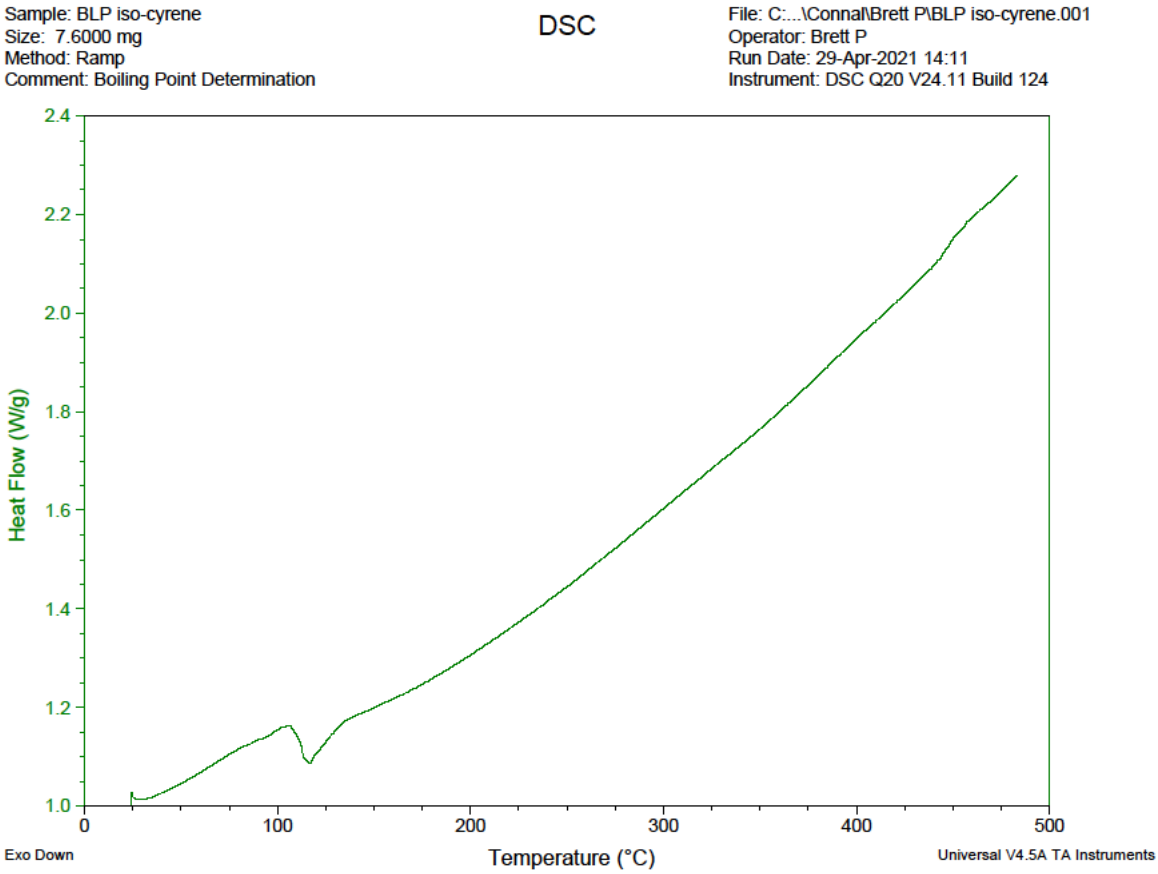

Figure S4: Trace arising from the DSC analysis of *iso*-Cyrene (**4**).

Computationally-derived xyz co-ordinates for compounds 1-4 in the gas phase

Table S1: M06-2X/6-31+G(d,p) optimised xyz coordinates for compounds **1**–**4** in gas phase

1. xyz

C	0.920723	1.340026	-0.278075
C	1.361668	-0.050955	0.000679
C	0.211048	-0.983650	0.403648
C	-0.369020	1.651526	-0.096049
C	-1.324322	0.592883	0.399841
C	-1.687538	-0.384445	-0.737350
H	-2.185613	1.007376	0.923628
H	1.666468	2.048613	-0.623453
H	-0.757993	2.640227	-0.325068
H	-1.800339	0.095298	-1.711866
H	-2.585906	-0.955903	-0.484242
O	2.502437	-0.439605	-0.115035
O	-0.556716	-1.250494	-0.764742
O	-0.643469	-0.299694	1.281092
H	0.570008	-1.909580	0.854316

2. xyz

C	0.834926	1.227279	-0.590226
C	1.354235	-0.094863	-0.052585
C	0.235433	-1.071716	0.328953
C	-0.434512	1.683592	0.158969
C	-1.328598	0.490749	0.492991
C	-1.673696	-0.371828	-0.729635
H	-2.204642	0.787471	1.072350
H	1.635649	1.967774	-0.544908
H	-0.155078	2.164631	1.101468
H	-1.732158	0.206959	-1.657078
H	-2.601490	-0.932690	-0.586308
O	2.523307	-0.373637	0.063851
O	-0.581543	-1.290912	-0.806333
O	-0.580284	-0.439307	1.283835
H	0.625270	-2.013167	0.718393
H	-0.988644	2.417025	-0.436345
H	0.602529	1.053569	-1.649187

Table S1 (contd):

3. xyz

C	-0.930377	1.340121	-0.280979
C	0.370503	1.638436	-0.176795
C	1.335919	0.579022	0.330736
C	-1.364550	-0.041387	0.047690
C	-0.221960	-0.956663	0.480483
C	0.658167	-1.305925	-0.748992
H	-0.599701	-1.817796	1.030587
H	-1.683986	2.037160	-0.632986
H	0.101652	-1.268623	-1.690468
H	1.130839	-2.283801	-0.633385
O	1.675727	-0.305180	-0.726812
O	0.692259	-0.223295	1.287187
H	2.249446	0.992273	0.757691
H	0.767138	2.604368	-0.476079
O	-2.499436	-0.444675	-0.093902

4. xyz

C	-1.048717	1.371580	-0.016713
C	0.420586	1.691146	-0.369500
C	1.347272	0.572341	0.121192
C	-1.315478	-0.117604	0.065375
C	-0.170291	-0.932090	0.670596
C	0.658429	-1.553146	-0.456317
H	-0.537282	-1.637210	1.417231
H	-1.267402	1.762593	0.984665
H	0.052648	-1.908017	-1.292826
H	1.296010	-2.358227	-0.077069
O	1.455139	-0.446786	-0.870172
O	0.781396	-0.052356	1.256674
H	2.346994	0.925013	0.381895
H	0.556788	1.793144	-1.448989
O	-2.329911	-0.654099	-0.316048
H	-1.760756	1.817941	-0.712418
H	0.709198	2.637319	0.096085

van der Waals surfaces of compounds 2 and 4

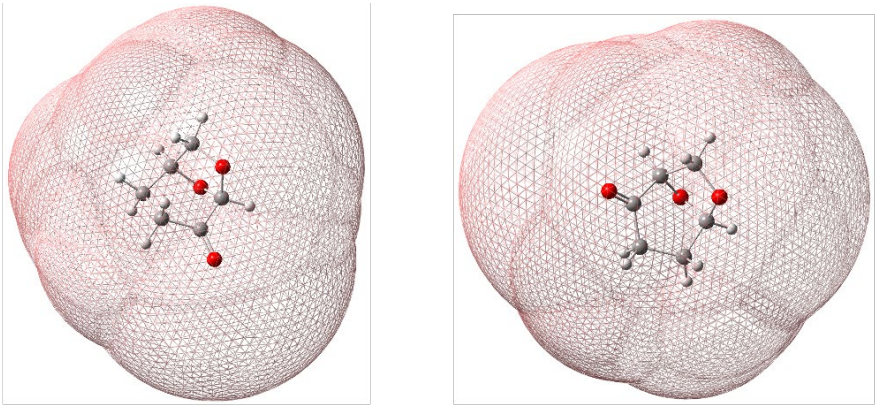

2 **4**

Cavity surface area: 528.712 Å^2 527.591 Å^2
Cavity volume : 1104.326 Å^3 1101.616 Å^3

Figure S5: (Top) Van der Waals surfaces of compound **2** and **4** representing the solute-solvent boundary in cyclohexane, as calculated with SMD/M062X/6-31+G(d,p), based on gas-phase optimised M062X/6-31+G(d,p) geometries; (Bottom) Solvent accessible surfaces of compound **2** and **4** representing the solute-solvent boundary in cyclohexane, as calculated with SMD/M062X/6-31+G(d,p) and based on gas-phase optimised M062X/6-31+G(d,p) geometries.

σ-Potential curves of NMP, Cyrene® and *iso*-Cyrene

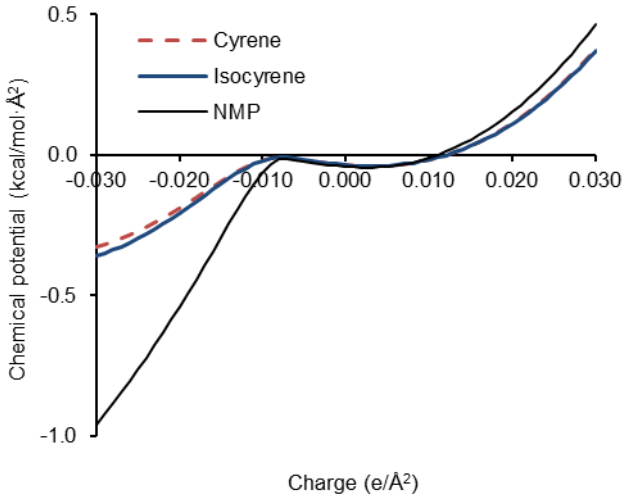

Figure S6: σ-Potential curves of NMP, Cyrene™, and *iso*-Cyrene derived from COSMO calculations.

400 MHz ^{1}H NMR Spectrum of Compound **3** (ex. Swern oxidation) (recorded in $CDCl_3$)

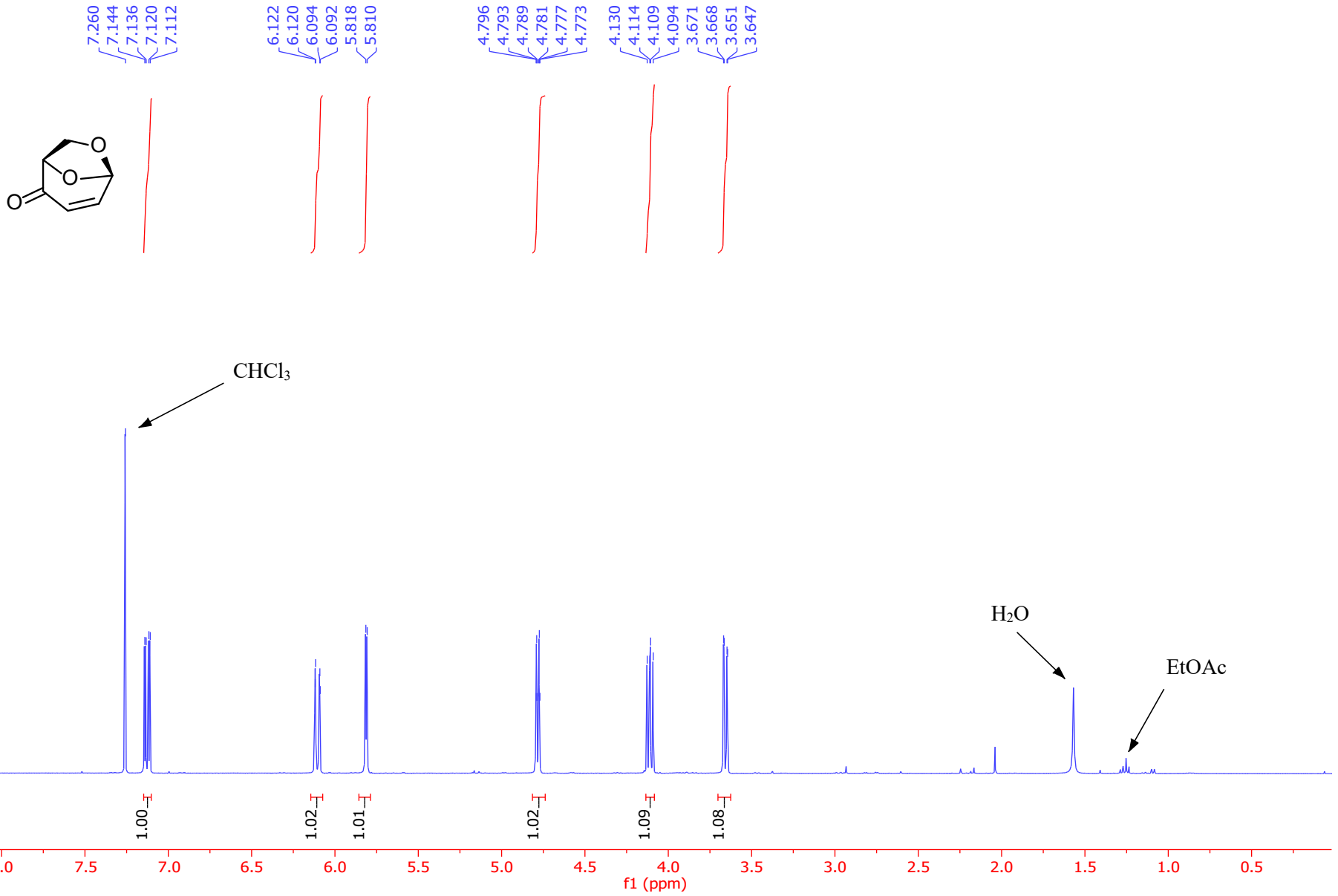

176 MHz $^{13}C\{^{1}H\}$ NMR Spectrum of Compound **3** (ex. Swern oxidation) (recorded in $CDCl_3$)

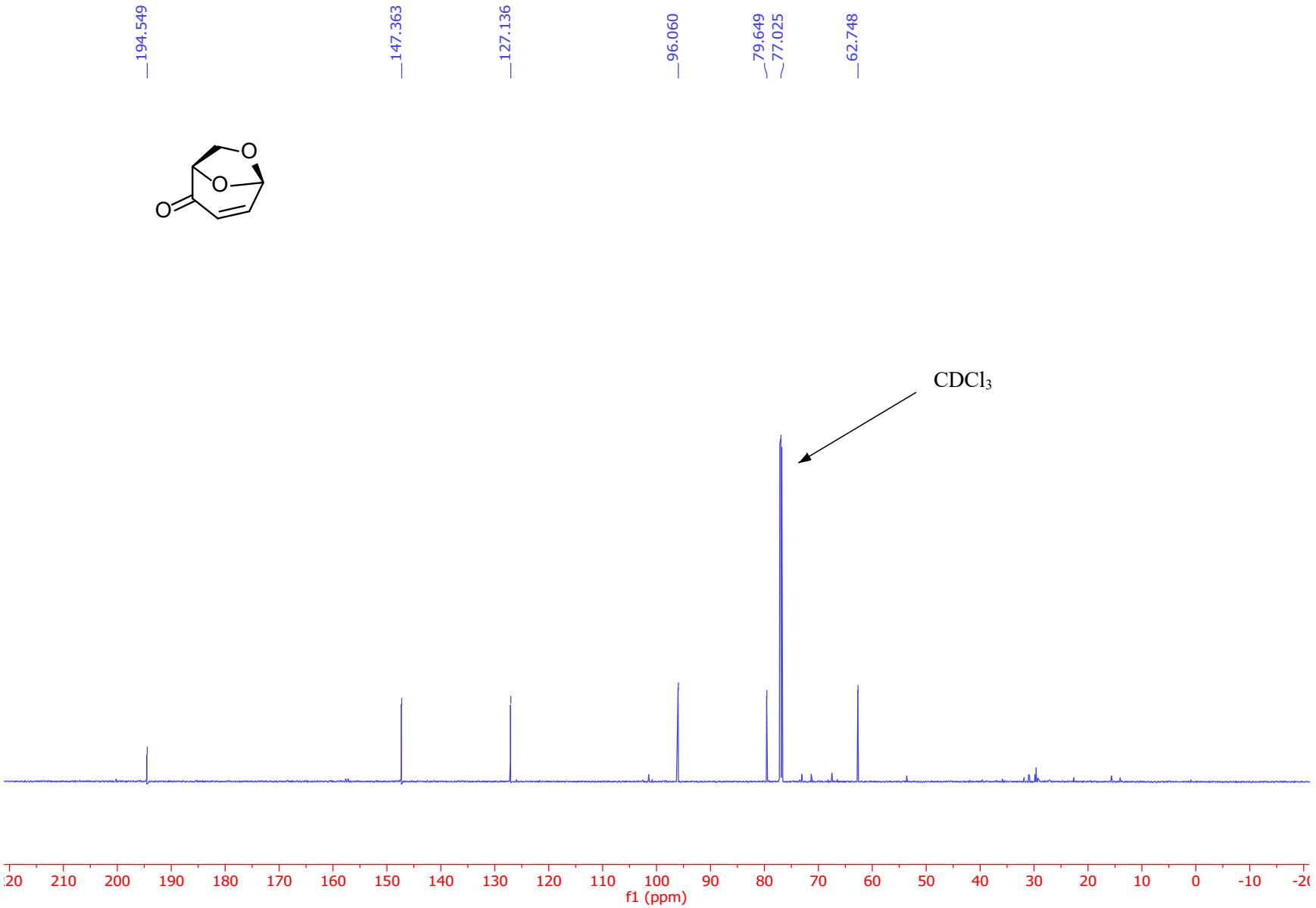

400 MHz ^{1}H NMR Spectrum of Compound **3** (ex. the Horton route) (recorded in $CDCl_3$)

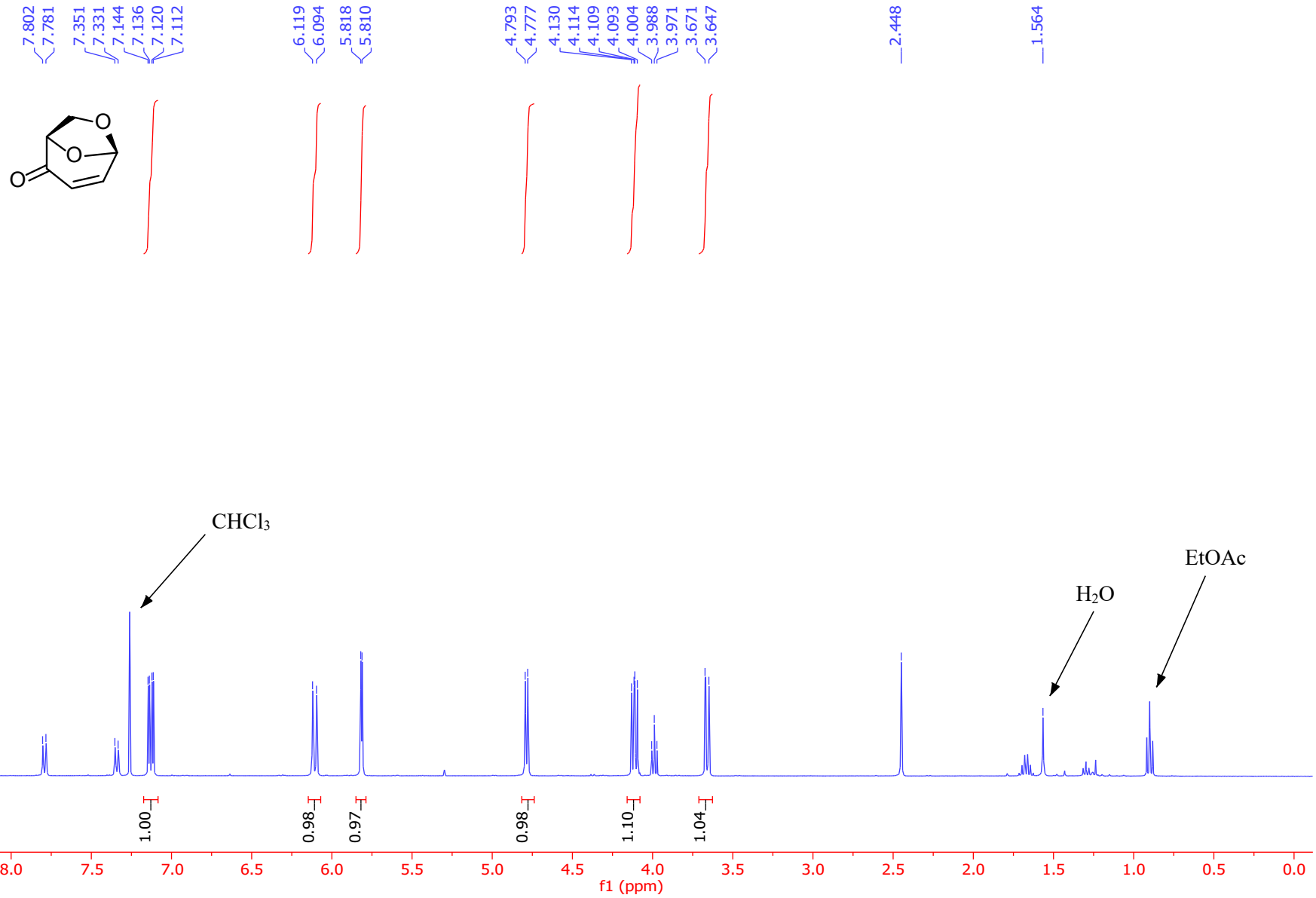

101 MHz $^{13}C\{^{1}H\}$ NMR Spectrum of Compound **3** (ex. the Horton route) (recorded in $CDCl_3$)

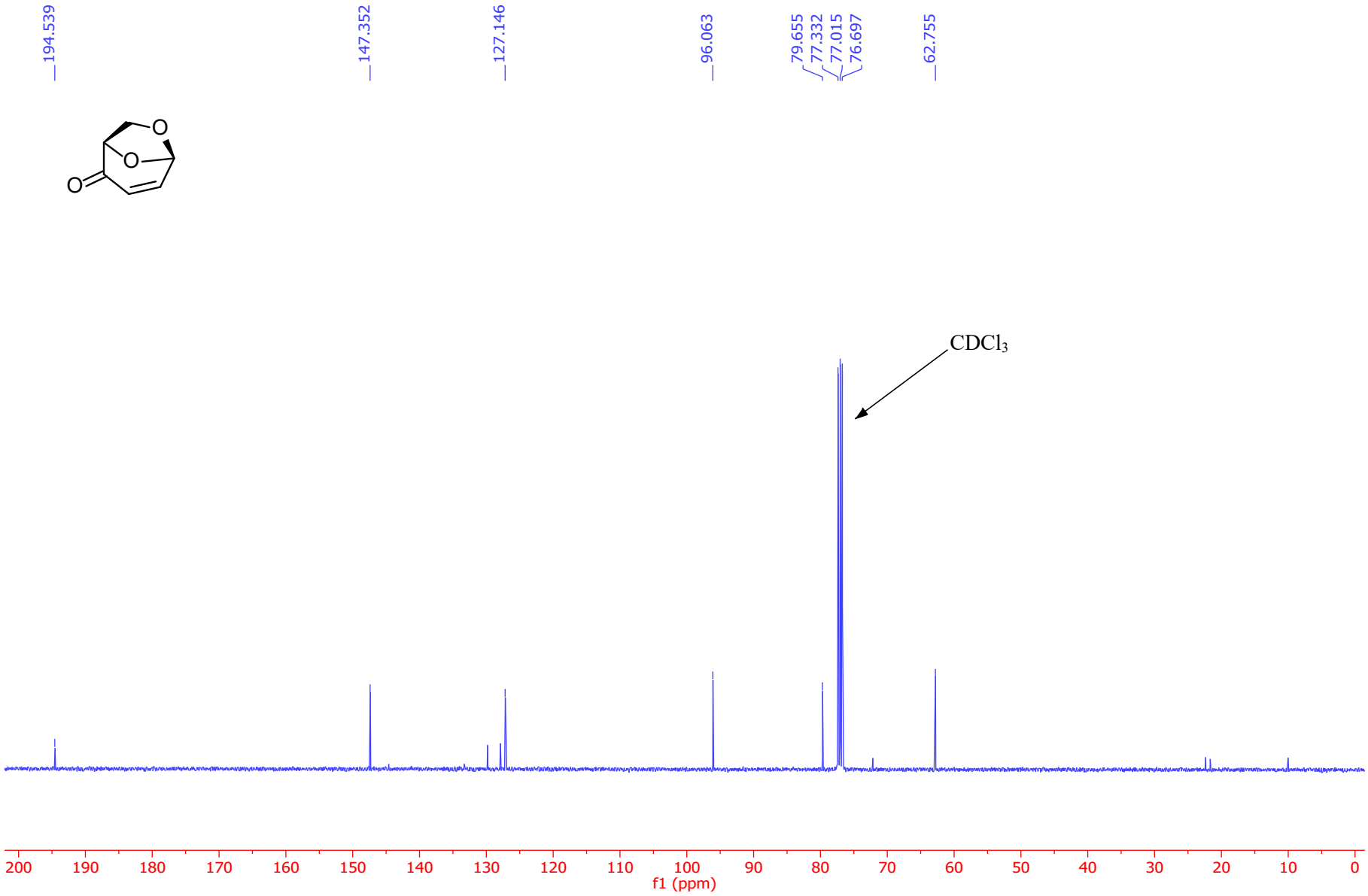

400 MHz ^{1}H NMR Spectrum of Compound **4** (recorded in $CDCl_3$)

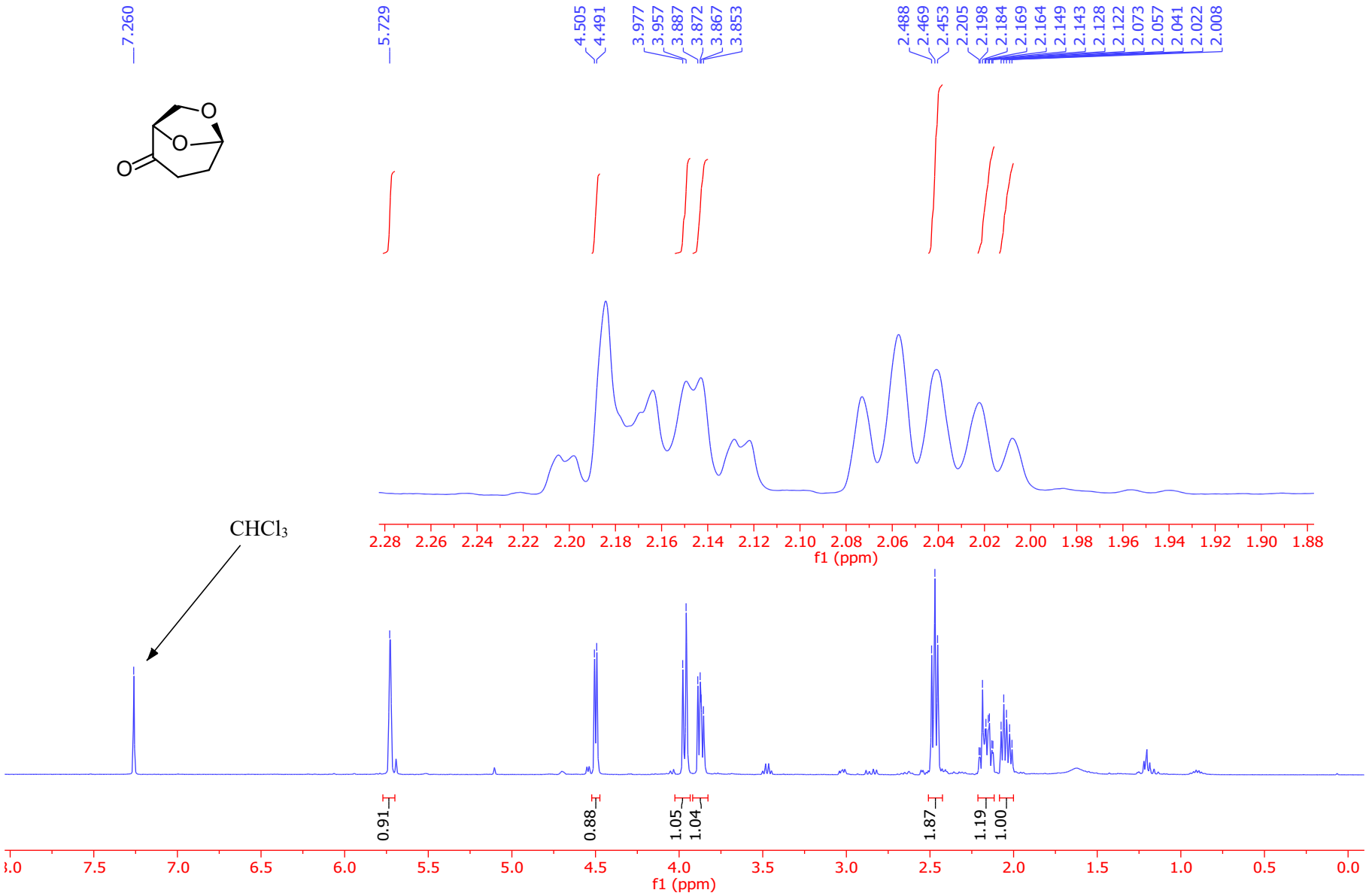

101 MHz $^{13}C\{^{1}H\}$ NMR Spectrum of Compound **4** (recorded in $CDCl_3$)

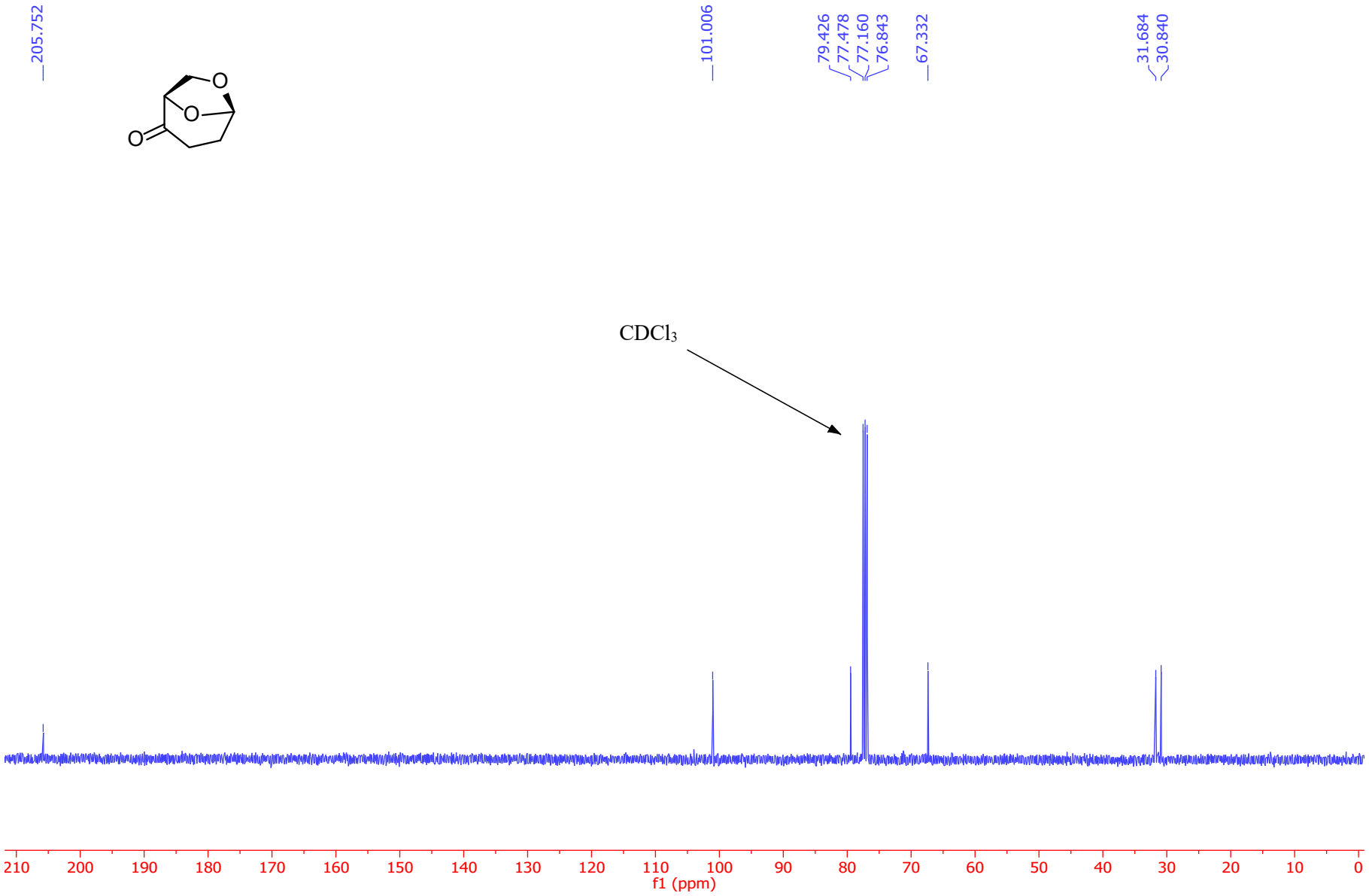

400 MHz ^{1}H NMR Spectrum of Compound **5** (recorded in $CDCl_3$)

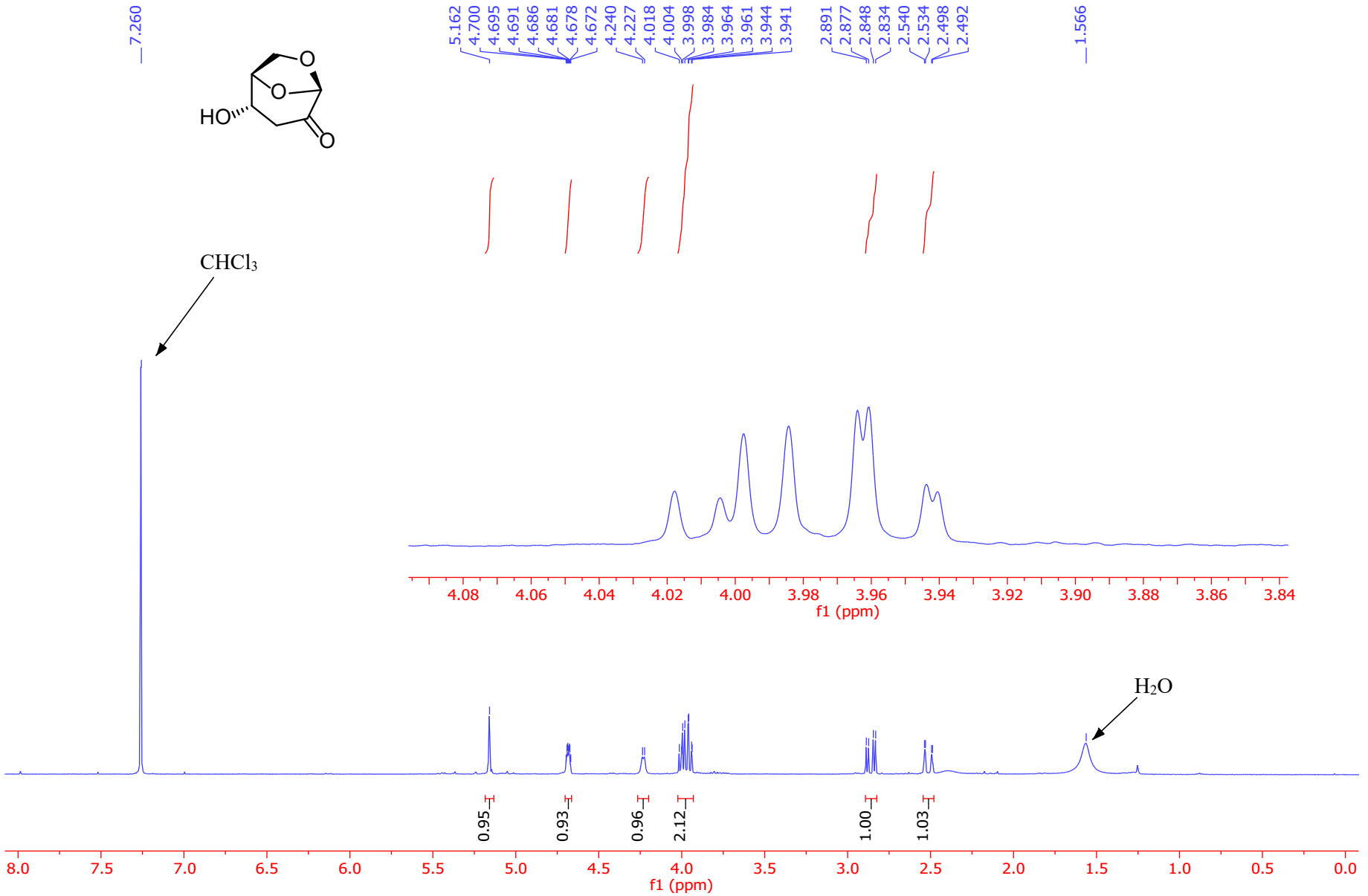

101 MHz $^{13}C\{^{1}H\}$ NMR Spectrum of Compound **5** (recorded in $CDCl_3$)

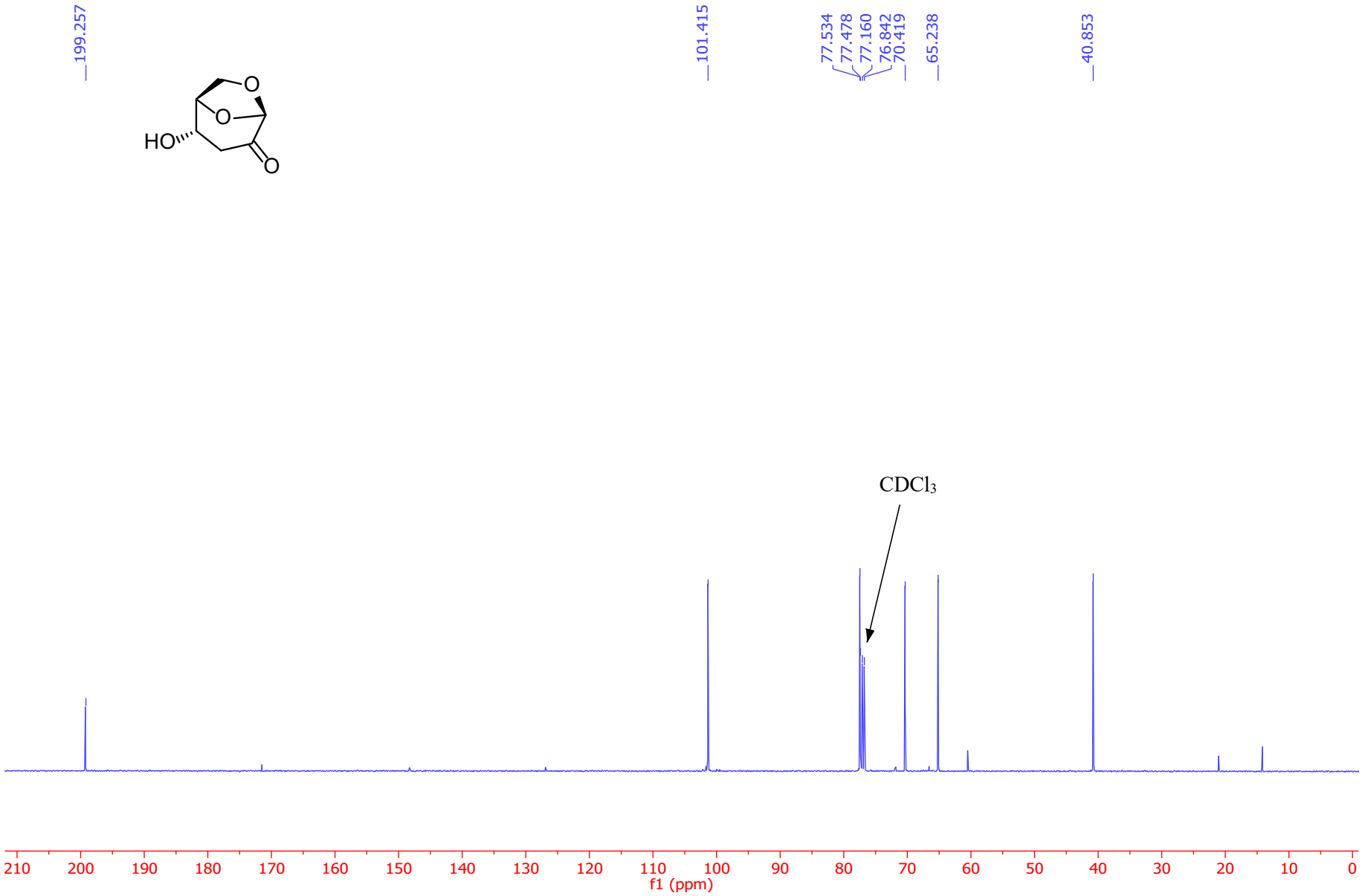

400 MHz ^{1}H NMR Spectrum of Compound **6** (recorded in $CDCl_3$)

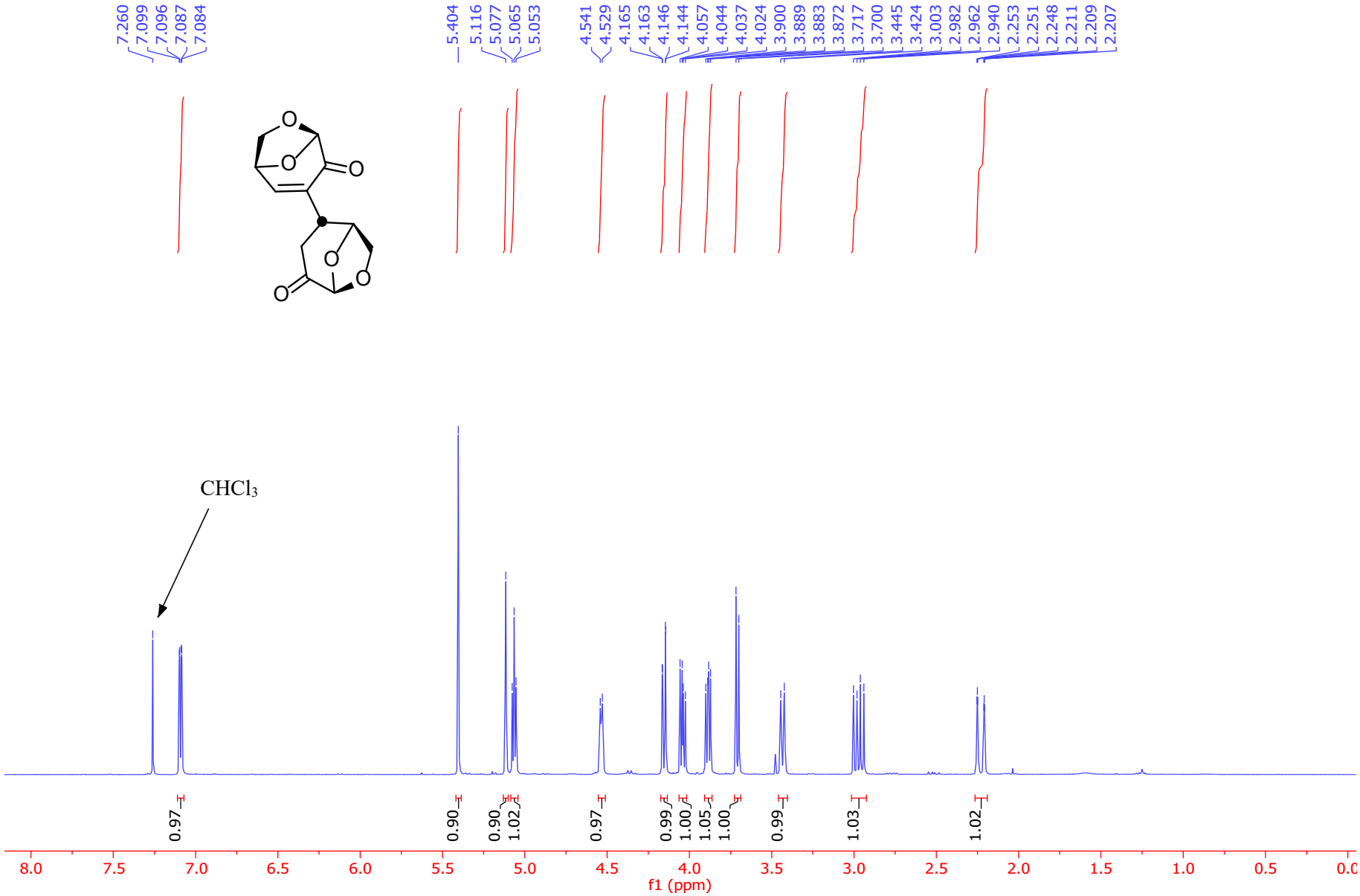

101 MHz $^{13}C\{^{1}H\}$ NMR Spectrum of Compound **6** (recorded in $CDCl_3$)

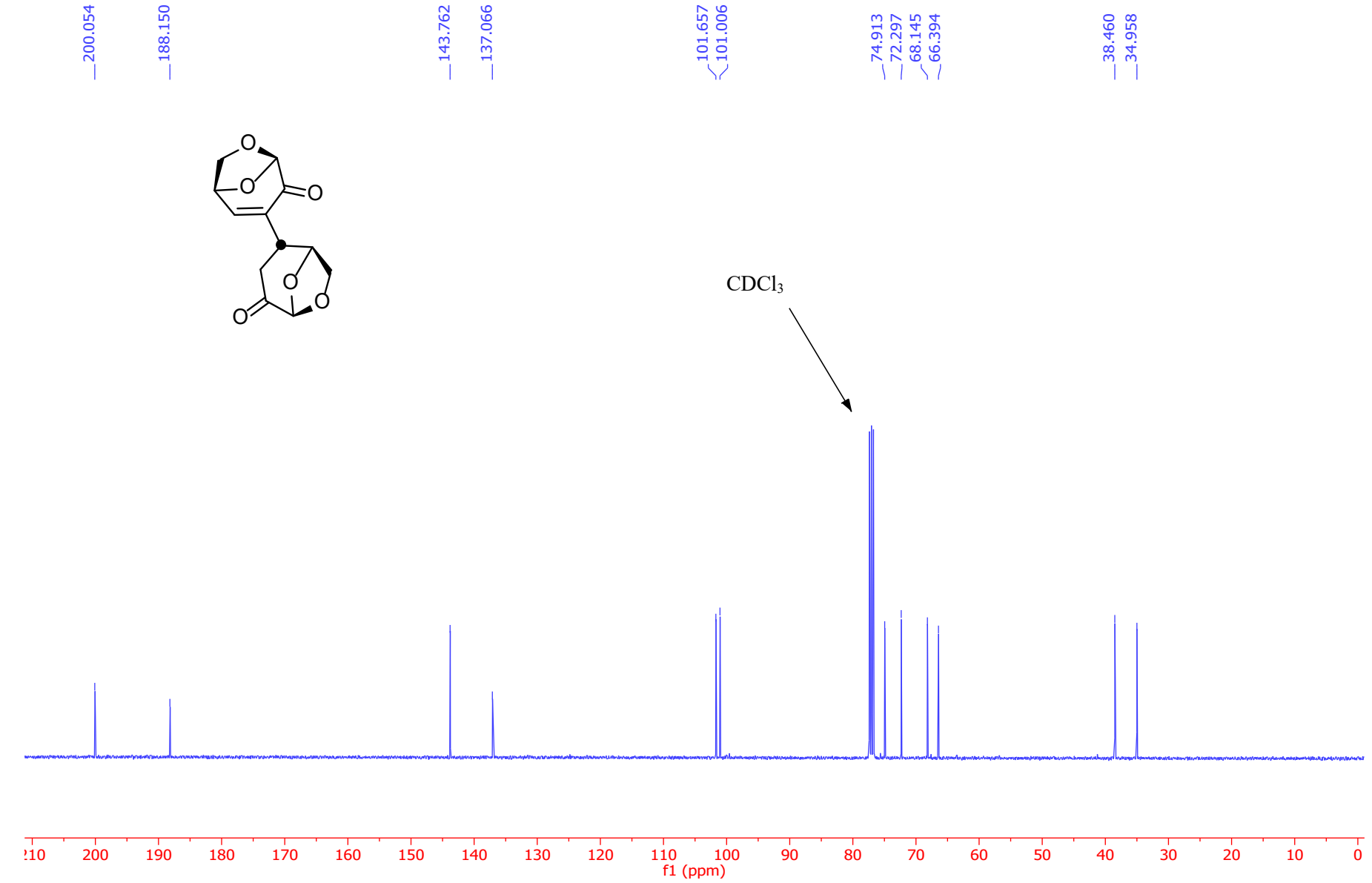

400 MHz ^{1}H NMR Spectrum of Compound **7** (recorded in $CDCl_3$)

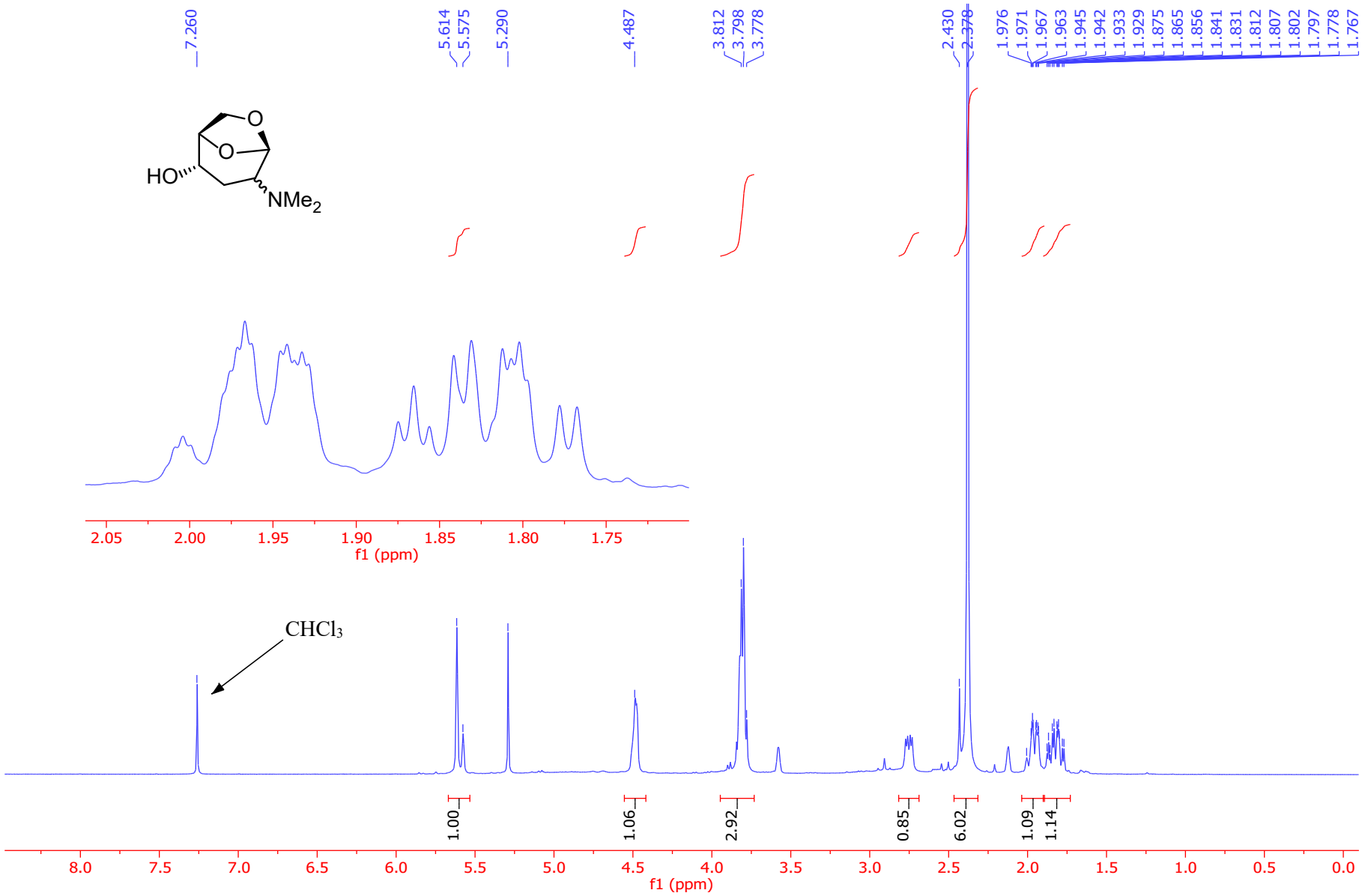

101 MHz $^{13}C\{^{1}H\}$ NMR Spectrum of Compound **7** (recorded in $CDCl_3$)

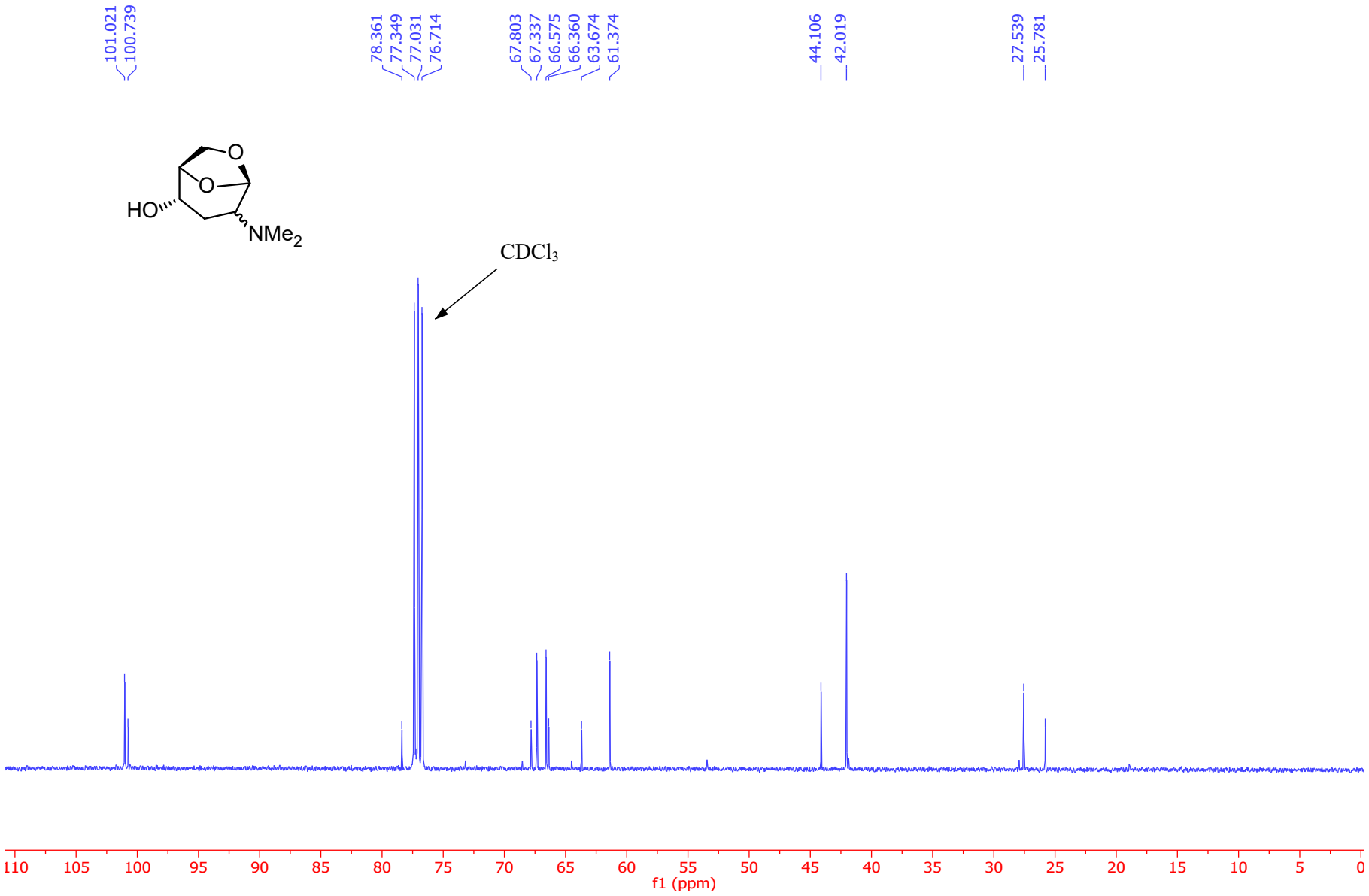

400 MHz ^{1}H NMR Spectrum of Compound **9** (recorded in $CDCl_3$)

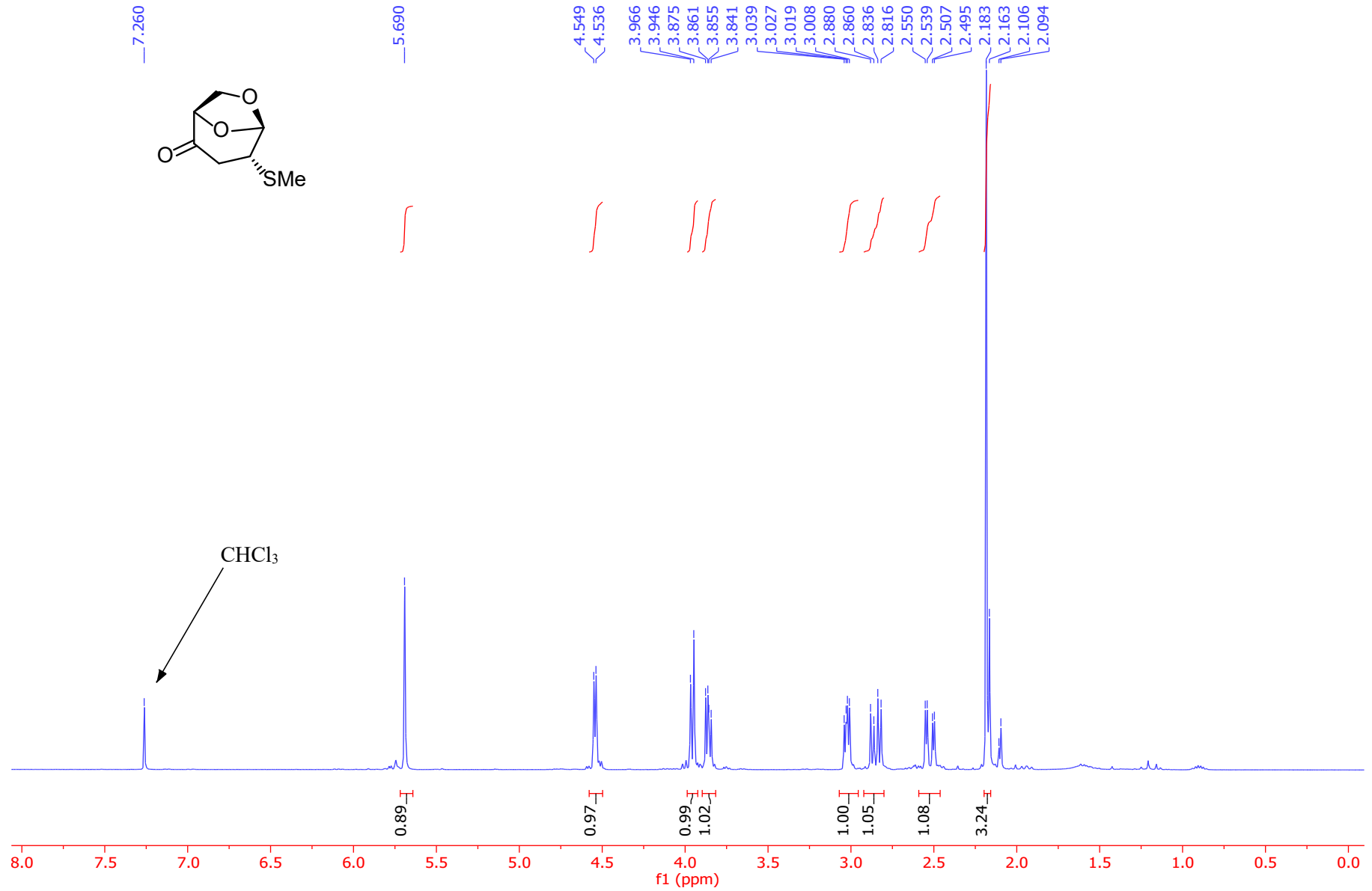

101 MHz $^{13}C\{^{1}H\}$ NMR Spectrum of Compound **9** (recorded in $CDCl_3$)

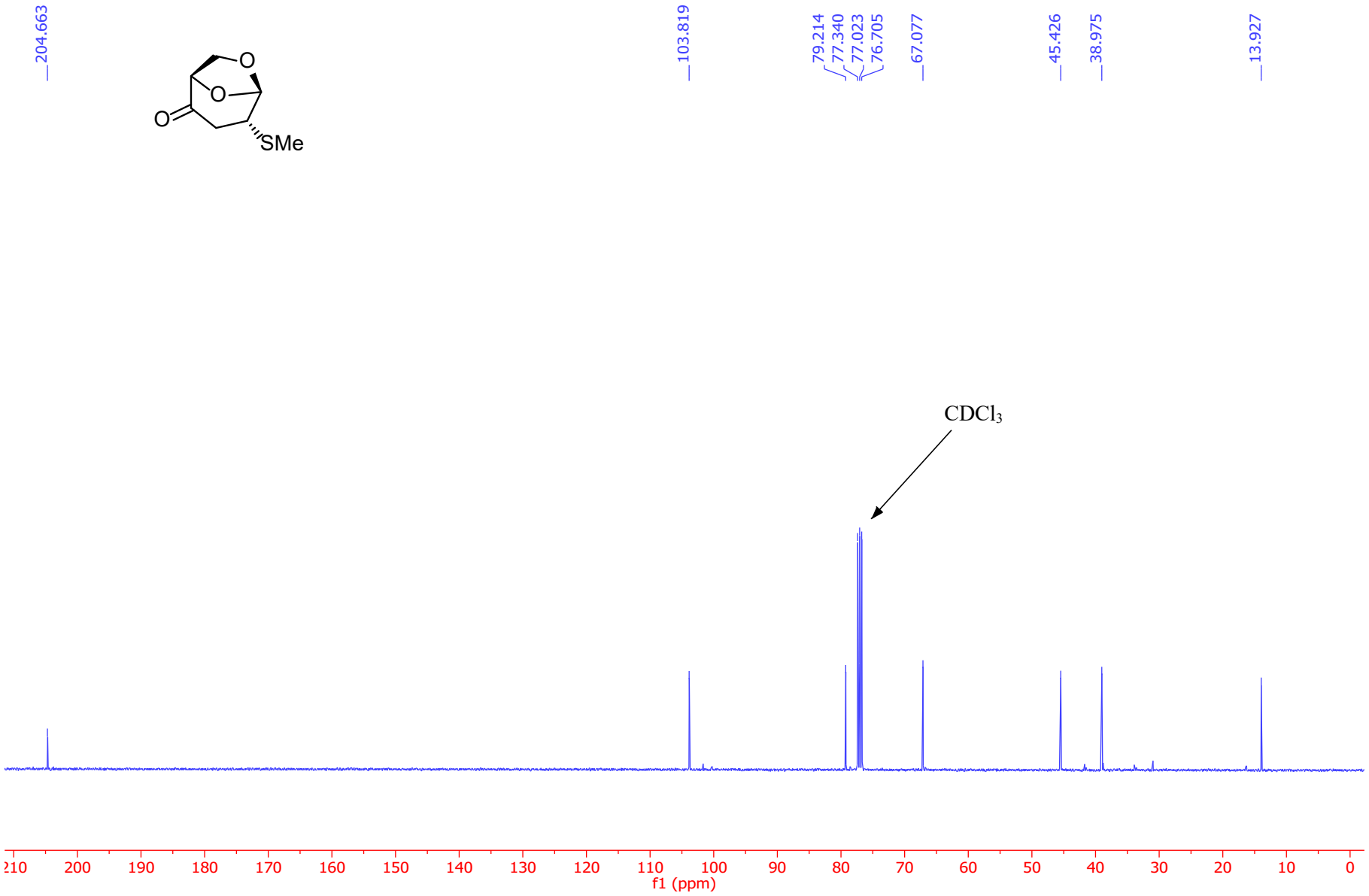

400 MHz ^{1}H NMR Spectrum of Compound **11** (recorded in $CDCl_3$)

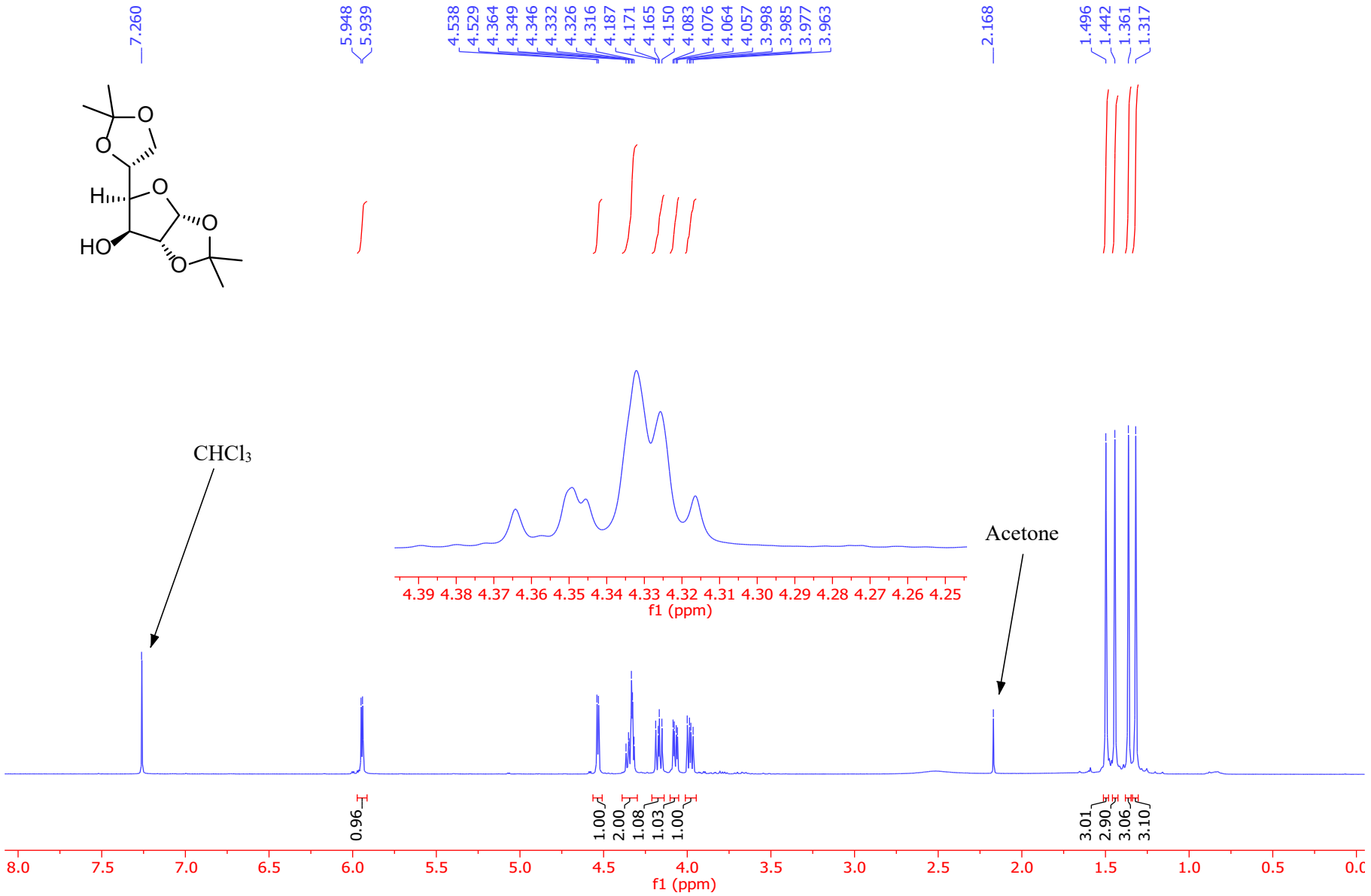

101 MHz $^{13}C\{^{1}H\}$ NMR Spectrum of Compound **11** (recorded in $CDCl_3$)

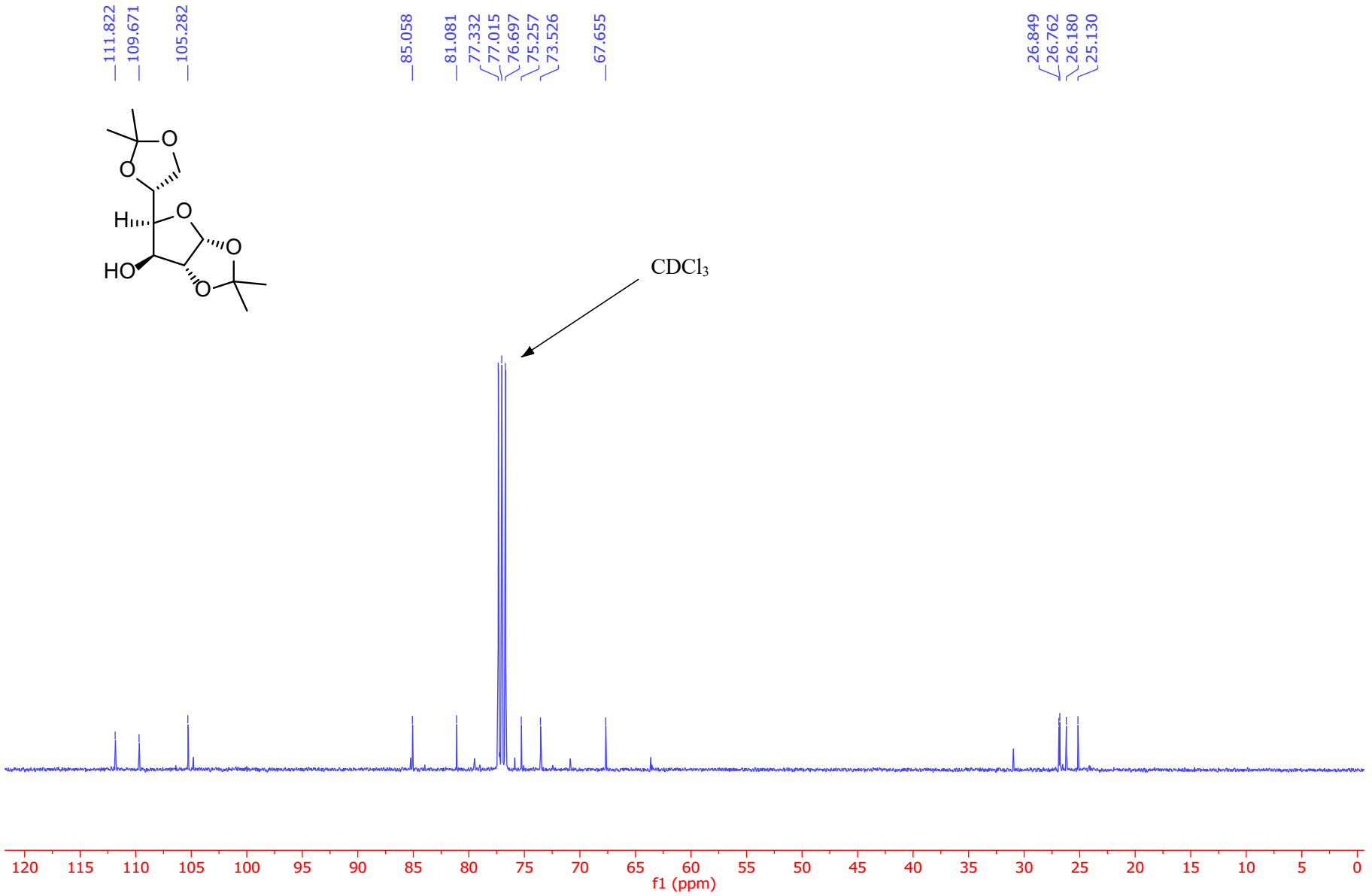

400 MHz ^{1}H NMR Spectrum of Compound **12** (recorded in $CDCl_3$)

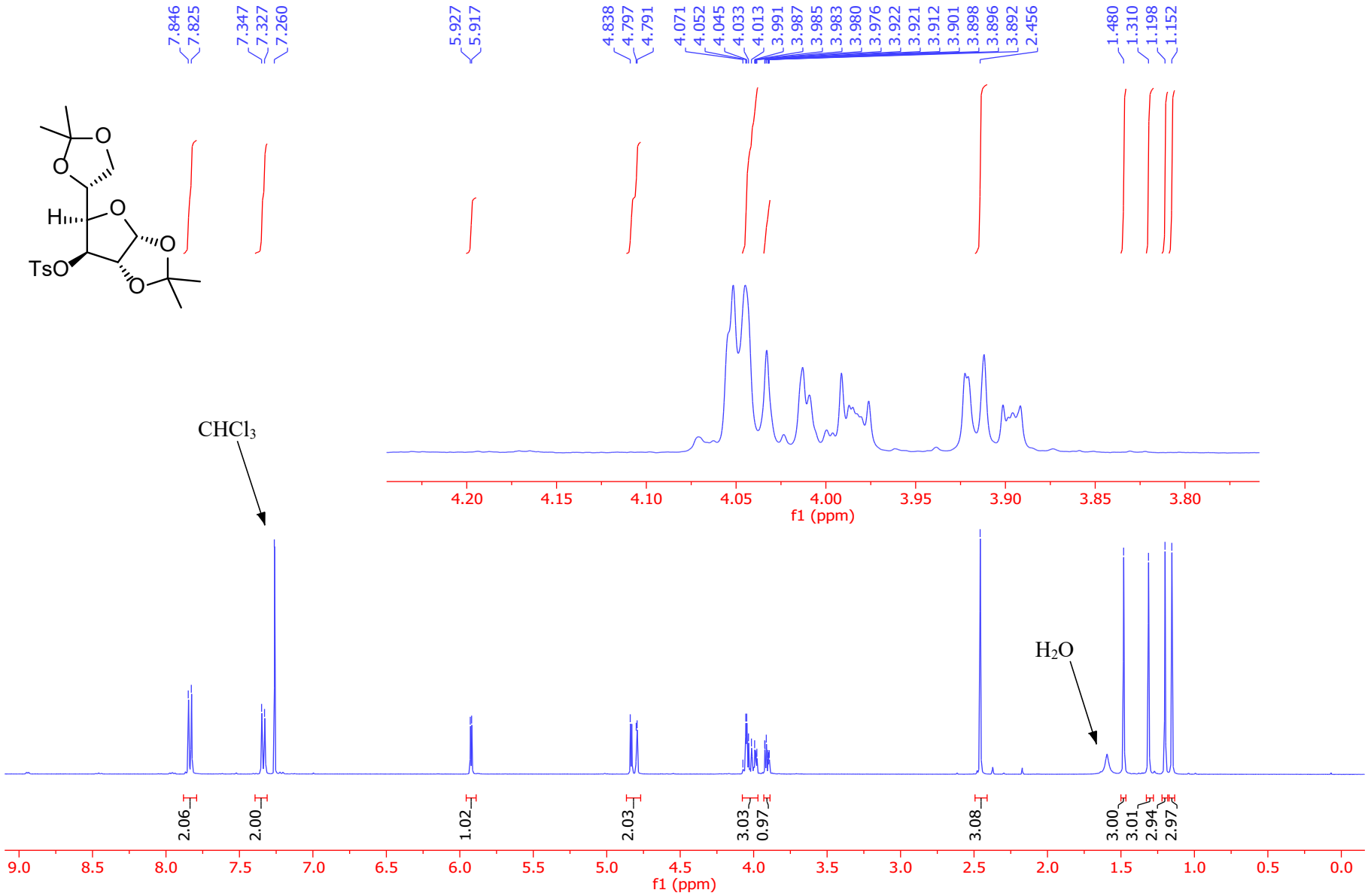

^{1}H NMR spectrum of the product mixture obtained after treating Cyrene® (**2**) with 2 M aq. HCl (recorded in DMSO-d_6)

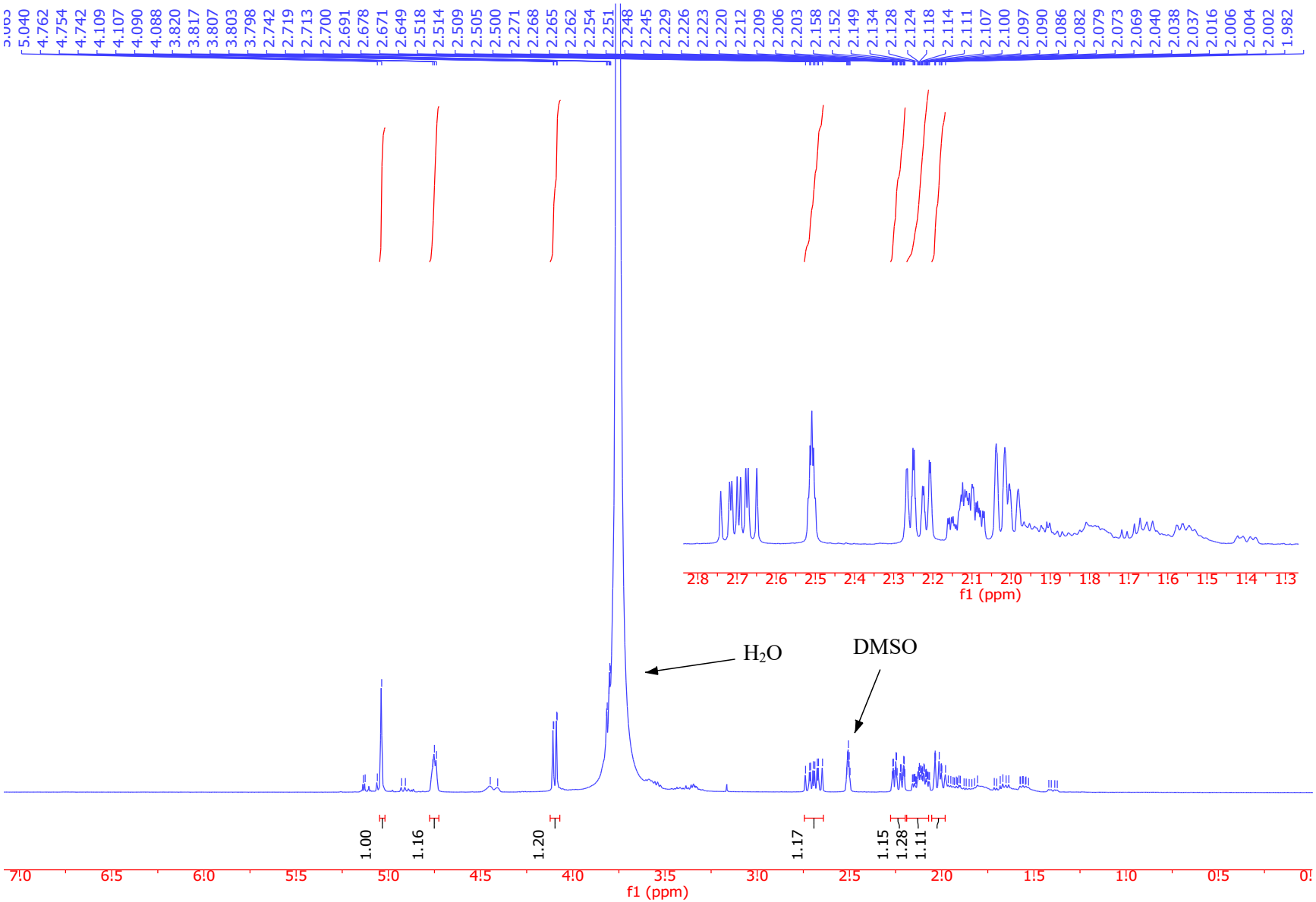

^{1}H NMR spectrum of the product mixture obtained after treating *iso*-Cyrene (**4**) with 2 M aq. HCl (recorded in DMSO-d_6)

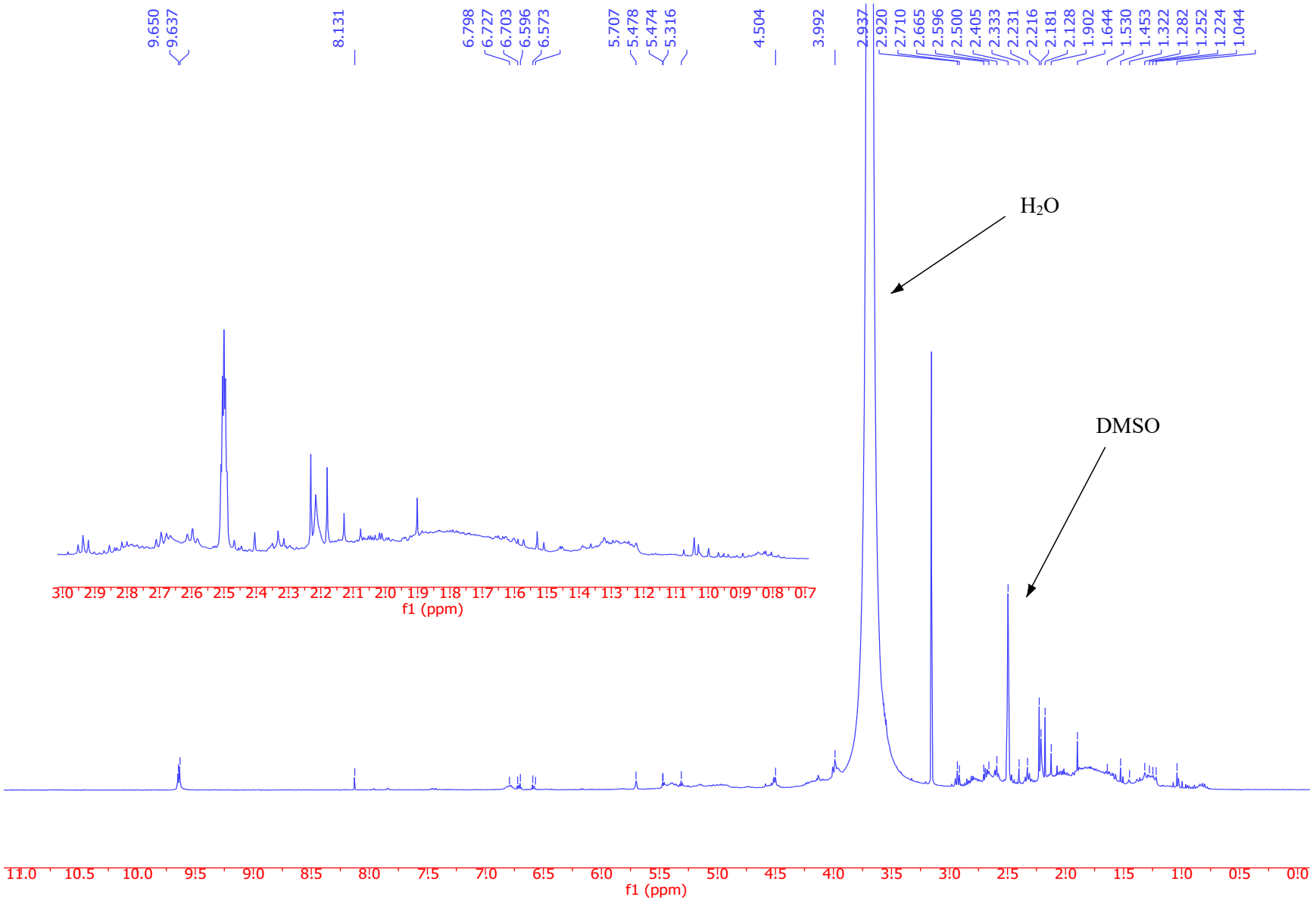

References and Footnotes

1. (a) Gu, Y. L.; Jerome F. *Chemical Society Reviews,* **2013**, *42*, 9550-9570; (b) Clarke, C. J.; Tu, W.-C.; Levers, O.; Bröhl, A.; Hallett, J. P. *Chemical Reviews*, **2018**, *118*, 747-800; (c) Jordan, A.; Hall, C. G. J.; Thorp, L. R.; Sneddon, H. F. *Chemical Reviews,* **2022**, *122*(6), 6749-6794.
2. Sherwood, J.; De bruyn, M.; Contantinou, A.; Moity, L.; McElroy, C. R.; Farmer, T. J.; Duncan, T.; Raverty, W.; Hunt, A. J.; Clark, J. H. *Chemical Commun*ications, **2014**, *50*, 9650-9652.
3. (a) Pacheco, A. A. C.; Sherwood, J.; Zhenova, A.; McElroy, C. R.; Hunt, A. J.; Parket, H. L.; Farmer, T. J.; Constantinou, A.; De bryun, M.; Whitwood, A. C.; Raverty, W.; Clark, J. H. *Chemistry Sustainable Chemistry*, **2016**, *9*, 3503-3512. Also, see: (b) Milescu, R. A.; Zhenova, A.; Vastano, M.;Gammons, R.; Lin, S.; Lau, C. H.; Clark, J. H.; McElroy, C. R.; Pellis, A. *Chemistry Sustainable Chemistry,* **2021**, *14*, 3367-3381.
4. Camp, J. E. *Chemistry Sustainable Chemistry*, **2018**, *11*, 3048-3055.
5. See https://www.circagroup.com.au/cyrene (accessed 26/02/2022).
6. (a) Zhang, J.; White, G. B.; Ryan, M. D.; Hunt, A. J.; Katz, M. J. *ACS Sustainable Chemical Engineering,* **2016**, *4*, 7186-7192; (b) Camp, J. E.; Nyamini, S. B.; Scott, F. J. *RSC Medicinal Chemistry,* **2020**, *11*, 111-117; (c) See https://echa.europa.eu/registration-dossier/-/registered-dossier/16252 (accessed 26/02/2022).
7. Ma, X.; Anderson, N.; White, L. V.; Bae, S.; Raverty, W.; Willis, A. C.; Banwell, M. G. *Australian Journal of Chemistry,* **2015**, *68*, 593-599.
8. (a) Ma, X.; Liu, X.; Yates, P.; Rafferty, W.; Banwell, M. G.; Ma, C.; Willis, A. C.; Carr, P. D. *Tetrahedron* **2018**, *74*, 5000-5011; (b) Diot-Néant, F.; Mouterde, L. M. M.; Couvreur, J.; Brunois, F.; Miller, S. A.; Allais, F. *European Polymer Journal*, **2021**, *159*, 110745.
9. (a) Pecka, J.; Stanek, J.; Cerny, M. *Collection of Czechoslovak Chemical Communications,* **1974**, *39*, 1192-1209; (b) Ton-That, T. *Nucleosides Nucleotides*, **1999**, *18*, 731-732.
10. Ledingham, E. T.; Greatrex, B. W. *Tetrahedron*, **2018**, *74*, 6107-6115.
11. Klepp, J.; Sumby, C. J.; Greatrex, B. W. *Synlett.* **2018**, *29*, 1441-1446.
12. (a) De bruyn, M.; Budarin, V. L.; Misefari, A.; Shimizu, S.; Fish, H.; Crockett, M.; Hunt, A. J.; Hofstetter, H.; Weckhuysen, B. M.; Clark, J. H.; Macquarie D. J. *ACS Sustainable Chemical Engineering* **2019**, *7*, 7878-7883; (b) Bousfield, T. W.; Pearce, K. P. R.; Nyamini, S. B.; Angelis-Dimakis, A.;, J. E. *Green Chemistry,* **2019**, *21*, 3675-3681
13. (a) Rennecke, R.-W.; Eberstein, K.; Köll, P. *Chemische Berichte,* **1975**, *108*, 3652-3655; (b) Shafizadeh, F.; Furneaux, R. H.; Stevenson, T. T. *Carbohydrate Research*, **1979**, *71*, 169-191.
14. Mouterde, L. M. M.; Allais, F.; Stewart, J. D. *Green Chemistry*, **2018**, *20*, 5528-5532.
15. (a) Shafizadeh, F.; Furneaux, R. H.; Pang, D.; Stevenson, T. T. *Carbohydrate Research,* **1982**, *100*, 303-313; (b) Kawai, T.; Isobe, M.; Peters, S. C. *Aust. J. Chem*. **1995**, *48*, 115-131; (c) Samet, A. V.;

Niyazymbetov, M. E.; Semenov, V. V.; Laikhter, A. L.; Evans, D. H. *Journal of Organic Chemistry,* **1996**, *61*, 8786-8791; (d) Sharipov, B. T.; Pilipenko, A. N.; Valeev, F. A. *Russian Journal of Organic Chem*istry, **2014**, *50*, 1628-1635; (e) Diot-Néant, F.; Mouterde, L.; Fadlallah, S.; Miller, S. A.; Allais, F. *Chemistry Sustainable Chemistry,* **2020**, *13*, 2613-2620.

16. Jeon, S.; Han, S. *Journal of the American Chemical Soc*iety, **2017**, *139*, 6302-6305 and references cited therein.
17. Mancuso, A. J.; Swern, D. *Synthesis*, **1981**, 165-185.
18. For examples of the reactions of episulfonium ions with nitrogen-centred nucleophiles see Fox, D. J.; Morley, T. J.; Taylor, S.; Warren, S. *Organic Biomolecular Chem*istry, **2005**, *3*, 1369-1371.
19. Horton, D.; Roski, J. P.; Norris, P. *Journal of Organic Chemistry,* **1996**, *61*, 3783-3793.
20. A single-crystal X-ray analysis of compound **12** has been reported previously although this did not establish, in contrast to the one reported here, its absolute configuration: Mamat, C.; Peppel, T.; Köckerling, M. *Crystals*, **2012**, *2*, 105-109.
21. Cantacuzene, J.; Petrissane, J.; Dang-Quoc-Quan. *Tetrahedron Letters*, **1967**, 2543-2545.
22. Hughes, L.; McElroy, C. R.; Whitwood, A.C.; Hunt, A. J. *Green Chemistry,* **2018**, *20*, 4423-4427 and references cited therein.
23. (a) Klamt, A.; Jonas, V.; Bürger, T.; Lohrenz, J. C. W. *Journal of Physical Chemistry,* **1998**, *102*, 5074-5085; (b) Klamt, A. *Wiley Interdiscip. Rev.: Computational. Molecular Science,* **2018**, *8*, e1338.
24. Trasande, L. *The Lancet Planetary Health*, **2017**, *1*, e88-e89 and references cited therein.
25. Piersma, A. H.; Bosgra, S.; van Duursen, M. B. M.; Hermsen, S. A. B.; Jonker, L. R. A.; Kroese, E. D.; van der Linden, S. C.; Man, H.; Roelofs, M. J. E.; Schulpen, S. H. W.; Schwarz, M.; Uibel, F.; van Vugt-Lussenburg, B. M. A.; Westerhout, J.; Wolterbeek, A. P. M.; van der Burg, B. *Reproductive Toxicology*, **2013**, *38*, 53-64.
26. Schenk, B.; Weimer, M.; Bremer, S.; van der Burg, B.; Cortvrindt, R.; Freyberger, A.; Lazzari, G.; Pellizzer, C.; Piersma, A.; Schäfer, W. R.; Seiler, A.; Witters, H.; Schwarz, M. *Reproductive Toxicology*, **2010**, *30*, 200-218
27. van der Burg, B.; Pieterse, B.; Buist, H.; Lewin, G.; van der Linden, S. C.; Man, H.-y.; Rorije, E.; Piersma, A. H.; Mangelsdorf, I.; Wolterbeek, A. P. M.; Kroese, E. D.; van Vugt-Lussenburg, B. *Reproductive Toxicology*, **2015**, *55*, 95-103.
28. A Panel of Quantitative Calux® Reporter Gene Assays for Reliable High-Throughput Toxicity Screening of Chemicals and Complex Mixtures in *High-Throughput Screening Methods in Toxicity Testing*, ed. Steinberg, P.; John Wiley & Sons (Hoboken, New Jersey, USA), 2013, pp 519-532.
29. van der Burg, B.; Wedebye, E. B.; Dietrich, D. R.; Jaworska, J.; Mangelsdorf, I.; Paune, E.; Schwarz, M.; Piersma, A. H.; Kroese, E. D. *Reproductive Toxicology*, **2015**, *55*, 114-123.

30. Krebs, A. et al. *Alternatives to Animal Experimentation*, **2019**, *36*, 682-699.
31. Krebs, A., et al., *Archives of Toxicology*, **2020**, *94*, 2435-2461.
32. Byrne, F. P.; Nussbaumer, C. M.; Savin, E. J.; Milescu, R. A.; McElroy, C. R.; Clark, J. H.; van Vugt-Lussenburg, B. M. A.; van der Burg, B.; Meima, M. Y.; Buist, H. E.; Kroese, E. D.; Hunt, A. J.; Farmer, T. J. *Chemistry Sustainable Chemistry*, **2020**, *13*, 3212-3221.
33. van Vugt-Lussenburg, B. M. A.; van Es, D. S.; Naderman, M.; le Notre, J.; Klis, F. v. d.; Brouwer, A.; van der Burg, B. *Green Chemistry*, **2020**, *22*, 1873-1883.
34. Brattoli, M.; Cisternino, E.; Dambruoso, P. R.; de Gennaro, G.; Giungato, P.; Mazzone, A.; Palmisiani, J.; Tutino, M. *Sensors*, **2013**, *13*, 16759-16800.
35. Banwell, M. G.; Pollard, B.; Liu, X.; Connal, L. A. *Chem. Asian J*. **2021**, *16*, 604-620.
36. Still, W. C.; Kahn, M.; Mitra, A. *Journal of Organic Chem*istry, **1978**, *43*, 2923–2925.
37. Pangborn, A. B.; Giardello, M. A.; Grubbs, R. H.; Rosen, R. K.; Timmers, F. J. *Organometallics,* **1996**, *15*, 1518–1520.
38. Tozuka, H.; Ota, M.; Kofujita, H.; Takahashi, K. Synthesis of dihydroxyphenacyl glycosides for biological and medicinal study: β-oxoacetoside from *Paulownia tomentosa*. *Journal of Wood Science*, **2005**, *51*, 48-59.
39. (a) Nagy, A.; Csordás, B.; Zsoldos-Mády, V.; Pintér, I.; Farkas, V.; Perczel, A. C-3 Epimers of sugar amino acids as foldamer building blocks: improved synthesis, useful derivatives, coupling strategies. *Amino Acids*, **2017**, *49*, 223-240; (b) Redlich, H.; Meyer, W.-U. *p*-Toluosulfinimidazolid als Reagenz zur haloenidfreien Sulfinesterbildung. *Liebigs Annalen der Chemie*, **1981**, 1354-1360.
40. Norris, P.; Fluxe, A. Preparation of a D-Glucose-Derived Alkene. *J. Chem. Ed*. **2011**, *78*, 1676-1678.
41. Dolomanov, O. V.; Bourhis, L. J.; Gildea, R. J.; Howard, J. A. K.; Puschmann, H. OLEX2: a complete structure solution, refinement and analysis program. *Journal of Applied Crystallography,* **2009**, *42*, 339-341.
42. Sheldrick, G. M. ShelXT-Integrated space-group and crystal-structure determination. *Acta Crystallographica*, **2015**, *A71*, 3-8
43. Sheldrick, G. M. Crystal structure refinement with *SHELXL*. *Acta Crystallographica,* **2015**, *C71*, 3-8.
44. Frisch, M. J.; Trucks, G. W.; Schlegel, H. B.; Scuseria, G. E.; Robb, M. A.; Cheeseman, J. R.; Scalmani, G.; Barone, V.; Petersson, G. A.; Nakatsuji, H., et al. *Gaussian 16 Revision C.01*, Wallingford, CT, 2016.
45. Lu, T.; Chen, F., Multiwfn: a multifunctional wavefunction analyzer. *Journal of Computational Chemistry,* **2012,** *33*, 580-592.

46. GaussView, Version 6, Dennington, Roy; Keith, Todd A.; Millam, John M. Semichem Inc., Shawnee Mission, KS, 2016.

47. See http://cidportal.jrc.ec.europa.eu/ftp/jrc-opendata/EURLECVAM/datasets/DBALM/-LATEST/online/dbalm.html (accessed 29/06/2021).

Chapter Four

The Synthesis and Manipulation of Certain Diels-Alder Adducts of Levoglucosenone and *iso*-Levoglucosenone

Brett Pollard, Xin Liu, Luke A. Connal, Martin G. Banwell, and Michael G. Gardiner

Aust. J. Chem. **2023**, ***76****(11)*, 797-811.

Australian National University

Statement of Contribution

This thesis is submitted as a Thesis by Compilation in accordance with https://policies.anu.edu.au/ppl/document/ANUP_003405

I declare that the research presented in this Thesis represents original work that I carried out during my candidature at the Australian National University, except for contributions to multi-author papers incorporated in the Thesis where my contributions are specified in this Statement of Contribution.

Title: The Synthesis and Manipulation of Certain Diels-Alder Adducts of Levoglucosenone and iso-Levoglucosenone

Authors: Brett Pollard, Xin Liu, Luke A. Connal, Martin G. Banwell, and Michael G. Gardiner

Publication outlet: Australian Journal of Chemistry, Accepted 17th August 2023, CH23130.

Current status of paper: Accepted

Contribution to paper: This is a full paper and the candidate carried out 75% of the experimental work reported within it. In addition, the candidate collated and formatted all of the spectral data presented in the Supporting Information document. The candidate also wrote the entirety of the Experimental Section and conducted relevant literature surveys. A preliminary outline was generated by the candidate and thereafter the body of the paper was written by Professor Martin Banwell and edited by the candidate.

Senior author or collaborating authors endorsement: M. G. Banwell

BRETT L POLLARD		21/8/2023
Candidate – Print Name	Signature	Date

Endorsed

Luke Connal		21/8/23
Primary Supervisor – Print Name	Signature	Date
Mark Humphrey	Mark Humphrey	22/8/23
Delegated Authority – Print Name	Signature	Date

Foreword

This chapter focuses on novel synthetic transformations of levoglucosenone, expanding on its valorisation in the realm of fine chemistry. Diels-Alder cycloaddition reactions between the biomass-derived platform molecule levoglucosenone and various cyclic dienes such as α-terpinene have produced a range of adducts. Transformations of these include intramolecular bromoetherifications and DAST-mediated Wagner-Meerwein rearrangements. The work presented in this chapter describes our manipulations of these functionalities and a suite of novel analogues with complex chemical structures, which have been extensively characterised (including X-ray diffraction). This chapter, of which I am first author, was accepted in August 2023 for publication in of the Australian Journal of Chemistry. My contribution to the manuscript includes the design of synthetic protocols, purifications, characterisation of the resulting materials, data analysis, as well as preparing and revising the manuscript and figures (overall 70%). The published version of the manuscript is presented here. Xin Liu contributed to the synthesis and characterisation of materials. Luke A. Connal contributed to revising the manuscript. Martin G. Banwell contributed to experimental design, project design, data analysis as well as preparing and revising the manuscript and figures. Michael G. Gardiner contributed through spectroscopic analysis.

Introduction

The pyrolytic conversion of acid-treated cellulose (**1**) (**Figure 1**) into levoglucosenone (LGO, **2**) is a transformation that has been known for decades and one that is currently being applied at the tonne scale to various forms of cellulosic waste including sawdust.[1] As a result, compound **2** is now considered a sustainably-generated platform molecule and it is attracting increasing attention as a starting point for the production of a remarkable array of end-products that include biologically active compounds and new materials.[1,2] During the course of our own studies on the formation and chemical manipulation of sustainably-derived platform molecules,[3] including LGO,[4] we devised simple methods for its conversion into the pseudo-enantiomeric *iso*-levoglucosenone (*iso*-LGO, **3**)[4b] and recently established[4c] that the Diels-Alder adducts **4** and **5** derived from their reactions with cyclopentadiene engaged in ring-opening metathesis polymerisations (ROMPs) to give polymers of the general forms **6** and **7**, respectively.[5] As part of these studies we established that the alcohols obtained on reduction of compounds **4** and **5** could be converted into a range of ethers that also engaged in ROMPs and so providing materials with properties distinct from those displayed by congeners **6** and **7**. The purpose of the work reported here was to undertake further manipulations of the Diels-Alder adducts, **4** and **5**, of compounds **2** and **3** as well as to study related systems so as to identify new monomeric systems that might eventually be engaged in useful polymerisation processes. The outcomes of such efforts are now reported.

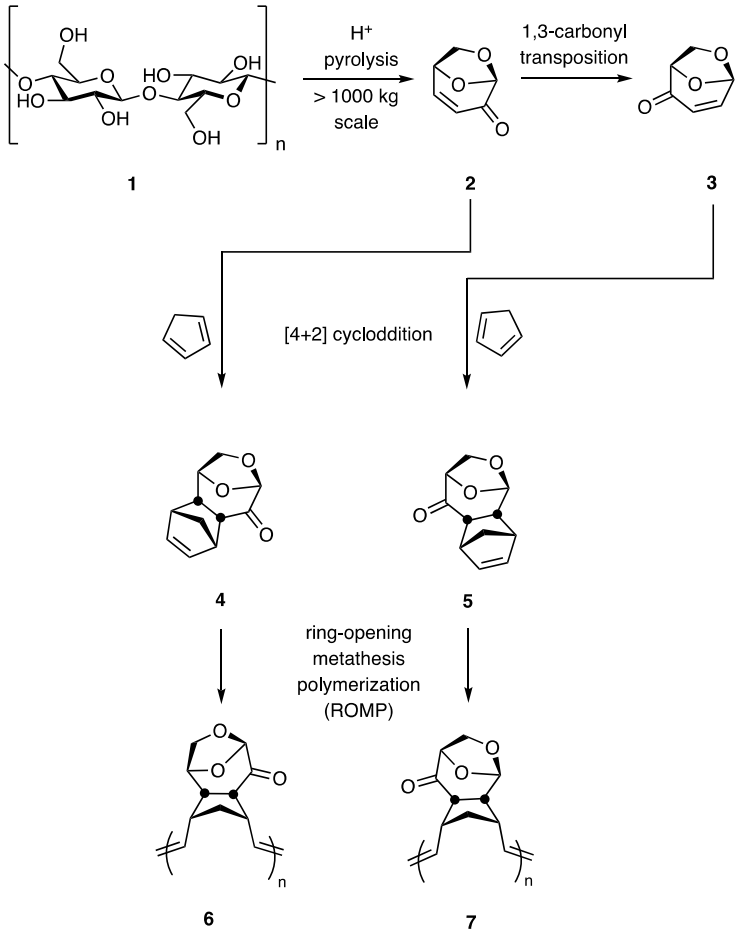

Figure 1: The Synthesis of the Diels-Alder Adducts, **4** and **5**, Arising from the Reaction of LGO and *iso*-LGO (**2** and **3**, respectively) with Cyclopentadiene and Their Engagement in ROMPs Leading to Polymers **6** and **7**.

Results and Discussion

(i) Further Manipulations of Diels-Alder Adducts 4 and 5.

In seeking to generate monomeric systems incorporating fluorine for use in ROMPs, the previously reported[4c] epimeric alcohols **8** and **9** (**Scheme 1**) obtained from the sodium borohydride-mediated reduction of the ketone carbonyl residue within LGO adducts were each treated with diethylaminosulfur trifluoride (DAST).[6] In the case of alcohol **9** the fluorination process involved a rearrangement reaction such that the associated acetal was transformed, *via*

initial ionisation of the free hydroxyl group, into a 1,4-dioxane-based oxonium ion that was then stereoselectively captured by fluoride ion to deliver compound **10** (64%).[7] All the spectral data derived from this material were in complete accord with the illustrated structure. Most notably, in the ^{1}H NMR spectrum a one-proton doublet (J_{HF} = 54.3 Hz) was observed at δ_H 5.09 and this resonance is assigned to the hydrogen on the fluorine-bearing carbon. In the corresponding $^{13}C\{^{1}H\}$ NMR spectrum one-, two- and three-bond C-F couplings are observed for those resonances appearing at δ_C 105.2, 76.6 and 76.2, respectively, and which are assigned to the oxygenated sp^3-hybridised carbons closest to the fluorine. That due to the analogous oxygenated sp^3-hybridised carbon remote from the halogen appears as a singlet at δ_C 67.6. Final confirmation of the structure of compound **10** came from a single-crystal X-ray analysis, details of which are provided in the Experimental and the Supplementary Material (SM). In the case of the epimeric alcohol **8**, when this was treated with DAST then a fluorinated compound lacking a carbon-carbon double bond was formed and this is tentatively assigned as the caged system **11** (28%) based on both mechanistic and spectroscopic considerations. So, in this conversion it is presumed that DAST-promoted ionisation of the free-hydroxyl group is accompanied by migration of the anti-disposed and vicinally related oxygen and that the oxonium ion so-formed then adds to the proximate olefin with the resulting carbocation then captured, in an *exo*-face addition reaction, by fluoride ion (or an equivalent thereof). The initial steps of such a pathway are supported by our observations of the operation of the related process for a homologue of compound **8** (see below). The ^{1}H NMR spectrum of product **11** displayed no resonances due to olefinic protons but, *inter alia*, a one-proton doublet (J_{HF} = 52.6 Hz) observed at δ_H 5.27 is assigned to the hydrogen on the fluorine-bearing sp^3-hybridised carbon with the lower field than expected chemical shift for this resonance being attributed to the deshielding effects of the proximate and "peri"-disposed oxygen. In the corresponding

$^{13}C\{^{1}H\}$NMR spectrum the fluorinated carbon appears as a doublet ($^{1}J_{CF}$ = 180 Hz) while a two-bond coupling ($^{2}J_{CF}$ = 24 Hz) to one of the adjacent methine carbons as well as to the methine carbons either side of the proximate oxygen (J_{CF} = ca. 30 and 10 Hz) are observed. The last two couplings presumably derive, to some extent at least, from through-space rather than through-bond interactions between the fluorine and relevant carbon nuclei.[8] Smaller couplings between the fluorine and two other, non-oxygenated sp^3-hybridised carbons are also observed (see Experimental for details).

When substrate **8** was reacted with *N*-bromosuccinimide rather than DAST then a smooth bromo-etherification reaction took place to deliver the pentacyclic and crystalline bromide **12** in 95% yield and upon which a single-crystal X-ray analysis was carried out (see Experimental and SM for details). On the other hand, treatment of substrate **8** with BF_3•Et_2O in dichloromethane at 22 °C afforded the previously reported[9] rearrangement product **13** (63%) that it has been suggested[9] results from initial cleavage of the acetal residue and with the ensuing oxonoium ion being attacked by the pendant olefin and the carbocation so formed being captured by the original secondary alcohol moiety.

Scheme 1: Formation and Manipulation of the Alcohols **8** and **9** Derived from the Diels-Alder Adduct, **4**, of Levoglucosenone (**2**) and Cyclopentadiene.

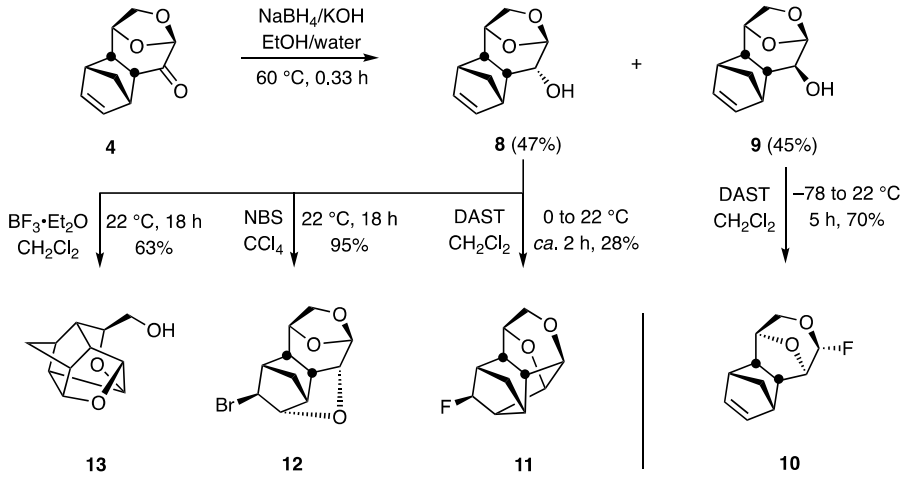

An analogous series of experiments involving the previously reported[10] Diels-Alder adduct, **5** (**Scheme 2**), derived from *iso*-levoglucosenone and cyclopentadiene was also carried out. Specifically, sodium borohydride-mediated reduction of adduct **5** gave a *ca*. 1:4 mixture of the chromatographically separable, known[10] and crystalline alcohols **14** (15%) and **15** (69%) and the structures of each of these was confirmed by single-crystal X-ray analysis[11] (see Experimental and SM for details). A comparison of the $^{13}C\{^{1}H\}$ NMR spectral data reported for compounds **14** and **15** with the analogous and previously reported data sets[10] (see the SM for tabular comparisons) were consistent with the assignments defined earlier.

When compound **15** was treated with DAST then fluorination with retention of configuration took place to afford the crystalline product **16** in 69% yield and the structure of which was confirmed by single-crystal X-ray analysis.

Scheme 2: Formation and Manipulation of the Alcohols **14** and **15** Derived from the Diels-Alder Adduct, **5**, of *iso*-Levoglucosenone (**3**) and Cyclopentadiene.

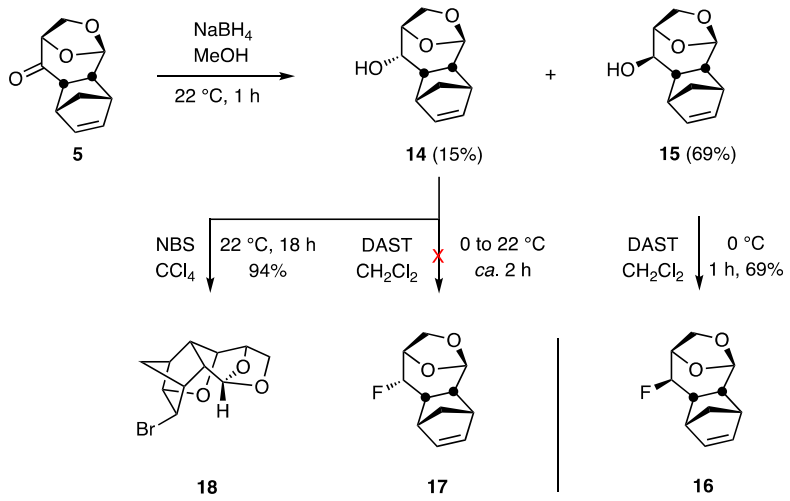

Analogous treatment of the epimeric alcohol with DAST did not, however, proceed cleanly and only an unstable tar was obtained – no evidence for the formation of, for example, fluoride **17** or any related product could be obtained. In contrast, on reacting substrate **14** with NBS then the anticipated bromo-etherification reaction took place to afford product **18** in 94% yield and the structure of which was again confirmed by single-crystal X-ray analysis. However, treatment of alcohol **14** with BF_3•Et_2O under the same conditions as employed in the conversion **8** → **13** only led to complex mixtures.

(ii) Manipulations of Diels-Alder Adducts Derived from LGO (2) and *iso*-LGO (3) with Cyclohexa-1,3-diene.

In an extension of the foregoing studies, LGO (**2**) was reacted with cyclohexa-1,3-diene (**Scheme 3**) under microwave irradiation conditions to give the anticipated and previously reported[12] and *endo*-configured adduct **19** (80%) and the structure of which was confirmed by single-crystal X-ray analysis (see Experimental and SM for details).

Scheme 3: Formation of the Diels-Alder Adduct, **19**, of Levoglucosenone (**2**) and Cyclohexa-1,3-diene and Its Conversion into Derivatives **20**-**23**.

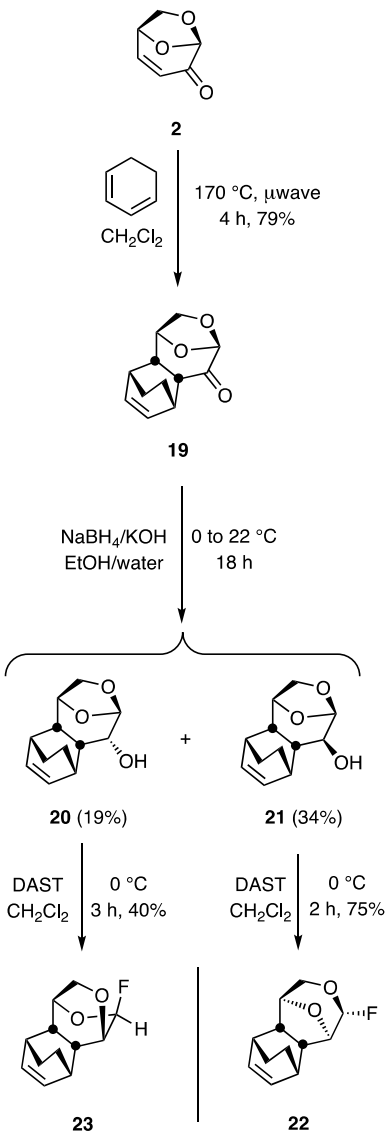

In keeping with the outcomes detailed above, on treating the tetracyclic ketone **19** with sodium borohydride then a non-stereoselective reduction took place to afford a *ca*. 2:3 mixture of the epimeric and chromatographically separable alcohols **20** (19%) and **21** (34%) and the structure of the first of these was confirmed by single-crystal X-ray analysis. The spectral data recorded on compounds **20** and **21** matched those reported previously[9] - see the SM for a tabular comparison of the relevant $^{13}C\{^{1}H\}$ NMR spectral data sets. On treating the latter alcohol with DAST under the same conditions as used earlier then a clean reaction took place to give

compound **22** in 75% yield. This product, the structure of which was confirmed by single-crystal X-ray analysis, is analogous to that formed from the lower homologue of the starting material, *viz*. the cyclopentadiene/LGO adduct **10**. Interestingly, treatment of the epimeric alcohol **20** with DAST under the same conditions afforded compound **23** (40%) and the structure of which was also confirmed by single-crystal X-ray analysis. This outcome contrasts with that observed for lower homologue **8** in that no product(s) arising from reaction(s) involving the carbon-carbon double-bond of substrate **20** is/are observed. This difference may be attributed to the varying geometries of the homologues and wherein, as judged by examination of molecular models, the acetal and alcohol residues of compound **8** are in closer proximity to the associated double bond. Consistent with such arguments, compound **20** could not be engaged in a bromo-etherification reaction using NBS - the substrate simply failed to react under a range of conditions. Similarly, attempts to effect a BF_3•Et_2O-induced rearrangement of alcohol **21** were also unsuccessful in that only highly unstable materials were formed.

iso-Levoglucosenone (**3**) also engaged in a Diel-Alder cycloaddition reaction with cyclohexa-1,3-diene (**Scheme 4**) and under microwave irradiation conditions a single, crystalline adduct **24** was obtained in 91% yield. All the spectral data acquired on this product were fully consistent with the assigned, *endo*-configured structure but final confirmation of this followed from a single-crystal X-ray analysis, details of which are provided in the Experimental and the SM. Rather surprisingly, the sodium-borohydride-mediated reduction of the ketone moiety within compound **24** was highly selective in that only the β-configured alcohol **25** (91%) could be isolated from the reaction mixture. The structure of this product was also confirmed by single-crystal X-ray analysis (see Experimental and SM for details). On treating this last compound with DAST under our now standard conditions then the starting material was rapidly

consumed. While, by analogy with conversion **15** → **16** (**Scheme 2**), the formation of fluoride **26** might have been anticipated under such conditions, no clear evidence for the formation of this product could be obtained and this being despite extensive chromatographic manipulations of the crude reaction mixture.

Scheme 4: Formation of the Diels-Alder Adduct, **24**, of *iso*-Levoglucosenone (**3**) and Cyclohexa-1,3-diene and Its Conversion into Alcohol **25**

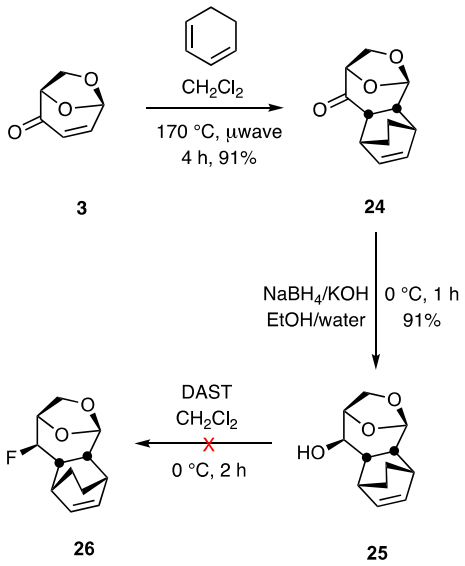

(iii) The Diels-Alder Adducts Derived from Reaction of LGO (2) and *iso*-LGO (3) with α-Terpinene.

In an effort to generate monomeric systems for ROMP that are entirely sustainably-derived in their constitution, the reaction of LGO (**2**) with α-terpinene (1-isopropyl-4-methylcyclohexa-1,3-diene), an abundant and commercially available monoterpene, was examined (**Scheme 5**). While attempts to effect a strictly thermally-induced cycloaddition reaction between this dienophile and diene failed, on using tin(IV) chloride as catalyst then a reaction did take place and so affording what is presumed to be a mixture of the two possible regio-isomeric *endo*-adducts **27** and **28** that could be separated chromtographically and then obtained in yields of *ca*. 2% and 30%, respectively.

Scheme 5: Formation of the Diels-Alder Adducts, **27** and **28**, of Levoglucosenone (**2**) and α-Terpinene and the Conversion of the Latter into Alcohol **29** and Fluoride **30**

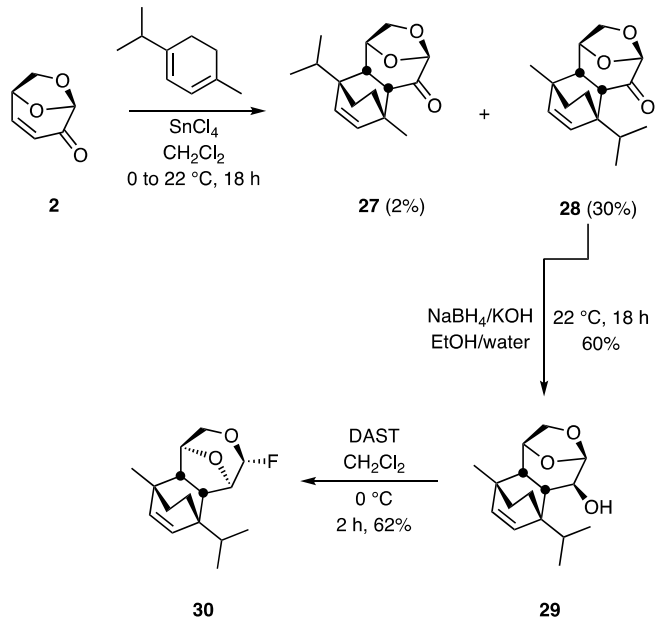

The spectral data obtained on each of these products were in accord with the illustrated structures but differentiating between them was less clear cut. Fortunately, upon subjecting the major adduct to reaction with sodium borohydride then a single epimeric alcohol **29** (60%) was obtained and the structure of this confirmed by single-crystal X-ray analysis. Of course, the structure assigned to precursor **28** follows from this (analysis) and, by inference, also serves to substantiate that assigned to regio-isomer **27**. Interestingly, the data recorded on the major Diels-Alder adduct **28** matches that reported[13] by Galimova *et al* (see the SM for a tabulated comparison of the $^{13}C\{^{1}H\}$ NMR spectral data sets) who prepared this adduct (in 37% yield) by reacting LGO with (±)-α-terpineol acetate in toluene at 100 °C and at a pressure of 10,000 atmospheres. These same workers suggested that this adduct arose through an *exo*-type [4+2]-cycloaddition reaction between LGO and *in situ* generated *a*-terpinene. Given the X-ray data just described, adduct **28** is clearly formed *via* an *endo*- rather than an *exo*-type process.

On treating compound **29** with DAST it underwent a smooth fluorination reaction analogous to those seen earlier (*cf* **21** → **22**) and thus providing the rearranged fluoride **30** in 62% yield and

which was obtained as a crystalline solid suitable for single-crystal X-ray analysis. Details of this analysis are presented in the Experimental Section and SM.

As was the case detailed above for enone **2**, isomer **3** also engages in a Diels-Alder cycloaddition reaction with α-terpinene (**Scheme 6**), although now a Lewis acid catalysed one, and so leading to the formation, as determined by ^{1}H NMR spectroscopic analysis of the crude reaction mixture, of a *ca*. >5:1 mixture of what is presume to be the regio-isomeric *exo*-adducts **31** and **32**. Only the latter adduct could be obtained in pure form (and 24% yield) with the structure of this being confirmed by single-crystal X-ray analysis (see Experimental and SM for details). The selective formation of *exo*-adduct **32** contrasts the outcome shown in **Scheme 5** and the origins of these seemingly differing preferences are unclear at the present time, not least because the relatively poor mass balances in each of the cycloaddition reactions is something of a confounding factor (as are the different modes used in effecting the processes – microwave irradiation *vs* $SnCl_4$ catalysis). The modest amounts of compounds **31** and **32** available using this Diels-Alder process has, at the present time, precluded any further investigations of their chemistries (for example the reactions of the derived alcohols with DAST) although the major one (*viz*. **32**) may itself serve as a monomer in ROMP processes.

Scheme 6: Formation of the *exo*-Configured Diels-Alder Adducts, **31** and **32**, of *iso*-Levoglucosenone (**3**) and α-Terpinene

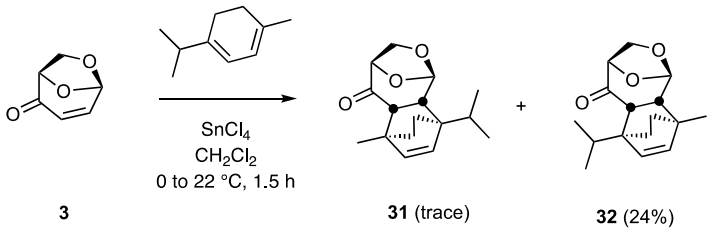

In efforts to generate new polymeric materials, the application of ROMP techniques to the Diels-Alder adducts **19**, **24**, **27**, **28** and **32** as well as to the corresponding $NaBH_4$-derived reduction products **20**, **21**, **25** and **29** and to the related or derived fluoroalkenes **10**, **16**, **22**, **23** and **30** will be the subject of future publications.

(iv) The Dihydroxylation of Diels-Alder Adduct 19

It is also conceiveable that the above-mentioned alkenes could be dihydroxylated and the resulting diols then engaged in alternative modes of polymerisation, including ones leading to poly-esters.[5d,5g] Accordingly, we concluded the present study by examining how readily or otherwise the representative Diels-Alder adduct **19** could participate in Upjohn-type dihydroxylation reactions. In the event, and as shown in **Scheme 7**, on treating this substrate under standard conditions and using osmium tetroxide as the catalytic oxidant then a single, crystalline diol **33** was formed (as the monohydrate), albeit in just 38% yield after chromatographic purification and recrystallisation. A single-crystal X-ray analysis of this material (see Experimental and SM) not only confirmed the anticipated *cis*-relationship between the vicinally-related hydroxy groups but that these were introduced, as expected, though oxidation at the less hindered *exo*-face of the precursor olefin. This outcome is in

keeping with that observed[14] when the LGO/cyclopentadiene adduct **4** is subjected to essentially the same conditions.

Another fraction arising from the chromatographic isolation of compound **33** led to the formation of crystalline material shown by X-ray analysis to be a non-hydrated form of compound **33** that incorporated the corresponding acyloin **34** as a co-crystallised impurity (18% refined occupancy). This is most likely formed through ketohydroxylation of substrate **19**. Certainly, catalytic combinations of osmium tetroxide and $Ni(mac)_2$ have been reported[15] to produce acyloins from olefins and in the present setting a possible source of the latter metal is the spatula used to dispense the reagents and reactant into the reaction vessel. Interestingly, the product resulting from dihydroxylation the LGO/cyclopentadiene adduct **4** undergoes a 1,4-hydride shift to afford an acyloin (of different regio-chemistry to that seen in compound **34**) and with the ketone carbonyl group derived from LGO being reduced stereoselectively during this isomerisation process.[14]

Scheme 7: The Dihydroxylation of Diels-Alder Adduct **19** Leading to the Formation of Diol **33** and Acyloin **34**.

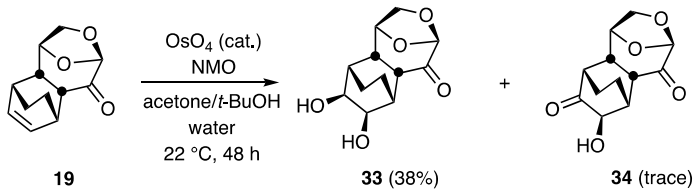

Conclusions

The present study demonstrates that various Diels-Alder adducts obtained from the biomass-derived platform molecule levoglucosenone (**2**) and its readily prepared isomer **3** can be converted into fluorinated derivatives through successive treatment with sodium borohydride then DAST. The fluorination step often involves rearrangement reactions. Such outcomes further emphasise the diverse chemistries displayed by the now abundantly available

levoglucosenone (**2**) and its derivatives and the potential that clearly exists to convert this compound into a wide-range of biomass-derived monomers for ROMP and other polymerisation processes.

Experimental

General Experimental Protocols.

Unless otherwise specified, proton (^{1}H) and proton-decoupled carbon (^{13}C{^{1}H}) NMR spectra were recorded at 18 °C in $CDCl_3$ on a spectrometer operating at 400 MHz for proton and 100 MHz for carbon nuclei. ^{1}H NMR data are recorded as follows: chemical shift (δ) [multiplicity, coupling constant(s) *J* (Hz), relative integral], where multiplicity is defined as s = singlet; d = doublet; t = triplet; q = quartet; m = multiplet, or combinations of the above. In relevant cases, the signal due to residual $CHCl_3$ appearing at δ_H 7.26 and the central resonance of the $CDCl_3$ "triplet" appearing at δ_C 77.0 were used to reference ^{1}H and ^{13}C{^{1}H} NMR spectra, respectively. Samples were analysed by FT infrared spectroscopy (ν_{max}) as thin films on KBr plates or as neat material resting on the sampling port. Low-resolution EI mass analyses were carried out on an Agilent HP 5973 gas chromatograph/mass spectrometer with a 7683 series injector fitted with an Agilent HP-5MS column (15 m length × 0.25 mm internal diameter × 0.25 μm film thickness) using EI+ ionisation mode at 70 eV. The data were analysed using MSDChem software. High-resolution EI analyses were carried out on Waters AutoSpec Premier mass spectrometer operating at 70 eV. Samples were injected by direct infusion with PFK as a reference standard and the data were analysed by MassLynx v4.1 software. HR EI experiments were also performed using an Agilent 7250 GC/Q-TOF mass spectrometer, fitted with an Agilent VF-5MS column (30 m length × 0.25 mm internal diameter × 0.25 μm film thickness) using EI+ ionisation mode at 70 eV. Gerstel autosampler was used to deliver the sample. The data were analysed using MassHunter Qualitative Analysis 10.0 software. Low-

resolution ESI were analyses were carried out on Agilent 6120 Quadrupole LC/MS instrument connected to an Agilent 1200 series LC unit. An isocratic elution mode was used to deliver the sample into MS. Capillary voltage was set at 5000v and desolvation temperature was set at 300 degrees, using API (+) ionisation. MSDChem software was used for data analyses. High resolution electrospray ionisation (ESI) analyses were performed on a Waters Synapt G2-Si HDMS qTOF mass spectrometer connected to a Waters Acquity UPLC I Class plus LC unit. An isocratic elution mode was used to deliver the sample into MS without chromatographic separation using methanol as the eluent at a flow rate of 0.2 mL/min. The mass spectrometer was operated in positive, full MS, resolution and TOF modes. Capillary voltage and cone voltage were set at 2kV and 30V respectively. Source temperature was set at 120 degrees and desolvation temperature was set at 200 degrees. Leucine Enkephalin was used as the Lockspray reference compound. Elemental composition reports were produced within 3 ppm error. Masslynx v4.1 software was used to process data. HR ESI experiments were also performed using an Orbitrap Elite mass spectrometer equipped with a HESI-II electrospray ionisation source coupled to an Ulti-Mate 3000 UHPLC (Thermo Scientific). Samples were introduced by direct infusion without chromatographic separation. Scans were performed on the orbitrap FTMS mass analyser at a resolution of 120 000 (m/z 200–2000). The spray voltage was set at 4.3kV, and the source heater temp at 300 Degrees. The data were analysed using Thermo Freestyle software. Melting points are uncorrected. Optical rotations were recorded in the indicated solvent at 20 °C on a Perkin Elmer Model 343 Polarimeter. Analytical thin layer chromatography (TLC) was performed on aluminum-backed 0.2 mm thick silica gel 60 F254 plates. Eluted plates were visualised using a 254 nm UV lamp and/or by treatment with a suitable dip, followed by heating. These dips included potassium permanganate/potassium carbonate/5% sodium hydroxide aqueous solution/water (3 g:20 g:5mL:300 mL), and *p*-anisaldehyde or vanillin/sulfuric acid (conc.)/ethanol (15 g:2.5 mL:250 mL). Flash

chromatographic separations were carried out following protocols defined by Still *et al.*[16] silica gel 60 (40−63 μm) as the stationary phase and using the AR- or HPLC-grade solvents indicated. The melting points of solids purified by such means were normally recorded directly (*viz*. after they had crystallised from the concentrated chromatographic fractions). A CEM Explorer system was employed for microwave-promoted reactions and these were undertaken using 10 mL vials fitted with polytetrafluoroethylene (PTFE) caps. An internal infrared probe was used to monitor and control reaction temperature.

Starting materials, reagents, drying agents, and other inorganic salts were generally commercially available and were used as supplied. Levoglucosenone was kindly supplied by Circa™ and was purified by vacuum distillation, collecting the distillate obtained at 95 ºC. *iso*-Levoglucosenone was prepared by the method of Ma *et al.*[4a] Tetrahydrofuran (THF), methanol, petroleum ether (40 to 60 °C fraction) and dichloromethane were dried using a solvent purification system that is based upon a technology originally described by Grubbs *et al.*[17] Where necessary, reactions were performed under a nitrogen atmosphere.

(1*R*,2*R*,5*S*,5a*S*,6*R*,9*S*,9a*R*)-2-Fluoro-1,2,4,5,5a,6,9,9a-octahydro-1,5-epoxy-6,9-methanobenzo[*d*]oxepine (10)

A magnetically stirred and deoxygenated solution of compound **9**[18] (194 mg, 1.00 mmol) in dry dichloromethane (5.0 mL) was cooled to –78 °C (acetone/dry-ice bath) then treated, *via* syringe, with diethylaminosulfur trifluoride (DAST) (163 mg, 1.01 mmol, 1 equiv.). After 5 h the reaction mixture was slowly warmed to 22 °C before being treated with flash chromatography-grade silica gel (200 mg). The ensuing mixture was concentrated under reduced pressure and the resulting free-flowing solid subjected to flash chromatography (silica gel, 1:1 *v/v* diethyl ether/hexane elution) to afford, after concentration of the appropriate fractions (R_f = 0.4), compound **10** (138 mg, 70%) as an off-white, crystalline solid, m.p. = 49-50 °C, $[\alpha]_D$ = +12.14

(*c* = 0.14, methanol). ^{1}H NMR (400 MHz, $CDCl_3$) δ 6.07 (s, 2H), 5.08 (d, J_{HF} = 54.3 Hz, 1H), 4.10 (d, *J* = 10.8 Hz, 1H), 3.80 (s, 2H), 3.38 (d, *J* = 10.8 Hz, 1H), 2.97 (broadened s, 1H), 2.92 (broadened s, 1H), 2.83 (m, 1H), 2.75 (m, 1H), 1.44 (ABq, *J* = 8.4 Hz, 2H); ^{13}C{^{1}H} NMR (100 MHz, $CDCl_3$) δ 134.2, 134.0, 105.2 (d, $^{1}J_{CF}$ = 230 Hz), 76.6 (d, $^{2}J_{CF}$ = *ca*. 21 Hz), 76.2 (d, $^{3}J_{CF}$ = *ca*. 1 Hz), 67.6, 52.4, 46.9, 46.8, 45.6, 45.3; IR (KBr) ν_{max} 3388, 3058, 2955, 2869, 1453, 1352, 1332, 1253, 1223, 1114, 1076, 1032, 996, 975, 897, 852, 797, 738 cm^{-1}; HRMS (EI, 70 eV) *m/z* $M^{+\bullet}$ calcd for $C_{11}H_{13}FO_2$ 196.0894; found 196.0895.

(3*S*,4a*R*,4b*R*,5*S*,6*S*,7a*R*,8*R*,8a*S*,9*R*)-5-Fluorodecahydro-3,6,8-(epimethanetriyl)pent-aleno-[1,2-*b*][1,4]dioxine (**11**)

A deoxygenated and magnetically stirred solution of compound **8**[18] (358 mg, 1.84 mmol) in dry dichloromethane (10.0 mL) maintained under nitrogen at 0 °C was treated, *via* syringe, with DAST (344 mg, 2.14 mmol, 1.2 equiv). After 1.5 h the reaction mixture allowed to warm to 22 °C then exposed to air before being treated with flash chromatography-grade silica gel (500 mg). The ensuing mixture was concentrated under reduced pressure and the resulting free-flowing solid subjected to flash chromatography (silica gel, 1:4 *v/v* diethyl ether/hexane elution) to afford, after concentration of the appropriate fractions (R_f = 0.2), compound **11** (100 mg, 28%) as a cloudy, orange-white oil, $[\alpha]_D$ = +0.50 (*c* = 1.0, MeOH). ^{1}H NMR (400 MHz, $CDCl_3$) δ 5.27 (d, J_{HF} = 52.6 Hz, 1H), 4.45-4.36 (complex m, 2H), 4.15 (d, *J* = 11.9, 1H), 4.07 (m, 1H), 3.72 (d, *J* = 11.9, 1H), 2.82 (broad s, 1H), 2.67 (broad s, 1H), 2.51 (m, 1H), 2.32 (m, 1H), 2.17 (m, 1H), 1.72 (d, *J* = 11.3 Hz, 1H), 1.53 (d, *J* = 11.3 Hz, 1H); ^{13}C{^{1}H} NMR (100 MHz, $CDCl_3$) δ 101.1 (d, $^{1}J_{CF}$ = 180 Hz), 82.9 (d, J_{CF} = 30 Hz), 81.9 (d, J_{CF} = 10 Hz), 75.1, 63.9, 50.0 (d, J_{CF} = 24 Hz), 48.5, 43.5 (d, J_{CF} = *ca*. 1 Hz), 40.0 (d, J_{CF} = *ca*. 5 Hz), 38.1, 30.0;

IR (KBr) ν_{max} 2927, 2871, 1576, 1077, 1007, 871, 834, 801 cm^{-1}; HRMS (EI, 70 eV) *m/z* $M^{+\bullet}$ calcd for $C_{11}H_{13}FO_2$ 196.0894; found 196.0891.

(2*S*,2a*R*,2a^1*R*,4*S*,4a*R*,5*S*,8*R*,8a*R*,10*S*)-10-Bromodecahydro-1,7,9-trioxa-2,4:5,8-dimethanocyclopenta[*cd*]azulene (12)

A magnetically stirred solution of compound **8** (97 mg, 0.50 mmol) in carbon tetrachloride (2.5 mL) maintained at 22 °C was treated, in one portion, with *N*-bromosuccinimide (NBS) (89 mg, 0.50 mmol, 1.0 equiv.). After 18 h the reaction mixture was concentrated under reduced pressure and the resulting brown solid subjected to flash chromatography (silica gel, 1:1 *v/v* diethyl ether/hexane elution) to afford, after concentration of the appropriate fractions (R_f = 0.1), compound **12** (129 mg, 95%) as a colourless, needles, m.p. = 93-94 °C, $[\alpha]_D$ = +60.0 (*c* = 1.0, methanol); ^{1}H NMR (400 MHz, $CDCl_3$) δ 5.38 (d, *J* = 2.4 Hz, 1H), 4.83 (d, *J* = 2.4 Hz, 1H), 4.65 (m, 2H), 3.89-3.84 (complex m, 2H), 3.79 (d, *J* = 7.0 Hz, 1H), 2.83 (m, 1H), 2.55-2.51 (complex m, 2H), 2.21 (d, *J* = 11.1 Hz, 1H), 1.85 (m, 1H) (one signal obscured or overlapping); ^{13}C{^{1}H} NMR (100 MHz, $CDCl_3$) δ 99.5, 90.2, 77.0, 73.9 69.2, 55.1, 48.5, 47.1, 42.5, 35.5, 34.1; IR (KBr) ν_{max} 2954, 2926, 2898, 1464, 1330, 1319, 1284, 1216, 1142, 1133, 1056, 994, 974, 936, 924, 859, 833, 700, 648 cm^{-1}; HRMS (EI, 70 eV) *m/z* $M^{+\bullet}$ calcd for $C_{11}H_{13}{}^{79}BrO_3$ 272.0048; found 272.0048.

((2*R*,2a*S*,2a^1*S*,4*R*,4a*R*,6*S*,7*S*,7a*S*,8*R*)-Octahydro-1*H*-3,5-dioxa-2,4,7-(epimethanetriyl)cyclopenta[*cd*]inden-6-yl)methanol (**13**) A magnetically stirred solution of compound **8** (97 mg, 0.48 mmol) in dichloromethane (5.0 mL) maintained at 22 °C was treated with BF_3•OEt_2 (177 mg, 1.25 mmol). After 18 h the reaction mixture was treated with flash chromatography-grade silica gel (150 mg) and the ensuing mixture concentrated under reduced pressure. The resulting free-flowing solid was subjected to subjected to flash chromatography

(silica 1:4 *v/v* diethyl ether/hexane elution) to afford, after concentration of the appropriate fractions (R_f = 0.3 in 1:1 *v/v* diethyl ether/hexane), compound **13**[9] (61 mg, 63%) as an off-white, oily solid, m.p. = 34-35 °C, $[\alpha]_D$ = –120.00 (*c* = 0.25, methanol) {lit.[9] $[\alpha]_D$ = +143.3 (*c* = 1.03, $CHCl_3$)}. ^{1}H NMR (400 MHz, $CDCl_3$) δ 4.64 (broadened s, 1H), 4.34 (broadened s, 1H), 4.02 (m, 1H), 3.76 (m, 1H), 3.61 (dd, *J* = 11.3 and 8.2 Hz, 1H), 3.53 (dd, *J* = 11.3 and 4.4 Hz, 1H), 2.57 (s, 1H), 2.33 (m, 1H), 2.23-2.16 (complex m, 2H), 1.87 (broadened s, 2H), 1.74 (m, 1H), 1.38 (m, 1H); ^{13}C{^{1}H} NMR (100 MHz, $CDCl_3$) δ 87.2, 76.7, 74.6, 72.1, 66.1, 49.3, 39.8, 39.5, 36.8, 36.2, 32.1; IR (KBr) ν_{max} 3411, 2956, 2876, 1369, 1321, 1310, 1141, 1117, 1052, 1018, 955, 911, 834 cm^{-1}; HRMS (TOF ESI, +ve) *m/z* $(M+Na)^+$ calcd for $C_{11}H_{14}O_3Na$ 217.0841; found 217.0851.

(1*R*,4*R*,5*S*,5a*S*,6*R*,9*S*,9a*R*)-1,3,4,5,5a,6,9,9a-octahydro-1,4-epoxy-6,9-methanobenzo[*c*]oxepin-5-ol (14) and (1*R*,4*R*,5*R*,5a*S*,6*R*,9*S*,9a*R*)-1,3,4,5,5a,6,9,9a-Octahydro-1,4-epoxy-6,9-methanobenzo[*c*]oxepin-5-ol (15) A magnetically stirred solution of compound **5** (268 mg, 1.39 mmol) in methanol (10 mL) maintained at 22 °C was treated with sodium borohydride (53 mg, 1.39 mmol). After 1 h the reaction mixture was treated with flash chromatography-grade silica gel (300 mg) and then concentrated under reduced pressure. The resulting free-flowing solid was subjected to subjected to flash chromatography (silica, 1:3 *v/v* ethyl acetate/petroleum ether) to afford two fractions, A and B.

Concentration of fraction A (R_f = 0.25) afforded compound **14**[10] (40 mg, 15%) as a colourless, crystalline solid, m.p. = 87-89 °C (lit.[10] m.p. = 90-92 °C), $[\alpha]_D$ = –5.8 (*c* = 0.5, methanol) {lit.[10] $[\alpha]_D$ = –61.1 (*c* = 1.2, $CHCl_3$)}. ^{1}H NMR (400 MHz, $CDCl_3$) δ 6.39 (dd, *J* = 5.6 and 2.8 Hz, 1H), 6.17 (dd, *J* = 5.6 and 3.2 Hz, 1H), 5.32 (s, 1H), 4.21 (dd, *J* = 6.8 and 2.8 Hz, 1H), 3.88 (m, 2H), 3.58 (dd, *J* = 8.0 and 2.4 Hz, 1H), 3.08 (broad s, 1H), 2.91 (broad s, 1H), 2.77 (m, 1H), 2.24 (dd, *J* = 10.0 and 3.6 Hz, 1H), 1.42 (d, *J* = 8.0 Hz, 1H), 1.28 (d, *J* = 8.0

Hz, 1H) (signal due to OH group proton not observed); $^{13}C\{^{1}H\}$ NMR (100 MHz, $CDCl_3$) δ 137.5, 133.2, 102.7, 76.6, 69.5, 64.5, 50.9, 47.0, 46.3, 44.5, 40.5; IR (KBr) ν_{max} 3356, 2962, 1357, 1341, 1114, 1015, 912, 881, 754, 631 cm^{-1}; HRMS (EI, 70 eV) *m/z* $M^{+\bullet}$ calcd for $C_{11}H_{14}O_3$ 194.0943; found 194.0944.

Concentration of fraction B (R_f = 0.2), afforded compound **15**[10] (186 mg, 69%) as a colourless, crystalline solid, m.p. = 100-103 °C (lit.[10] m.p. = 111-113 °C), $[\alpha]_D$ = +21.8 (*c* = 0.7, methanol) {lit.[10] $[\alpha]_D$ = +18.8 (*c* = 1.4, $CHCl_3$)}. ^{1}H NMR (400 MHz, $CDCl_3$) δ 6.22 (m, 1H), 5.32 (s, 1H), 4.21 (m, 1H), 3.94 (dd, *J* = 8.0 and 2.0 Hz, 1H), 3.67-3.61 (complex m, 2H), 3.07 (broad s, 1H), 2.87 (broad s, 1H), 2.39 (dd, *J* = 10.0 and 3.6 Hz, 1H), 2.28 (m, 1H), 1.46 (dd, *J* = 8.3 and 1.8 Hz, 1H), 1.44 (d, *J* = 8.4 Hz, 1H), 1.31 (d, *J* = 8.4 Hz, 1H) (signal due to OH group proton not observed); $^{13}C\{^{1}H\}$ NMR (100 MHz, $CDCl_3$) δ 136.1, 135.7, 101.8, 73.3, 68.6, 61.6, 50.8, 48.6, 46.2, 46.0, 44.1; IR (KBr) ν_{max} 3479, 2969, 1340, 1236, 1124, 1059, 957, 881, 736 cm^{-1}; HRMS (TOF ESI, +ve) *m/z* $(2M + Na)^+$ calcd for $C_{22}H_{28}NaO_6$ 411.1784; found 411.1801.

(1*R*,4*R*,5*R*,5a*S*,6*R*,9*S*,9a*R*)-5-Fluoro-1,3,4,5,5a,6,9,9a-octahydro-1,4-epoxy-6,9-methanobenzo[*c*]oxepine (16)

A deoxygenated and magnetically stirred solution of compound **15** (97 mg, 0.50 mmol) in dry dichloromethane (5.0 mL), maintained at 0 °C under nitrogen was treated with DAST (122 mg, 0.76 mmol, 1.5 equiv.). After 1.5 h the reaction mixture was exposed to air then treated with flash chromatography-grade silica gel (150 mg) and then concentrated under reduced pressure. The resulting free-flowing solid was subjected to subjected to flash chromatography (silica gel, 1:4 *v/v* diethyl ether/hexane) to afford, after concentration of the appropriate fractions (R_f = 0.4) a colourless, crystalline solid. Recrystallisation (hexane) of this material gave compound **16** (68 mg, 69%) as colourless needles, m.p. = 46-47 °C, $[\alpha]_D$ = 10.5 (*c* = 0.2, methanol). ^{1}H

NMR (400 MHz, $CDCl_3$) δ 6.22 (s, 2H), 5.34 (d, J = 6.8 Hz, 1H), 4.49 (partially obscured dt, J_{HF} = 52 Hz and J_{HH} = 5.2 Hz, 1H), 4.37 (partially obscured m, 1H), 3.93 (dd, J = 8.4 and 2.4 Hz, 1H), 3.68 (m, 1H), 3.11 (broad s, 1H), 2.89 (broad s, 1H), 2.57 (m, 1H), 2.48 (m, 1H), 1.47 (d, J = 8.4 Hz, 1H), 1.32 (d, J = 8.4 Hz, 1H); $^{13}C\{^1H\}$ NMR (100 MHz, $CDCl_3$) δ 136.1, 135.7, 101.8, 88.5 ($^1J_{CF}$ = 180 Hz), 70.7 ($^2J_{CF}$ = 20 Hz), 62.0, 50.7, 49.5, 46.0, 41.4, 41.2; IR (KBr) ν_{max} 2967, 1353, 1338, 1118, 1003, 914, 906, 737, 652 cm^{-1}; HRMS (EI, 70 eV) *m/z* $M^{+\bullet}$ calcd for $C_{11}H_{13}FO_2$ 196.0900; found 196.0901.

(2*R*,2a*S*,2a^1*R*,4*R*,4a*R*,5*R*,8*R*,8a*S*,10*R*)-10-Bromodecahydro-1,6,9-trioxa-2,4:5,8-dimethanocyclopenta[*cd*]azulene (18)

A magnetically stirred solution of compound **14** (63 mg, 0.33 mmol) in carbon tetrachloride (3.0 mL) maintained at 22 °C was treated with NBS (120 mg, 0.66 mmol). After 18 h the reaction mixture was concentrated under reduced pressure and the brown solid so-formed subjected to flash chromatography (1:1 *v/v* diethyl ether/hexane) to afford, after concentration of the appropriate fractions (R_f = 0.1), compound **18** (83 mg, 94%) as a yellow, crystalline solid, m.p. = 113-115 °C, $[\alpha]_D$ = –7.2 (*c* = 1.0, methanol); ^1H NMR (400 MHz, $CDCl_3$) δ 5.55 (s, 1H), 4.70 (d, J = 2.1 Hz, 1H), 4.65 (d, J = 5.0 Hz, 1H), 4.52 (m, 1H), 3.95 (dd, J = 5.6 and 2.4 Hz, 1H), 3.75-3.73 (complex m, 2H), 2.81 (t, J = 4.8 Hz, 1H), 2.54 (m, 1H), 2.42 (broadened s, 1H), 2.21 (d, J = 11.0 Hz, 1H), 1.98 (broadened d, J =11.2 Hz, 1H), 1.55 (d, J = 11.2 Hz, 1H); $^{13}C\{^1H\}$ NMR (100 MHz, $CDCl_3$) δ 101.4, 89.8, 77.9, 73.9, 64.6, 54.7, 48.4, 44.6, 43.9, 36.0, 34.2; IR (KBr) ν_{max} 3151, 1371, 1291, 1185, 837, 818, 638 cm^{-1}; HRMS (EI, 70 eV) *m/z* $(M\text{-}Br\bullet)^+$ calcd for $C_{11}H_{13}O_3$ 193.0859; found 193.0852.

(1*S*,4*R*,5a*R*,6*S*,9*R*,9a*S*)-1,2,5a,6,9,9a-Hexahydro-1,4-epoxy-6,9-ethanobenzo[*d*]oxe-pin-5(4*H*)-one (19)

A magnetically stirred solution of levoglucosenone (**2**) (1.49 g, 11.8 mmol) and 1,3-cyclohexadiene (2.37 g, 29.54 mmol, 2.5 equiv.) in dry dichloromethane (1.0 mL) was deoxygenated then placed under nitrogen before being subjected to microwave irradiation at 170 °C for 4 h. The cooled reaction mixture was treated with flash chromatography-grade silica gel (2.00 g) and the ensuing mixture concentrated under reduced pressure. The resulting free-flowing solid was subjected to flash chromatography (silica gel, 3:2 *v/v* diethyl ether/hexane) to afford, after concentration of the appropriate fractions (R_f = 0.5), compound **19**[12] (1.92 g, 79%) as a colourless, crystalline solid, m.p. = 59-61 °C (lit.[12a] m.p. = 44-45 °C), $[\alpha]_D$ = –150.5 (*c* = 1.0, methanol) {lit.[12b] $[\alpha]_D$ = –178.8 (*c* = 1.07, $CHCl_3$)}. ^{1}H NMR (400 MHz, $CDCl_3$) δ 6.40 (t, *J* = 7.3 Hz, 1H), 6.10 (t, *J* = 7.3 Hz, 1H), 4.87 (s, 1H), 4.54 (broadened s, 1H), 3.82 (s, 2H), 3.23 (broadened s, 1H), 2.74 (dd, *J* = 9.4 and 3.5 Hz, 1H), 2.65 (m, 1H), 2.10 (d, *J* = 9.4 Hz, 1H), 1.64 (m, 1H), 1.52 (m, 1H), 1.39 (m, 1H), 1.27 (m, 1H); ^{13}C{^{1}H} NMR (100 MHz, $CDCl_3$) δ 200.7, 134.1, 132.3, 99.7, 78.0, 69.5, 46.9, 43.3, 35.7, 32.9, 27.5, 22.2; IR (KBr) ν_{max} 2954, 2867, 1722, 1119, 995, 902, 870, 677 cm^{-1}; HRMS (EI, 70 eV) *m/z* $M^{+\bullet}$ calcd for $C_{12}H_{14}O_3$ 206.0937; found 206.0929.

(1*S*,4*R*,5*R*,5a*R*,6*S*,9*R*,9a*S*)-1,2,4,5,5a,6,9,9a-Octahydro-1,4-epoxy-6,9-ethanobenzo[*d*]-oxepin-5-ol (20) and (1*S*,4*R*,5*S*,5a*R*,6*S*,9*R*,9a*S*)-1,2,4,5,5a,6,9,9a-Octahydro-1,4-epoxy-6,9-ethanobenzo[*d*]oxepin-5-ol (21)

A magnetically stirred solution of compound **19** (250 mg, 1.21 mmol) in ethanol (100 mL) maintained at *ca*. 0 °C (ice-bath) was treated with potassium hydroxide (two drops of a 40% w/v aqueous solution) then, in portions, with a solution of sodium borohydride (50 mg, 1.21 mmol, 1.0 equiv.) in water (413 μL). The ensuing mixture was allowed to warm to ambient temperatures and, after 18 h, filtered through a pad of diatomaceous earth contained in a sintered-glass funnel and the filtrate then dried (Na_2SO_4) and filtered again. The solution thus obtained was adsorbed onto flash chromatography-grade silica gel (300 mg) and the ensuing

mixture concentrated under reduced pressure. The free-flowing solid thus obtained was subjected to flash chromatography (silica gel, 1:1 *v/v* diethyl ether/hexane) to afford two fractions, A and B.

Concentration of fraction A (R_f = 0.3) afforded compound **20**[9] (47 mg, 19%) as a colourless, crystalline solid, m.p. = 110-112 °C (lit.[9] m.p. = 112-113 °C), $[\alpha]_D$ = +4.60 (*c* = 5.0, methanol) {lit.[9] $[\alpha]_D$ = +29.8 (*c* = 0.97, $CHCl_3$)}. ^{1}H NMR (400 MHz, $CDCl_3$) δ 6.42 (t, *J* = 7.3 Hz, 1H), 6.33 (t, *J* = 7.3 Hz, 1H), 5.14 (s, 1H), 4.31 (d, *J* = 4.3 Hz, 1H), 3.74 (d, *J* = 6.8 Hz, 1H), 3.68 (dd, *J* = 6.8 and 4.5 Hz, 1H), 3.62 (dd, *J* = 12.8 and 8.4 Hz, 1H), 2.81 (broadened s, 1H), 2.54-2.49 (complex m, 2H), 1.84 (d, *J* = 12.8 Hz, 1H), 1.79 (d, *J* = 10.4 Hz, 1H), 1.61-1.48 (complex m, 2H), 1.37 (m, 1H), 1.20 (m, 1H); ^{13}C{^{1}H} NMR (100 MHz, $CDCl_3$) δ 134.6, 133.4, 102.5, 77.0, 71.7, 68.6, 44.5, 39.7, 36.7, 33.2, 29.1, 23.4; IR (KBr) ν_{max} 2934, 1133, 1026, 931, 843, 721, 642, 592, 570, 537 cm^{-1}; HRMS (EI, 70 eV) *m/z* $M^{+\bullet}$ calcd for $C_{12}H_{16}O_3$ 208.1099; found 208.1096.

Concentration of fraction B (R_f = 0.1) gave compound **21** (85 mg, 34%) as a voluminous white solid, m.p. = 155-157 °C (lit.[9] m.p. = 157-158 °C), $[\alpha]_D$ = –81.8 (*c* = 5.0, methanol) {lit.[9] $[\alpha]_D$ = –106.0 (*c* = 0.99, $CHCl_3$)}. ^{1}H NMR (400 MHz, $CDCl_3$) δ 6.44 (t, *J* = 7.3 Hz, 1H), 6.16 (t, *J* = 7.3 Hz, 1H), 5.18 (d, *J* = 3.1 Hz, 1H), 4.37 (d, *J* = 5.0 Hz, 1H), 3.76 (dd, *J* = 7.0 and 5.0 Hz, 1H), 3.70 (d, *J* = 7.0 Hz, 1H), 3.33 (m, 1H), 2.88 (broadened s, 1H), 2.49 (m, 1H), 1.94 (m, 1H), 1.83 (d, *J* = 10.0 Hz, 1H), 1.75 (d, *J* = 11.0 Hz, 1H), 1.59-1.52 (complex m, 1H), 1.50-1.33 (complex m, 2H), 1.16 (m, 1H); ^{13}C{^{1}H} NMR (100 MHz, $CDCl_3$) δ 135.3, 132.4, 100.9, 77.2, 71.2, 70.2, 46.3, 45.4, 36.2, 34.0, 28.7, 22.4; IR (KBr) ν_{max} 2971, 2945, 2874, 1143, 1050, 1043, 965, 907, 862, 707 cm^{-1}; HRMS (EI, 70 eV) *m/z* $M^{+\bullet}$ calcd for $C_{12}H_{16}O_3$ 208.1099; found 208.1100.

(1*R*,2*R*,5*S*,5a*S*,6*R*,9*S*,9a*R*)-2-Fluoro-1,2,4,5,5a,6,9,9a-octahydro-1,5-epoxy-6,9-ethanobenzo[*d*]oxepine (22)

A deoxygenated and magnetically stirred solution of compound **21** (61 mg, 0.29 mmol) in dry dichloromethane (5.0 mL), maintained at 0 °C under nitrogen was treated with DAST (43 mg, 0.27 mmol, 1.0 equiv.). After 2 h the reaction mixture was exposed to air then treated with flash chromatography-grade silica gel (100 mg) then concentrated under reduced pressure. The resulting free-flowing solid was subjected to flash chromatography (silica gel, 1:1 *v/v* diethyl ether/hexane elution) to afford, after concentration of the appropriate fractions (R_f = 0.4), an off-white, crystalline solid. Recrystallisation (dichloromethane) of this material gave compound **22** (46 mg, 75%) as a yellow, crystalline solid, m.p. = 99-102 °C, $[\alpha]_D$ = +15.00 (*c* = 1.0, methanol). ^{1}H NMR (400 MHz, $CDCl_3$) δ 6.22-6.16 (complex m, 2H), 5.07 (d, J_{HF} = 54.4 Hz, 1H), 4.13 (d, *J* = 10.8 Hz, 1H), 3.87 (s, 2H), 3.39 (d, *J* = 10.8 Hz, 1H), 2.71 (m, 2H), 2.45 (d, *J* = 2.8 Hz, 1H), 2.43 (d, *J* = 2.8 Hz, 1H), 1.55 (m, 2H), 1.24 (m, 2H); ^{13}C{^{1}H} NMR (100 MHz, $CDCl_3$) δ 132.4, 132.1, 105.2 (d, $^1J_{CF}$ = 229 Hz), 80.1 (d, $^2J_{CF}$ = 21 Hz), 68.0, 45.3 (d, J_{CF} = *ca*. 1 Hz), 45.1(0), 45.0(6), 33.6, 33.4, 24.6, 24.4; IR (KBr) ν_{max} 2943, 1151, 1084, 1060, 973, 866, 851, 842, 838, 706, 570 cm^{-1}; HRMS (EI, 70 eV) *m/z* $M^{+\bullet}$ calcd for $C_{12}H_{15}FO_2$ 210.1056; found 210.1060.

(1*S*,3*S*,4*S*,4a*R*,5*S*,8*R*,8a*S*)-3-Fluoro-3,4,4a,5,8,8a-hexahydro-1*H*-4,1-(epoxymethano)-5,8-ethanoisochromene (23)

A deoxygenated and magnetically stirred solution of compound **20** (63 mg, 0.30 mmol) in dry dichloromethane (3.0 mL) maintained under nitrogen at 0 °C was treated with DAST (54 mg, 0.33 mmol, 1.1 equiv.). After 3 h the reaction mixture was exposed to air then treated calcium

carbonate (33 mg, 0.33 mmol, 1.1 equiv.). The resulting mixture was subjected to subjected to flash chromatography (silica gel, 1:1 *v/v* diethyl ether/hexane elution) to afford, after concentration of the appropriate fractions (R_f = 0.5), a clear, yellow oil. Crystallisation (dichloromethane) of this material gave compound **23** (19 mg, 40%) as a colourless, crystalline solid, m.p. = 90-92 °C, $[\alpha]_D$ = +2.3 (*c* = 1.3, methanol). ^{1}H NMR (400MHz, $CDCl_3$) δ 6.25 (t, *J* = 7.3 Hz, 1H), 6.01 (t, *J* = 7.3 Hz, 1H), 5.40 (d, J_{HF} = 66.4 Hz, 1H), 4.21 (dd, *J* = 9.3 and 2.1 Hz, 1H), 3.90 (s, 1H), 3.79 (d, *J* = 9.3 Hz, 1H), 3.66 (broadened s, 1H), 2.62 (m, 1H), 2.58-2.49 (complex m, 2H), 2.04 (m, 1H), 1.63 (m, 2H), 1.43-1.20 (complex m, 2H); ^{13}C{^{1}H} NMR (100 MHz, $CDCl_3$) δ 134.3, 127.7, 107.1 (d, $^1J_{CF}$ = 220 Hz), 70.0, 69.2, 67.8 (d, $^2J_{CF}$ = 18 Hz), 43.3, 40.7, 33.2, 30.5, 26.0 (one signal obscured or overlapping); IR (KBr) ν_{max} 2934, 2907, 2864, 1172, 1121, 1114, 1087, 1076, 982, 878, 858, 837, 726, 718, 617, 599 cm^{-1}; MS (EI, 70 eV) *m/z* 210 [(M+)$^+$, 100%]; HRMS (EI, 70 eV) *m/z* $M^{+\bullet}$ calcd for $C_{12}H_{15}FO_2$ 210.1056; found 210.1058.

(1*R*,4*R*,5a*S*,6*R*,9*S*,9a*R*)-3,4,5a,6,9,9a-Hexahydro-1,4-epoxy-6,9-ethanobenzo[*c*]oxe-pin-5(1*H*)-one (24)

A magnetically stirred solution of *iso*-levoglucosenone (**3**) (200 mg, 1.59 mmol) and 1,3-cyclohexadiene (640 mg, 7.99 mmol, 5.0 equiv.) and dry dichloromethane (1.0 mL) maintained under nitrogen was subjected to microwave irradiation at 170 °C for 4 h. Thereafter, the cooled reaction mixture was treated with flash chromatography-grade silica gel (250 mg) and the ensuing mixture concentrated under reduced pressure. The resulting free-flowing solid was subjected to flash chromatography (silica gel, 1:1 *v/v* diethyl ether/hexane elution) to afford, after concentration of the appropriate fractions (R_f = 0.5) compound **24**[10] (300 mg, 91%) as a colourless, crystalline solid, m.p. = 54-56 °C. (lit.[10] m.p. = 78-79 °C), $[\alpha]_D$ = +43.6 (*c* = 0.1, acetonitrile) {lit.[10] $[\alpha]_D$ = +67.2 (*c* = 0.5, $CHCl_3$)}. ^{1}H NMR (400 MHz, $CDCl_3$) δ 6.31 (t, *J* = 7.4 Hz, 1H), 6.13 (t, *J* = 7.4 Hz, 1H), 5.45 (s, 1H), 4.25 (t, *J* = 3.6 Hz, 1H), 3.81 (d, *J* = 3.6 Hz,

2H), 3.20 (broadened s, 1H), 2.64 (m, 2H), 2.24 (d, J = 9.2 Hz, 1H), 1.62-1.47 (complex m, 2H), 1.34 (m, 1H), 1.23 (m, 1H); $^{13}C\{^1H\}$ NMR (100 MHz, $CDCl_3$) δ 206.6, 134.1, 131.8, 104.9, 77.9, 66.7, 48.5, 44.6, 33.3, 32.7, 26.8, 23.1; IR (KBr) ν_{max} 2937, 2865, 1721, 1224, 1126, 1007, 911, 853, 704, 471 cm^{-1}; HRMS (EI, 70 eV) *m/z* $M^{+\bullet}$ calcd for $C_{12}H_{14}O_3$ 206.0943; found 206.0949.

(1*R*,4*R*,5*R*,5a*S*,6*R*,9*S*,9a*R*)-1,3,4,5,5a,6,9,9a-Octahydro-1,4-epoxy-6,9-ethanobenzo-[*c*]oxepin-5-ol (25)

A magnetically stirred solution of compound **24** (300 mg, 1.45 mmol) in ethanol (10.0 mL) maintained at *ca*. 0 °C was treated with potassium hydroxide (2 drops of a 40% w/v aqueous solution) then with sodium borohydride (55 mg, 1.46 mmol). After 1 h the reaction mixture was treated with flash chromatography-grade silica gel (500 mg) then concentrated under reduced pressure. The resulting free-flowing solid was subjected to flash chromatography (silica, 1:1 *v/v* diethyl ether/hexane elution) to afford, after concentration of the appropriate fractions (R_f = 0.2), compound **25** (277 mg, 91%) as a crystalline solid, m.p. = 74-76 ºC, $[\alpha]_D$ = +6.5 (c = 0.4, acetone). ^1H NMR (400 MHz, $CDCl_3$) δ 6.37 (m, 1H), 6.16 (t, J = 7.3 Hz, 1H), 5.28 (s, 1H), 4.28-4.23 (complex m, 1H), 3.91 (d, J = 8.9 Hz, 1H), 3.81 (m, 1H), 3.58-3.54 (complex m, 1H), 2.81 (broadened s, 1H), 2.48-2.40 (complex m, 1H), 2.00-1.85 (complex m, 1H), 1.58-1.32 (complex m, 2H), 1.46 (m, 1H), 1.35 (m, 1H), 1.15 (m, 1H) (signal due to OH group proton not observed); $^{13}C\{^1H\}$ NMR (100 MHz, $CDCl_3$) δ 135.0, 132.6, 104.1, 73.7, 69.4, 61.2, 47.5, 44.3, 33.6, 33.3, 28.5, 22.5; IR (KBr) ν_{max} 3429, 2936, 2865, 1342, 1119, 1062, 1002, 979, 958, 870, 851, 709, 643, 527 cm^{-1}; HRMS (EI, 70 eV) *m/z* $M^{+\bullet}$ calcd for $C_{12}H_{16}O_3$ 208.1099; found 208.1091.

(1*S*,4*R*,5a*S*,6*S*,9*S*,9a*R*)-9-Isopropyl-6-methyl-1,2,5a,6,9,9a-hexahydro-1,4-epoxy-6,9-ethanobenzo[*d*]oxepin-5(4*H*)-one (27) and (1*S*,4*R*,5a*S*,6*R*,9*R*,9a*R*)-6-Isopropyl-9-methyl-1,2,5a,6,9,9a-hexahydro-1,4-epoxy-6,9-ethanobenzo[*d*]oxepin-5(4*H*)-one (28)

A magnetically stirred and deoxygenated solution of levoglucosenone (**2**) (2.40 g, 19.0 mmol) and α-terpinene (2.85 g, 20.9 mmol) in dichloromethane (50 mL), maintained at *ca*. 0 °C (ice-bath) was treated with tin(IV) chloride (300 mL of a 1.0 M solution in dichloromethane, 1.6 mole %). The ensuing mixture was allowed to warm to ambient temperatures and after 18 h treated with flash chromatography-grade silica gel (3.00 g) then concentrated under reduced pressure. The free-flowing solid thus obtained was subjected to flash chromatography (silica, hexane → 1:1 *v/v* diethyl ether/hexane gradient elution) to afford two fractions, A and B.

Concentration of fraction A [R_f = 0.6(2) in 1:1 *v/v* diethyl ether/hexane] gave compound **27** (99 mg, 2%) as a clear, yellow oil, $[\alpha]_D$ = –8.19 (*c* = 0.6, methanol); ^{1}H NMR (400 MHz, $CDCl_3$) δ 6.03 (d, *J* = 8.4 Hz, 1H), 5.92 (d, *J* = 8.4 Hz, 1H), 4.77 (m, 1H), 3.87 (t, *J* = 7.2 Hz, 1H), 3.76 (dd, *J* = 7.2 and 1.2 Hz, 1H), 3.00 (p, *J* = 6.8 Hz, 1H), 2.89 (d, *J* = 8.4 Hz, 1H), 1.86, (d, *J* = 8.8 Hz, 1H), 1.35-0.80 (complex m, 14H); ^{13}C{^{1}H} NMR (100 MHz, $CDCl_3$) δ 201.0, 138.4, 135.7, 100.8, 73.3, 68.5, 49.5, 48.8, 45.1, 38.3, 35.8, 30.1, 22.9, 21.0, 18.8, 16.9; IR (KBr) ν_{max} 2959, 2872, 1722, 1464, 1371, 1118, 991, 913, 882, 674 cm^{-1}; HRMS (EI, 70 eV) *m/z* $M^{+\bullet}$ calcd for $C_{16}H_{22}O_3$ 262.1563; found 262.1554.

Concentration of fraction B [R_f = 0.6(0) in 1:1 *v/v* diethyl ether/hexane] gave compound **28** (1.49 g, 30%) as a clear, yellow oil, $[\alpha]_D$ = –86.3 (*c* = 6.0, methanol) {lit.[13] $[\alpha]_D$ = –167.2 (*c* = 1.0, $CHCl_3$)}. ^{1}H NMR (400 MHz, $CDCl_3$) δ 6.03 (d, *J* = 8.3 Hz, 1H), 5.93 (d, *J* = 8.3 Hz, 1H), 4.79-4.76 (complex m, 2H), 3.88 (dd, *J* = 7.2 and 5.8 Hz, 1H), 3.75 (dd, *J* = 7.2 and 1.1 Hz, 1H), 2.98 (m, 1H), 2.90 (d, *J* = 8.6 Hz, 1H), 1.86 (d, *J* = 8.6 Hz, 1H), 1.44-1.32 (complex m, 3H), 1.29 (s, 3H), 1.14-1.03 (complex m, 3H), 0.94 (d, *J* = 6.8 Hz, 3H), 0.93 (d, *J* = 6.8 Hz,

3H); $^{13}C\{^{1}H\}$NMR (100 MHz, $CDCl_3$) δ 200.9, 138.2, 135.5, 100.6, 73.1, 68.3, 49.3, 48.6, 45.0, 38.1, 35.6, 30.0, 22.8, 20.8, 18.7, 16.8; IR (KBr) ν_{max} 2959, 2931, 1724, 1464, 1371, 1117, 991, 913, 882, 674 cm^{-1}; HRMS (EI, 70 eV) *m/z* $M^{+\bullet}$ calcd for $C_{16}H_{22}O_3$ 262.1563; found 262.1560.

(1*S*,4*R*,5*S*,5a*S*,6*R*,9*R*,9a*R*)-6-Isopropyl-9-methyl-1,2,4,5,5a,6,9,9a-octahydro-1,4-epoxy-6,9-ethanobenzo[*d*]oxepin-5-ol (29)

A magnetically stirred solution of compound **28** (600 mg, 2.29 mmol) in ethanol (45 mL) maintained at ambient temperatures was treated with potassium hydroxide (3 drops of a 40% w/v aqueous solution) then, in portions, with a solution of sodium borohydride (86 mg, 2.29 mmol, 1.0 equiv.) in water (780 μL). After 18 h the reaction mixture was filtered through a short pad of diatomaceous earth contained in a sintered glass funnel. The filtrate was then dried (Na_2SO_4), filtered and the filtrate treated with flash chromatography-grade silica gel (750 mg) then concentrated under reduced pressure. The free-flowing solid thus obtained was subjected to flash chromatography (silica, 1:1 *v/v* diethyl ether/hexane elution) to afford, after concentration of the appropriate fractions (R_f = 0.3), compound **29** (360 mg, 60%) as a yellow, crystalline solid, m.p. = 146-149 °C, $[\alpha]_D$ = –96.7 (*c* = 1.0, methanol). ^{1}H NMR (400 MHz, $CDCl_3$) δ 6.09 (d, *J* = 8.4 Hz, 1H), 5.96 (d, *J* = 8.4 Hz, 1H), 5.15 (d, *J* = 3.3 Hz, 1H), 4.61 (d, *J* = 5.6 Hz, 1H), 3.82 (t, *J* = 6.8 Hz, 1H), 3.65 (d, *J* = 7.0 Hz, 1H), 3.33 (m, 1H), 2.22 (p, *J* = 6.8 Hz, 1H), 2.07 (dd, *J* = 9.1 and 6.5 Hz, 1H), 1.74 (d, *J* = 11.3 Hz, 1H), 1.59 (d, *J* = 9.3 Hz, 1H), 1.40-1.26 (complex m, 3H), 1.20 (s, 3H), 1.05 (m, 1H), 0.97 (d, *J* = 6.8 Hz, 3H), 0.96 (d, *J* = 6.8 Hz, 3H); $^{13}C\{^{1}H\}$ NMR (100 MHz, $CDCl_3$) δ 139.4, 135.0, 101.3, 72.6, 69.4, 69.1, 51.8, 47.1, 45.1, 39.0, 35.8, 30.1, 22.8, 21.1, 18.6, 17.0; IR (KBr) ν_{max} 3462, 2958, 2946, 1465, 1340, 1066, 1058, 919, 697, 676, 508 cm^{-1}; HRMS (EI, 70 eV) *m/z* $M^{+\bullet}$ calcd for $C_{16}H_{24}O_3$ 264.1720; found 264.1719.

(1*R*,2*R*,5*S*,5a*R*,6*R*,9*R*,9a*S*)-2-Fluoro-9-isopropyl-6-methyl-1,2,4,5,5a,6,9,9a-octahyd-ro-1,5-epoxy-6,9-ethanobenzo[*d*]oxepine (30)

A deoxygenated and magnetically stirred solution of compound **29** (73 mg, 0.28 mmol) in dry dichloromethane (5.0 mL) maintained at 0 °C under nitrogen was treated with DAST (50 mg, 0.31 mmol, 1.1 equiv.). After 2 h the reaction mixture was exposed to air then treated with calcium carbonate (31 mg, 0.31 mmol, 1.1 equiv.). The resulting mixture was subjected to flash chromatography (silica gel, 1:1 *v/v* diethyl ether/hexane) to afford, after concentration of the appropriate fractions (R_f = 0.6), a yellow solid. Recrystallisation (methanol/dichloromethane) of this material gave compound **30** (46 mg, 62%) as yellow crystals, m.p. = 91-93 °C, $[\alpha]_D$ = +3.7 (*c* = 1.0, MeOH). ^{1}H NMR (400 MHz, $CDCl_3$) δ 5.96 (d, *J* = 8.5 Hz, 1H), 5.87 (d, *J* = 8.5 Hz, 1H), 5.05 (d, J_{HF} = 54.1 Hz, 1H), 4.16 (d, *J* = 12.3 Hz, 1H), 4.01 (m, 2H), 3.33 (d, *J* = 10.8 Hz, 1H), 2.44 (d, *J* = 8.3 Hz, 1H), 2.22 (d, *J* = 8.3 Hz, 1H), 2.04 (m, 1H), 1.47-1.39 (complex m, 2H), 1.20 (s, 3H), 1.19-1.14 (complex m, 2H), 0.99 (d, *J* = 6.8 Hz, 3H), 0.86 (d, *J* = 7.0 Hz, 3H); ^{13}C{^{1}H} NMR (100 MHz, $CDCl_3$) δ 135.8(6), 135.7(6), 105.4 (d, $^1J_{CF}$ = 230 Hz), 76.3 (d, $^2J_{CF}$ = 22 Hz), 68.4, 52.9, 48.4(2), 48.3(8), 41.6, 35.4, 34.2, 31.3, 24.0, 23.8, 19.0, 16.8; IR (KBr) ν_{max} 2956, 2932, 1463, 1375, 1151, 977, 901, 842, 693, 679, 609 cm^{-1}; HRMS (EI, 70 eV) *m/z* $M^{+\bullet}$ calcd for $C_{16}H_{23}FO_2$ 266.1682; found 266.1685.

(1*R*,4*R*,5a*S*,6*S*,9*S*,9a*R*)-6-Isopropyl-9-methyl-3,4,5a,6,9,9a-hexahydro-1,4-epoxy-6,9-ethanobenzo[*c*]oxepin-5(1*H*)-one (32)

A magnetically stirred and deoxygenated solution of *iso*-levoglucosenone (135 mg, 1.07 mmol) and α-terpinene (160 mg, 1.17 mmol) in dichloromethane (5 mL), maintained at *ca*. 0 °C (ice-bath) was treated with tin(IV) chloride (2 μL). The ensuing mixture was allowed to warm to ambient temperatures and after a further 1.5 h it treated with flash chromatography-grade silica gel (150 mg). The ensuing mixture was concentrated under reduced pressure and the resulting

free-flowing solid subjected to flash chromatography (silica, hexane → 1:5 *v/v* diethyl ether/hexane gradient elution) to afford, after concentration of the appropriate fractions (R_f = 0.5), compound **32** (67 mg, 24%) as colourless, needle-like crystals, m.p. = 64-67 °C, $[\alpha]_D$ = +8.2 (*c* = 0.1, methanol). ^{1}H NMR (400 MHz, $CDCl_3$) δ 6.02 (d, *J* = 8.4 Hz, 1H), 5.91 (d, *J* = 8.4 Hz, 1H), 5.65 (s, 1H), 4.18 (d, *J* = 5.2 Hz, 1H), 3.79 (d, *J* = 7.8 Hz, 1H), 3.70 (dd, *J* = 7.8 and 5.2 Hz, 1H), 2.77 (d, *J* = 8.6 Hz, 1H), 2.63 (m, 1H), 2.02 (d, *J* = 8.6 Hz, 1H), 1.45 (m, 1H), 1.33 (d, *J* = 12.8 Hz, 1H), 1.28 (s, 3H), 1.12-1.00 (complex m, 2H), 0.98 (d, *J* = 6.8 Hz, 3H), 0.93 (d, *J* = 6.9 Hz, 3H); ^{13}C{^{1}H} NMR (100 MHz, $CDCl_3$) δ 207.6, 138.6, 134.5, 102.3, 79.2, 68.4, 51.5, 49.4, 45.4, 37.2, 35.2, 30.3, 22.8, 22.4, 18.8, 17.1; IR (KBr) ν_{max} 2958, 2925, 2872, 1713, 1472, 1472, 1369, 1173, 1120, 905, 897, 865, 671 cm^{-1}; HRMS (EI, 70 eV) *m/z* $M^{+\bullet}$ calcd for $C_{16}H_{22}O_3$ 262.1569; found 262.1568.

(1*S*,4*R*,5a*R*,6*R*,7*R*,8*S*,9*S*,9a*S*)-7,8-Dihydroxyoctahydro-1,4-epoxy-6,9-ethanobenzo-[*d*]oxepin-5(4*H*)-one (33)

A magnetically stirred solution of compound **19** (107 mg, 0.52 mmol) in acetone/water/*t*-BuOH (18 mL of a 1:1:1 *v/v/v* mixture) maintained at ambient temperatures was treated with *N*-methylmorpholine *N*-oxide (82 mg, 0.70 mmol) then osmium tetroxide (8.0 mg, 0.03 mmol). After 48 h the reaction mixture was treated with sodium sulfite (7.5 mL of a 0.15 M aqueous solution) then flash chromatography-grade silica gel (200 mg). The ensuing mixture was concentrated under reduced pressure and the resulting free-flowing solid subjected to flash chromatography (silica, 95:5 *v/v* dichloromethane/methanol elution) to afford, after concentration of the appropriate fractions (R_f = 0.4), compound **33** (47 mg, 38%) as a colourless crystalline monohydrate, m.p. = 169-171 °C, $[\alpha]_D$ = –5.0 (*c* = 1.2, methanol). ^{1}H NMR (400 MHz, $CDCl_3$) δ 5.08 (s, 1H), 4.68 (m, 1H), 4.47 (dd, *J* = 5.4 Hz, 1H), 3.91 (m, 1H), 3.84 (dd, *J* = 8.4 and 3.6 Hz, 1H), 2.72 (dd, *J* = 11.2 and 4.0 Hz, 1H), 2.45 (m, 1H), 2.23 (d, *J* = 11.0 Hz, 1H), 2.11-1.95 (complex m, 3H), 1.92 (m, 1H), 1.33 (m, 2H), 0.85 (m, 2H); ^{13}C{^{1}H} NMR (100

MHz, $CDCl_3$) δ 201.5, 100.3, 77.4, 70.0, 64.3, 64.0, 42.1, 41.6, 37.7, 35.0, 18.5, 17.7; IR (KBr) ν_{max} 3426, 2928, 1721, 1119, 1066, 1023, 1000, 941 cm^{-1}; HRMS (TOF ESI, +ve) *m/z* $(M+Na)^+$ calcd for $C_{12}H_{16}O_5Na$ 263.0895; found 263.0905.

Crystallographic Studies

Crystallographic Data for Compound 10

$C_{11}H_{13}FO_2$, M = 196.21, T = 150 K, monoclinic, space group $P2_1$, Z = 4, a = 9.6766(2), b = 6.1686(2), c = 15.2100(2) Å; β = 96.633(2)°; V = 901.82(4) $Å^3$, D_x = 1.445 g cm^{-3}, 3240 unique data ($2\Theta_{max}$ = 147.696°), R = 0.0336 [for 3106 reflections with $I > 2.0\sigma(I)$]; Rw = 0.0852 (all data), S = 1.040.

Crystallographic Data for Compound 12

$C_{11}H_{13}BrO_3$, M = 273.12, T = 150 K, orthorhombic, space group $P2_12_12_1$, Z = 12, a = 6.13730(10), b = 13.3744(2), c = 37.1971(5) Å; V = 3053.24(8) $Å^3$, D_x = 1.782 g cm^{-3}, 6146 unique data ($2\Theta_{max}$ = 147.768°), R = 0.0372 [for 5929 reflections with $I > 2.0\sigma(I)$]; Rw = 0.0781 (all data), S = 1.053.

Crystallographic Data for Compound 14

$C_{11}H_{14}O_3$, M = 194.22, T = 150 K, monoclinic, space group $C2$, Z = 8, a = 22.8328(5), b = 7.6093(2), c = 10.8801(2) Å; β = 100.254(2)°; V = 1860.13(7) $Å^3$, D_x = 1.387 g cm^{-3}, 3716 unique data ($2\Theta_{max}$ = 147.598°), R = 0.0300 [for 3577 reflections with $I > 2.0\sigma(I)$]; Rw = 0.0799 (all data), S = 1.046.

Crystallographic Data for Compound 15

$C_{11}H_{14}O_3$, M = 192.22, T = 150 K, orthorhombic, space group $P2_12_12_1$, Z = 4, a = 6.3231(3), b = 10.4166(3), c = 13.8634(5) Å; V = 913.12(6) Å^3, D_x = 1.413 g cm^{-3}, 1819 unique data ($2\Theta_{max}$ = 147.674°), R = 0.0329 [for 1781 reflections with $I > 2.0\sigma(I)$]; Rw = 0.0841 (all data), S = 1.088.

Crystallographic Data for Compound 16

$C_{11}H_{13}FO_2$, M = 196.21, T = 150 K, orthorhombic, space group $P2_12_12_1$, Z = 8, a = 8.01597(4), b = 11.19036(5), c = 20.45824(9) Å; V = 1835.136(15) Å^3, D_x = 1.420 g cm^{-3}, 3700 unique data ($2\Theta_{max}$ = 147.57°), R = 0.0278 [for 3646 reflections with $I > 2.0\sigma(I)$]; Rw = 0.0736 (all data), S = 1.049.

Crystallographic Data for Compound 18

$C_{11}H_{13}BrO_3$, M = 273.12, T = 150 K, orthorhombic, space group $P2_12_12_1$, Z = 4, a = 6.51262(3), b = 10.13334(5), c = 15.30877(7) Å; V = 1010.296(8) Å^3, D_x = 1.796 g cm^{-3}, 2036 unique data ($2\Theta_{max}$ = 147.666°), R = 0.0152 [for 2035 reflections with $I > 2.0\sigma(I)$]; Rw = 0.0395 (all data), S = 1.064.

Crystallographic Data for Compound 19

$C_{12}H_{14}O_3$, M = 206.23, T = 150 K, orthorhombic, space group $P2_12_12_1$, Z = 4, a = 6.79360(10), b = 8.81770(10), c = 16.7440(2) Å; V = 1003.03(2) Å^3, D_x = 1.366 g cm^{-3}, 2023 unique data ($2\Theta_{max}$ = 147.392°), R = 0.0272 [for 1988 reflections with $I > 2.0\sigma(I)$]; Rw = 0.0696 (all data), S = 1.067.

Crystallographic Data for Compound 20

$C_{12}H_{16}O_3$, M = 208.25, T = 150 K, orthorhombic, space group $P2_12_12_1$, Z = 4, a = 6.64130(10), b = 9.23670(10), c = 16.4248(2) Å; V = 1007.56(2) Å^3, D_x = 1.373 g cm^{-3}, 2034 unique data

($2\Theta_{max}$ = 147.354°), R = 0.0245 [for 2026 reflections with $I > 2.0\sigma(I)$]; Rw = 0.0629 (all data), S = 1.073.

Crystallographic Data for Compound 22

$C_{12}H_{15}FO_2$, M = 210.24, T = 150 K, monoclinic, space group $P2_1$, Z = 2, a = 6.31320(10), b = 9.05670(10), c = 8.62950(10) Å; β = 92.4200(10) °; V = 492.967(11) Å^3, D_x = 1.416 g cm^{-3}, 1995 unique data ($2\Theta_{max}$ = 147.576°), R = 0.0261 [for 1969 reflections with $I > 2.0\sigma(I)$]; Rw = 0.0675 (all data), S = 1.055.

Crystallographic Data for Compound 23

$C_{12}H_{15}FO_2$, M = 210.24, T = 150 K, orthorhombic, space group $P2_12_12_1$, Z = 4, a = 6.17990(10), b = 8.86940(10), c = 17.8628(2) Å; V = 979.10(2) Å^3, D_x = 1.426 g cm^{-3}, 1974 unique data ($2\Theta_{max}$ = 147.55°), R = 0.0308 [for 1952 reflections with $I > 2.0\sigma(I)$]; Rw = 0.0825 (all data), S = 1.074.

Crystallographic Data for Compound 24

$C_{12}H_{14}O$, M = 206.23, T = 150 K, monoclinic, space group $P2_1$, Z = 2, a = 8.3349(3), b = 7.04620(10), c = 9.4300(3) Å; β = 116.220(4)°; V = 496.83(3) Å^3, D_x = 1.379 g cm^{-3}, 2015 unique data ($2\Theta_{max}$ = 147.500°), R = 0.0249 [for 1990 reflections with $I > 2.0\sigma(I)$]; Rw = 0.0639 (all data), S = 1.052.

Crystallographic Data for Compound 25

$C_{12}H_{16}O_3$, M = 208.25, T = 150 K, orthorhombic, space group $P2_12_12_1$, Z = 4, a = 16.4965(6), b = 9.6802(3), c = 6.4328(4) Å; V = 1027.25(8) Å^3, D_x = 1.347 g cm^{-3}, 2488 unique data ($2\Theta_{max}$

= 57.678°), R = 0.0718 [for 1936 reflections with $I > 2.0\sigma(I)$]; Rw = 0.1908 (all data), S = 1.085.

Crystallographic Data for Compound 29

$C_{16}H_{24}O_3$, M = 264.35, T = 150 K, monoclinic, space group $P2_1$, Z = 2, a = 9.37870(10), b = 5.99750(10), c = 12.60630(10) Å; Θ = 105.3830(10) °; V = 683.685(15) Å^3, D_x = 2 g cm^{-3}, 2508 unique data ($2\Theta_{max}$ = 147.724°), R = 0.0290 [for 2473 reflections with $I > 2.0\sigma(I)$]; Rw = 0.0768 (all data), S = 1.079.

Crystallographic Data for Compound 30

$C_{16}H_{23}FO_2$, M = 266.34, T = 150 K, monoclinic, space group $P2_1$, Z = 2, a = 8.1256(5), b = 6.6884(3), c = 13.2704(7) Å; β = 105.386(6) °; V = 695.36(7) Å^3, D_x = 1.272 g cm^{-3}, 3869 unique data ($2\Theta_{max}$ = 59.148°), R = 0.0514 [for 3448 reflections with $I > 2.0\sigma(I)$]; Rw = 0.1156 (all data), S = 1.037.

Crystallographic Data for Compound 32

$C_{16}H_{22}O_3$, M = 262.33, T = 150 K, monoclinic, space group $P2_1$, Z = 2, a = 10.3300(9), b = 5.8129(4), c = 11.94370(10) Å; β = 105.337(9) °; V = 691.64(10) Å^3, D_x = 1.260 g cm^{-3}, 3058 unique data ($2\Theta_{max}$ = 57.18°), R = 0.0578 [for 2493 reflections with $I > 2.0\sigma(I)$]; Rw = 0.1202 (all data), S = 1.067.

Crystallographic Data for Compound 33 (monohydrated form)

$C_{12}H_{18}O_6$, M = 258.26, T = 150 K, monoclinic, space group $P2_1$, Z = 2, a = 9.0086(9), b = 6.8556(7), c = 9.6657(11) Å; β = 97.622(11) °; V = 591.67(11) Å^3, D_x = 1.450 g cm^{-3}, 2009 unique data ($2\Theta_{max}$ = 140.136°), R = 0.0459 [for 1853 reflections with $I > 2.0\sigma(I)$]; Rw = 0.1213 (all data), S = 1.036.

Crystallographic Data for Compound 34

$C_{12}H_{15.639}O_5$, M = 239.88, T = 150 K, monoclinic, space group $P2_1$, Z = 2, a = 8.4848(3), b = 6.58213(18), c = 9.5820(3) Å; β = 90.171(3) °; V = 535.14(3) Å^3, D_x = 1.489 g cm^{-3}, 1859 unique data ($2\Theta_{max}$ = 133.200°), R = 0.0295 [for 1751 reflections with $I > 2.0\sigma(I)$]; Rw = 0.0710 (all data), S = 1.042. Difference electron density maps towards the end of the refinement revealed unaccounted for features in the refinement model for compound **33** that were handled by the incorporation of compound **34** as a cocrystallised impurity (refined occupancy of 18%) after discussion with co-authors over the spectroscopic data of the bulk sample. This model yielded an improved refinement relative to that of the diol as a diastereomeric mixture that was also investigated.

Structure Determinations

Data for compounds **10**, **12**, **14**, **15**, **16**, **18**, **19**, **20**, **22**, **23**, **24**, **29**, **33** and the **33/34** cocrystallised mixture were measured on an Agilent SuperNova X-ray diffractometer (CuKα, graphite monochromator, λ = 1.54184 Å, except for **25**, **30** and **32** that used MoKα, graphite monochromator, λ = 0.71073 Å). Using OLEX2,[19] structures were solved by dual-space methods with the ShelXT[20] program and refined, using least squares minimisation, with the ShelXL[21] package. Atomic coordinates, bond lengths and angles, and displacement parameters have been deposited at the Cambridge Crystallographic Data Centre (CCDC numbers 2268350-2268366). These data can be obtained free-of-charge *via* www.ccdc.cam.ac.uk/data_request/cif, by emailing data_request@ccdc.cam.ac.uk, or by contacting The Cambridge Crystallographic Data Centre, 12 Union Road, Cambridge CB2 1EZ, UK; fax: +44 1223 336033.

Plots derived from the single-crystal X-ray analyses of compounds 10, 12, 14, 15, 16, 18, 19, 20, 22, 23, 24, 25, 29, 30, 32, 33 and the aggregate of compounds 33 and 34

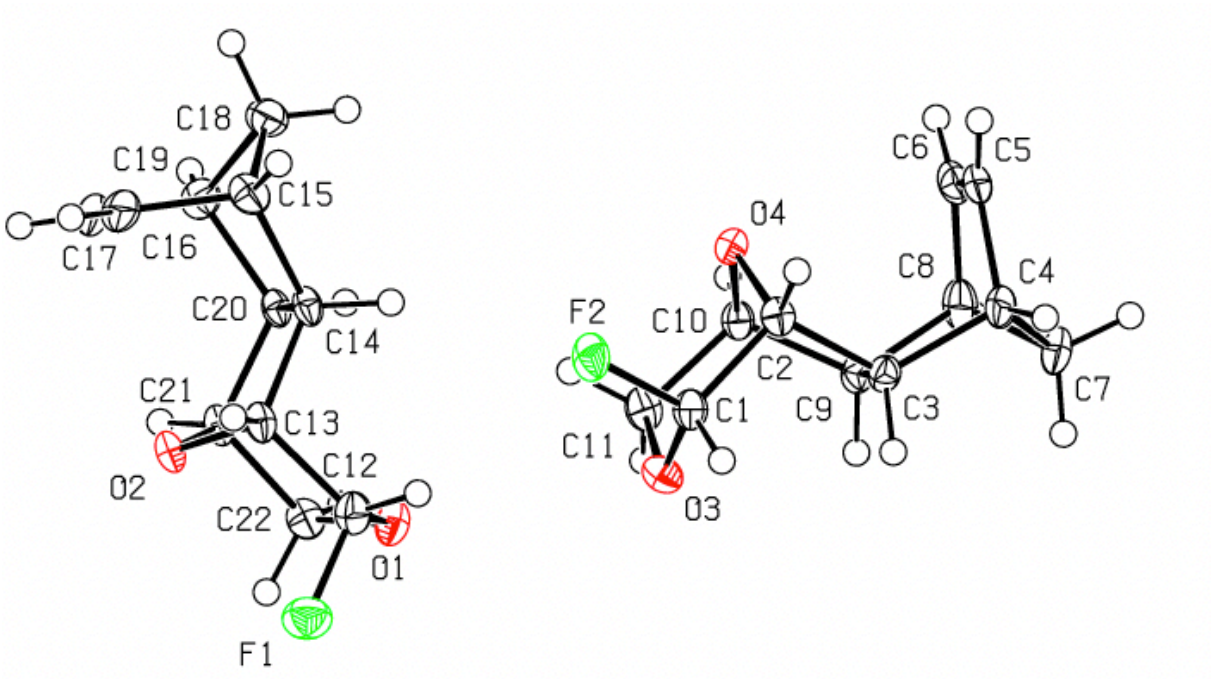

Figure S1: Molecular structure of compound **10** (CCDC 2268350) showing both crystallographically independent molecules in the asymmetric unit. Atomic displacement parameters shown at 50% probability level (crystal grown from hexane).

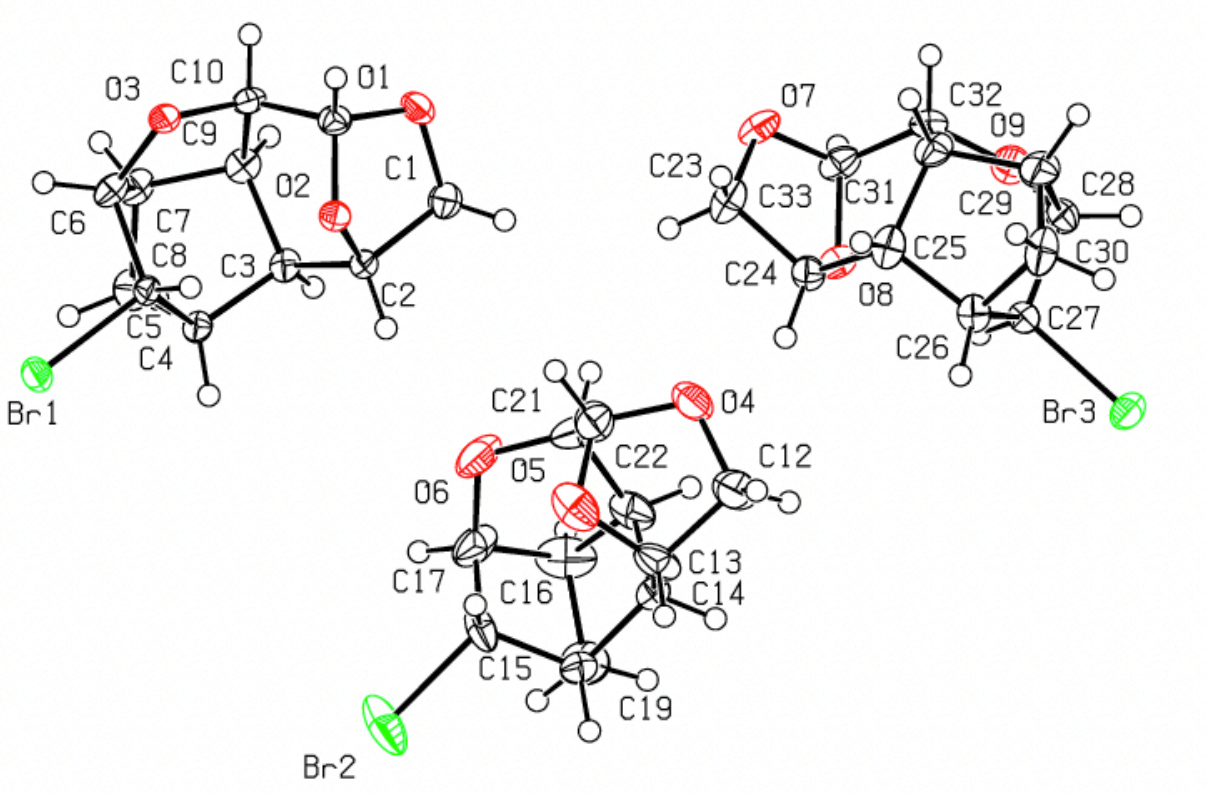

Figure S2: Molecular structure of compound **12** (CCDC 2268351) and showing the three crystallographically independent molecules in the asymmetric unit. Atomic displacement parameters shown at 50% probability level (crystal grown from methanol/dichloromethane).

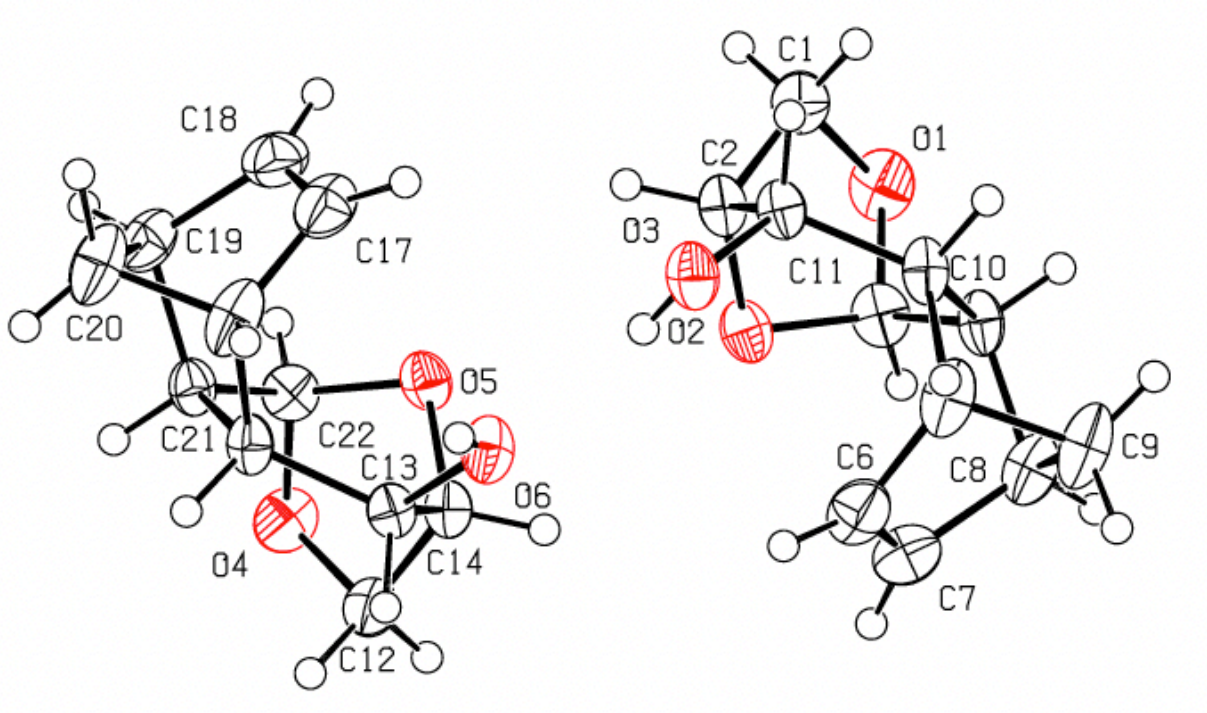

Figure S3: Molecular structure of compound **14** (CCDC 2268353) and showing both crystallographically independent molecules in the asymmetric unit (hydrogen bonding is not shown and the extended structure arising from hydrogen bonding is also not shown). Atomic displacement parameters shown at 50% probability level (crystal grown from diethyl ether/petroleum ether).

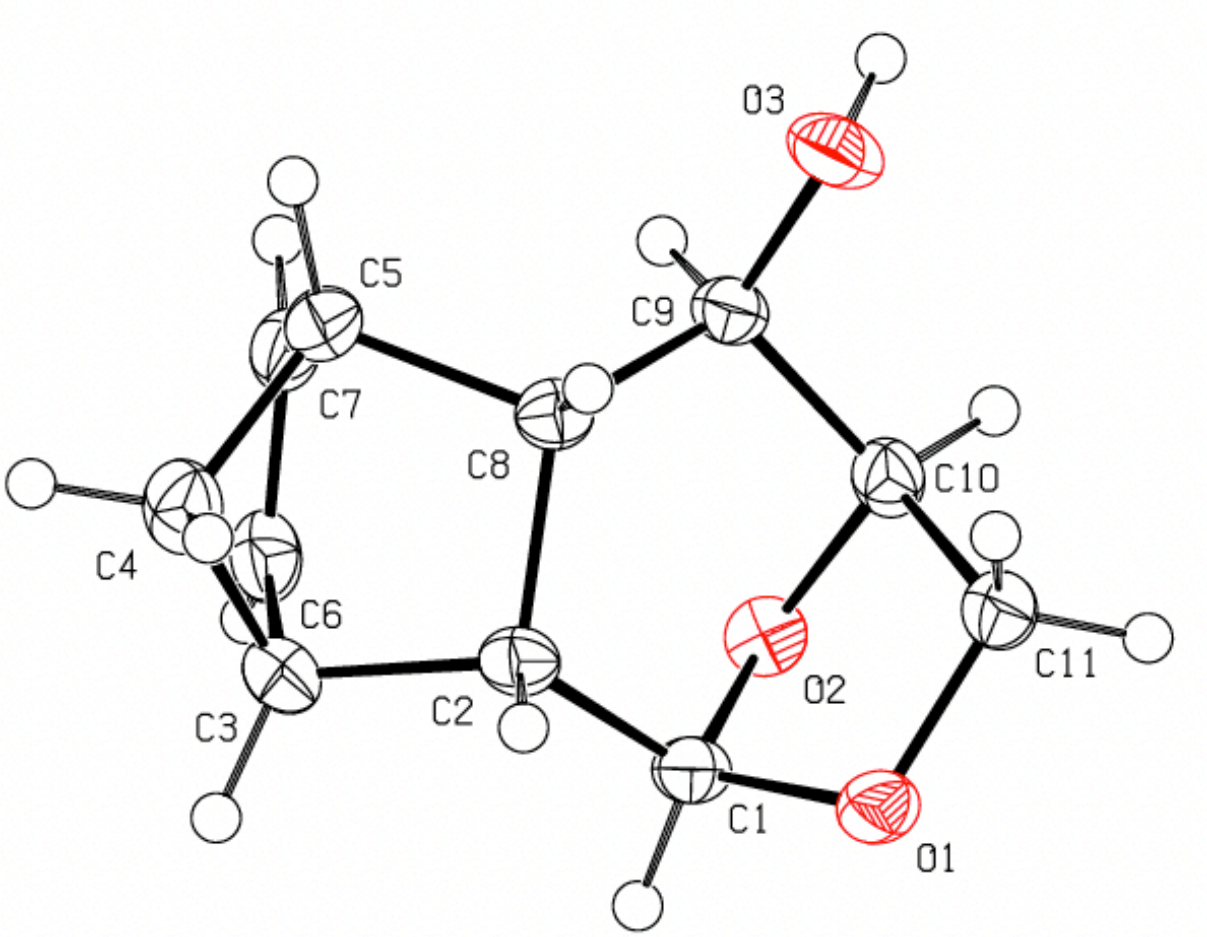

Figure S4: Molecular structure of compound **15** (CCDC 2268352). The extended structure arising from hydrogen bonding is not shown. Atomic displacement parameters shown at 50% probability level (crystal grown from ethyl acetate/petroleum ether).

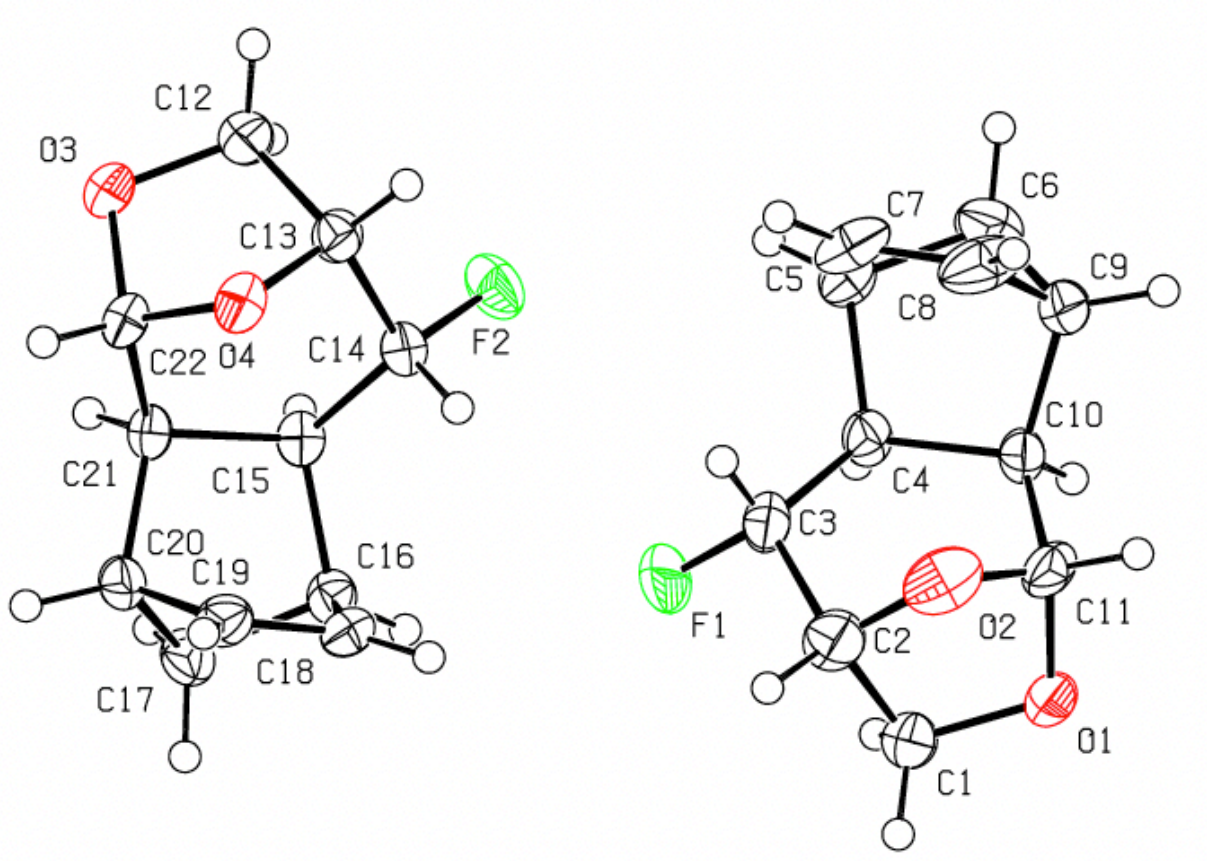

Figure S5: Molecular structure of compound **16** (CCDC 2268354) showing both crystallographically independent molecules in the asymmetric unit. Atomic displacement parameters shown at 50% probability level (crystal grown from hexane).

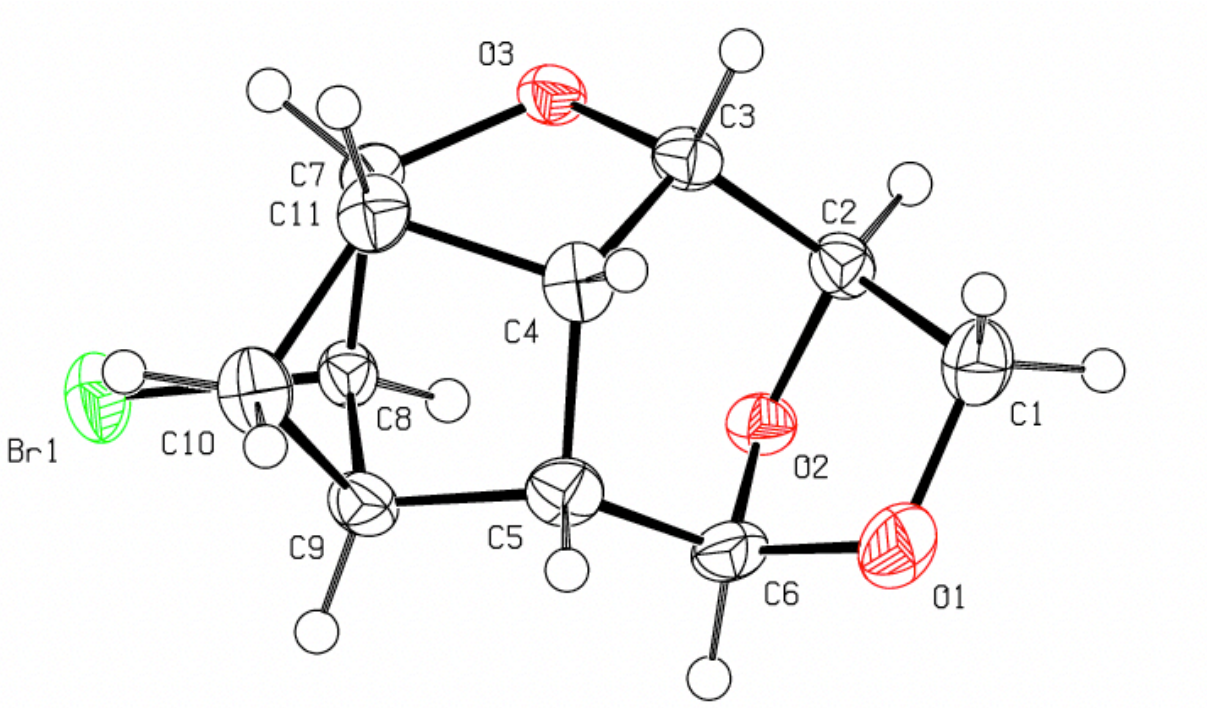

Figure S6: Molecular structure of compound **18** (CCDC 2268355). Atomic displacement parameters shown at 50% probability level (crystal grown from ethyl acetate/hexane/methanol).

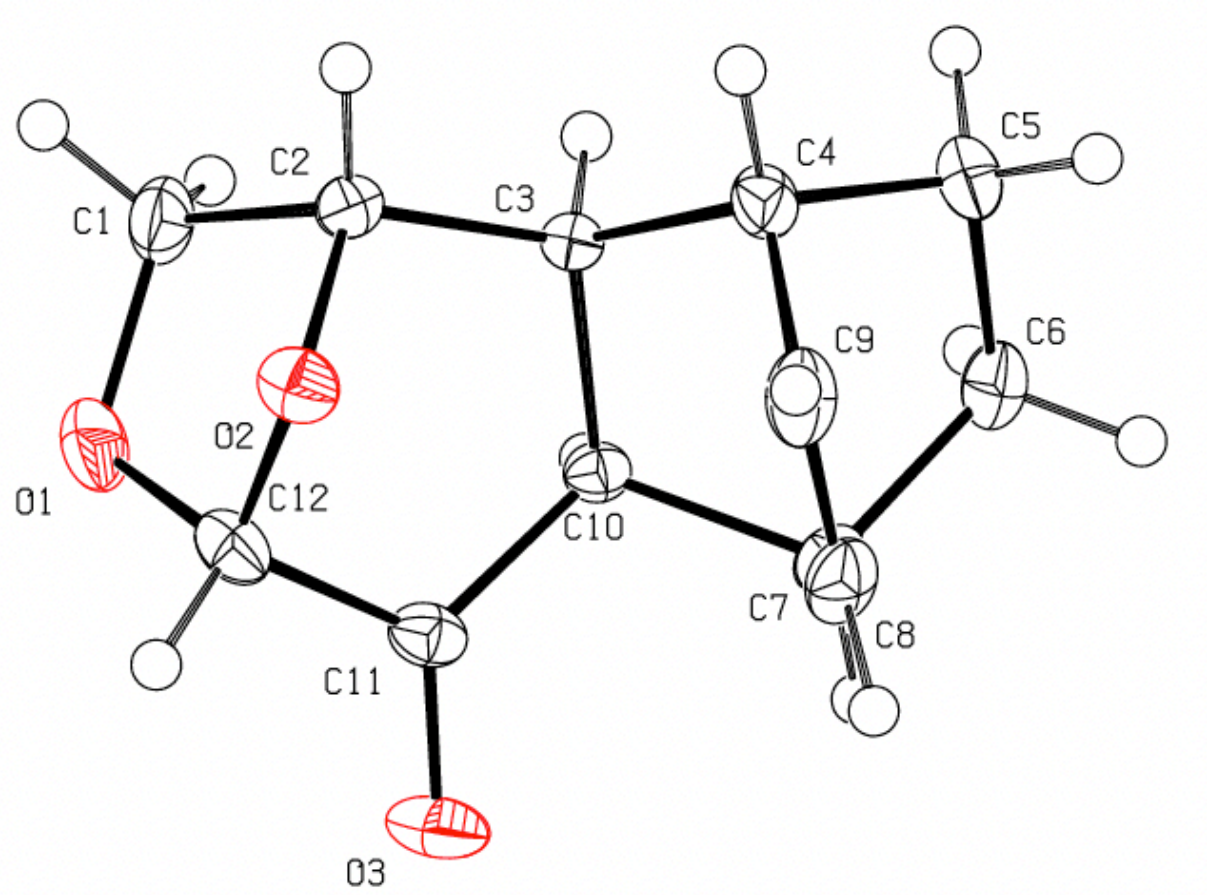

Figure S7: Molecular structure of compound **19** (CCDC 2268356). Atomic displacement parameters shown at 50% probability level (crystal grown from diethyl ether/hexane).

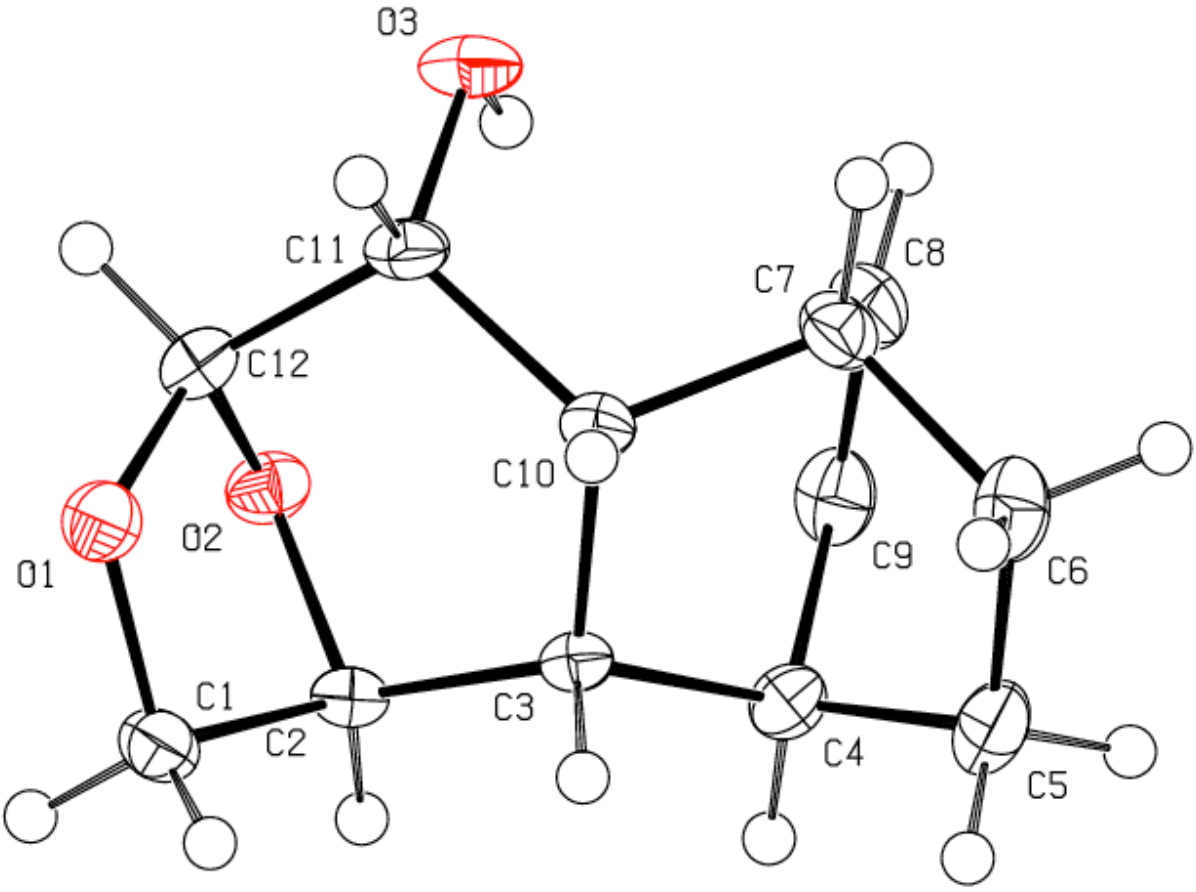

Figure S8: Molecular structure of compound **20** (CCDC 2268357). The extended structure arising from hydrogen bonding is not shown. Atomic displacement parameters shown at 50% probability level (crystal grown from diethyl ether/hexane).

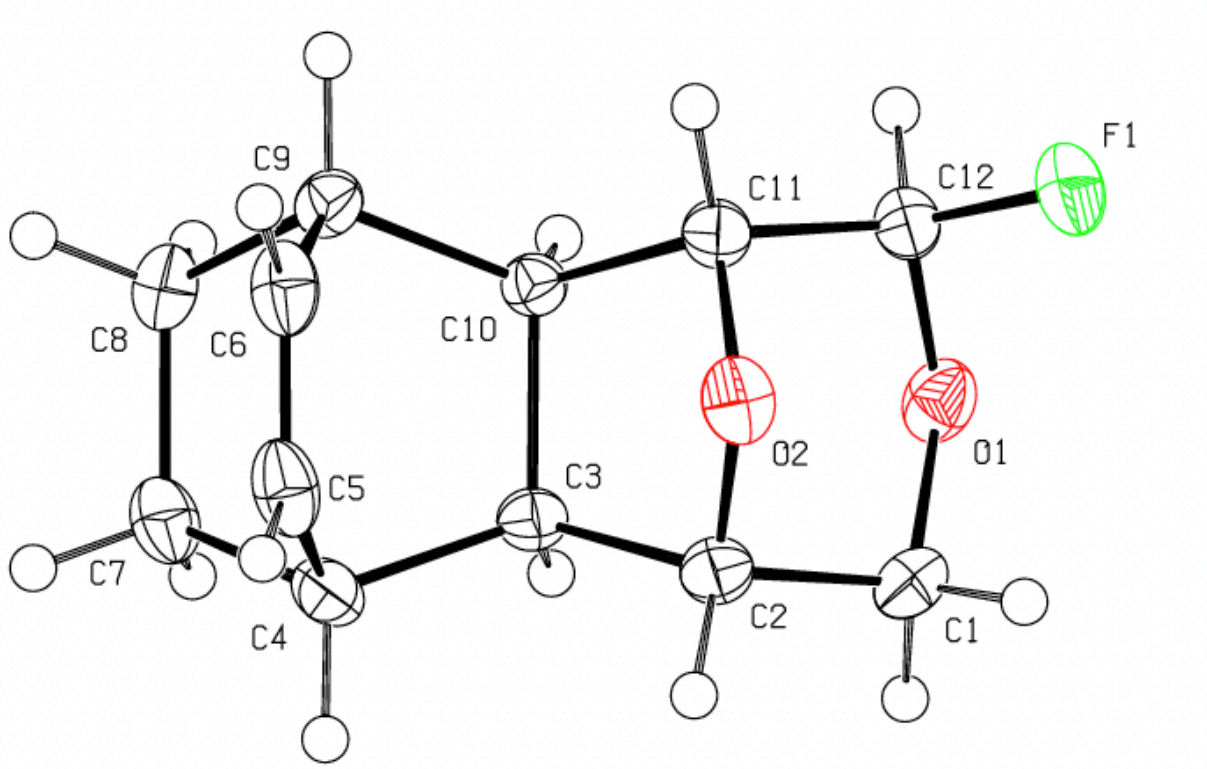

Figure S9: Molecular structure of compound **22** (CCDC 2268358). Atomic displacement parameters shown at 50% probability level (crystal grown from dichloromethane).

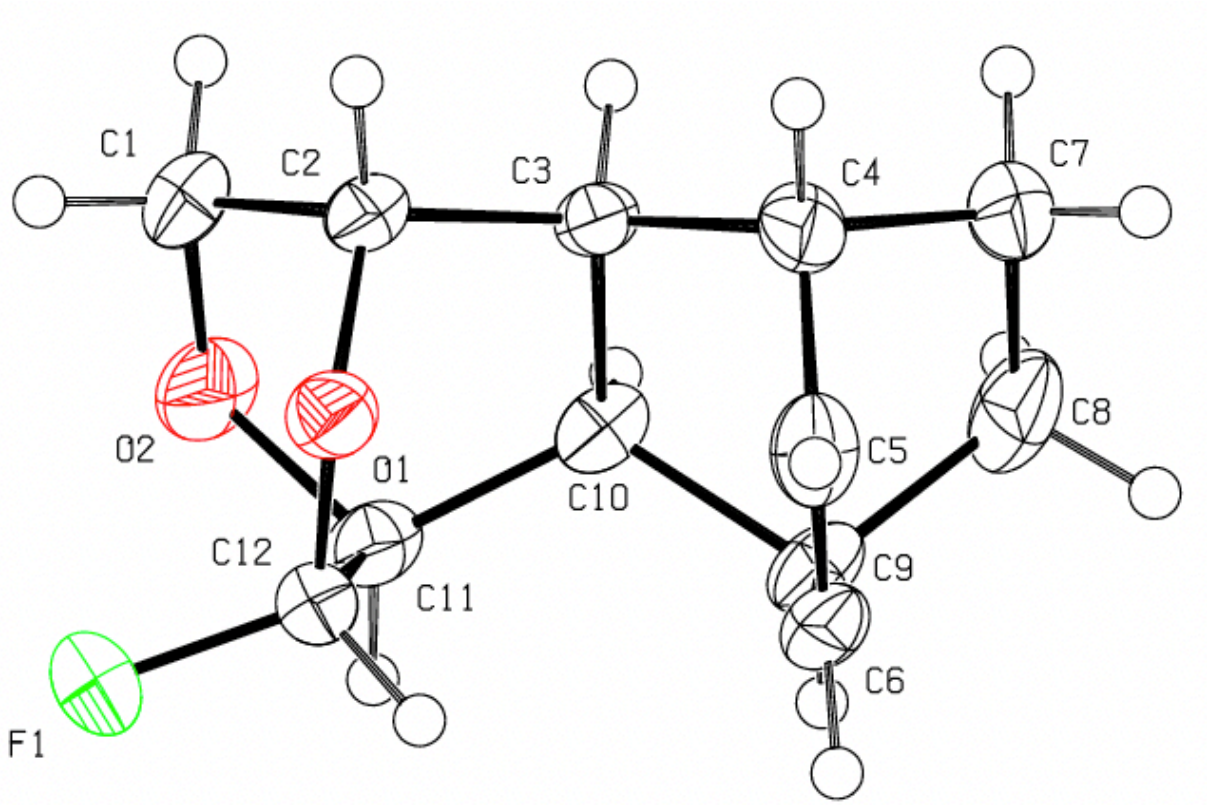

Figure S10: Molecular structure of compound **23** (CCDC 2268359). Atomic displacement parameters shown at 50% probability level (crystal grown from dichloromethane/methanol).

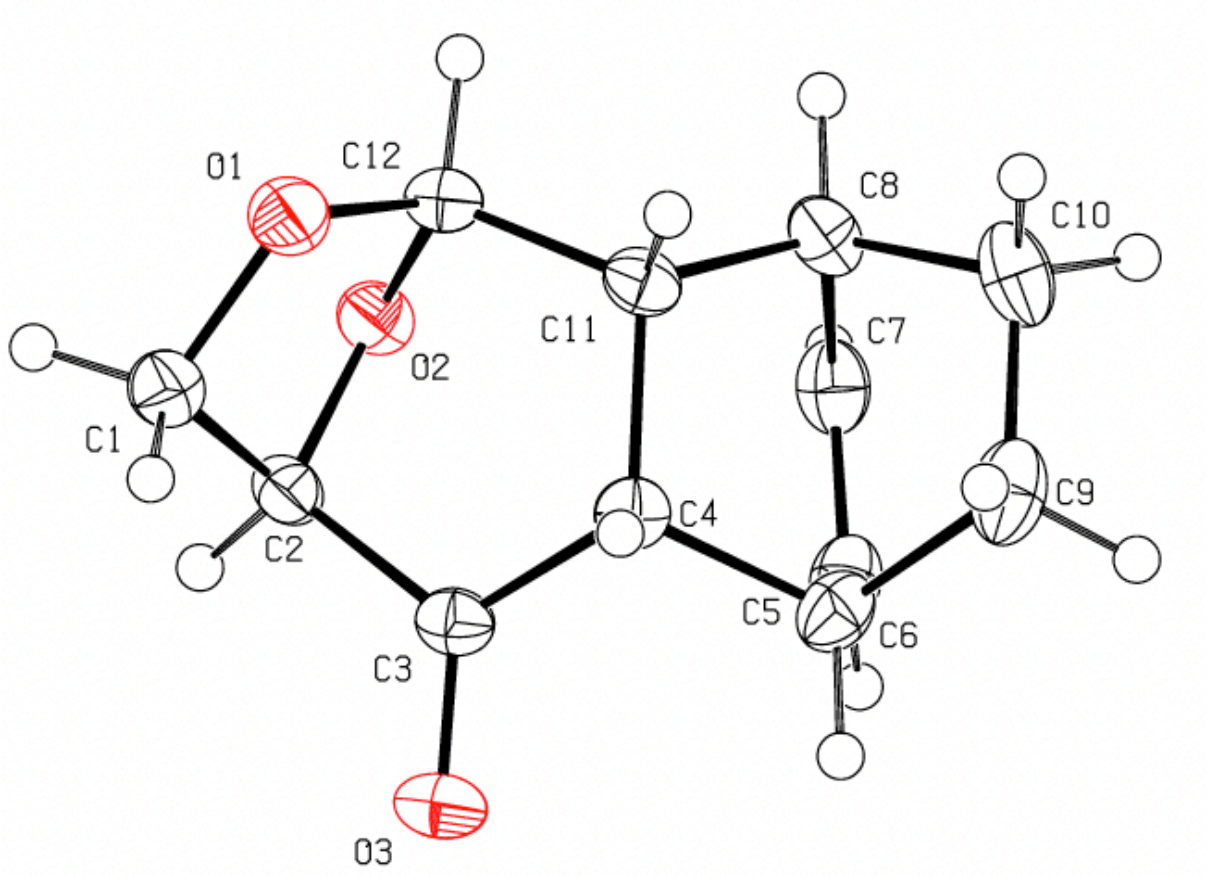

Figure S11: Molecular structure of compound **24** (CCDC 2268360). Atomic displacement parameters shown at 50% probability level (crystal grown from diethyl ether/hexane).

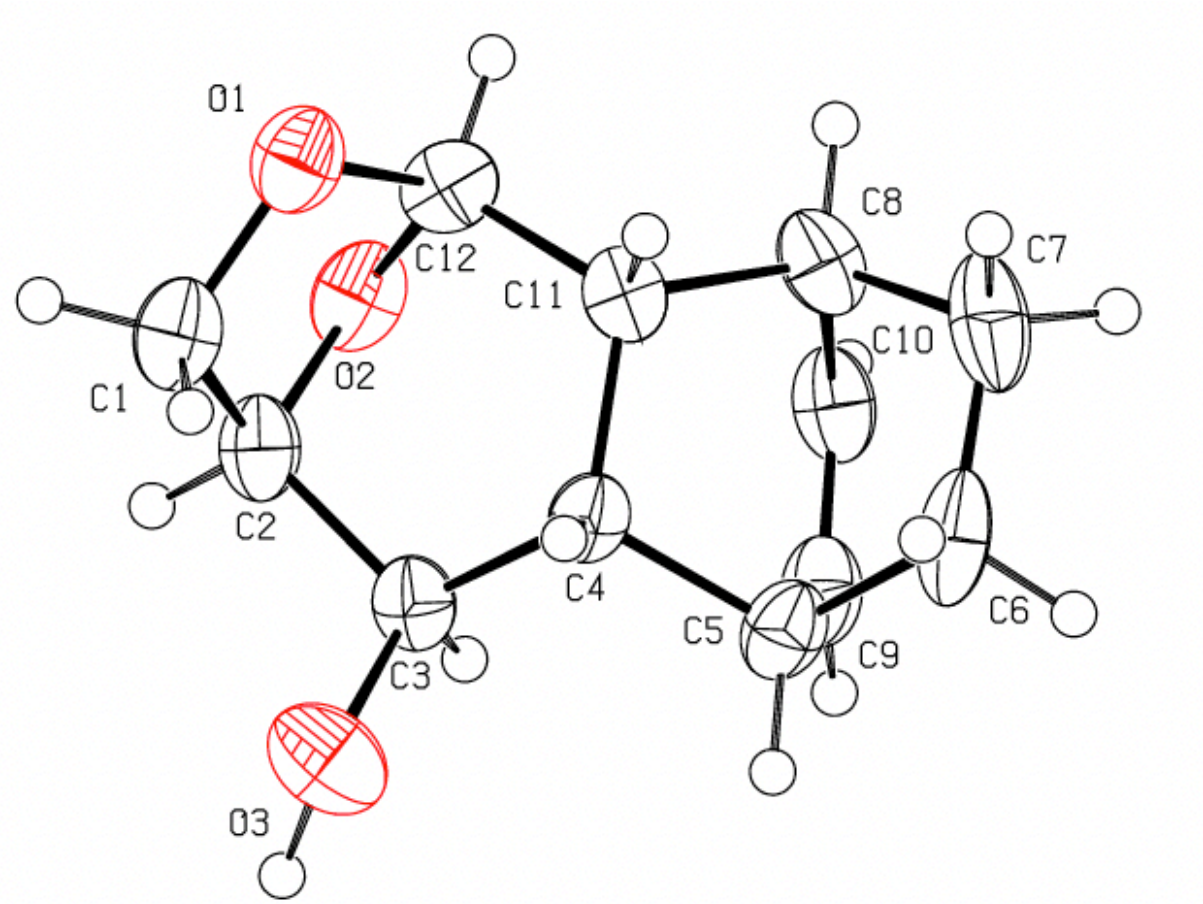

Figure S12: Molecular structure of compound **25** (CCDC 2268361). The extended structure arising from hydrogen bonding is not shown. Atomic displacement parameters shown at 50% probability level (crystal grown from dichloromethane).

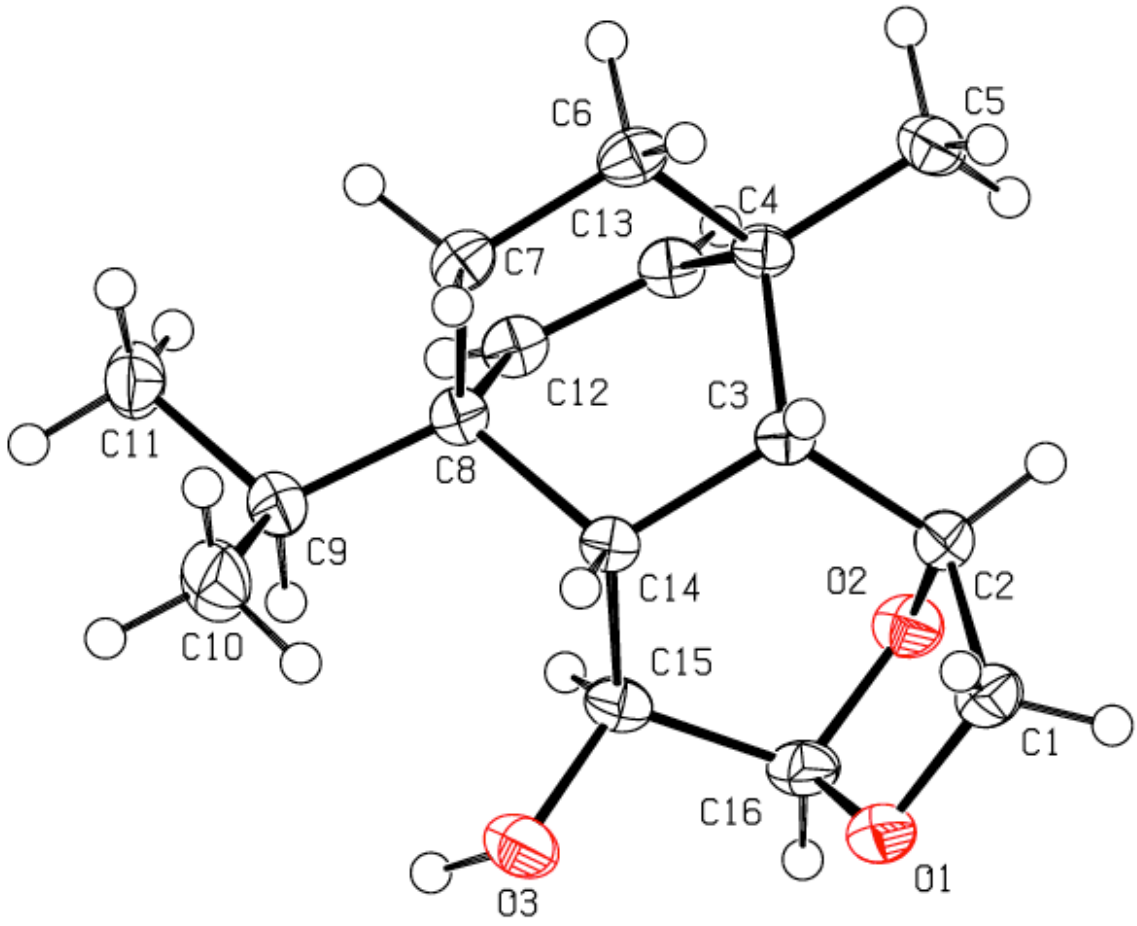

Figure S13: Molecular structure of compound **29** (CCDC 2268362). The extended structure arising from hydrogen bonding is not shown. Atomic displacement parameters shown at 50% probability level (crystal grown from dichloromethane/methanol).

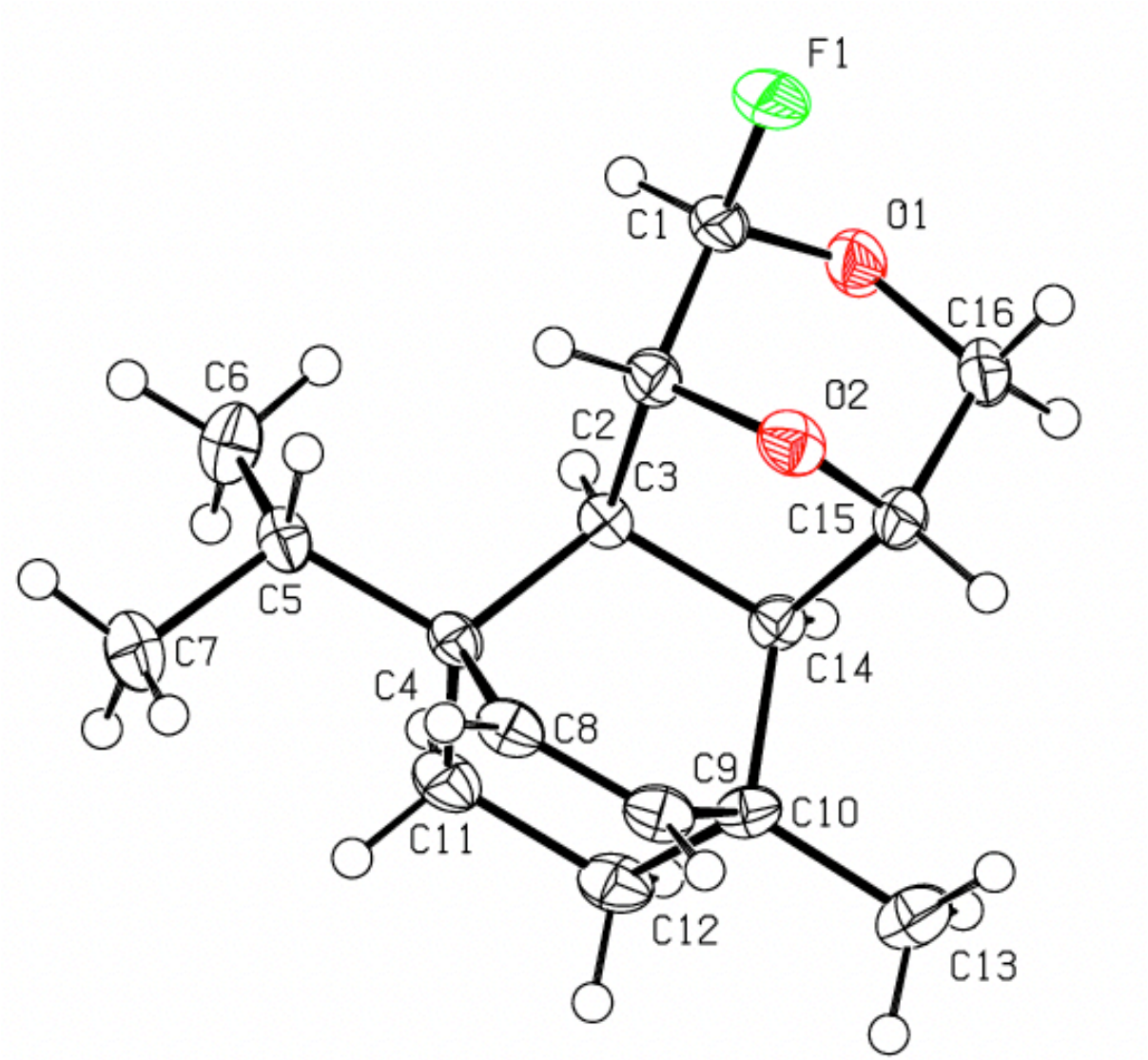

Figure S14: Molecular structure of compound **30** (CCDC 2268363). Atomic displacement parameters shown at 50% probability level (crystal grown from dichloromethane/methanol).

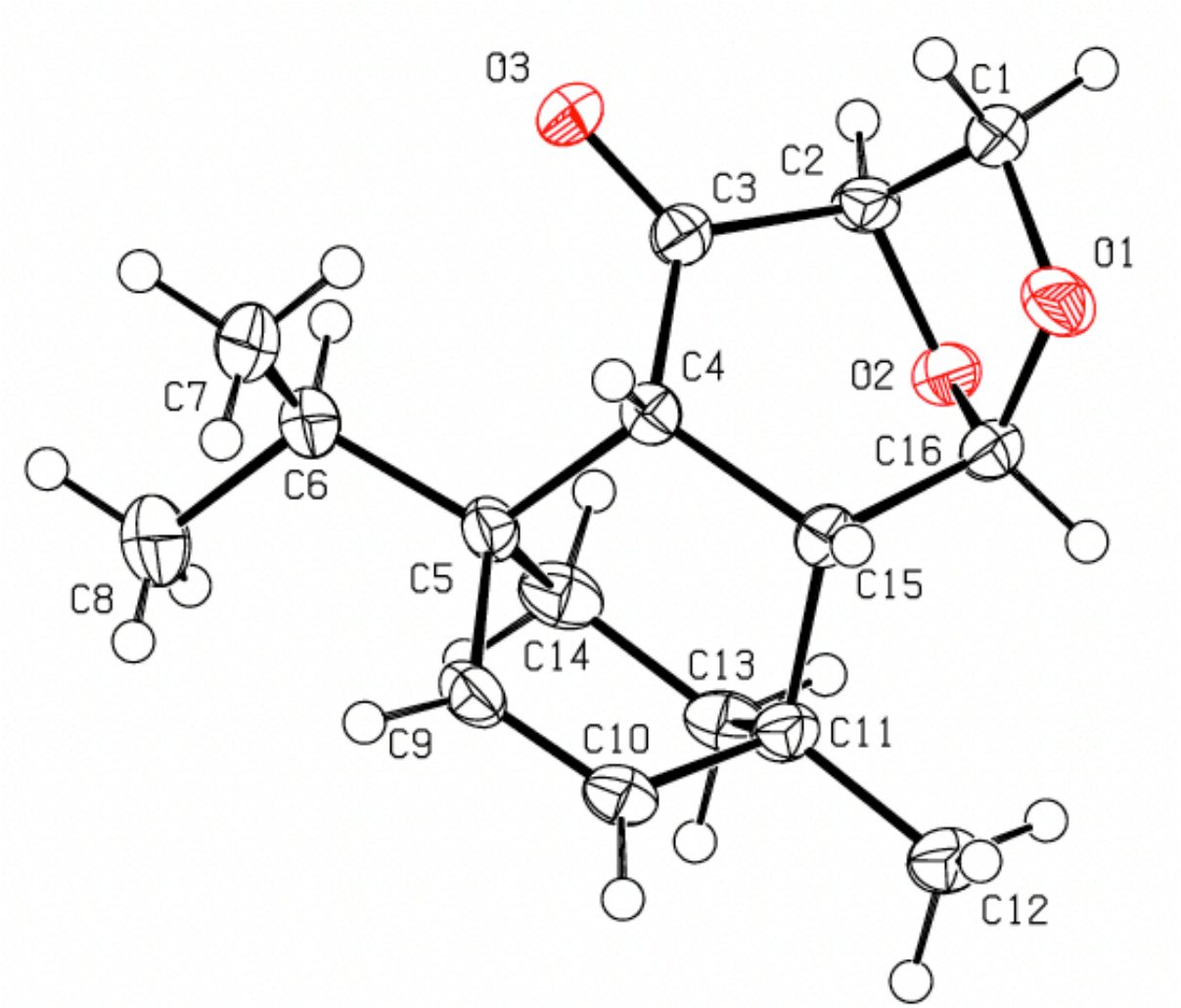

Figure S15: Molecular structure of compound **32** (CCDC 2268364). Atomic displacement parameters shown at 50% probability level (crystal grown from diethyl ether/hexane).

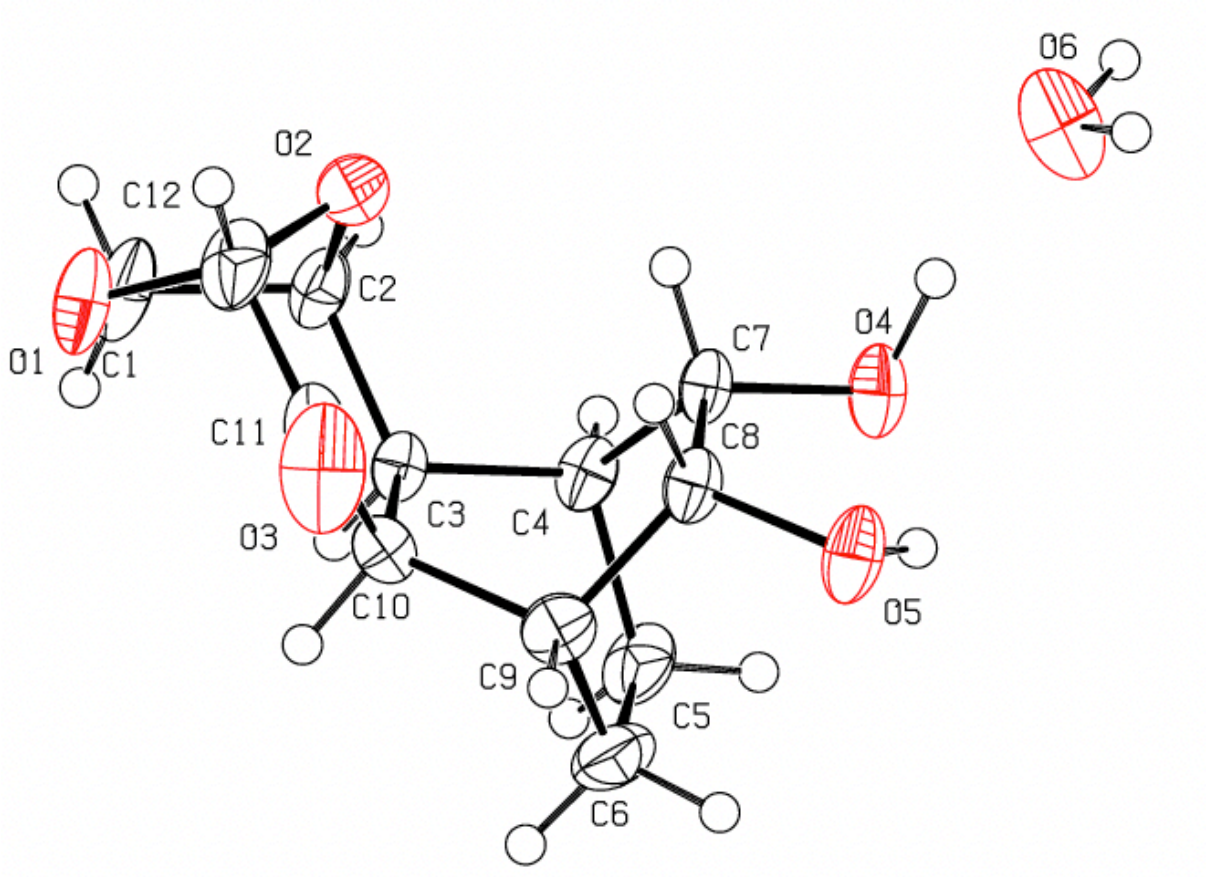

Figure S16: Molecular structure of compound **33** (CCDC 2268365) showing the water molecule in the asymmetric unit for the monohydrate (hydrogen bonding is not shown and the extended structure arising from the hydrogen bonding is also not shown). Atomic displacement parameters shown at 50% probability level (crystal grown from dichloromethane).

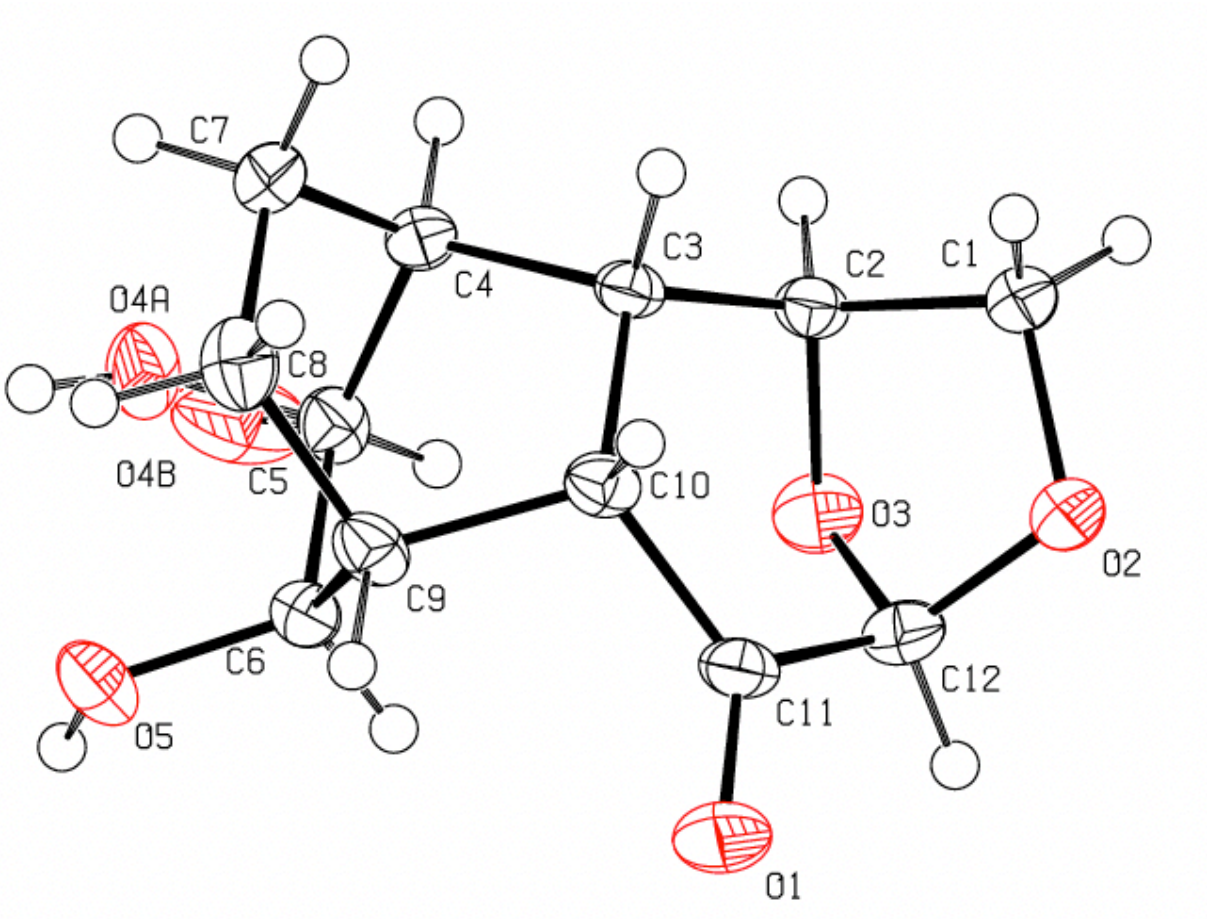

Figure S17: Molecular structure of compounds **33** and **34** CCDC 2268366) present in the non-hydrated form of compoound **33** that was found to contain a minor co-crystallised impurity of compound **34**. The extended structure arising from hydrogen bonding is not shown for compound **33**. Atomic displacement parameters shown at 50% probability level (crystal grown from chloroform)

Tabular comparisons of the $^{13}C\{^1H\}$ NMR spectral data recorded on compounds 14 and 15 with those reported by Horton *et al.*

Table S1: Comparison of the $^{13}C\{^1H\}$NMR spectral data reported by Horton *et al* for the chromatographically more mobile alcohol derived from reduction of the Diels-Alder adduct of LGO and cyclopentadiene (compound **14**) with those derived from compound **15** prepared during the course of the present study.

Compound **14** reported by Horton *et al*[a,b] δ_C	Compound **15**[c] δ_C	$\Delta\delta$[d]
135.8	136.1	+0.3
135.5	135.7	+0.2
101.7	101.8	+0.1
73.2	73.3	+0.1
68.4	68.6	+0.2
61.4	61.6	+0.2
50.6	50.8	+0.2
48.6	48.6	0
46.5	46.2	–0.3
45.8	46.0	+0.2
43.9	44.1	+0.2

[a] Data obtained from Horton *et al*. *J. Org. Chem*. **1996**, *61*, 3783; [b]Data recorded in $CDCl_3$ at 125 MHz; [c]Data recorded in $CDCl_3$ at 100 MHz; [d]Calculated by subtracting the δ_C values in the first column from those in the second.

Table S2: Comparison of the $^{13}C\{^{1}H\}$NMR spectral data reported by Horton *et al* for the chromatographically less mobile alcohol derived from reduction of the Diels-Alder adduct of LGO and cyclopentadiene (compound **15**) with those derived from compound **14** prepared during the course of the present study.

Compound **15** reported by Horton *et al*[a,b] δ_C	Compound **14**[c] δ_C	$\Delta\delta$[d]
137.4	137.5	+0.1
133.0	133.2	+0.2
102.6	102.7	+0.1
76.4	76.6	+0.2
69.4	69.5	+0.1
64.3	64.5	+0.2
50.7	50.9	+0.2
46.8	47.0	+0.2
46.1	46.3	+0.2
44.3	44.5	+0.2
40.3	40.5	+0.2

[a] Data obtained from Horton *et al*. *J. Org. Chem*. **1996**, *61*, 3783; [b]Data recorded in $CDCl_3$ at 125 MHz; [c]Data recorded in $CDCl_3$ at 100 MHz; [d]Calculated by subtracting the δ_C values in the first column from those in the second.

Tabular comparisons of the $^{13}C\{^{1}H\}$ NMR spectral data recorded on compounds 20 and 21 with those reported by Zurita *et al*

Table S3: Comparison of the $^{13}C\{^{1}H\}$NMR spectral data reported by Zurita *et al* for the major alcohol derived from reduction of the Diels-Alder adduct of LGO and cyclohexadiene (compound **10**) with those derived from compound **20** prepared during the course of the present study.

Compound **10** reported by Zurita *et al*[a,b] δ_C	Compound **20**[c] δ_C	$\Delta\delta$[d]
134.5	134.6	+0.1
133.3	133.4	+0.1
102.5	102.5	0
77.0	77.0	0
71.7	71.7	0
68.6	68.6	0
44.5	44.5	0
39.7	39.7	0
36.7	36.7	0
33.2	33.2	0
29.1	29.1	0
23.3	23.4	+0.1

[a] Data obtained from Zurita *et al*. *Carbohydr*. *Res*. **2015**, *401*, 67; [b]Data recorded in $CDCl_3$ at 75 MHz; [c]Data recorded in $CDCl_3$ at 100 MHz; [d]Calculated by subtracting the δ_C values in the first column from those in the second.

Table S4: Comparison of the $^{13}C\{^{1}H\}$NMR spectral data reported by Zurita *et al* for the minor alcohol derived from reduction of the Diels-Alder adduct of LGO and cyclohexadiene (compound **17**) with those derived from compound **21** prepared during the course of the present study.

Compound **17** reported by Zurita *et al*[a,b] δ_C	Compound **21**[c] δ_C	$\Delta\delta$[d]
135.3	135.3	0
132.4	132.4	0
100.9	100.9	0
77.2	77.2	0
71.2	71.2	0
70.2	70.2	0
46.3	46.3	0
45.3	45.4	+0.1
36.1	36.2	+0.1
33.9	34.0	+0.1
28.7	28.7	0
22.3	22.4	+0.1

[a]Data obtained from Zurita *et al*. *Carbohydr*. *Res*. **2015**, *401*, 67; [b]Data recorded in $CDCl_3$ at 75 MHz; [c]Data recorded in $CDCl_3$ at 100 MHz; [d]Calculated by subtracting the δ_C values in the first column from those in the second.

Tabular comparisons of the $^{13}C\{^{1}H\}$ NMR spectral data recorded on compounds 27 and 28 with those reported by Galimova *et al*

Table S5: Comparison of the $^{13}C\{^{1}H\}$NMR spectral data reported by Galimova *et al* for the Diels-Alder adduct of LGO and *in situ*-generated α-terpinene (Compound V) with those derived from compound **27** prepared during the course of the present study.

Compound V reported by Galimova *et al*[a,b] δ_C	Compound **27**[c] δ_C	$\Delta\delta$[d]
200.96	201.0	0
138.26	138.4	+0.1
135.53	135.7	+0.2
100.61	100.8	+0.2
73.12	73.3	+0.2
68.29	68.5	+0.2
49.29	49.5	+0.2
48.58	48.8	+0.2
44.98	45.1	+0.1
38.13	38.3	+0.2
35.59	35.8	+0.2
29.97	30.1	+0.1
22.76	22.9	+0.1
20.80	21.0	+0.2
18.70	18.8	+0.1
16.76	16.9	+0.1

[a] Data obtained from Galimova *et al*. *Russ. J. Org. Chem*. **2014**, *50*, 1848; [b]Data recorded in $CDCl_3$ at 75.47 MHz; [c]Data recorded in $CDCl_3$ at 100 MHz; [d]Calculated by rounding the δ_C values for compound V to the first decimal place and then subtracting these from the corresponding value for compound **27**.

Table S6: Comparison of the $^{13}C\{^{1}H\}$NMR spectral data reported by Galimova *et al* for the Diels-Alder adduct of LGO and *in situ*-generated α-terpinene (Compound V) with those derived from compound **28** prepared during the course of the present study

Compound V reported by Galimova *et al*[a,b] δ_C	Compound **28**[c] δ_C	$\Delta\delta$[d]
200.96	200.9	–0.1
138.26	138.2	–0.1
135.53	135.5	0
100.61	100.6	0
73.12	73.1	0
68.29	68.3	0
49.29	49.3	0
48.58	48.6	0
44.98	45.0	0
38.13	38.1	0
35.59	35.6	0
29.97	30.0	0
22.76	22.8	0
20.80	20.8	0
18.70	18.7	0
16.76	16.8	0

[a] Data obtained from Galimova *et al*. *Russ. J. Org. Chem*. **2014**, *50*, 1848; [b]Data recorded in $CDCl_3$ at 75.47 MHz; [c]Data recorded in $CDCl_3$ at 100 MHz; [d]Calculated by rounding the δ_C values for compound V to the first decimal place and then subtracting these from the corresponding value for compound **27**.

400 MHz ^{1}H NMR Spectrum of Compound **10** (Recorded in $CDCl_3$)

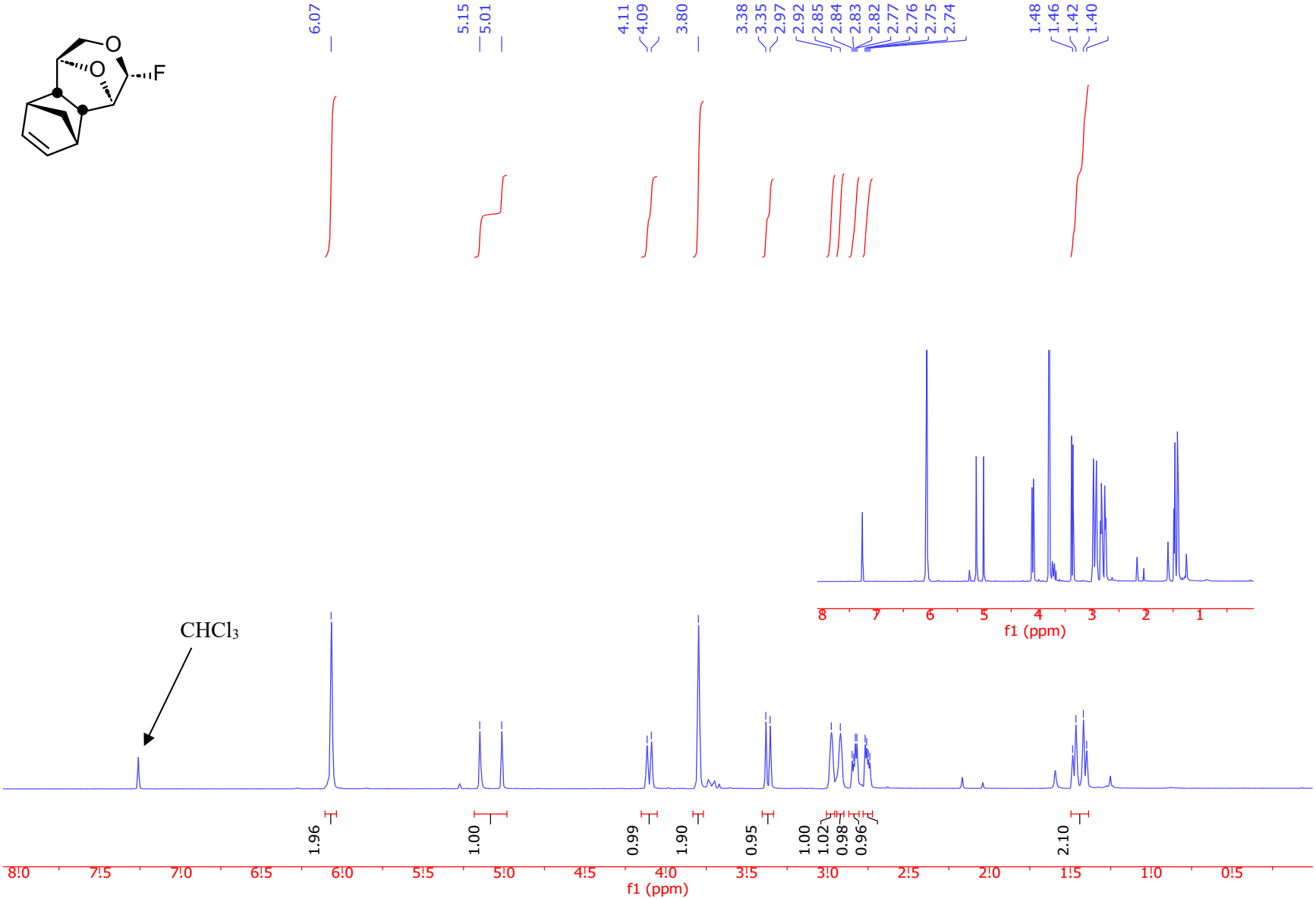

101 MHz $^{13}C\{^{1}H\}$ NMR Spectrum of Compound **10** (Recorded in $CDCl_3$)

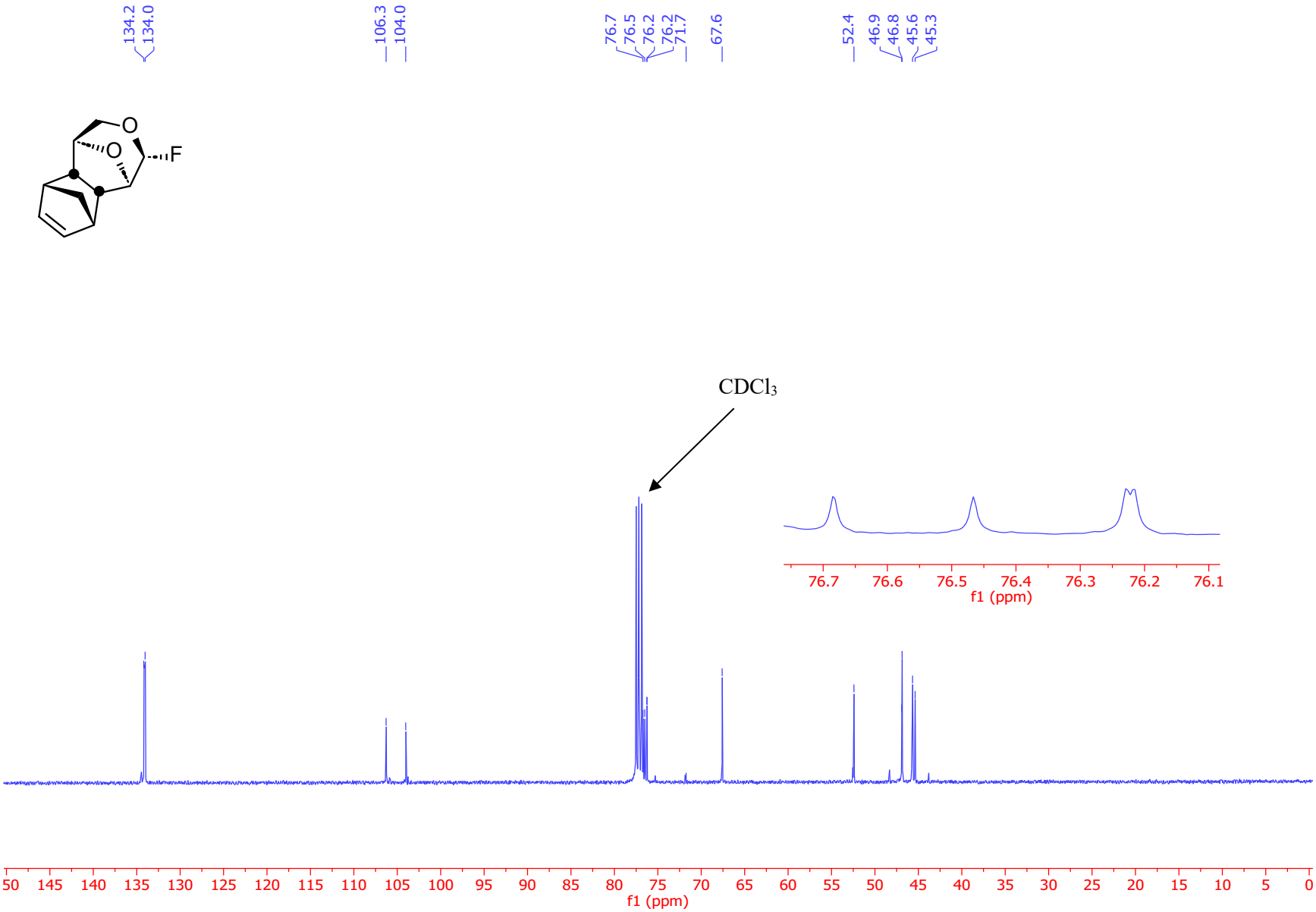

400 MHz ^{1}H NMR Spectrum of Compound **11** (Recorded in $CDCl_3$)

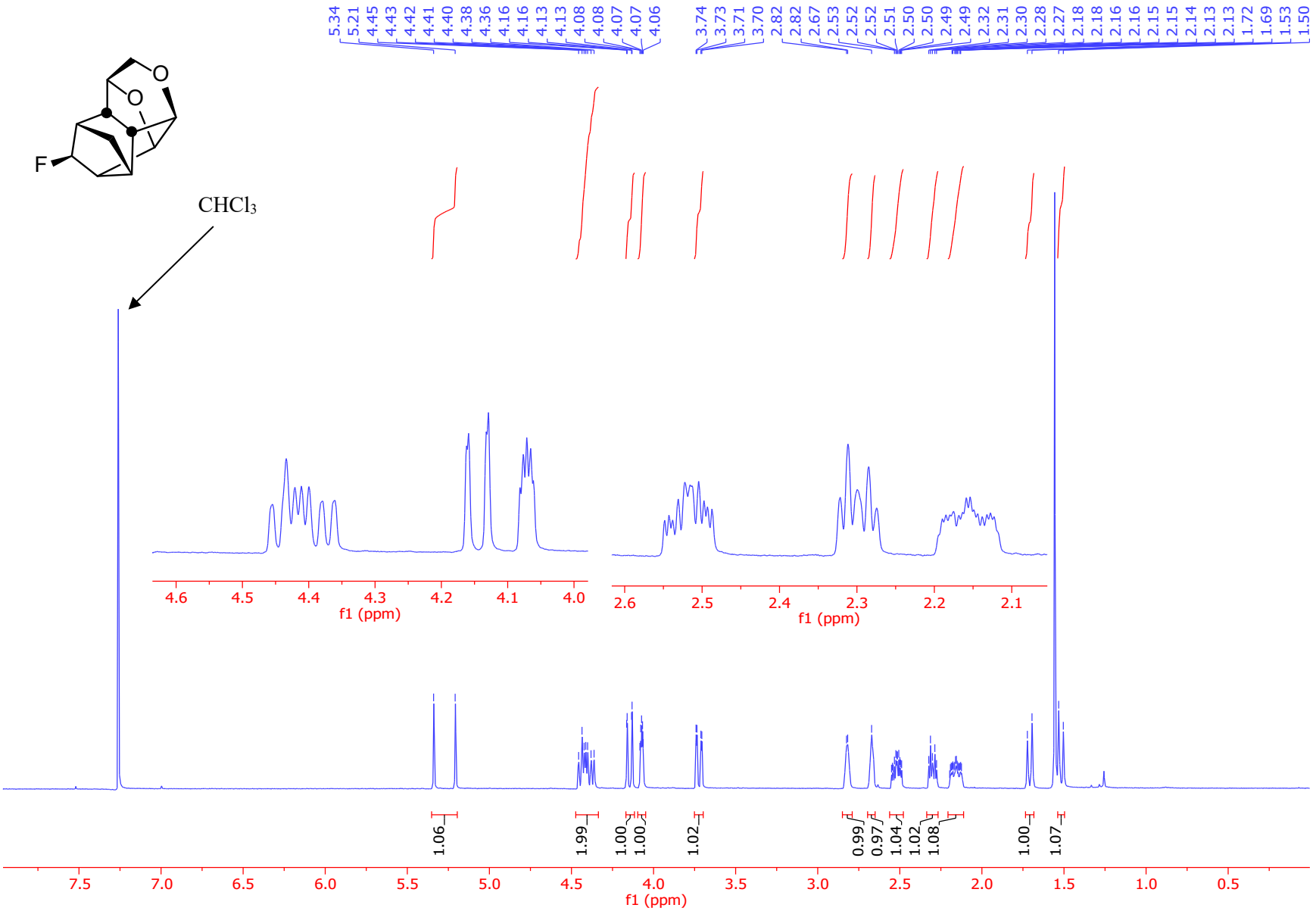

101 MHz $^{13}C\{^{1}H\}$ NMR Spectrum of Compound **11** (Recorded in $CDCl_3$)

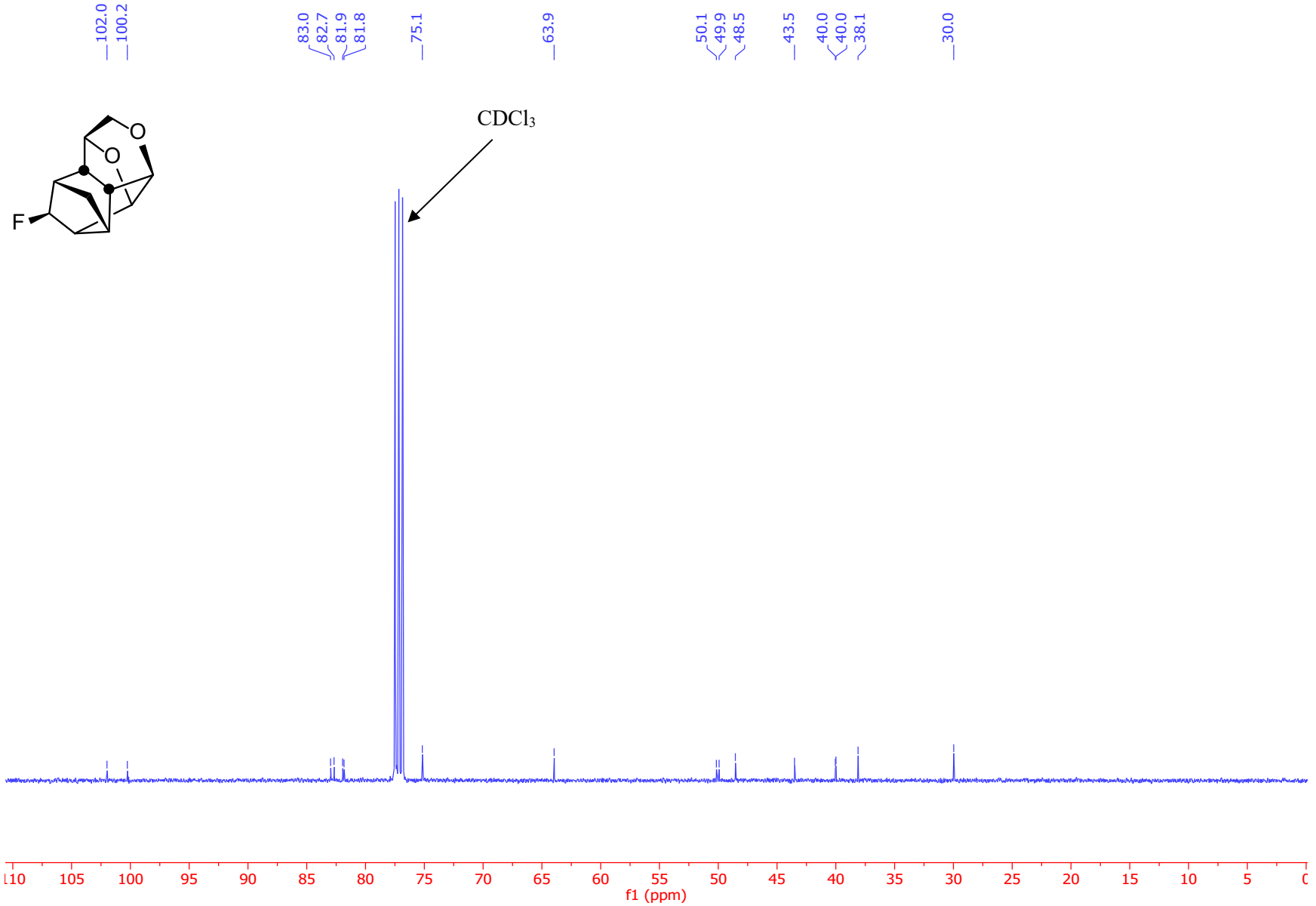

400 MHz ^{1}H NMR Spectrum of Compound **12** (Recorded in $CDCl_3$)

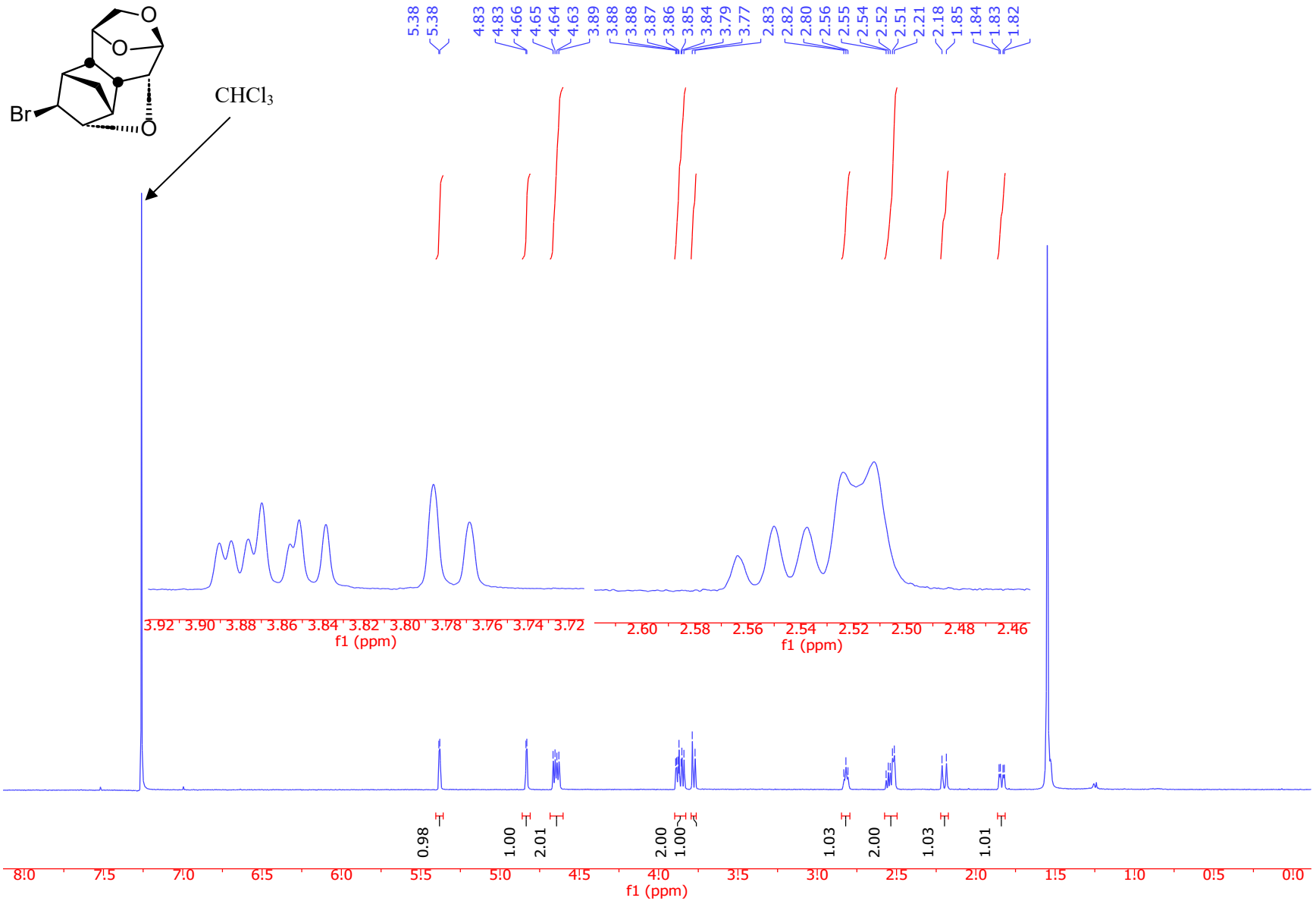

101 MHz $^{13}C\{^{1}H\}$ NMR Spectrum of Compound **12** (Recorded in $CDCl_3$)

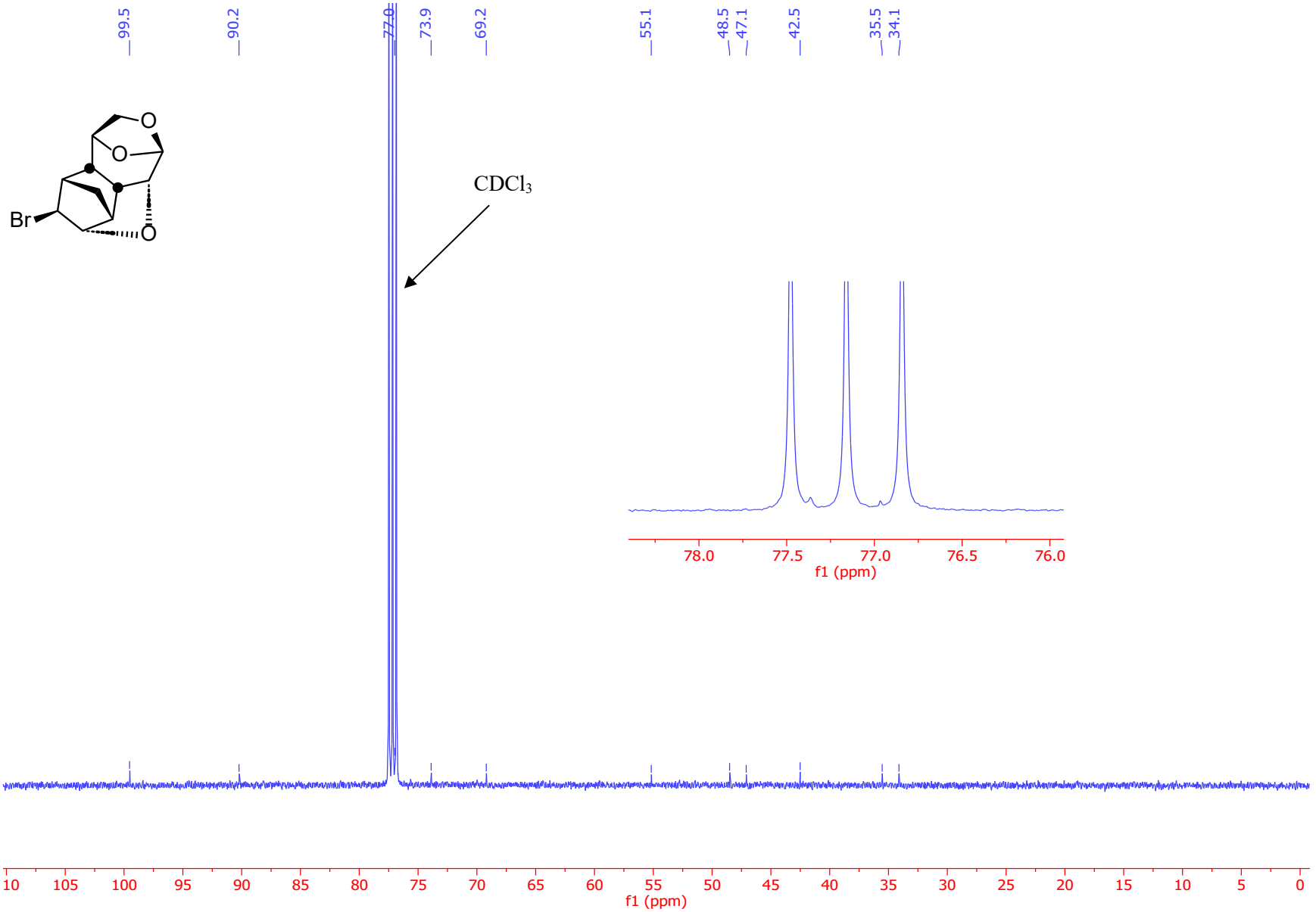

400 MHz ^{1}H NMR Spectrum of Compound **13** (Recorded in $CDCl_3$)

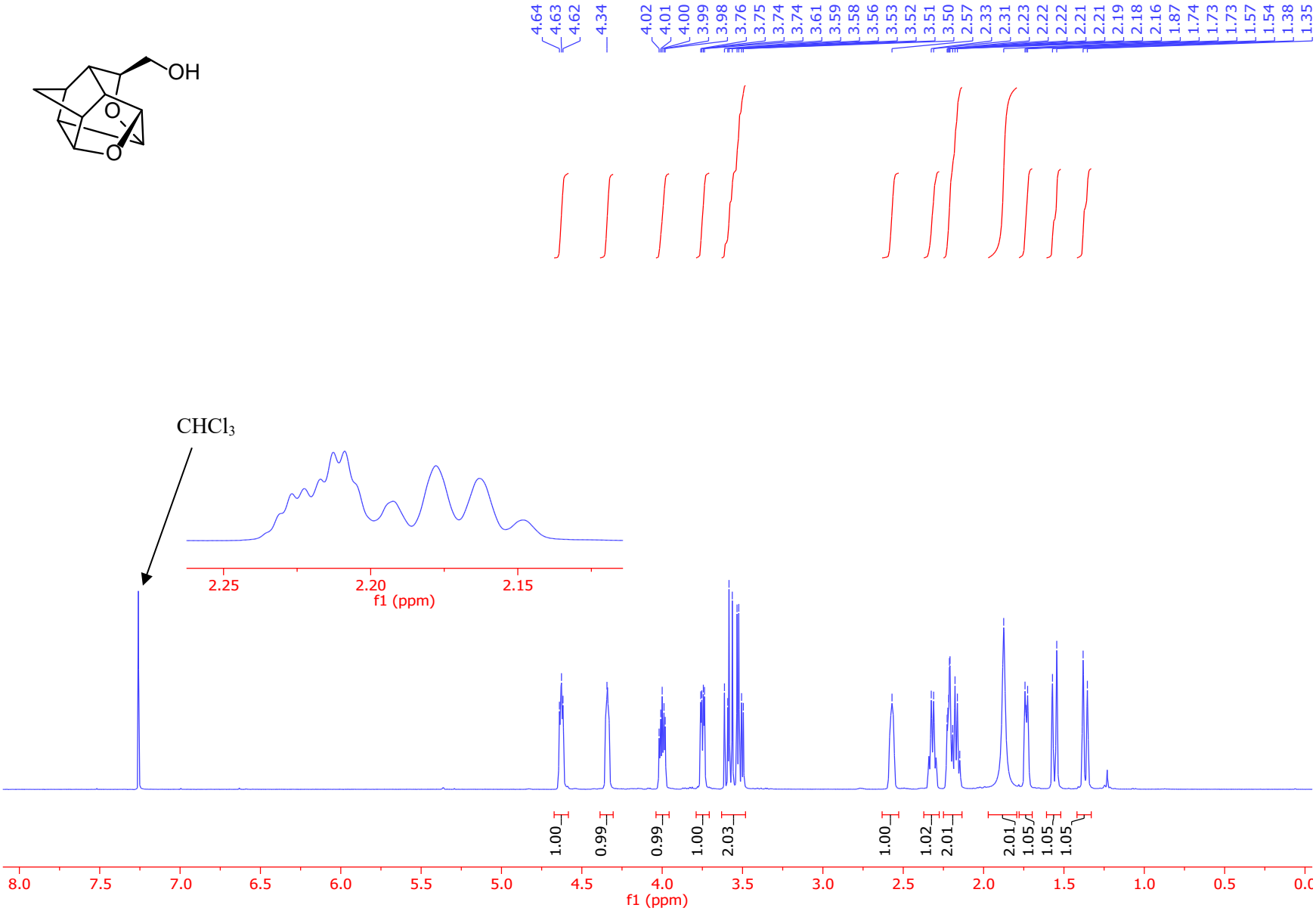

101 MHz $^{13}C\{^{1}H\}$ NMR Spectrum of Compound **13** (Recorded in $CDCl_3$)

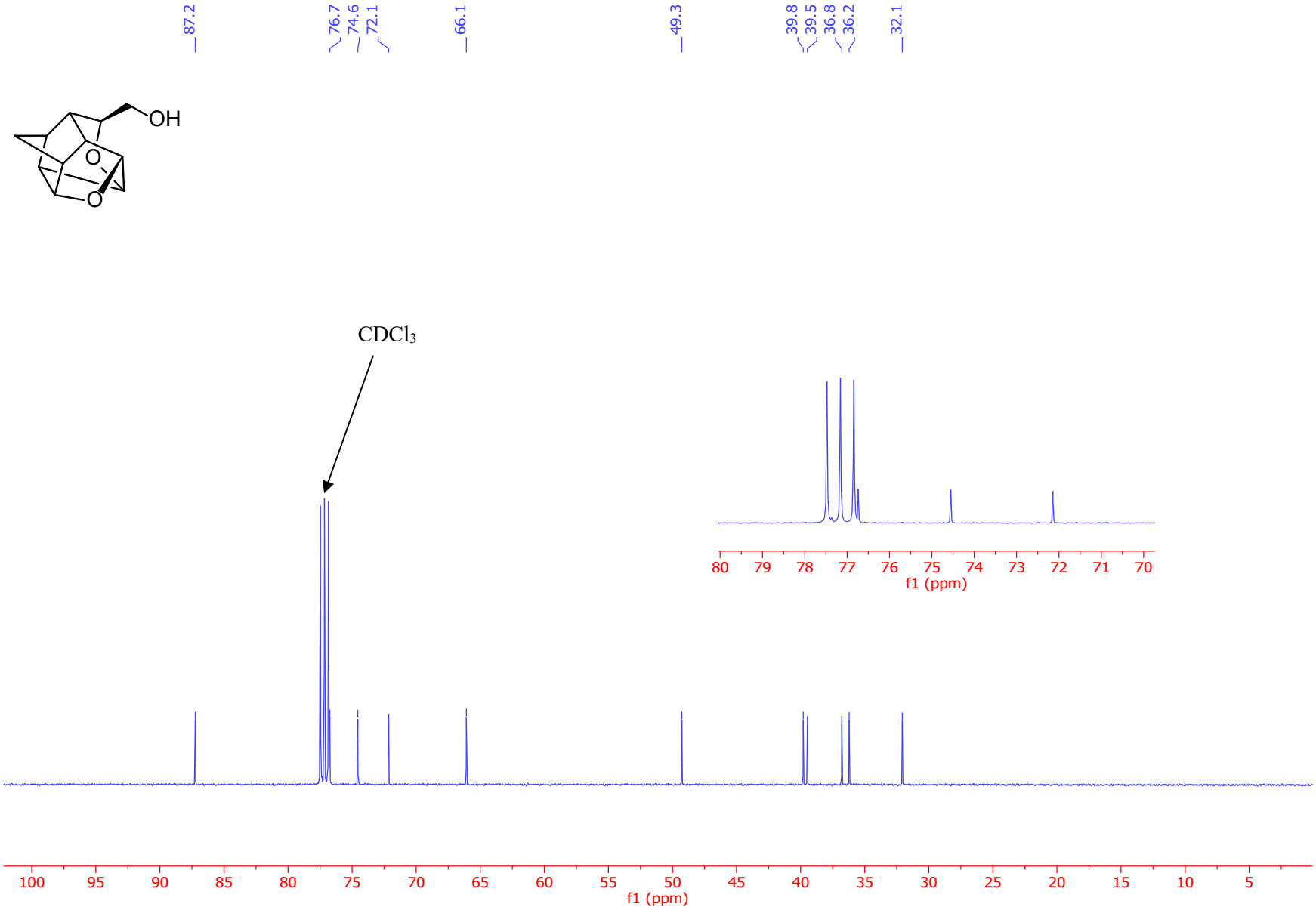

400 MHz ^{1}H NMR Spectrum of Compound **14** (Recorded in $CDCl_3$)

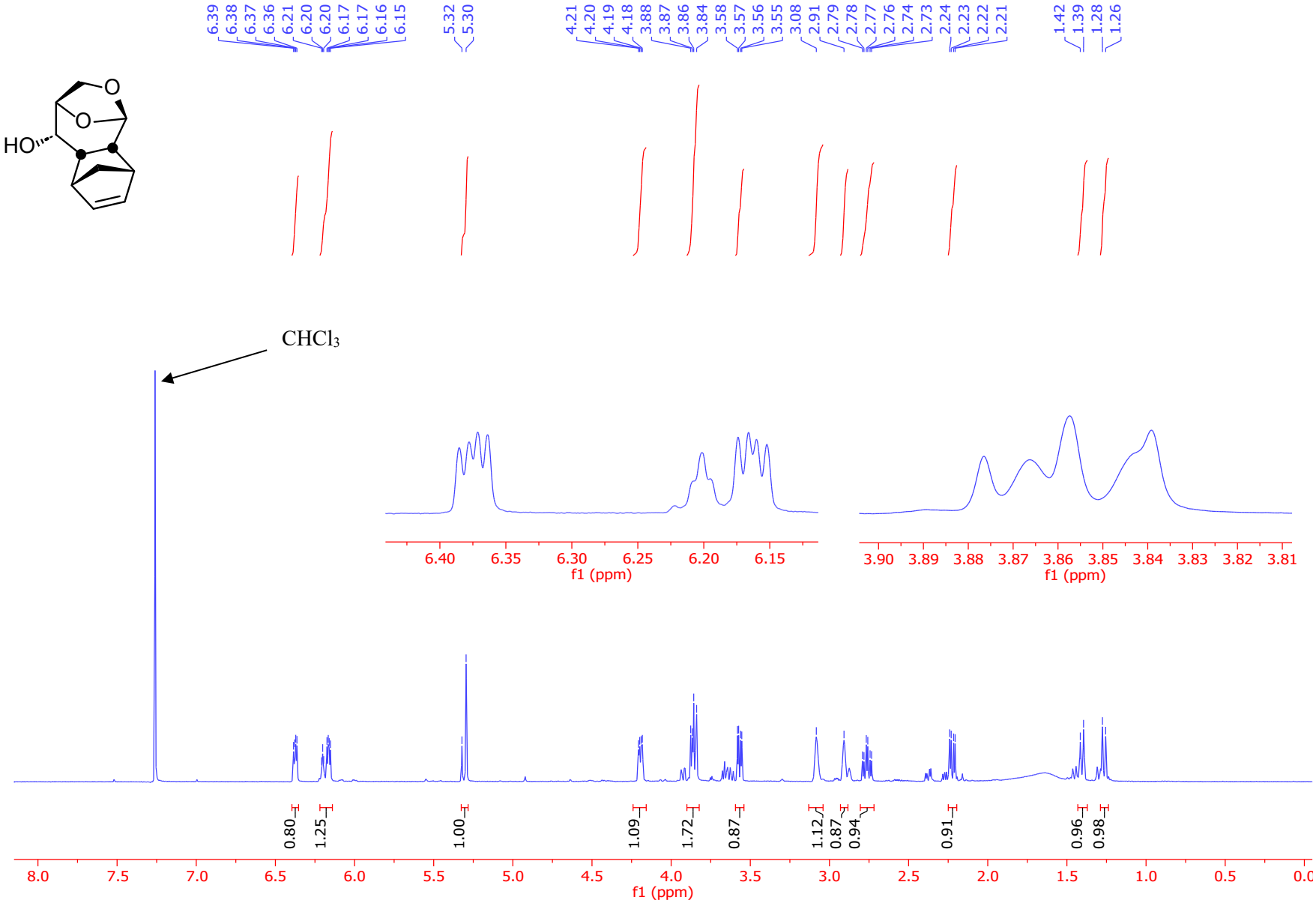

101 MHz $^{13}C\{^{1}H\}$ NMR Spectrum of Compound **14** (Recorded in $CDCl_3$)

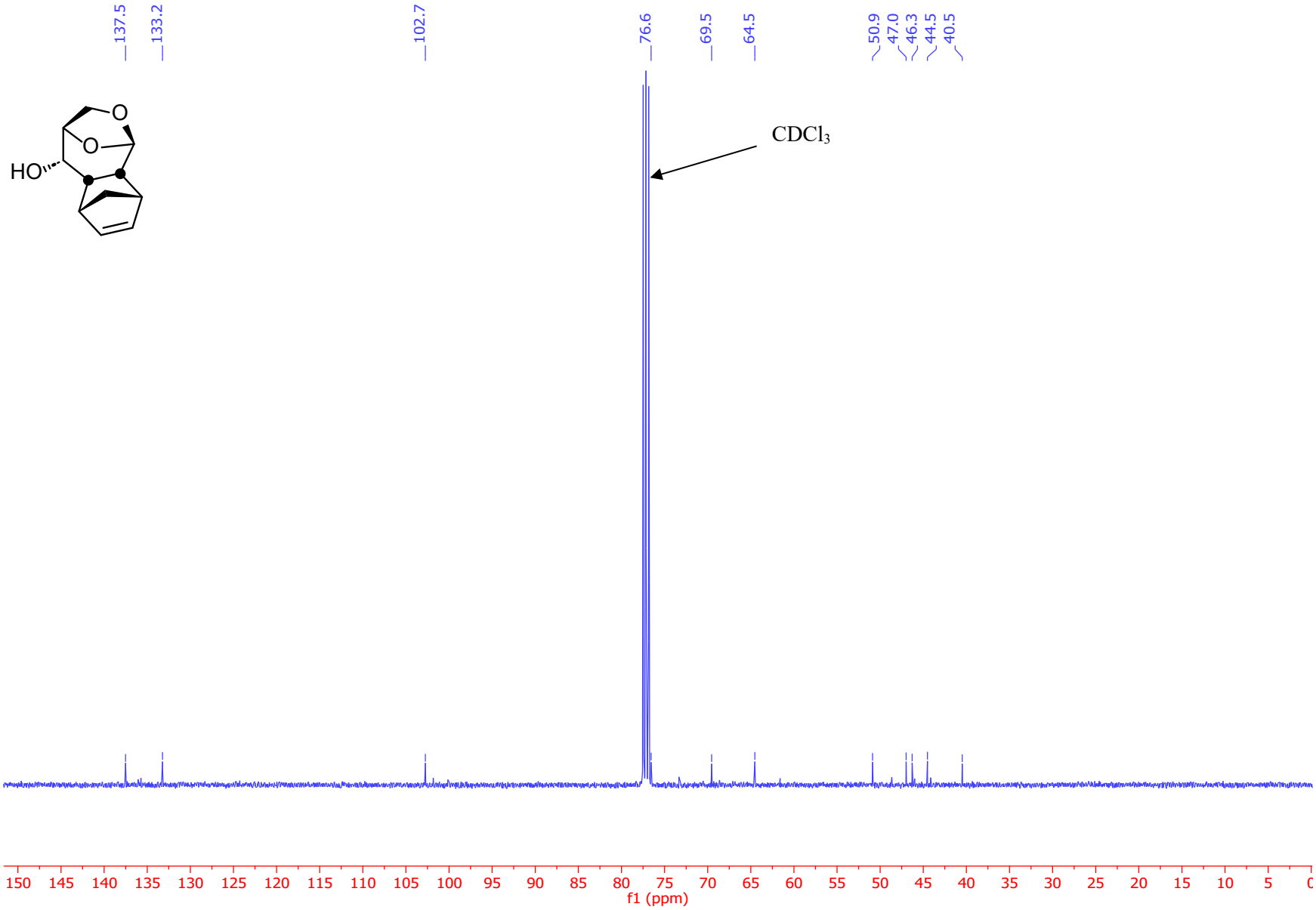

400 MHz ^{1}H NMR Spectrum of Compound **15** (Recorded in $CDCl_3$)

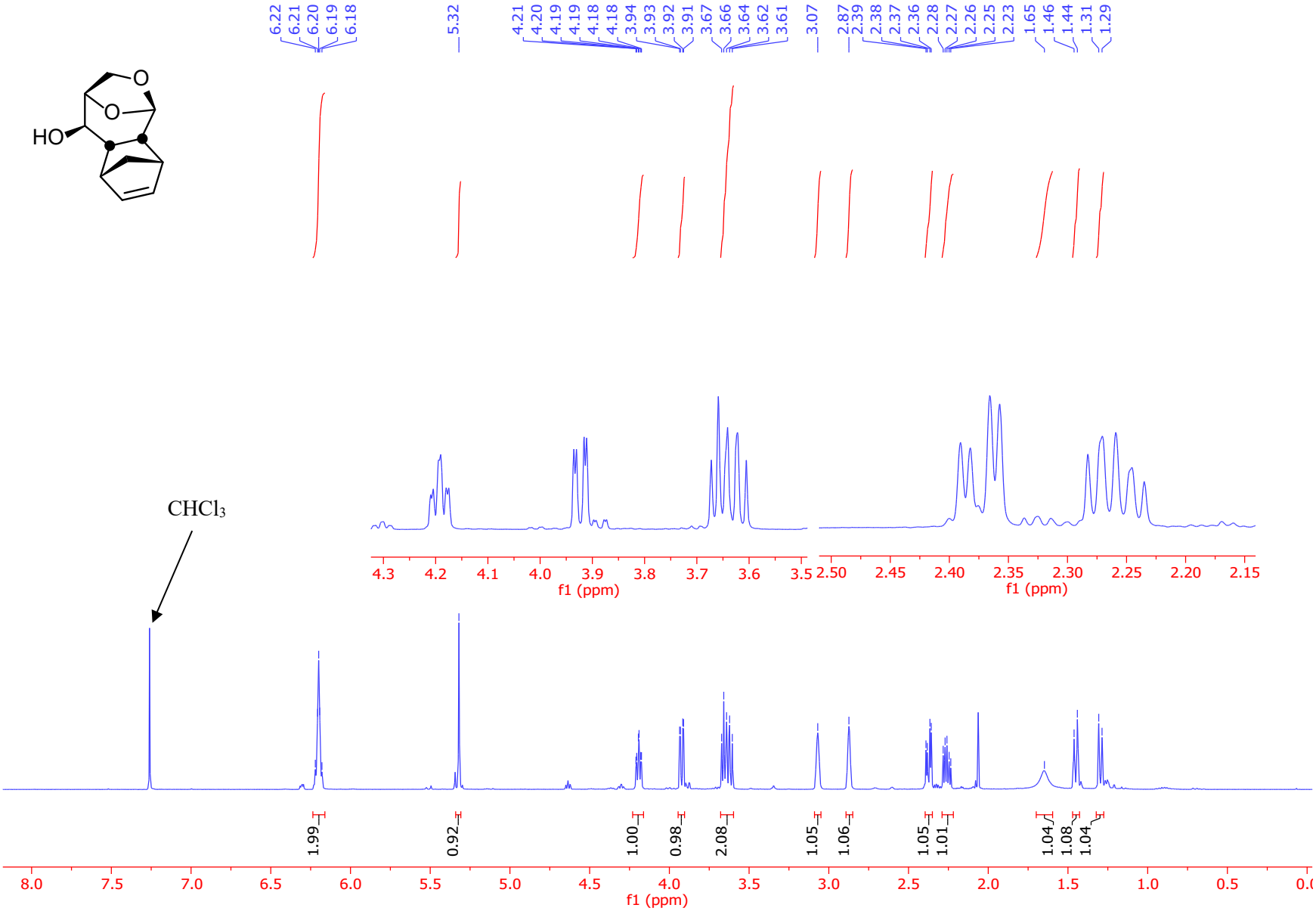

101 MHz $^{13}C\{^{1}H\}$ NMR Spectrum of Compound **15** (Recorded in $CDCl_3$)

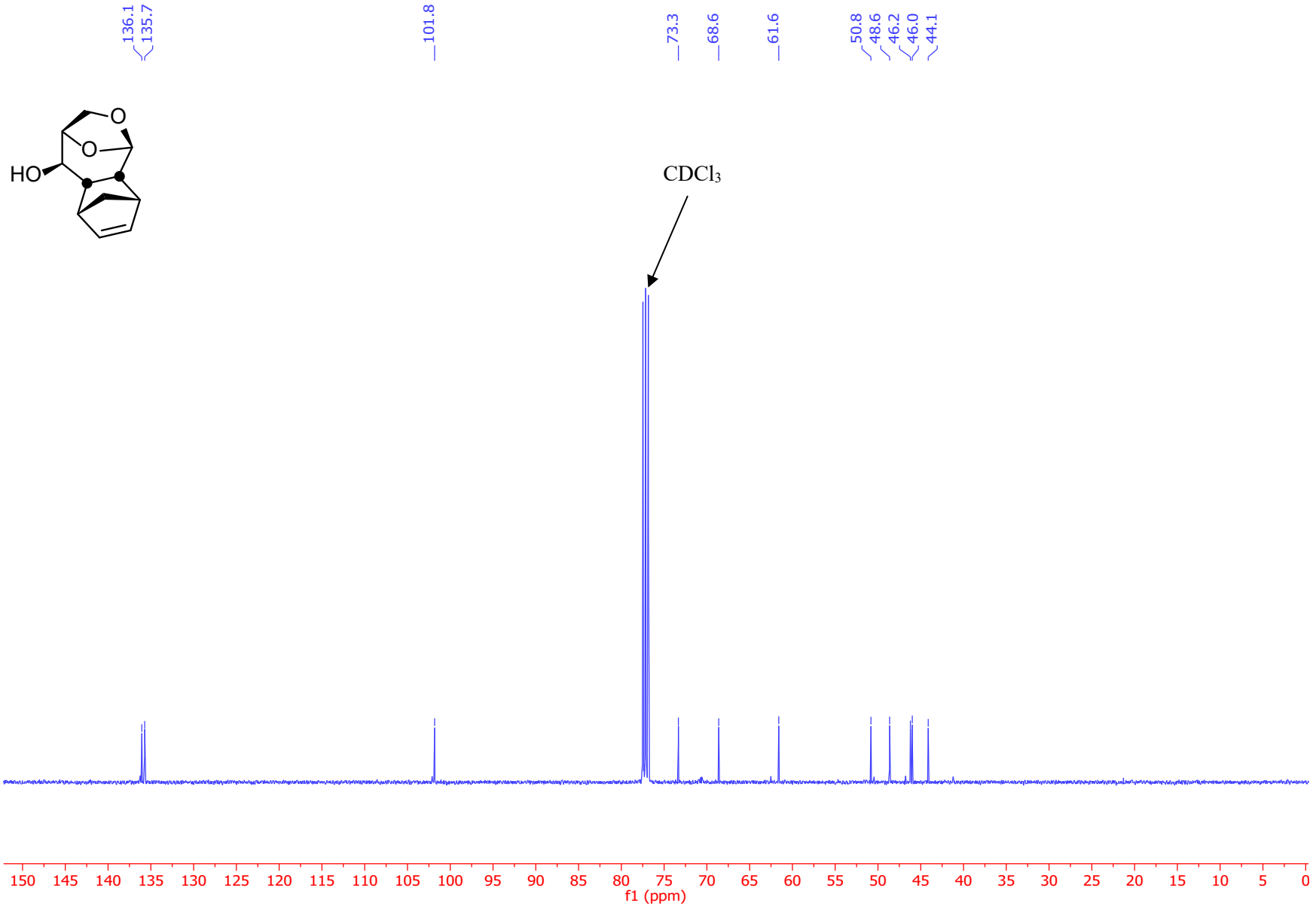

400 MHz ^{1}H NMR Spectrum of Compound **16** (Recorded in $CDCl_3$)

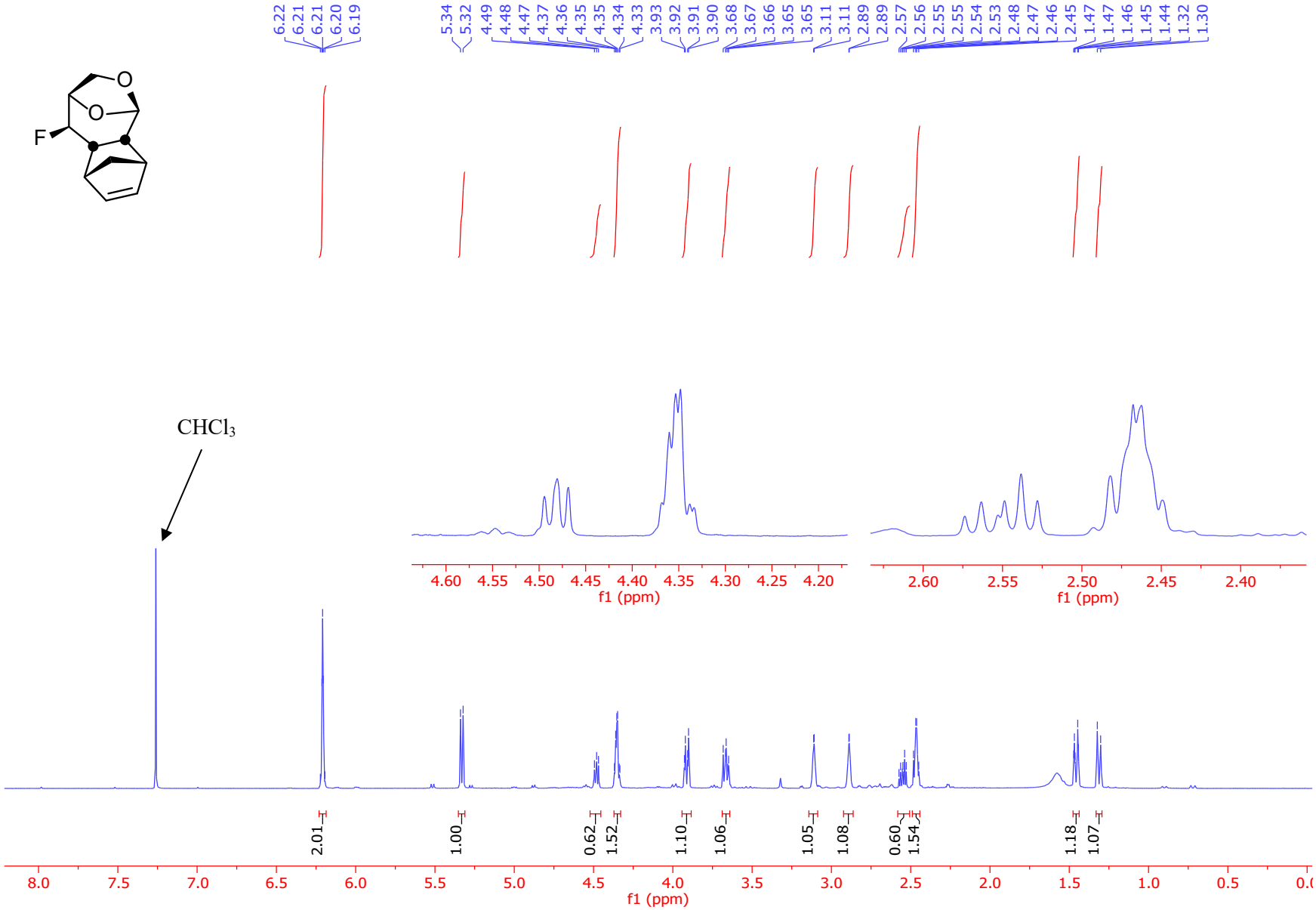

101 MHz $^{13}C\{^{1}H\}$ NMR Spectrum of Compound **16** (Recorded in $CDCl_3$)

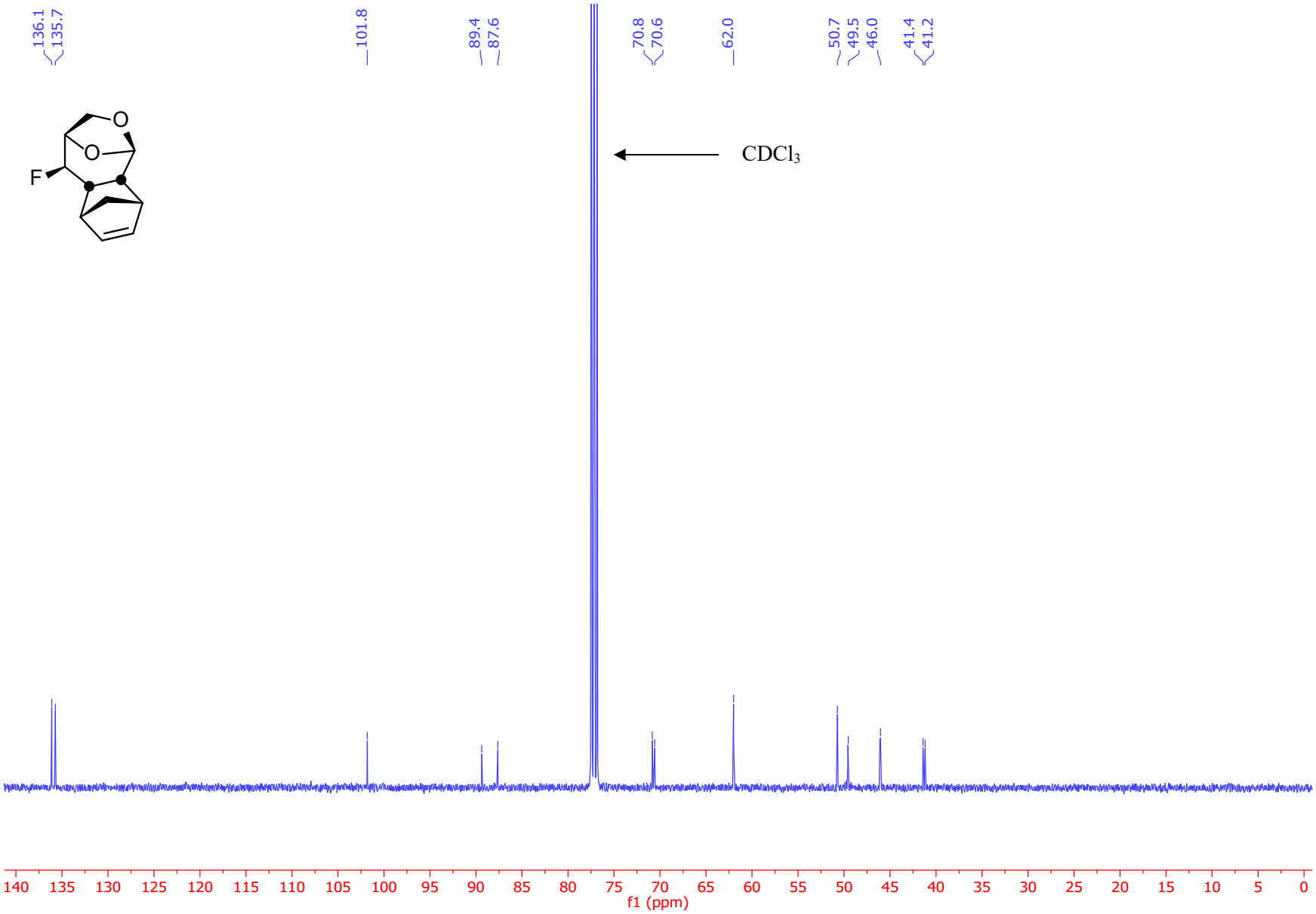

400 MHz ^{1}H NMR Spectrum of Compound **18** (Recorded in $CDCl_3$)

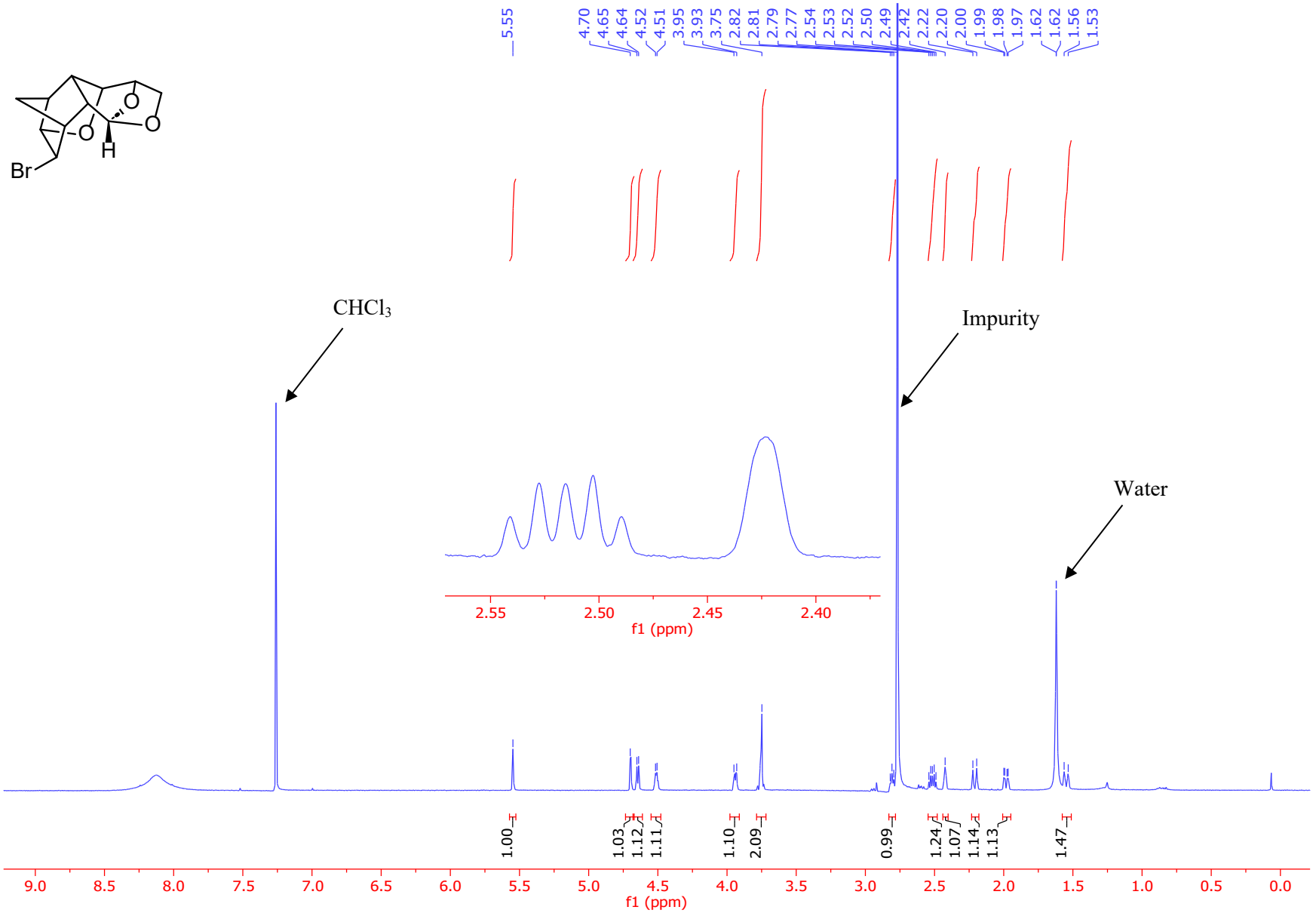

101 MHz $^{13}C\{^{1}H\}$ NMR Spectrum of Compound **18** (Recorded in $CDCl_3$)

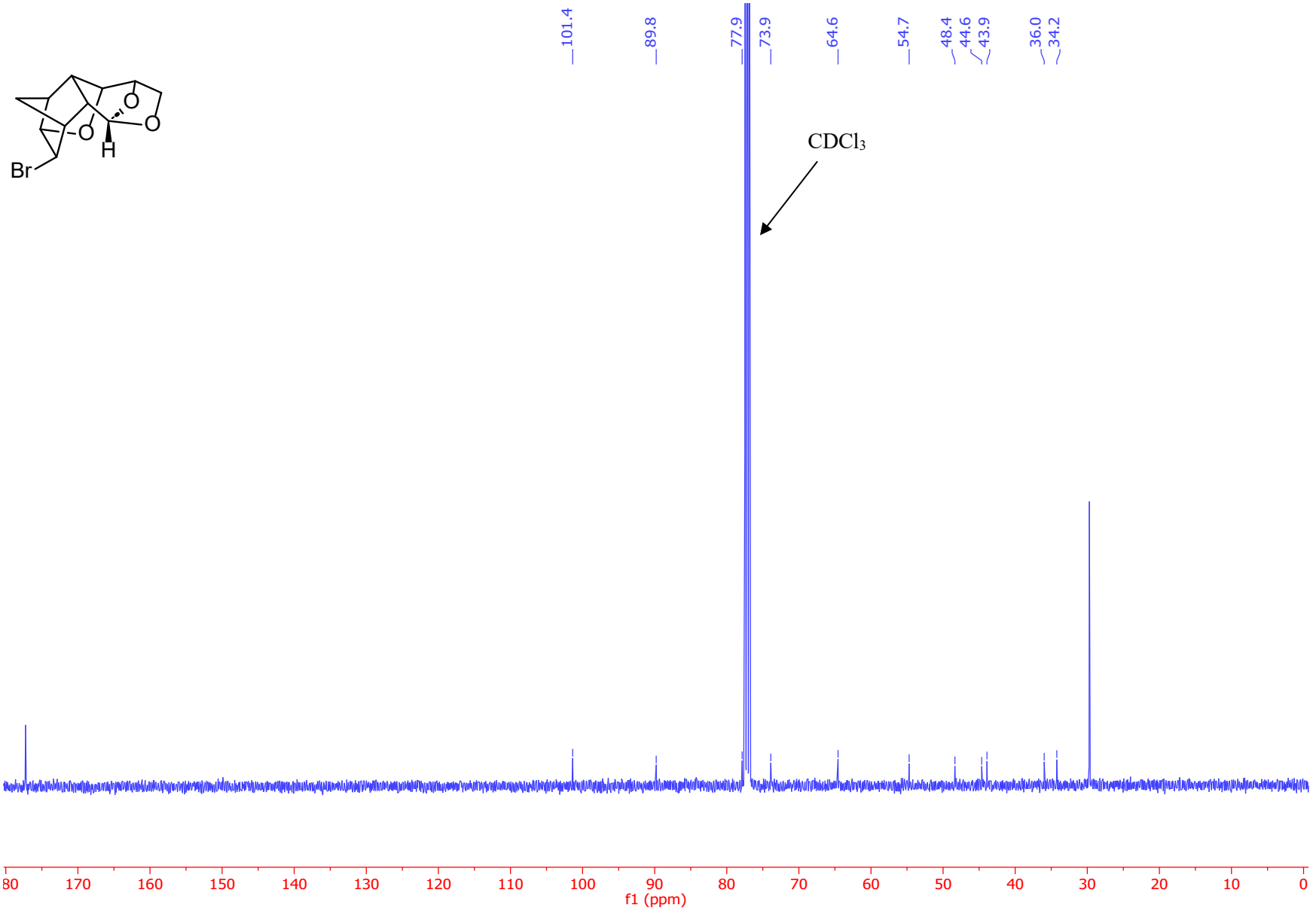

400 MHz ^{1}H NMR Spectrum of Compound **19** (Recorded in $CDCl_3$)

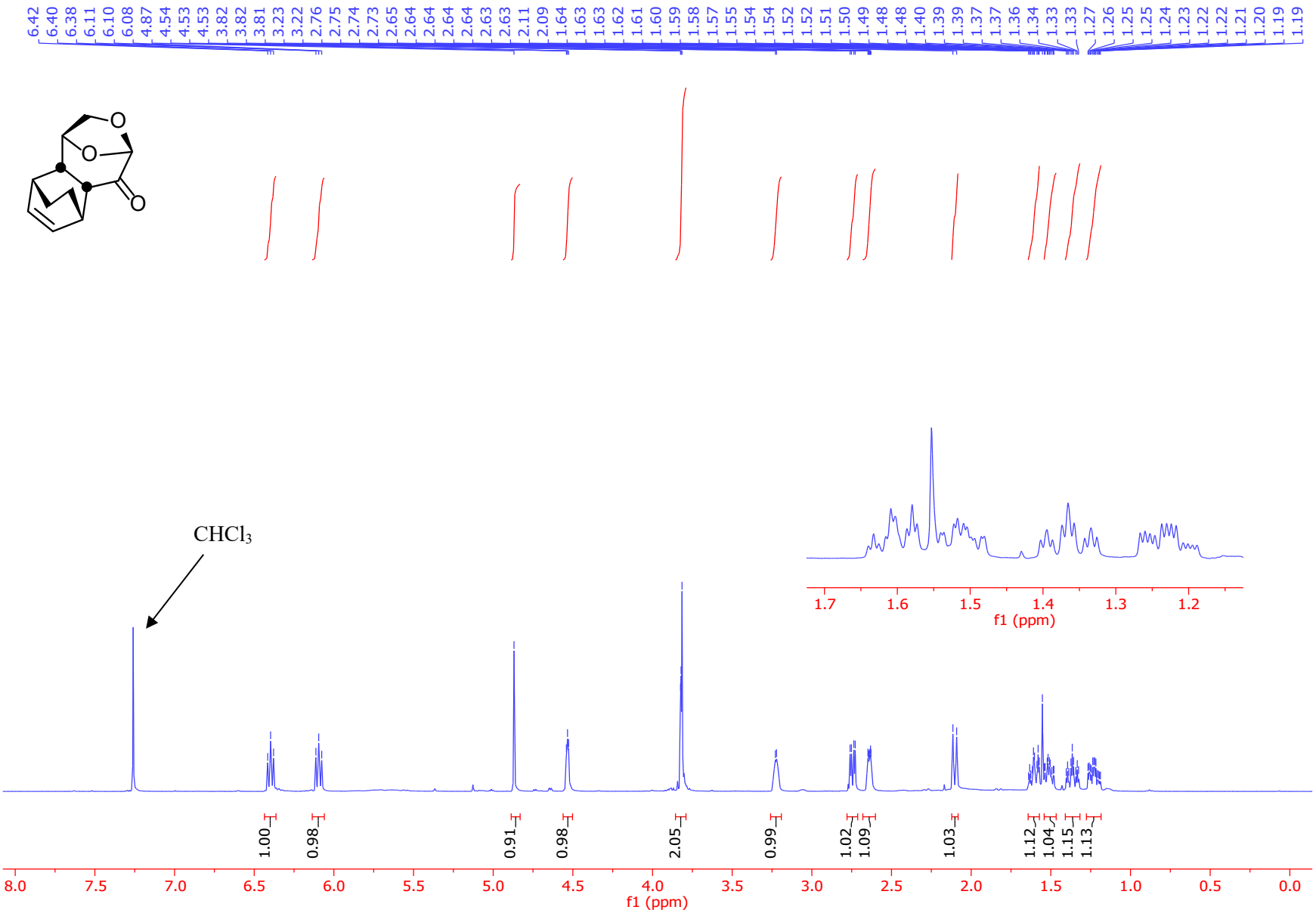

101 MHz $^{13}C\{^{1}H\}$ NMR Spectrum of Compound **19** (Recorded in $CDCl_3$)

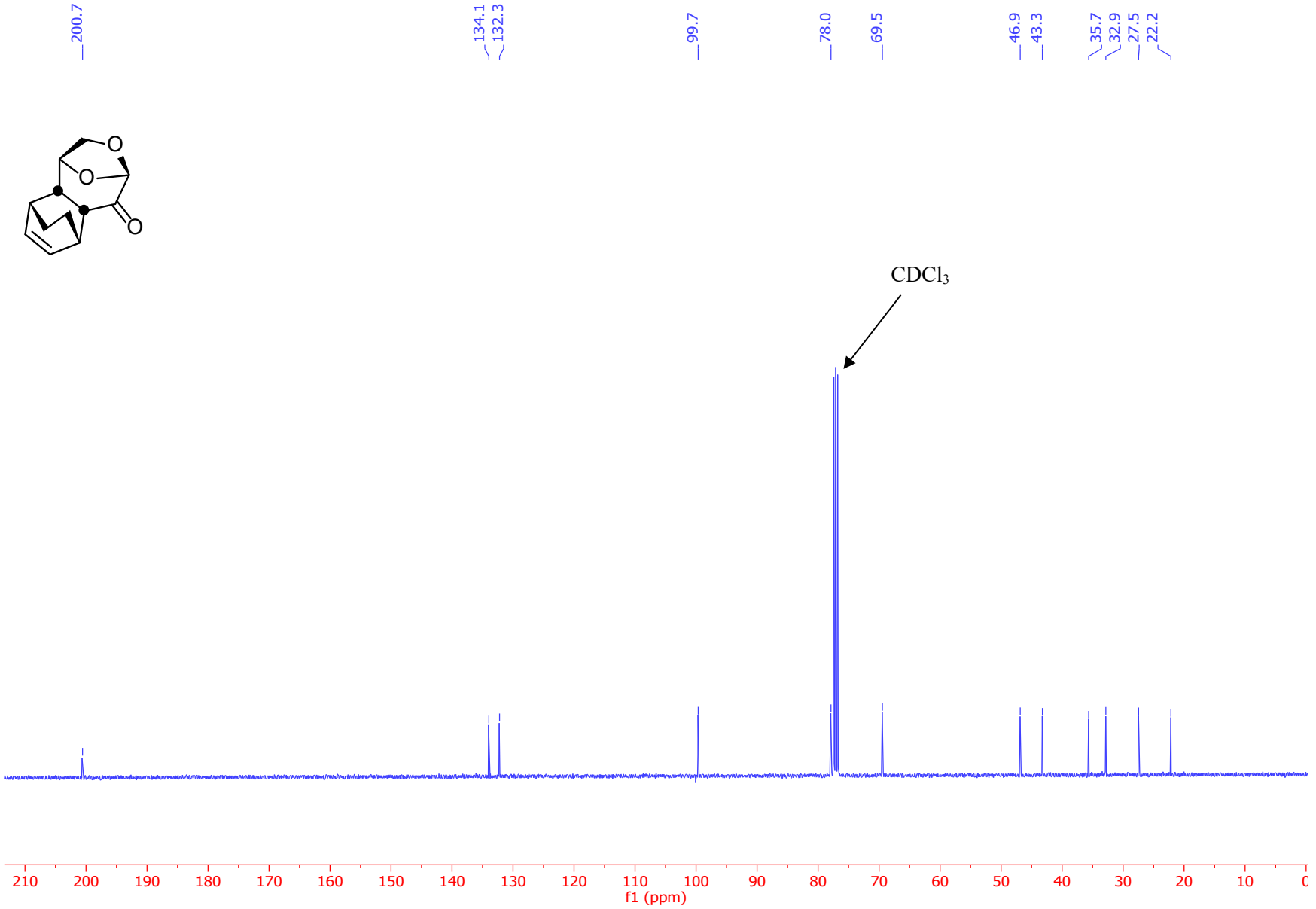

400 MHz ^{1}H NMR Spectrum of Compound **20** (Recorded in $CDCl_3$)

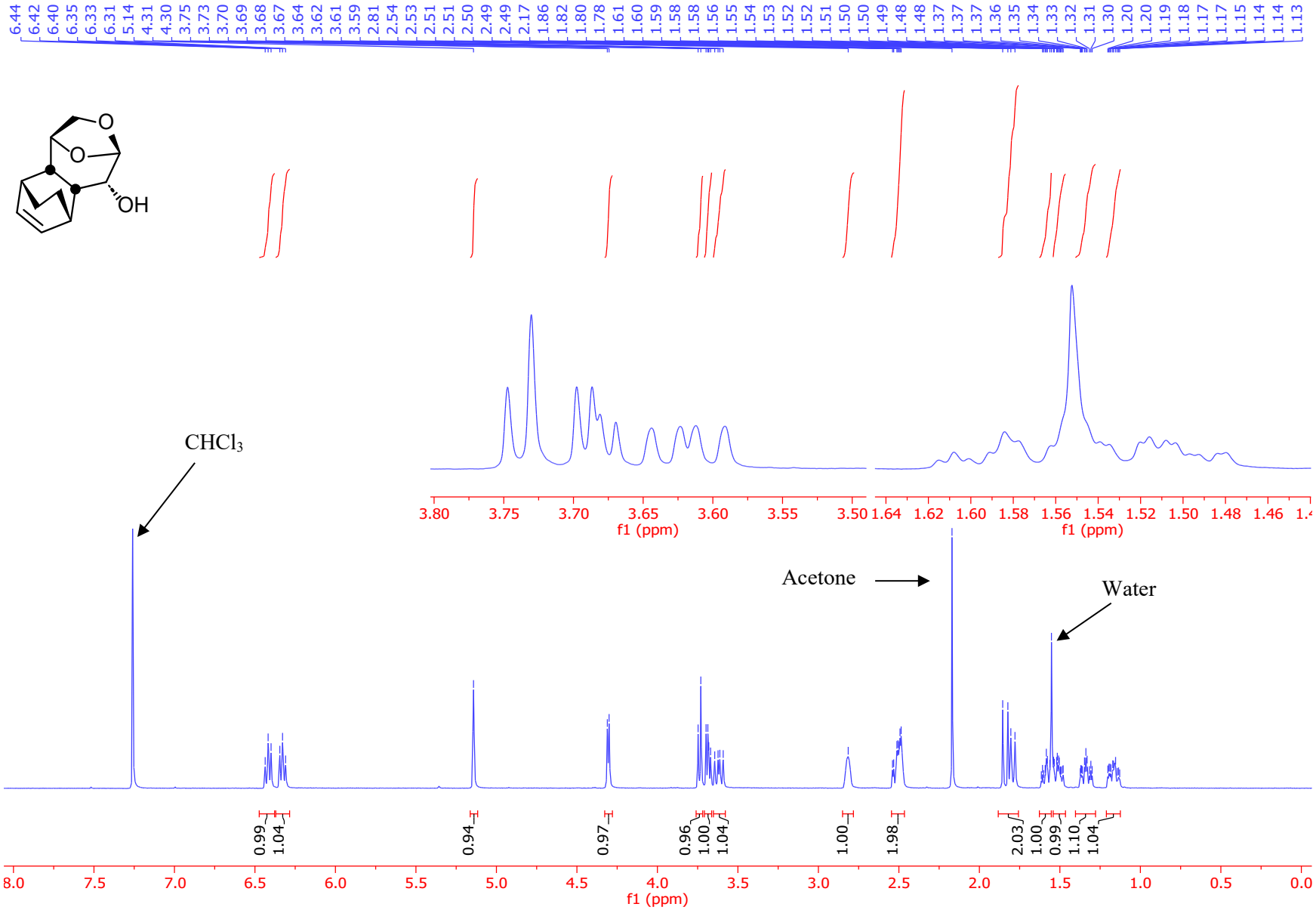

101 MHz $^{13}C\{^{1}H\}$ NMR Spectrum of Compound **20** (Recorded in $CDCl_3$)

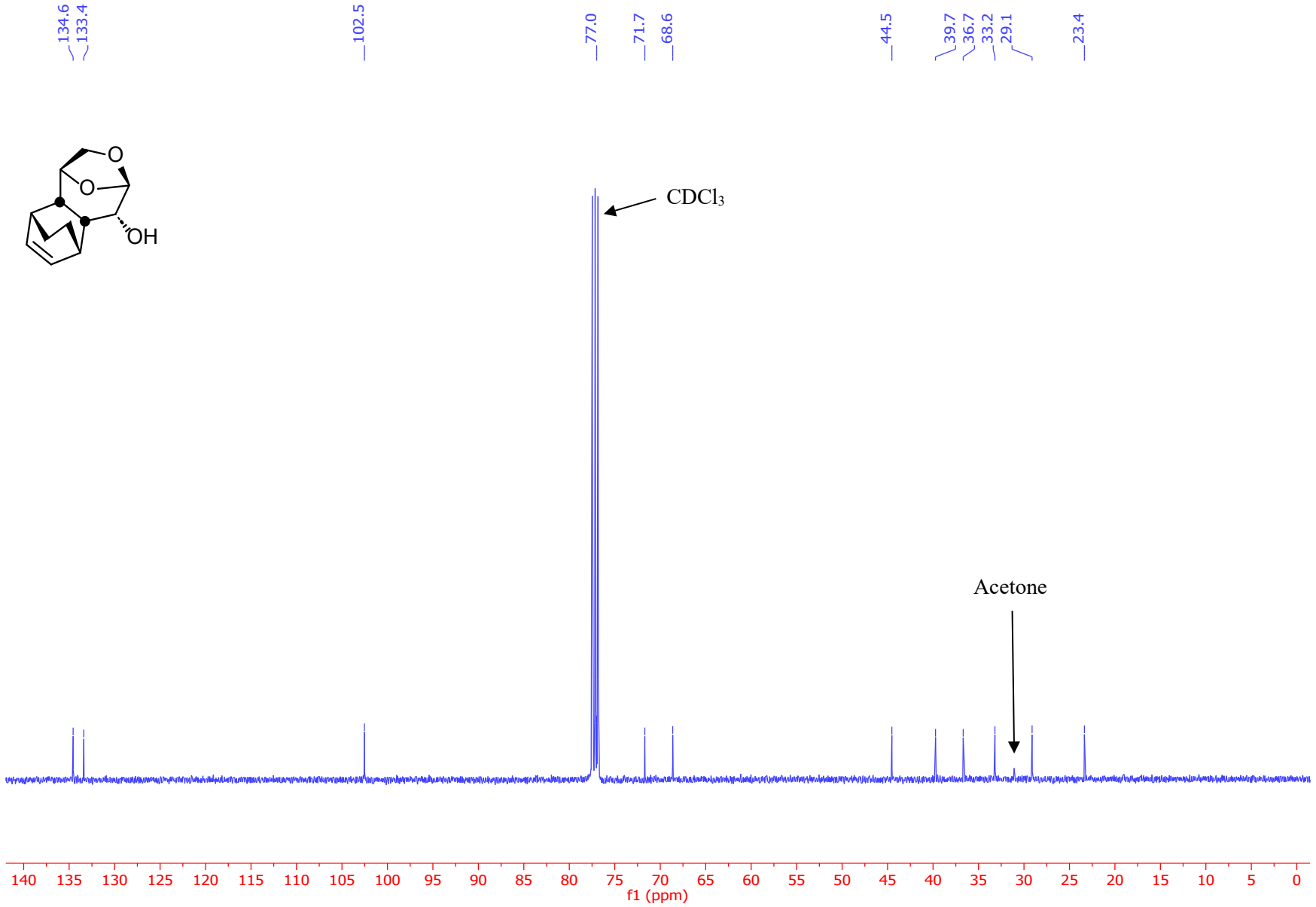

400 MHz ^{1}H NMR Spectrum of Compound **21** (Recorded in $CDCl_3$)

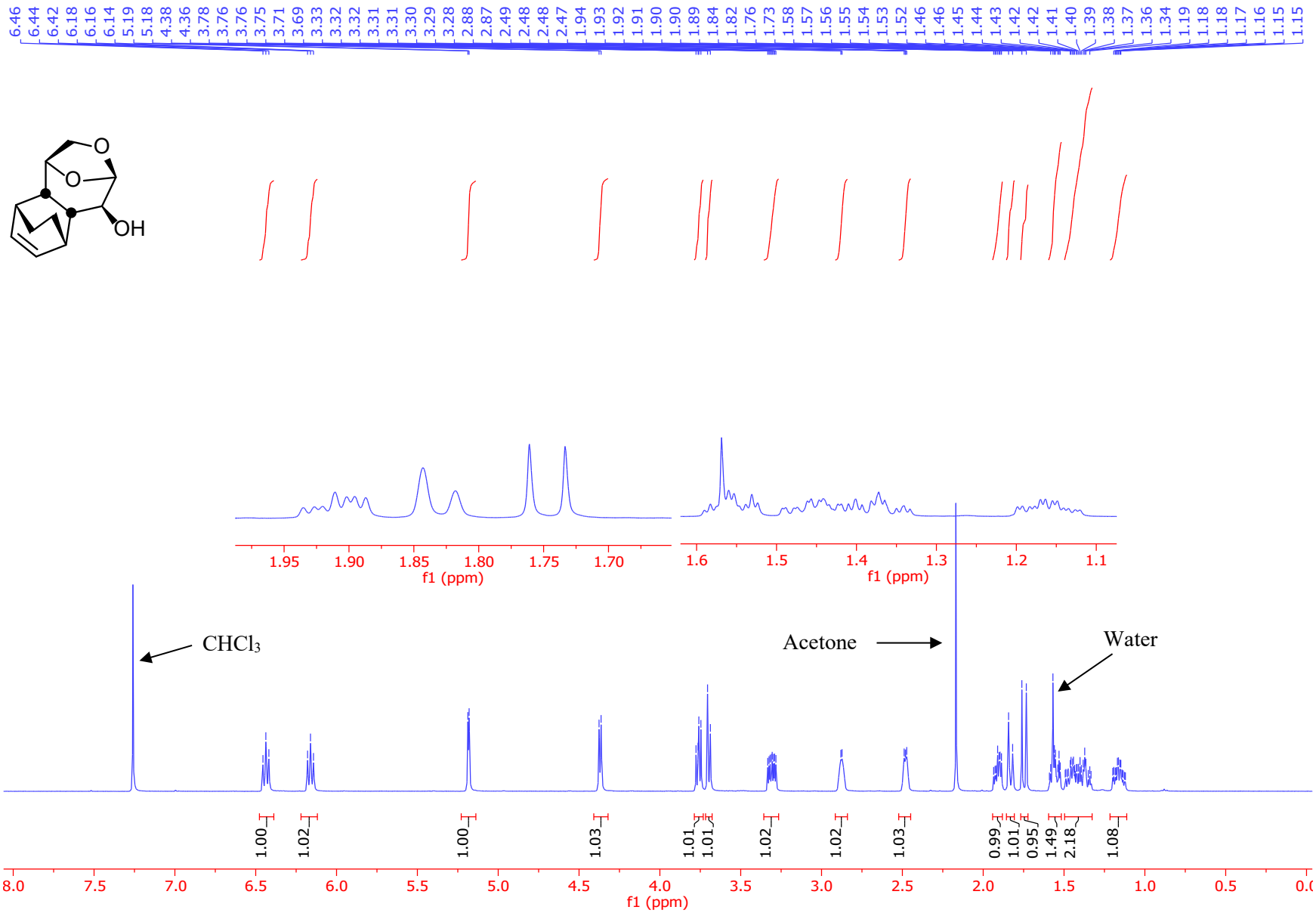

101 MHz $^{13}C\{^{1}H\}$ NMR Spectrum of Compound **21** (Recorded in $CDCl_3$)

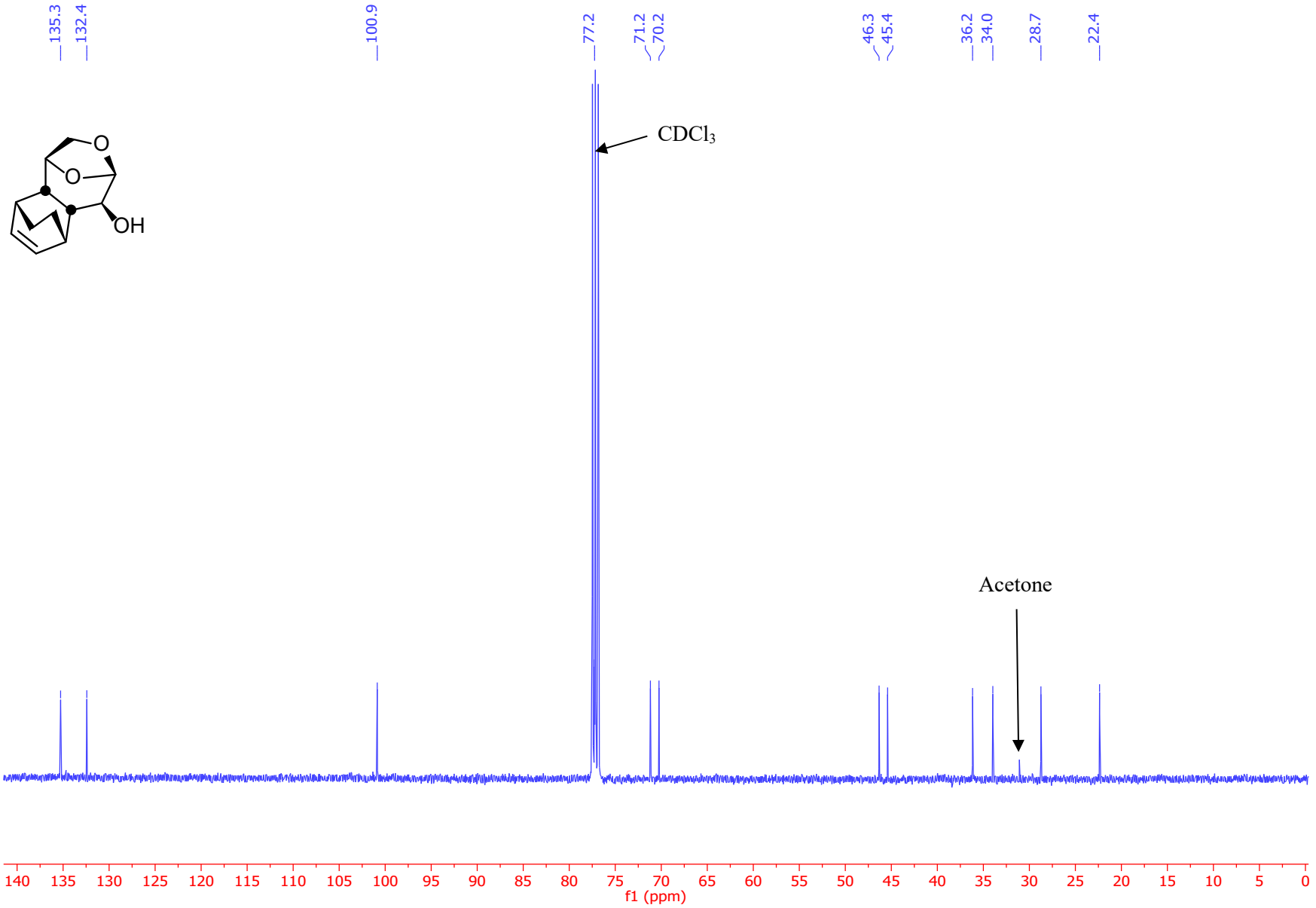

400 MHz ^{1}H NMR Spectrum of Compound **22** (Recorded in $CDCl_3$)

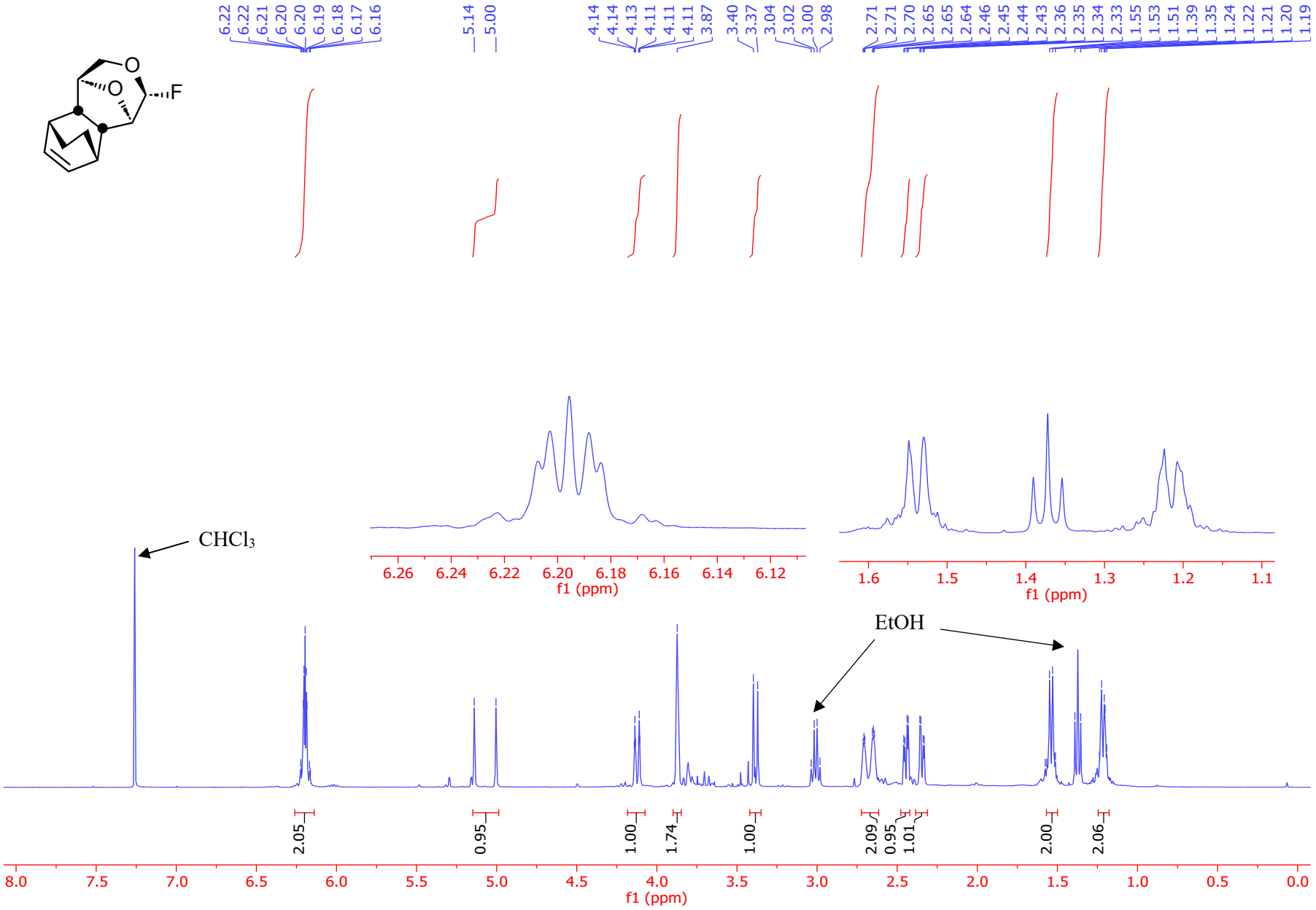

101 MHz $^{13}C\{^{1}H\}$ NMR Spectrum of Compound **22** (Recorded in $CDCl_3$)

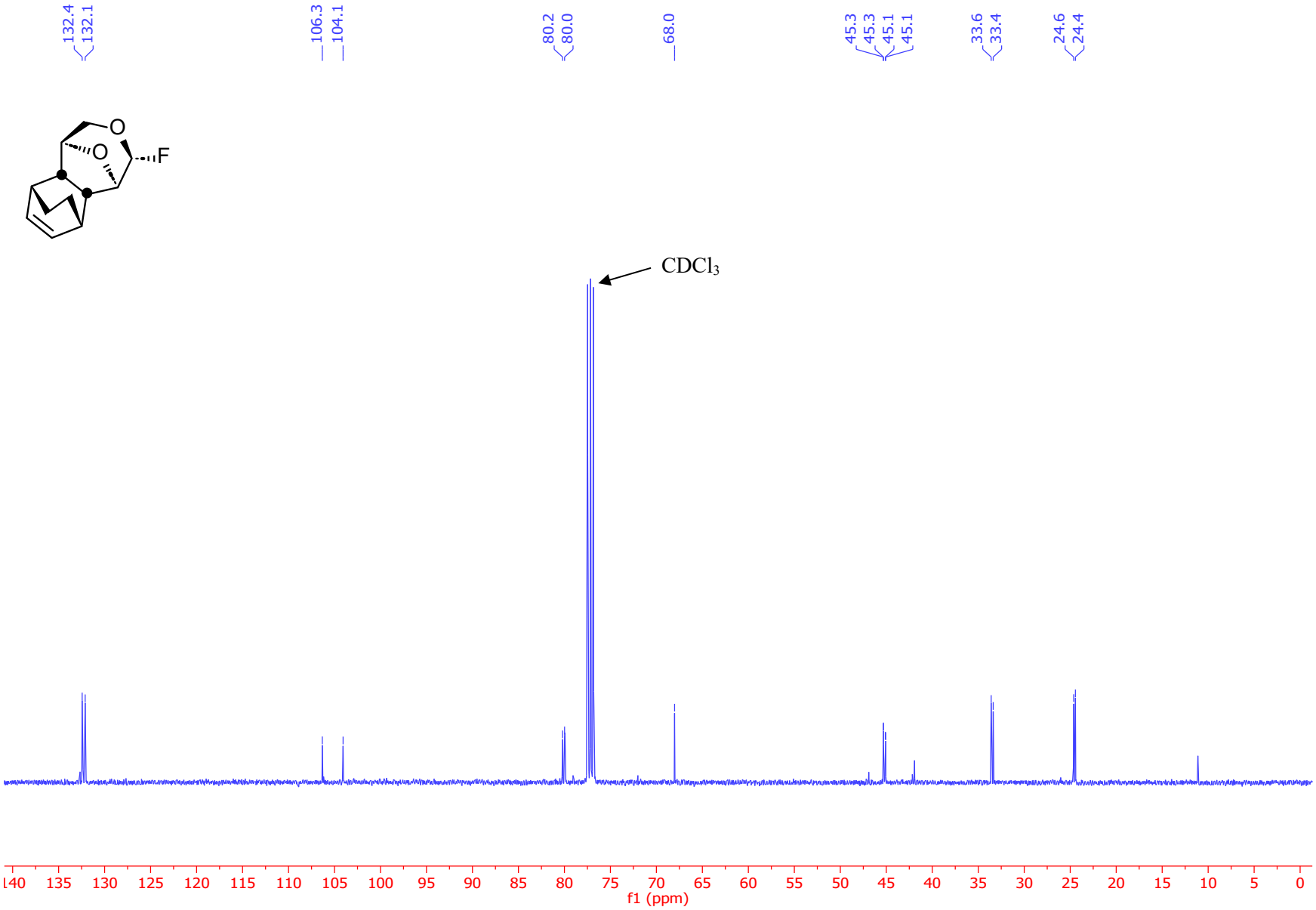

400 MHz ^{1}H NMR Spectrum of Compound **23** (Recorded in $CDCl_3$)

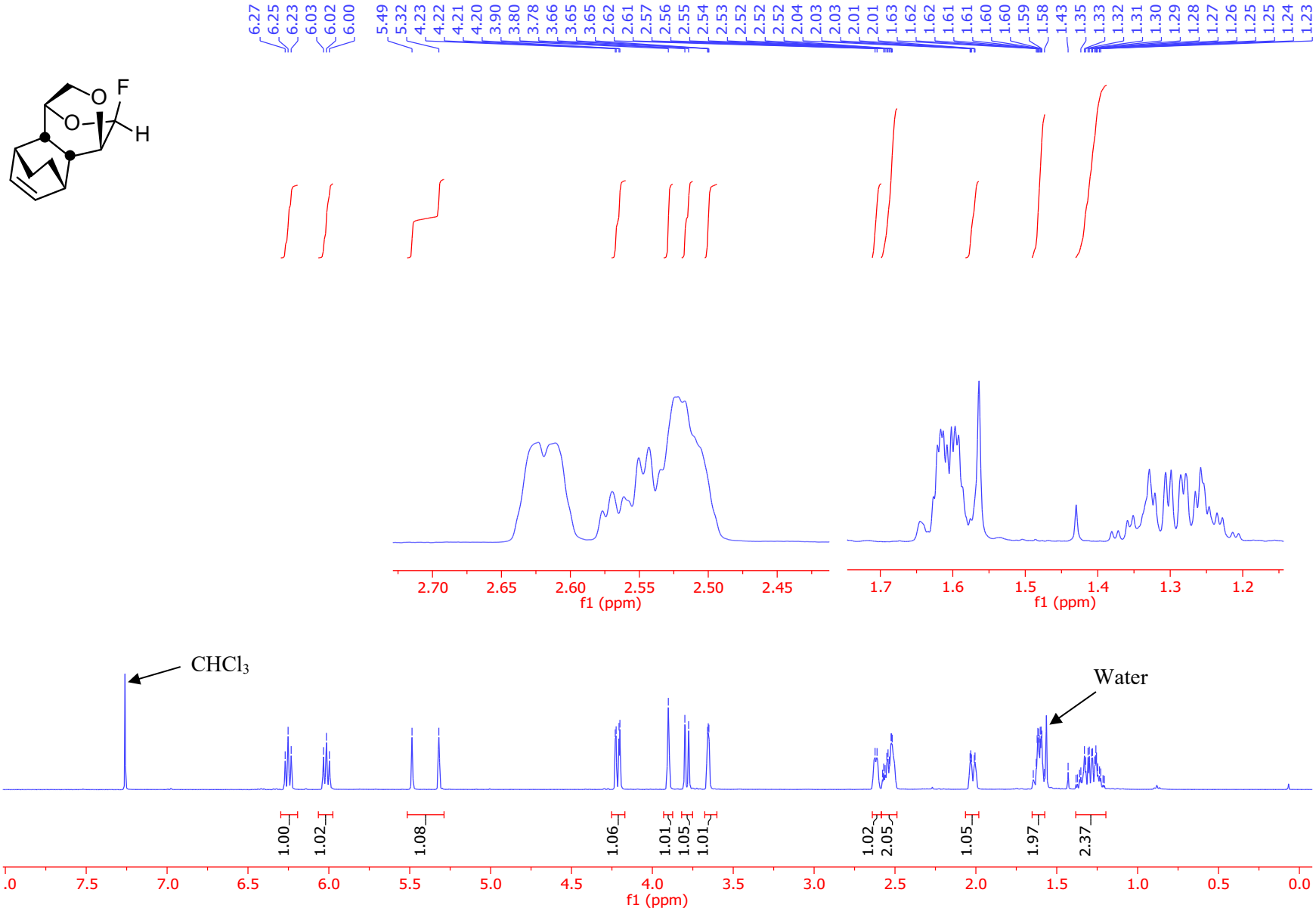

101 MHz $^{13}C\{^{1}H\}$ NMR Spectrum of Compound **23** (Recorded in $CDCl_3$)

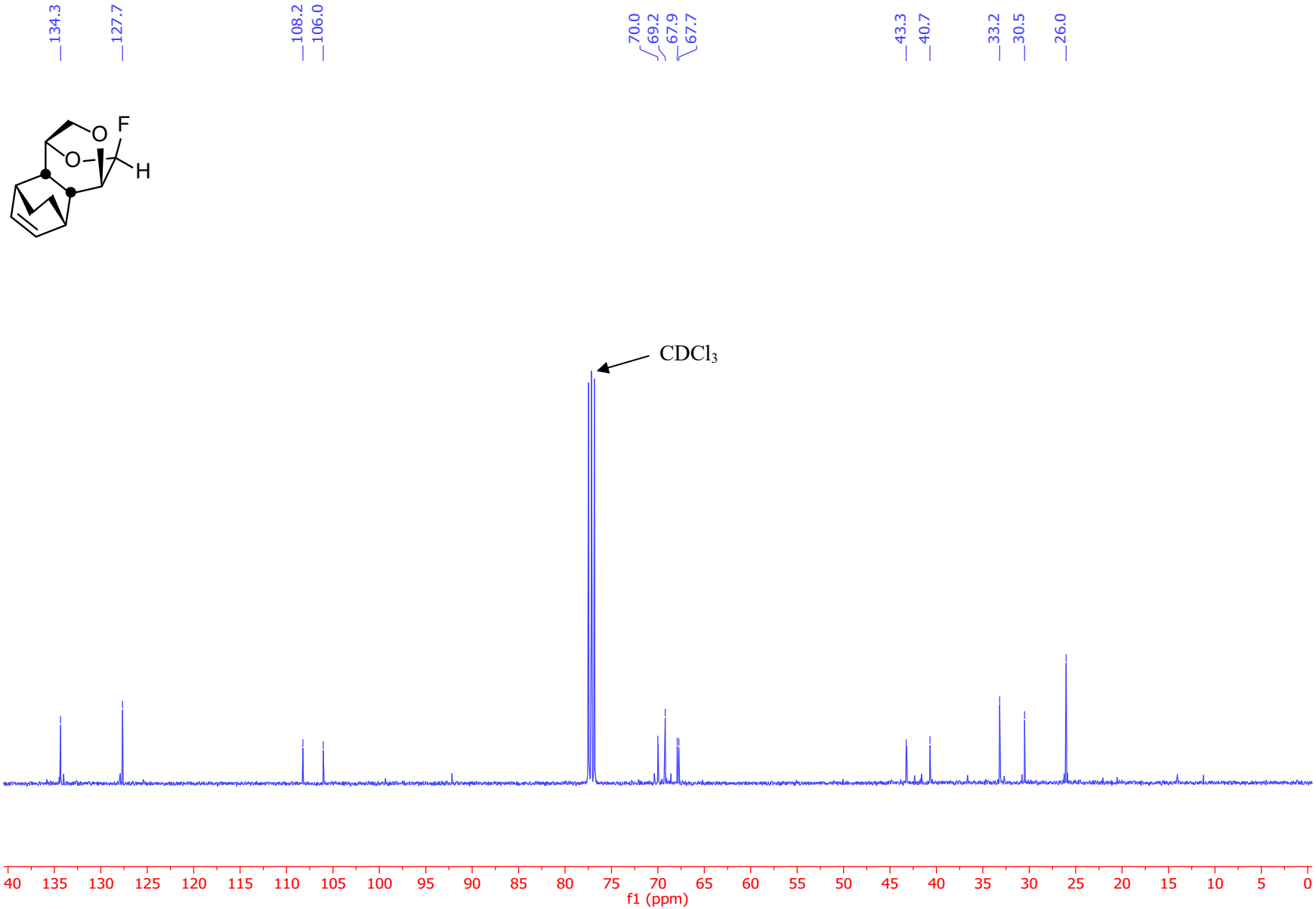

400 MHz ^{1}H NMR Spectrum of Compound **24** (Recorded in $CDCl_3$)

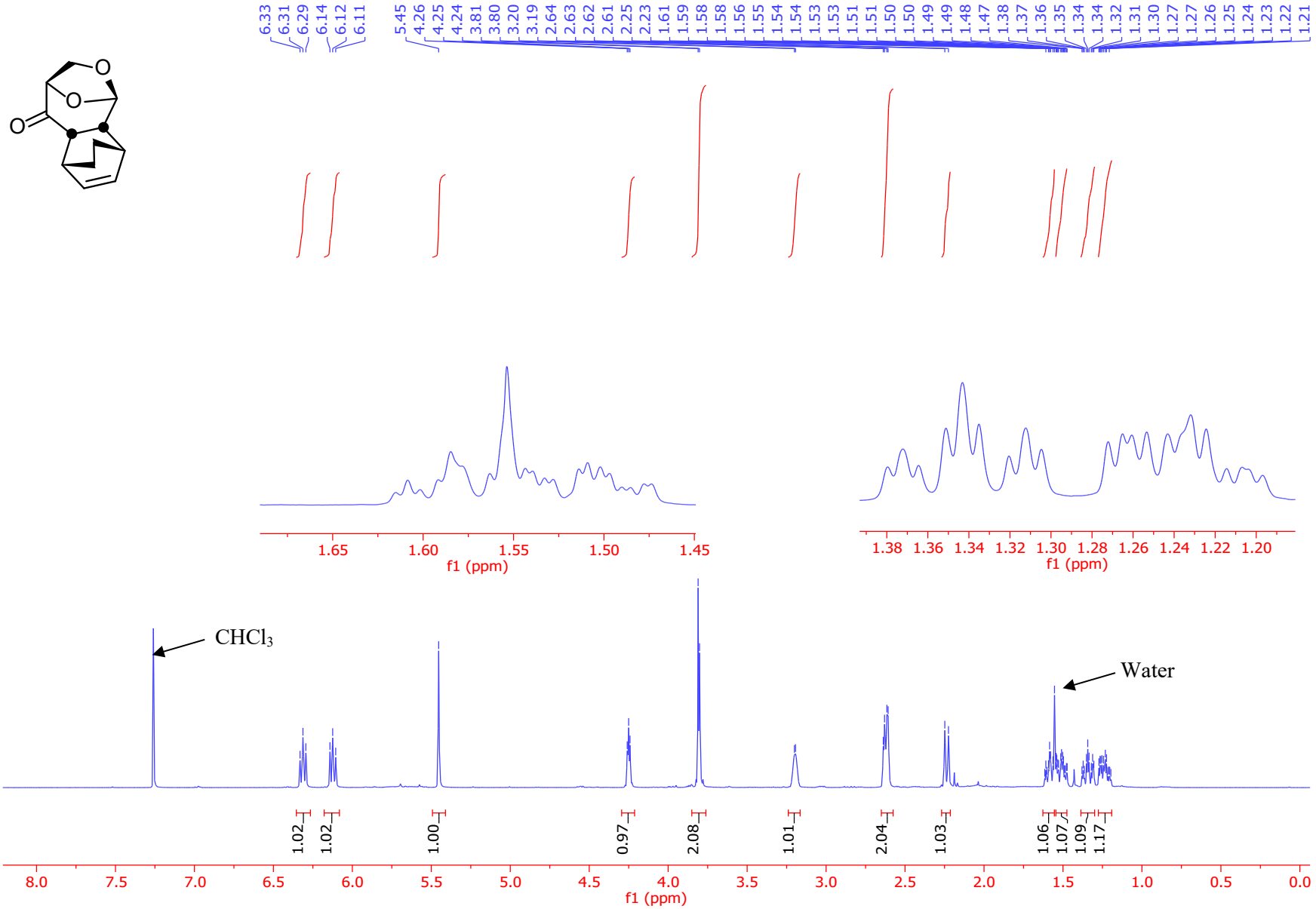

101 MHz $^{13}C\{^{1}H\}$ NMR Spectrum of Compound **24** (Recorded in $CDCl_3$)

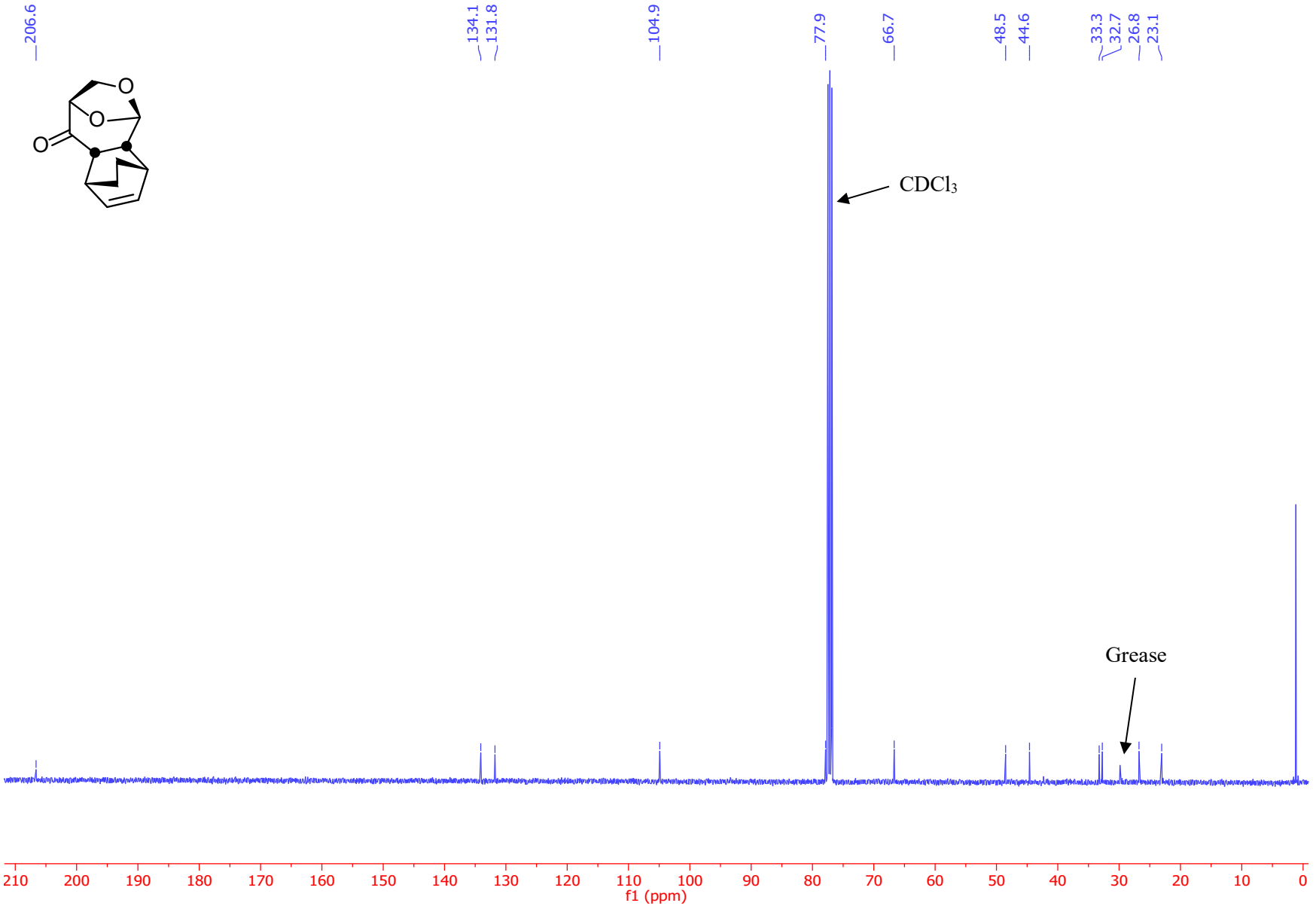

400 MHz ^{1}H NMR Spectrum of Compound **25** (Recorded in $CDCl_3$)

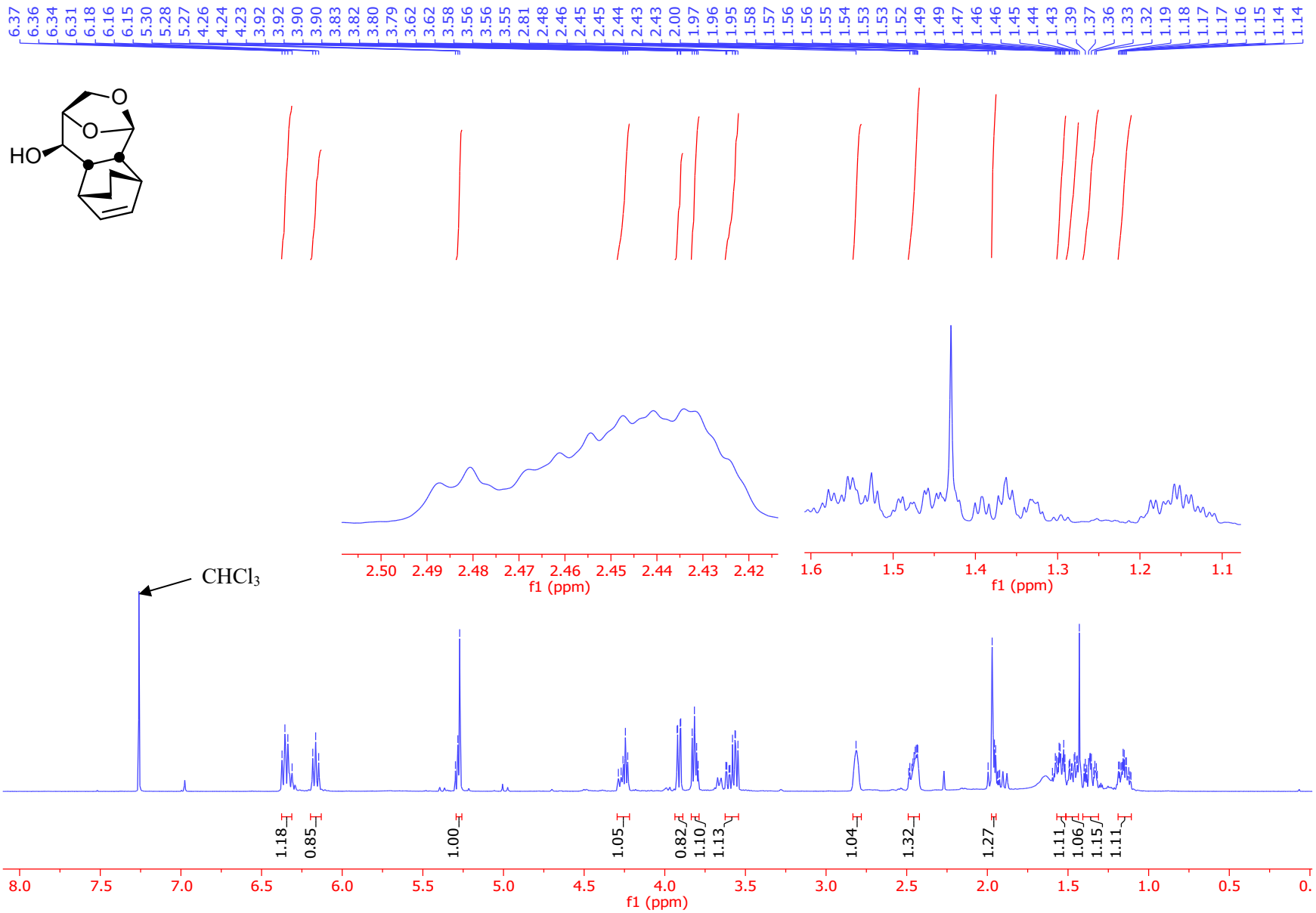

101 MHz $^{13}C\{^{1}H\}$ NMR Spectrum of Compound **25** (Recorded in $CDCl_3$)

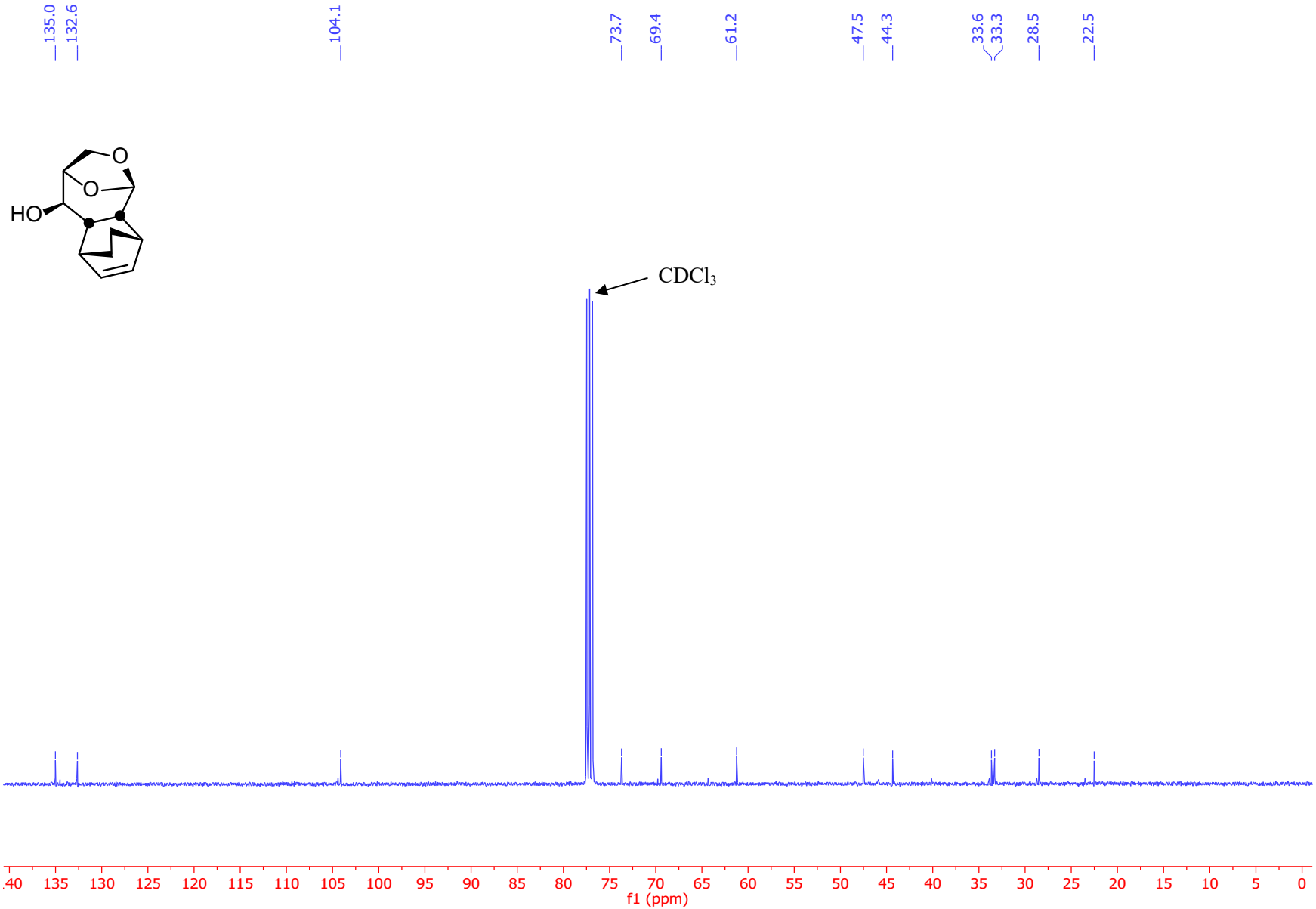

400 MHz ^{1}H NMR Spectrum of Compound **27** (Recorded in $CDCl_3$)

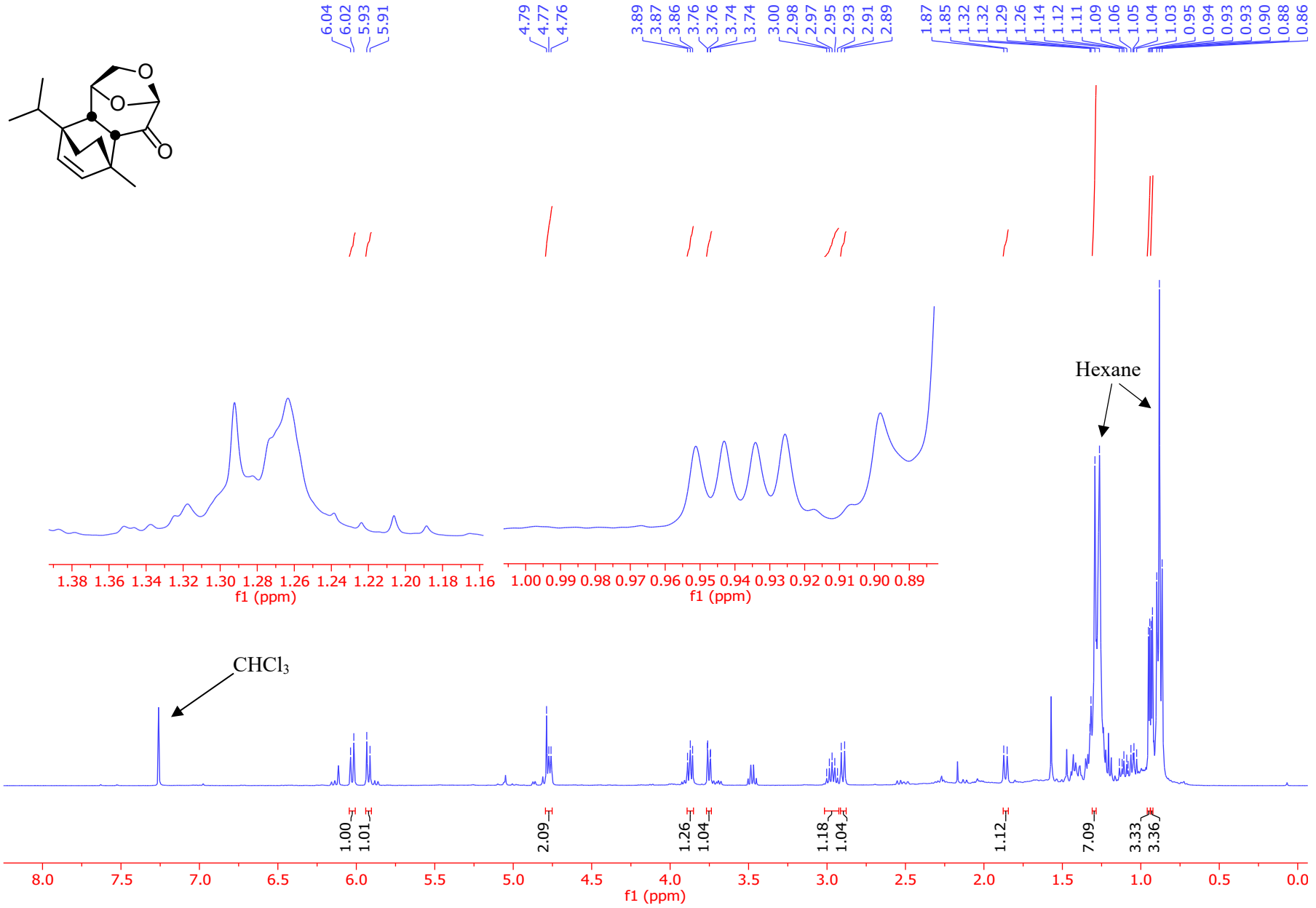

101 MHz $^{13}C\{^{1}H\}$ NMR Spectrum of Compound **27** (Recorded in $CDCl_3$)

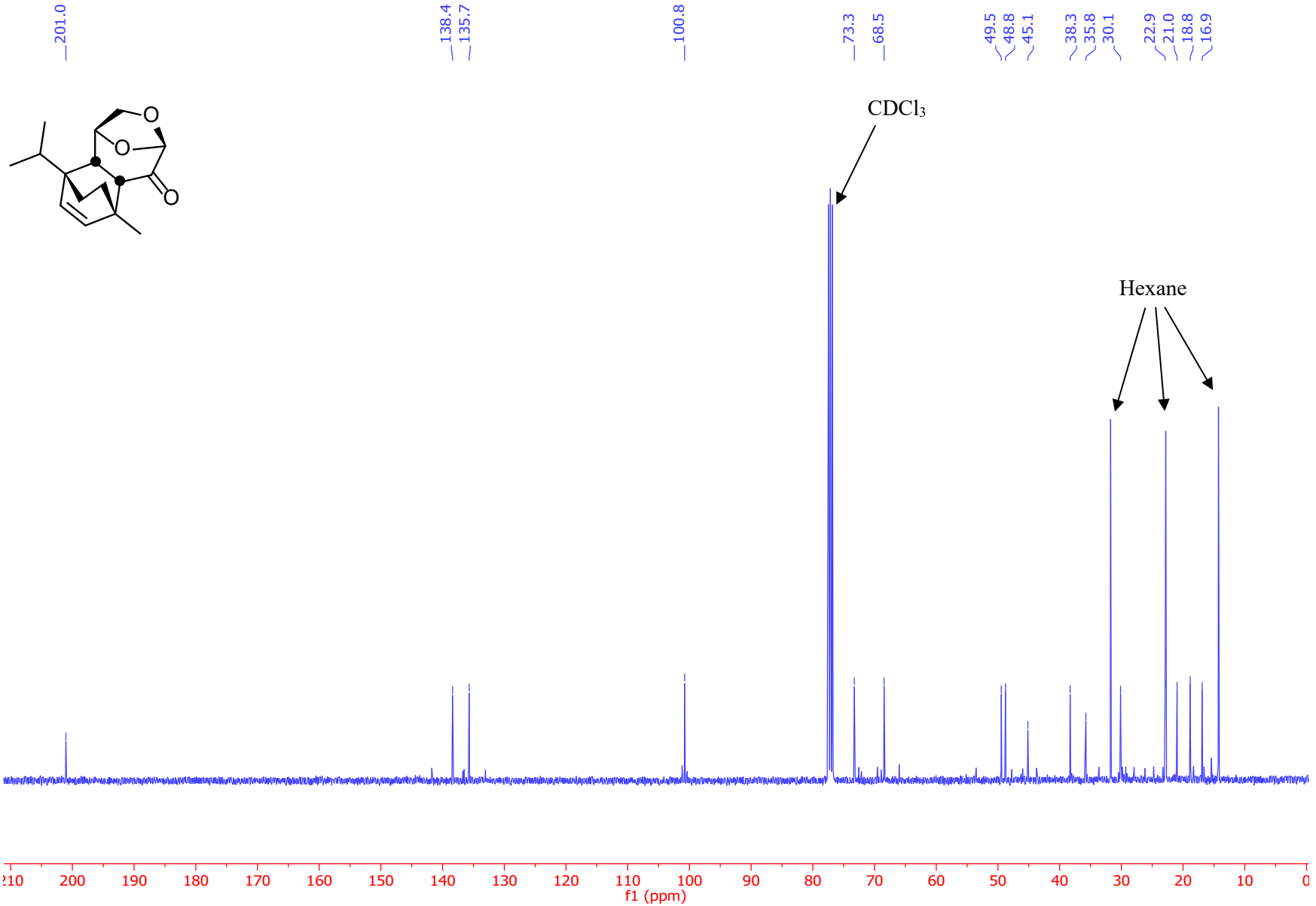

400 MHz ^{1}H NMR Spectrum of Compound **28** (Recorded in $CDCl_3$)

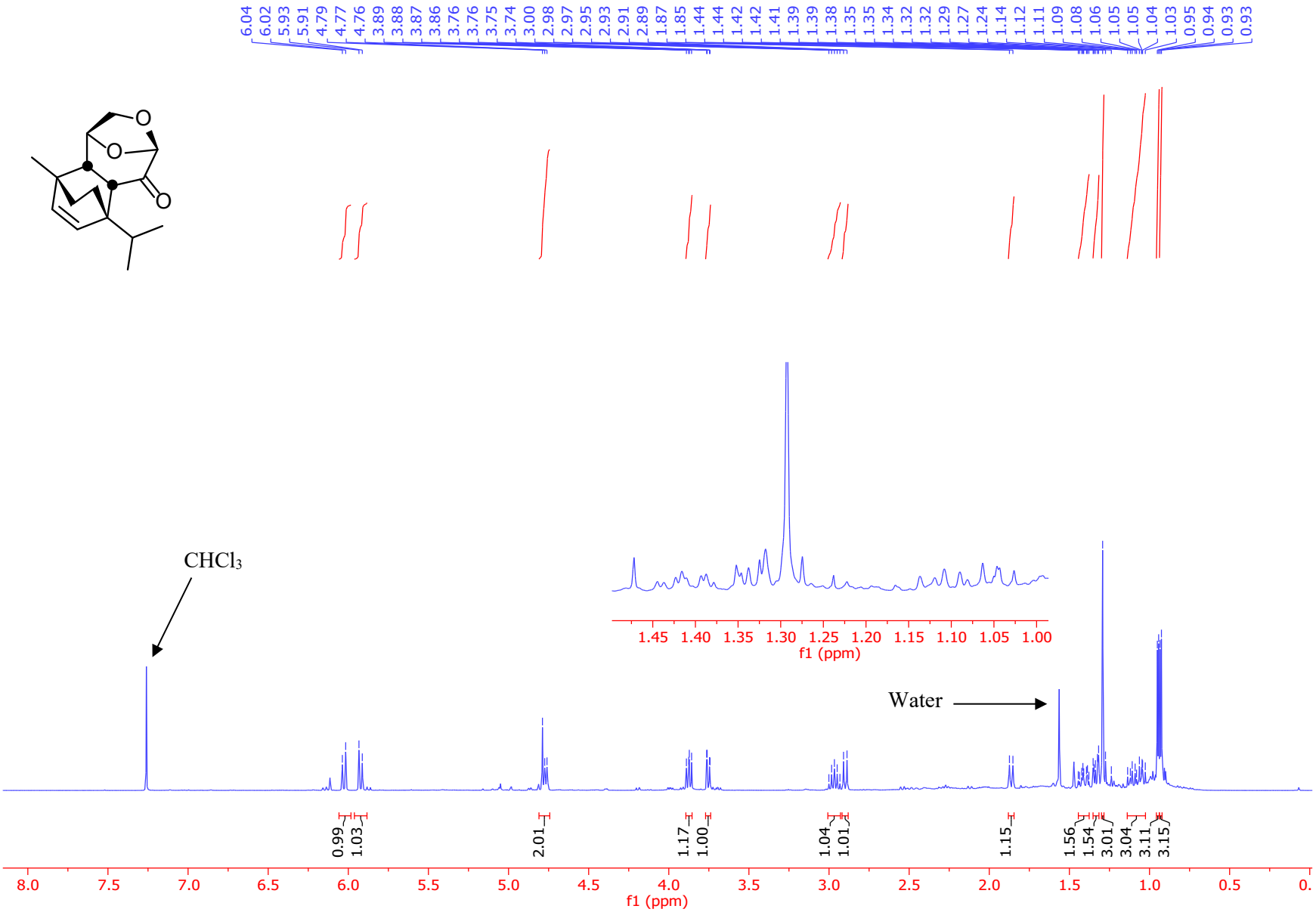

101 MHz $^{13}C\{^{1}H\}$ NMR of Compound **28** (Recorded in $CDCl_3$)

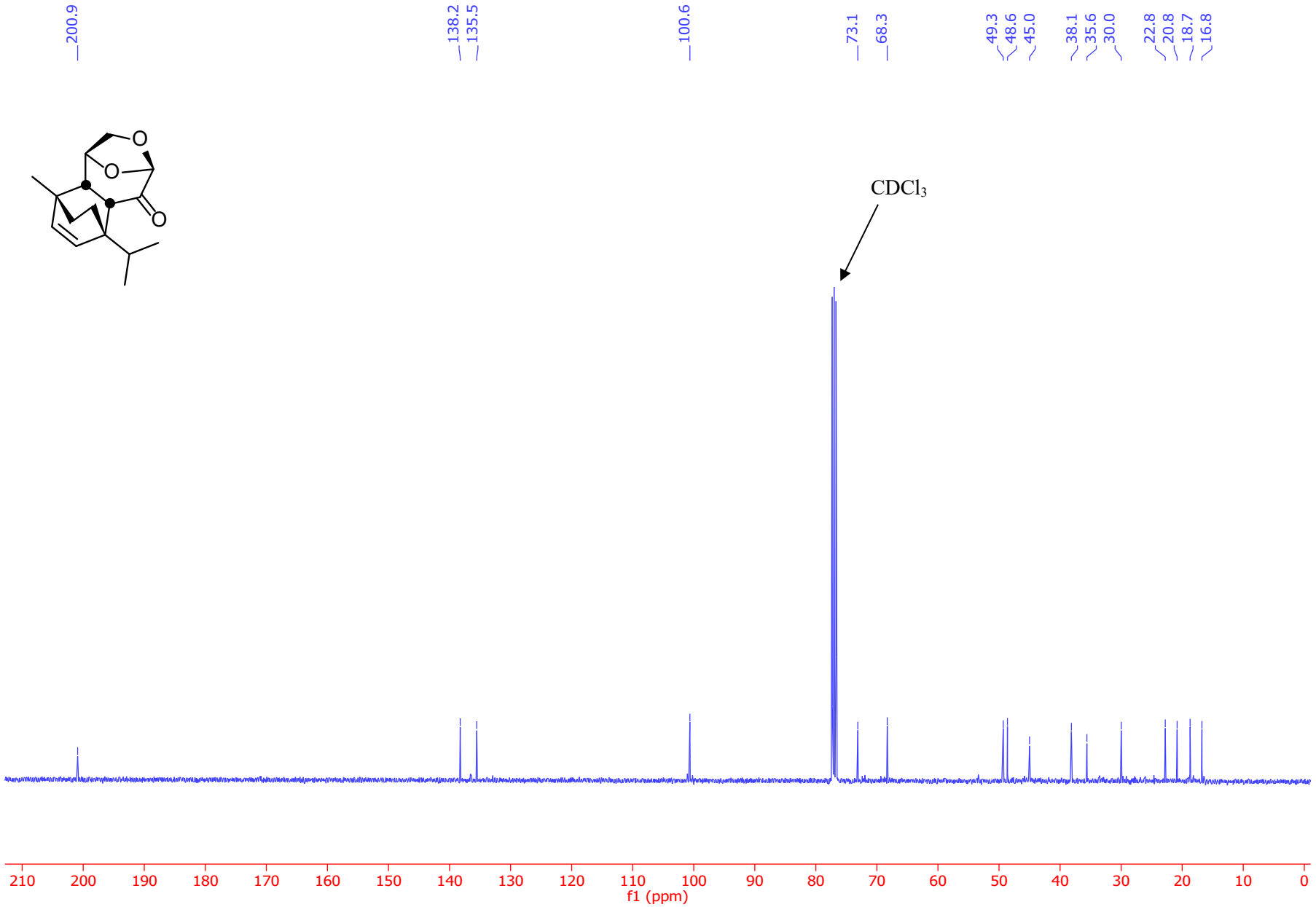

400 MHz ^{1}H NMR of Compound **29** (Recorded in $CDCl_3$)

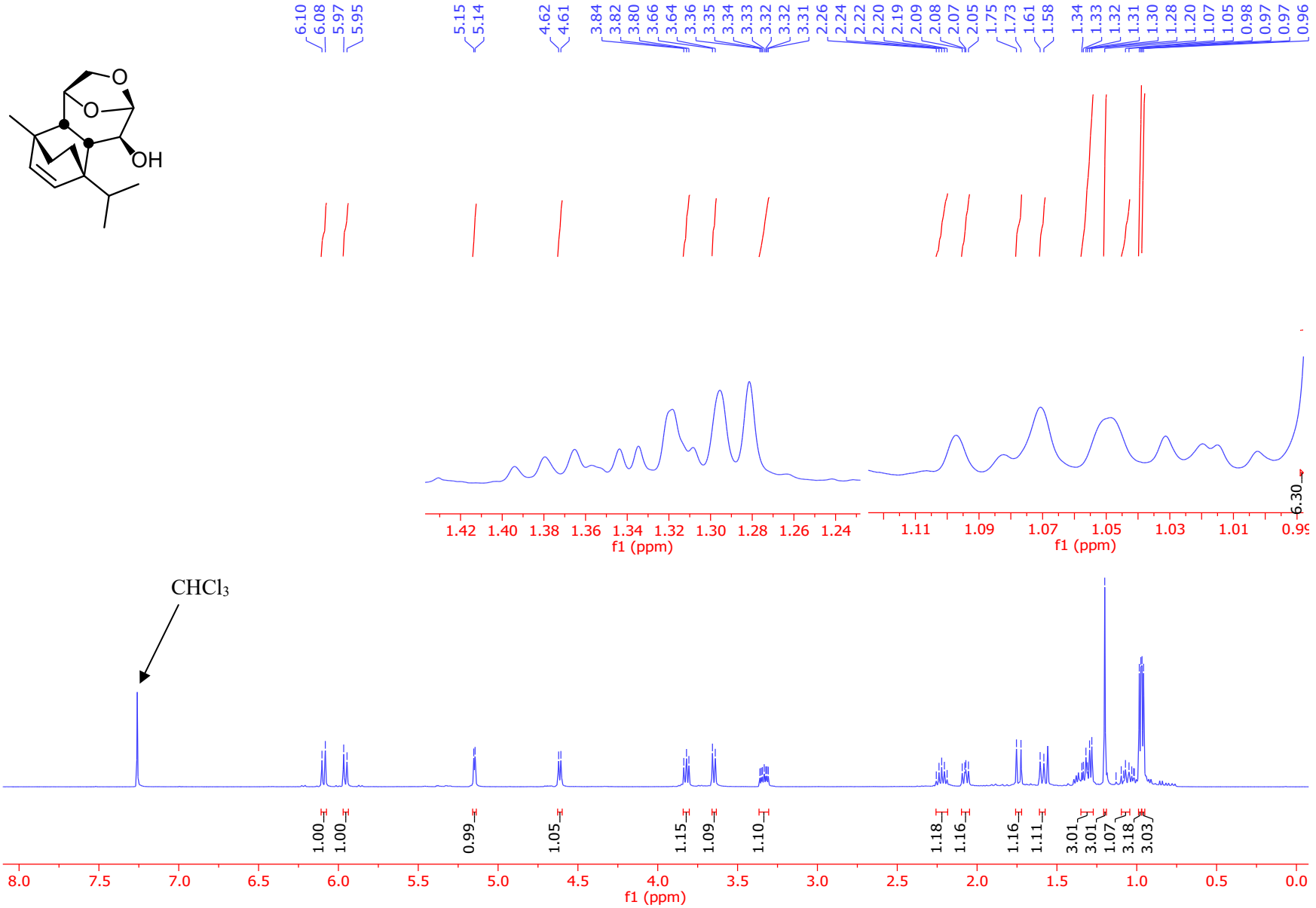

101 MHz $^{13}C\{^{1}H\}$ NMR Spectrum of Compound **29** (Recorded in $CDCl_3$)

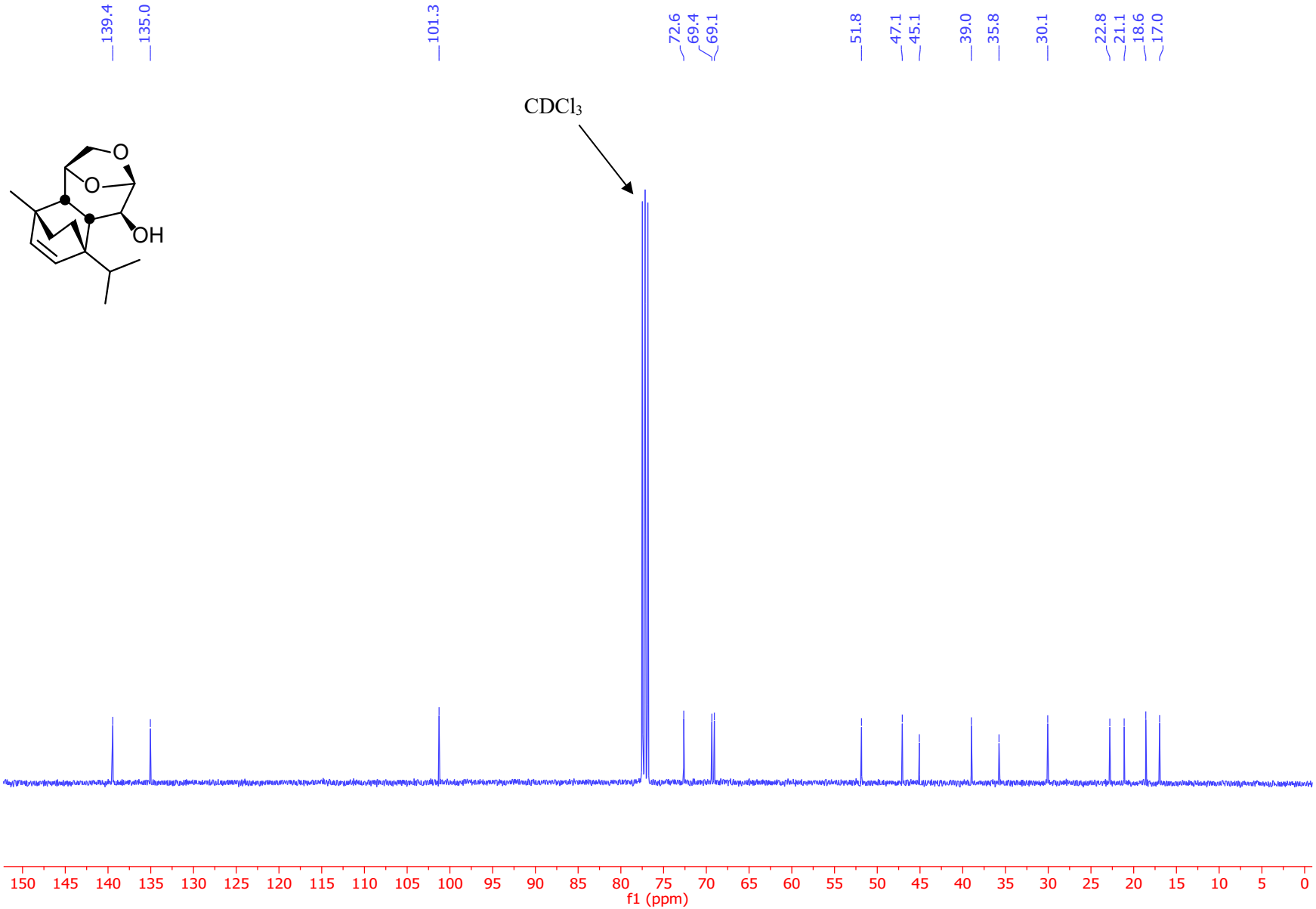

400 MHz ^{1}H NMR Spectrum of Compound **30** (Recorded in $CDCl_3$)

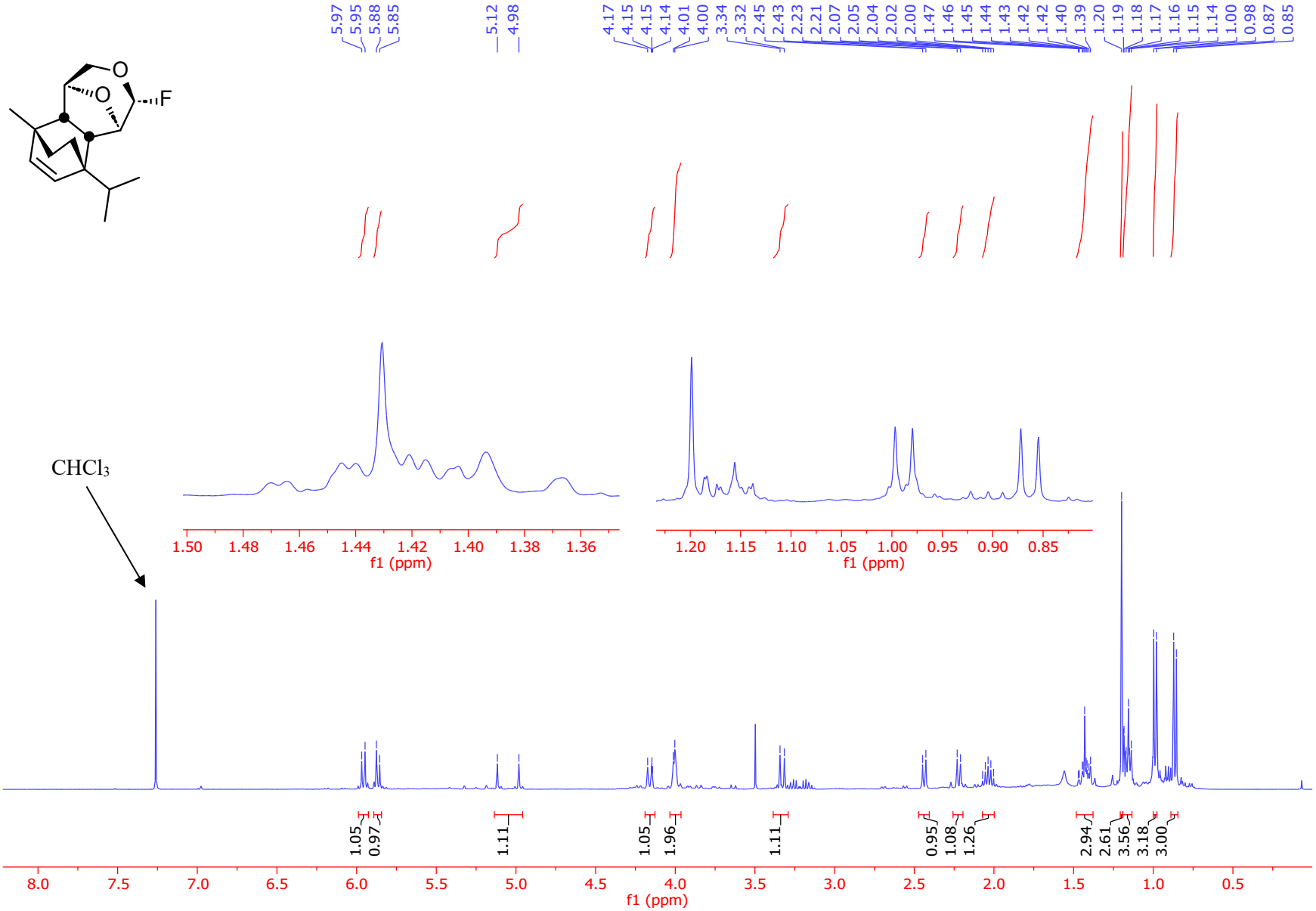

101 MHz $^{13}C\{^{1}H\}$ NMR Spectrum of Compound **30** (Recorded in $CDCl_3$)

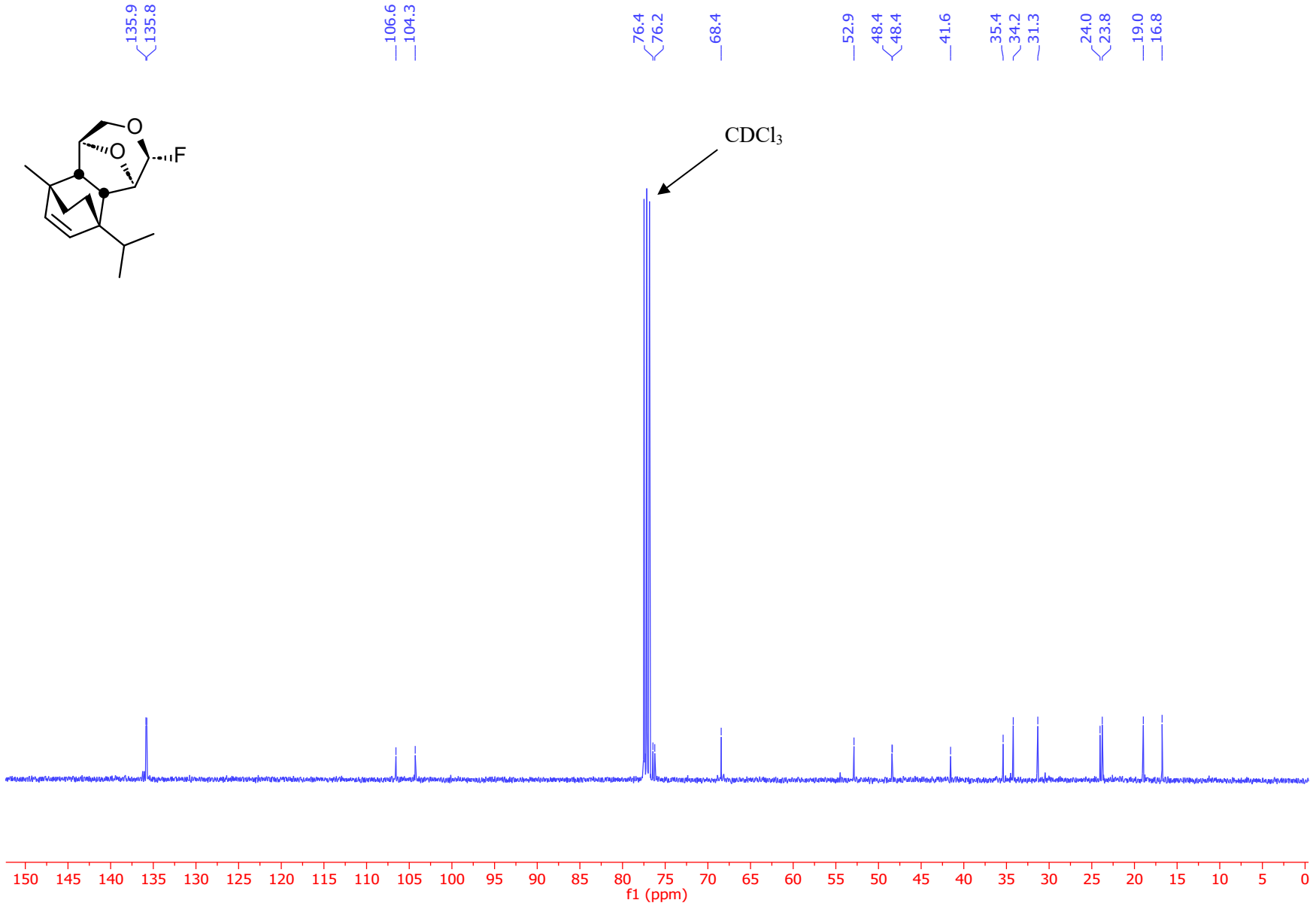

400 MHz ^{1}H NMR Spectrum of Compound **32** (Recorded in $CDCl_3$)

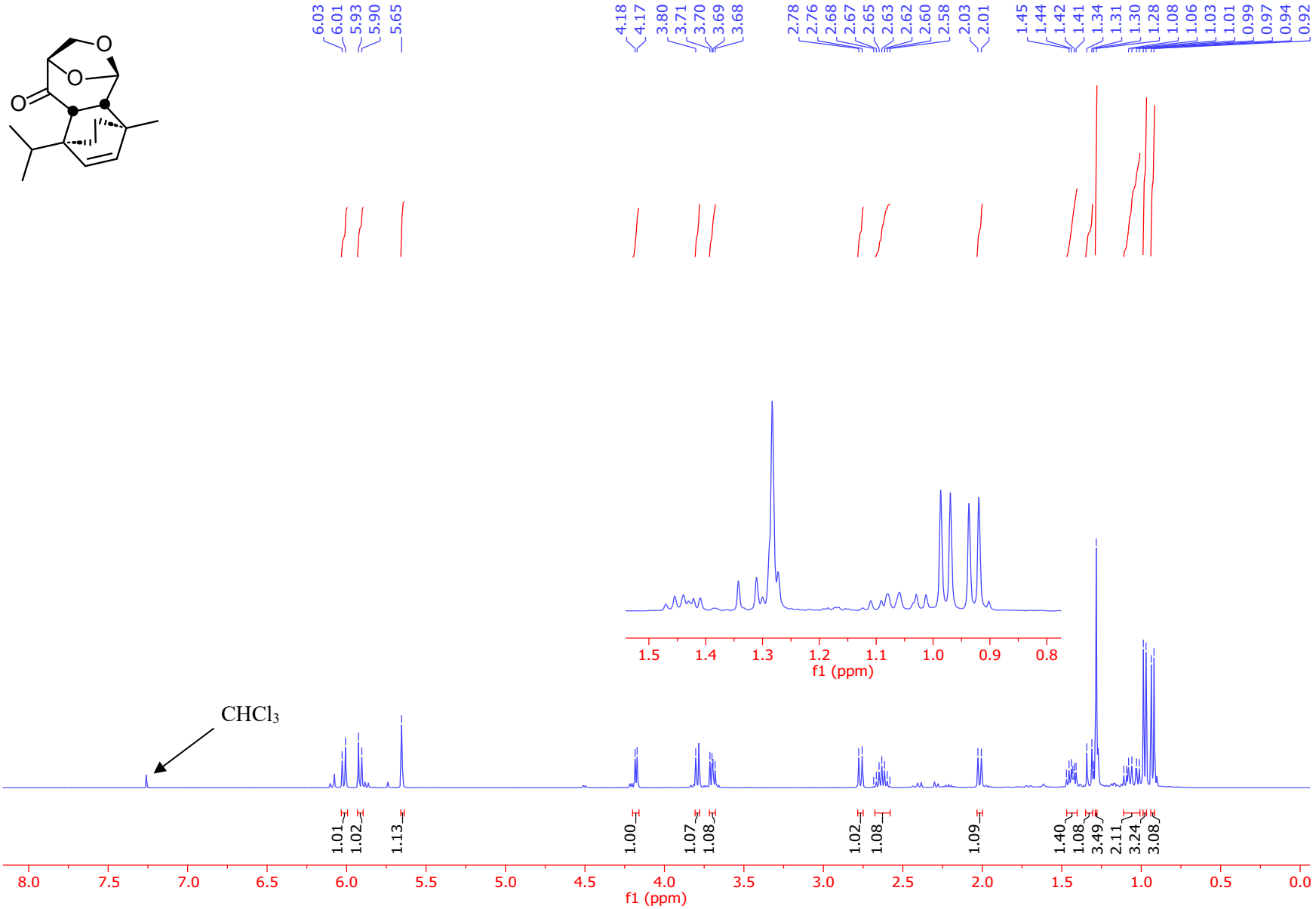

101 MHz $^{13}C\{^{1}H\}$ NMR Spectrum of Compound **32** (Recorded in $CDCl_3$)

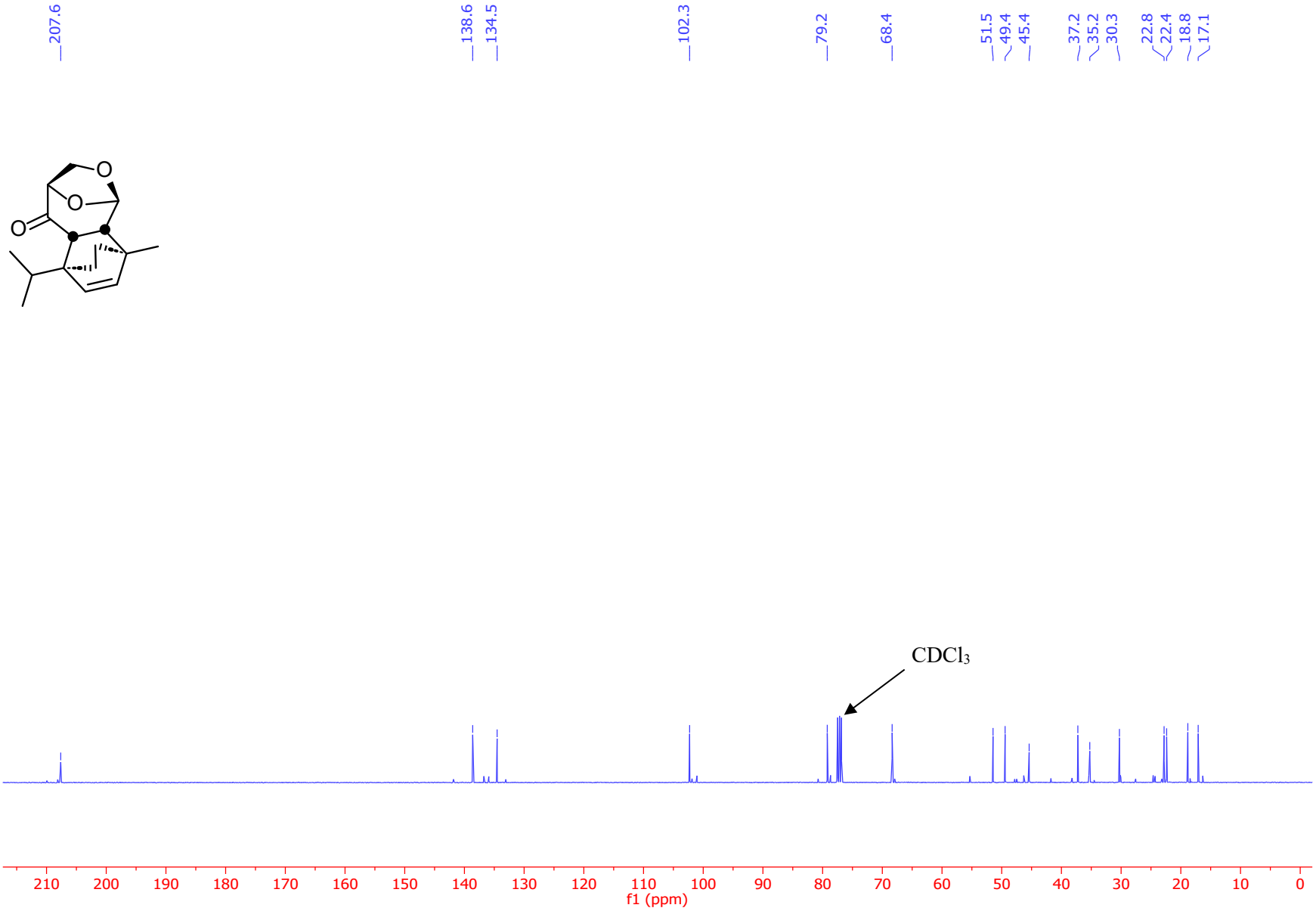

400 MHz ^{1}H NMR Spectrum of Compound **33** (Recorded in $CDCl_3$)

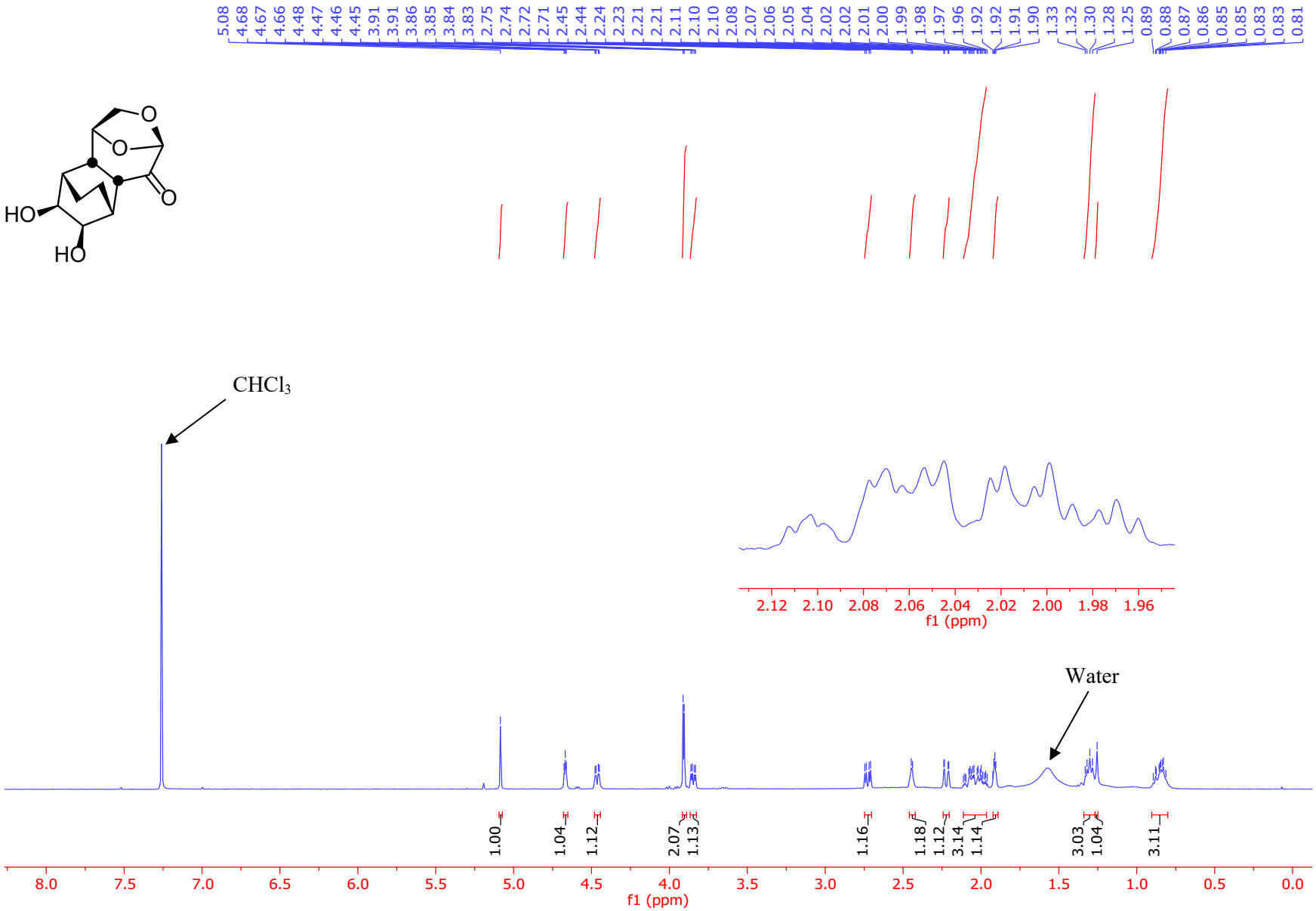

101 MHz $^{13}C\{^{1}H\}$ NMR Spectrum of Compound **33** (Recorded in $CDCl_3$)

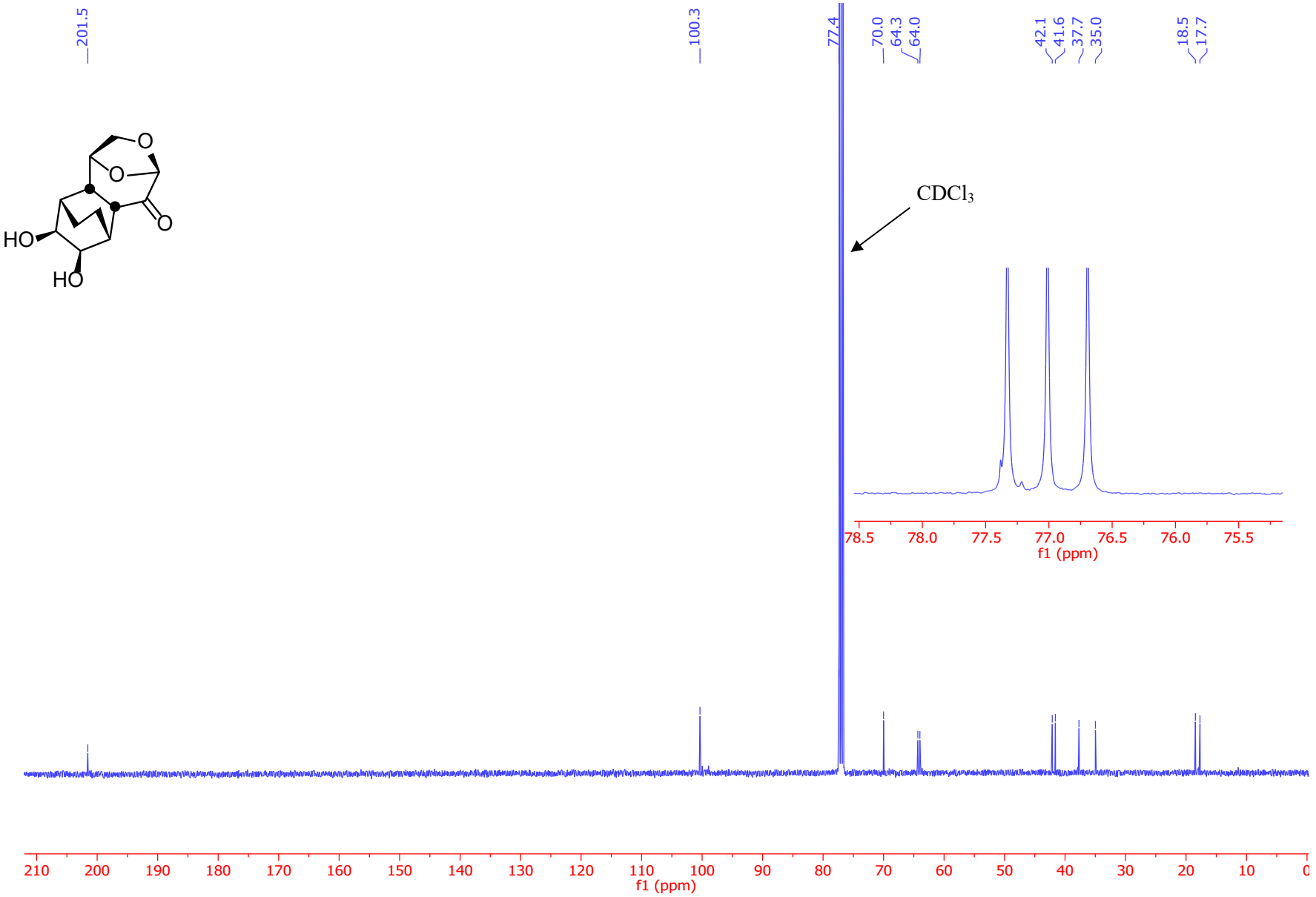

References

1. For some recent points-of-entry into the relevant literature, see: (a) M. B. Comba, Y.-h.Tsai, A. M. Sarotti, M. I. Mangione, A. G. Suárez, R. A. Spanevello, *European Journal of Organic Chemistry*, **2018**, 590; (b) M. G. Banwell, B. Pollard, X. Liu, L. A. Connal, *Chemistry An Asian Journal,* **2021**, *16*, 604; (c) F. Allais, *Curr. Opin. Green Sustain. Chem*. **2023**, *40*, 100744.
2. See, for example: (a) J. E. Camp, B. W. Greatrex, *Front. Chem*. **2022**, *10*, 902239; (b) J. Klepp, T. Bousfield, H. Cummins, S. V. A.-M. Legendre, J. E. Camp, B. W. Greatrex, *Beilstein Journal of Organic Chemistry*, **2022**, *18*, 1457 and references cited therein.
3. (a) M. Nikahd, J. Mikusek, L.-J. Yu, M. L. Coote, M. G. Banwell, C. Ma, M. G. Gardiner, *J. Org. Chem*. **2020**, *85*, 4583; (b) M. Nikahd, J. Mikusek, M. G. Banwell, L.-J. Yu, M. L. Coote, M. G. Gardiner, *Australian Journal of Chemistry,* **2020**, *73*, 1186.
4. (a) X. Ma, N. Anderson, L. V. White, S. Bae, W. Raverty, A. C. Willis, M. G. Banwell, *Australian Journal of Chemistry*, **2015**, *68*, 593; (b) X. Ma, X. Liu, P. Yates, W. Raverty, M. G. Banwell, C. Ma, A. C. Willis, P. D. Carr, *Tetrahedron*, **2018**, *74*, 5000; (c) M. G. Banwell, X. Liu, L. A. Connal, M. G. Gardiner, *Macromolecules*, **2020**, *53*, 5308; (d) X. Liu, P. Carr, M. G. Gardiner, M. G. Banwell, A. H. Elbanna, Z. G. Khalil, R. J. Capon, *ACS Omega*, **2020**, *5*, 13926; (e) X. Liu, B. Pollard, M. G. Banwell, L.-J. Yu, M. L. Coote, M. G. Gardiner. B. M. A. van Vugt-Lussenburg, B. van der Burg, F. L. Grasset, E. Campillo, J. Sherwood, F. P. Byrne, T. J. Farmer, *Australian Journal of Chemistry,* **2022**, *75*, 331.
5. For other recent studies concerned with the formation of LGO-derived polymers, see: (a) F. Diot-Néant, L. Mouterde, S. Fadlallah, S. A. Miller, F. Allais, *Chemistry Sustainable Chemistry*, **2020**, *13*, 2613; (b) S. Fadlallah, A. A. M. Peru, A. L. Flourat, F. Allais, *Eur. Polym. J*. **2020**, *138*, 109980; (c) F. Diot-Néant, L. M. M. Mouterde, J. Couvreur, F. Brunois, S. A. Miller, F. Allais, *European Polymer Journal*, **2021**, *159*, 110745; (d) A. Kayishaer, S. Fadlallah, L. M. M. Mouterde, A. A. M. Peru, Y. Werghi, F. Brunois, Q. Carboué, M. Lopez, F. Allais, *Molecules*, **2021**, *26*, 7672; (e) S. Fadlallah, A. L. Flourat, L. M. M. Mouterde, M. Annatelli, A. A. M. peru, A. Gallos, F. Aricó, F. Allais, *Macromolecular Rapid Communications*, **2021**, *42*, 2100284; (f) T. Debsharma, B. Schmidt, A. Laschewsky, H. Schlaad, *Marcomolecules*, **2021**, *54*, 2720; (g) F. Diot-Néant, L. M. M. Mouterde, C. Veith, J. Couvreur, S. A. Miller, F. Allais, *ACS Sustainable Chemical Engineering*, **2022**, *10*, 10132; (h) S. Fadlallah, A. Kayishaer, M. Annatelli, L. M. M. Mouterde, A. A. M. Peru, F. Aricó, F. Allais, *Green Chemistry,* **2022**, *24*, 2871; (i) S. Fadlallah, Q. Carboué, L. M. M. Mouterde, A. Kayishaer, Y. Werghi, A. M. M. Peru, M. Lopez, F. Allais, *Polymers*, **2022**, *14*,
   2082; (j) C. M. Warne, S. Fadlallah, A. C. Whitwood, J. Sherwood, L. M. M. Mouterde, F. Allais, G. M. Guebitz, C. R. McElroy, A. Pellis, *Green Chemistry Letters and Reviews*, **2023**, *16*, 2154573.

6. W. J. Middleton, *Journal of Organic Chemistry,* **1975**, *40*, 574.
7. For a related DAST-induced rearrangement of a simpler anhydropyranose see: F. Oberdorfer, R. Haeckel, G. Lauer, *Synthesis*, **1998**, 201.
8. J.-C. Hierso, *Chemical Reviews,* **2014**, *114*, 4838.
9. M. A. Zurita, A. Avila, R. A. Spanevello, A. G. Suárez, A. M. Sarotti, *Carbohydrate Research*, **2015**, *402*, 67.
10. D. Horton, J. P. Roski, P. Norris, *Journal of. Organic Chemistry,* **1996**, *61*, 3783.
11. A single-crystal X-ray analysis of compound **14** has been reported previously – see ref. 10.
12. (a) D. D. Ward, F. Shafizadeh, *Carbohydr. Res*. **1981**, *95*, 155; (b) A. M. Sarotti, R. A. Spanevello, A. G. Suárez, *Tetrahedron Letters*, **2011**, *52*, 4145; (c) A. N. Davydova, A. A. Pershin, B. T. Sharipov, F. A. Valeev, *Mendeleev* Communications, **2015**, *25*, 271.
13. Y. S. Galimova, Y. A. Khalilova, B. T. Sharipov, L. V. Spirikhin, S. R. Rameev, R. L. Safiullin, F. A. Valeev, *Russian Journal of Organic Chemistry,* **2014**, *50*, 2848.
14. M. G. Essig, T. T. Stevenson, F. Shafizadeh, R. E. Stenkamp, L. H. Jensen, *Journal of Organic Chemistry,* **1984**, *49*, 3652.
15. B. Plietker, *Tetrahedron Asymmetry* **2005**, *16*, 3453 and references cited therein.
16. W. C. Still, M. Kahn, A. Mitra, A. *Journal of Organic Chemistry,* **1978**, *43*, 2923.
17. A. B. Pangborn, M. A. Giardello, R. H. Grubbs, R. K. Rosen, F. J. Timmers, *Organometallics*, **1996**, *15*, 1518.
18. (a) P. Bhate, D. Horton, *Carbohydr. Res*. **1983**, *122*, 189; (b) A. M. Sarotti, R. A. Spanevello, C. Duhayon, J.-P. Tuchagues, A. G. Suárez, *Tetrahedron*, **2007**, *63*, 241.
19. O. V. Dolomanov, L. J. Bourhis, R. J. Gildea, J. A. K. Howard, H. J. Puschmann, *Journal of Applied Crystallography,* **2009**, *42*, 339−341.
20. G. M. Sheldrick, *Acta Crystallographica., Sect. A: Found. Adv*. **2015**, *A71*, 3−8.
21. G. M. Sheldrick, *Acta Crystallographica., Sect. C: Struct. Chem*. **2015**, *C71*, 3.

Chapter Five

Polymers From Cellulosic Waste:

Direct Polymerisation of Levoglucosenone Using DBU as a Catalyst

Brett Pollard, Martin G. Banwell, Luke A. Connal

ChemSusChem, **2023**, e202301165.

Australian National University

Statement of Contribution

This thesis is submitted as a Thesis by Compilation in accordance with https://policies.anu.edu.au/ppl/document/ANUP_003405

I declare that the research presented in this Thesis represents original work that I carried out during my candidature at the Australian National University, except for contributions to multi-author papers incorporated in the Thesis where my contributions are specified in this Statement of Contribution.

Title: Polymers from cellulosic waste: Direct polymerisation of levoglucosenone using DBU as a catalyst

Authors: Brett Pollard, Martin G. Banwell, Luke A. Connal

Publication outlet: ChemSusChem

Current status of paper: Submitted

Contribution to paper: This is a full paper and the candidate carried out all of the experimental work reported within it. In addition, the candidate collated and formatted all of the spectral data presented in the Supporting Information document. The candidate also wrote the entirety of the manuscript and Experimental Section and conducted relevant literature surveys. A preliminary outline was generated and revised by the candidate.

Senior author or collaborating authors endorsement: M. G. Banwell

BRETT L POLLARD		21/8/2023
Candidate – Print Name	Signature	Date

Endorsed

Luke Connal		21/8/23
Primary Supervisor – Print Name	Signature	Date
Mark Humphrey	Mark Humphrey	22/8/23
Delegated Authority – Print Name	Signature	Date

Foreword

Given the scale and utility of polymeric materials, the efficient formation of a polymer from a BMDPM is arguably the most impactful valorisation of renewable biomass in the sphere of commodity chemicals. As detailed in **Chapters 1** and **3**, levoglucosenone has been manipulated to form various derivatives which provide scope for polymerisation. However, as of the preparation of this thesis, the use of unmodified levoglucosenone as a monomer for the synthesis of polymers remains unreported. This chapter outlines our discovery and characterisation of a polymer prepared directly from levoglucosenone which we have described as "poly-Cyrene". Herein we report the direct (one-step) and operationally simple polymerisation of LGO that provides a highly sustainable method for polymer synthesis. Specifically, the ability of LGO to act as an electrophile has been harnessed so as to deliver high molecular weight polymers (M_n = 235,500 g/mol, Đ = 2.41) possessing excellent thermal stabilities ($T_{D5\%}$ = 249 °C). Furthermore, there is a significant capacity for the effective chemical manipulation of these polymers as exemplified by treatment of them under Baeyer-Villiger conditions, creating a simple and green route to hydrophilic polymers. These one- and two-step transformations provide the most direct route to new, LGO-derived polymer scaffolds yet reported. E-factors of *ca*. 0.012 and atom economies of up to 99% have been realised.

This chapter was submitted to *ChemSusChem* in August 2023, and I am its first and corresponding author. My contribution to the manuscript includes the project design, design of synthetic protocols, purifications, characterisation of resulting materials, data analysis, as well as preparing and revising the manuscript and figures (overall 80%). The unpublished, submitted manuscript is presented here. Luke A. Connal contributed to the project design, design of

synthetic protocols, data analysis and revising of the manuscript and figures. Martin G. Banwell contributed to the project design, data analysis, as well as revising the manuscript and figures.

Introduction

Consumer societies depend upon polymeric materials in essentially all facets of contemporary life. For the most part, the production of these materials relies on non-renewable, petrochemically-derived monomers. While such monomers are relatively cheap, their polymeric derivatives are environmentally persistent, often toxic and lacking any viable end-of-life utility. Furthermore, given the finite availability of petrochemical feedstocks, the costs of such polymers are likely to increase, possibly significantly, over time.

Such challenges could be addressed by using, as chemical feedstocks, renewable platform molecules such as naturally-occurring polymers and their degradation products.[1] Levoglucosenone (LGO, **1**) (**Figure 1**), a lower molecular weight compound formed by the pyrolysis of cellulose waste, is one such platform molecule and is currently produced in >5,000 tonne quantities annually[2] It has been explored extensively as a chiral auxiliary[3] and chemical building block[4,5] while its hydrogenation product dihydrolevoglucosenone (a.k.a. Cyrene™) is now a commercially available solvent.[6]

Levoglucosenone (**1**) is known to undergo intermolecular self-addition on treatment with aqueous base (typically triethylamine or potassium carbonate) to form the dimer **2** as well as two structurally distinct trimers **3** and **4** (**Figure 1**).[7] During our previous work concerned with effecting a 1,3-carbonyl transposition within LGO (**1**) so as to generate the pseudo-enantiomer *iso*-levoglucosenone (**5**),[8] we observed that when the former compound was treated, at ambient temperatures, with 0.1 equivalents of triethylamine in water then the desired hydration product

6 was accompanied by the dimeric side-product **2** (*ca.* 0.5% yield). Interestingly, Diot-Néant *et al.* have optimised the synthesis of this dimer and exploited it, through functional group manipulations then cross-linking using diacyl chlorides, in the formation of new polymers.[10]

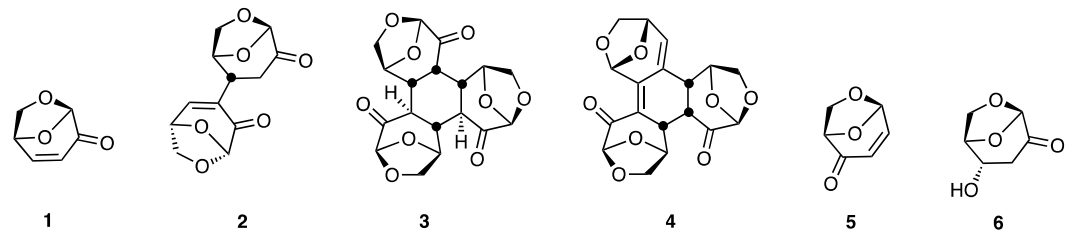

Figure 1: The structures of levoglucosenone (LGO, **1**), the derived dimer **2** and trimers **3** and **4** as well as *iso*-levoglucosenone (*iso*-LGO, **5**) and that of the product, **6**, arising from conjugate addition of water to LGO in the presence of triethylamine. The structures of compounds **2**, **3** and **4** have been confirmed by single-crystal X-ray analysis.[6,7,8]

The dimerisation process leading to compound **2** involves a vinylogous Morita-Baylis-Hillman (MBH) or Rauhut-Currier (RC) reaction.[11] Such reactions are known for their high atom-efficiencies and excellent rates of conversion when they are effected (catalysed) using organophosphines such as tributylphosphine. On the other hand, MBH reactions are most often effected using 1,4-diazabicyclo[2.2.2]octane (DABCO) as a catalyst.[12] Accordingly, we anticipated that treating the monomer LGO with either of these catalysts, rather than triethylamine, under solvent-free conditions or in a suitable polar, aprotic solvent, could promote sequential RC processes and so afford, for the first time, and in a direct and atom-economic fashion, oligo- or poly-meric products. The realisation and extension of such outcomes are reported below and thus provide a new and exceptionally efficient means for the sustainable formation of novel polymers from an abundant and bio-mass derived platform molecule.

Results and Discussion

Screening Suitable Bases for the Polymerisation of LGO (1)

Treating neat LGO with DABCO, the "traditional" MBH catalyst, only led to the formation of the previously observed dimer (**4**) and two trimers (compounds **5** and **6**) – *viz.* no polymerisation was observed. Since 1,8-diazabicyclo[5.4.0]undec-7-ene (DBU) has been described as the "optimum catalyst" for the MBH reaction[13] the use of this was investigated. In the event, on adding, at ambient temperatures, DBU (a liquid) to neat LGO (also a liquid) then an exothermic reaction took place and this was accompanied by rapid solidification (within 30 seconds) and so leading to the formation of an amber and semi-crystalline material that could contain "poly-Cyrene" (**7**) (***Upper Section***, **Figure 2**). This material was soluble in *N,N*-dimethylacetamide (DMAc) and the resulting solution was subjected to gel-permeation chromatographic (GPC) analysis. Polymer formation was evident although with high dispersity ($Đ \approx 30$).

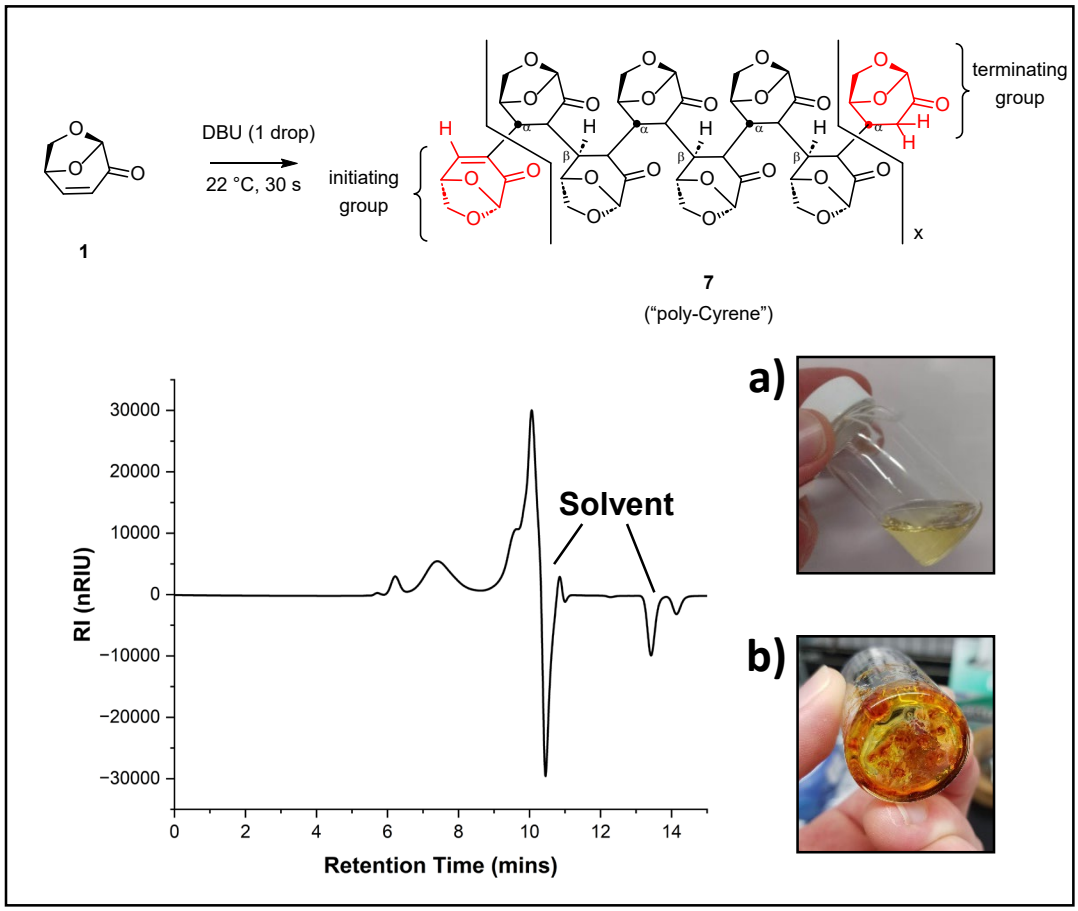

Figure 2: ***Upper Section***: Proposed structure of "poly-Cyrene" (**7**) derived from treating LGO (**1**) with catalytic quantities of DBU at *ca*. 22 °C for 30 s; ***Lower Section***: Gel permeation chromatogram recorded on the crude reaction mixture (*N,N*-dimethylacetamide used as eluting solvent); ***Insets***: ***(a)*** photograph of the starting levoglucosenone and, ***(b)***, photograph of the crude polymerisation product.

The use of tributylphosphine (Bu_3P), regarded as the premier RC catalyst, was also investigated as an agent for promoting the polymerisation of LGO and at loadings as low as 2 mol% a violent and highly exothermic reaction took place with accompanying solidification. However, ^1H NMR spectroscopic analysis of the resulting material revealed that very little polymer formation had occurred (<5%). Given this result, the increased toxicity, air-sensitivity and malodour associated with Bu_3P as well as its expense (Bu_3P costs roughly twice as much as DBU) we abandoned further studies of its use in the present setting.

In order to gain insights into how the above-described polymerisation process might be proceeding, a series of ^{1}H NMR spectroscopic experiments was conducted using a 4.5 M solution of LGO in $(CD_3)_2SO$ that had been treated, at *ca*. 22 °C, with DBU (8 mole %). Spectra were recorded at t = 0, 1, 20, 40, 60, 80, 100 and 340 min. Over time, the two distinct resonances associated with the alkenic protons in substrate **1** [H_A: δ 7.51 (dd, *J* =10.0, 4.7 Hz, 1H), H_B: δ 6.09 (d, *J* = 10.0 Hz, 1H] began to broaden as chain propagation commenced and then these signals eventually disappeared (**Figure 3**). Attending this process was the gradual emergence, at δ 7.00 ppm (s), of a distinct resonance that could be attributed to the olefinic proton $\mathbf{H_G}$ of the new alkene residue associated with the initiating groups of the "poly-Cyrene" chains and that is formed when the β-located and catalysing DBU is eventually eliminated. This signal is reminiscent of that due to the alkene-associated proton present in dimer **4**.[9] Significantly, other signals characteristic of this dimer were not observed in the reaction mixture and so reinforcing the notion that oligomers and polymers are the major products being formed in this DBU-catalysed process.

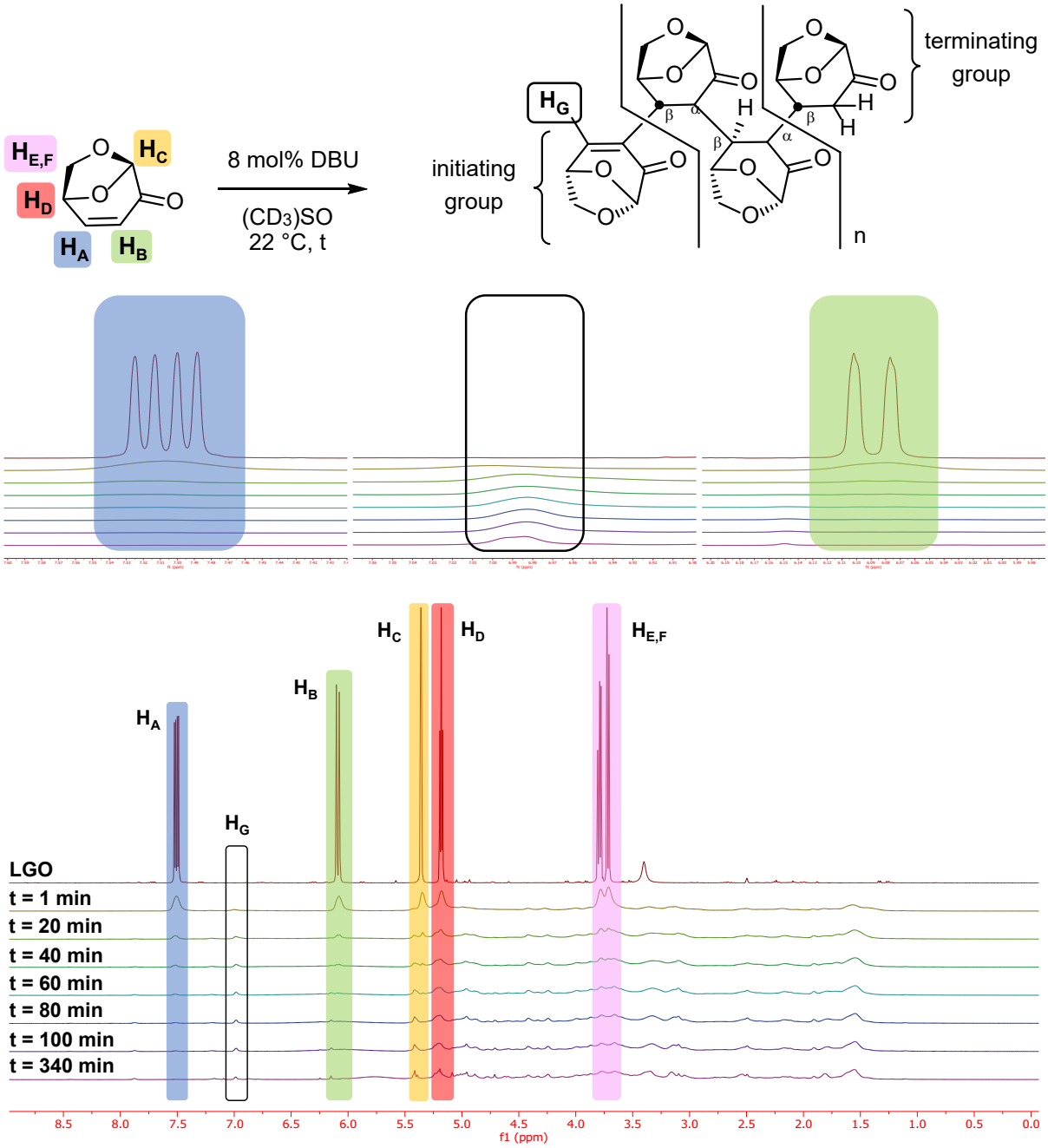

Figure 3: Stacked ^{1}H NMR spectra, recorded at regular intervals, of the reaction mixture obtained on treating, at 22 °C, a 4.5 M solution of LGO in $(CD_3)_2SO$ with 8 mol% DBU.

It is worth noting, at this point, that the pseudo-enantiomer of LGO, namely *iso*-levoglucosenone (**5**),[9] failed to undergo polymerisation under any of the conditions investigated. Such outcomes are consistent with previous observations[9] that the latter compound does not undergo conjugate hydration or form dimers upon treatment with base, a

feature attributed to the significantly lower dipole moment of this compound compared to that of levoglucosenone (2.09 and 4.69 Debye, respectively). This results in a markedly different reactivity profile including it being a weaker Michael-acceptor.[9]

Identifying a Suitable Solvent for Polymerisation of LGO (1)

One possible mechanism by which DBU catalyses the polymerisation of LGO (**1**) is shown in **Scheme 1**. Thus, this adds as a nucleophile and in a conjugate manner to the substrate **1** with the ensuing enolate anion **8** adding in a second Michael addition process to another molecule of LGO and this taking place at the α-face (*viz*. that face opposite to the anhydro-bridge).[7] The ensuing adduct **9** may, in an overall sense, either eliminate the elements of DBU to form the LGO-Cyrene dimer **2**, or, under the conditions defined above, continue to add, presumably with high degrees of stereoselectivity, to further molecules of LGO and so eventually delivering oligomers and polymers of the general form **7** and of (presumably) well-defined configuration (**Scheme 1**). Chain-termination would involve enolate protonation while the initially introduced DBU residue could also be removed in an E1cb process that re-establishes the C-C double bond at the "starting- or initiating-end" of the polymer chain. Regardless of the detail, with DBU having been identified as a particularly effective catalyst, optimising the reaction conditions for the polymerisation of LGO was pursued. In particular, the identification of a solvent that would facilitate mixing and so improve the dispersity of the product polymer was prioritised.

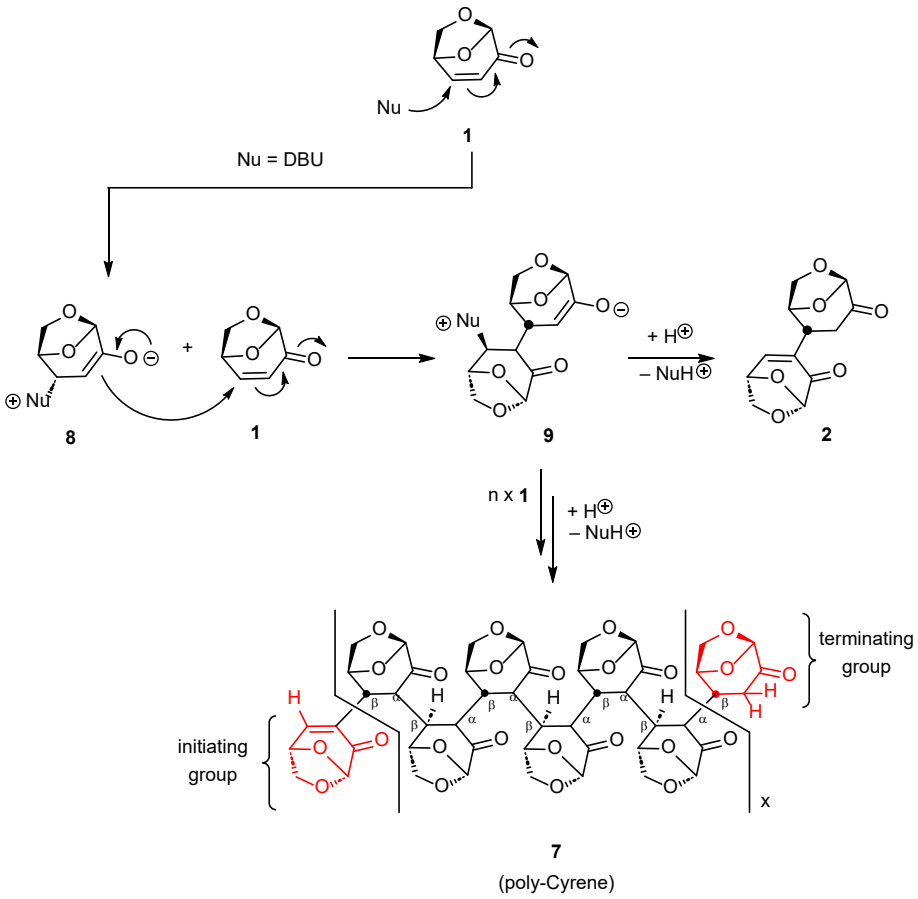

Scheme 1: A Rauhut-Currier type pathway for the conversion of LGO (**1**) into "poly-Cyrene" (**7**)

Based on the proposed mechanism of polymerisation (**Scheme 1**), it was expected that a polar, aprotic solvent would best facilitate polymerisation by suppressing chain-termination through protonation. A seemingly obvious solvent choice was the levoglucosenone-derived Cyrene®, a "green", polar and notionally aprotic solvent[14] that embodies the same heterocyclic framework as levoglucosenone (**1**) but lacking the alkene residue. However, attempts to effect such a conversion with a 9.5 M solution of compound **1** in Cyrene® at 90 °C and using DBU (8 mol%) failed to afford any polymer. Rather, the solvent appeared to undergo a self-aldol condensation,[15] generating an insoluble mixture of complex products, the components of which were not characterised. Acetone, which is considered a non-toxic, affordable and "green" solvent,[16] was next explored but under the conditions initially used (0.08 M LGO maintained at 22 °C and containing 0.2 mol% DBU) no polymerisation took place (as determined by GPC).

In contrast, upon increasing both the catalyst loading (to 8 mol%) and the concentration of LGO (to 9.5 M)[9,16] as well as performing the reaction at elevated temperature and pressure (90 °C, sealed tube) then an immediate reaction was observed. After 21 h a product mixture comprised of a dark-brown solution and a tan precipitate was obtained. The product was precipitated in chilled water (5 °C) and the tan powder thus obtained, after gravity filtration, in 76% overall yield. The product showed sparing solubility but was able to be characterised *via* GPC after being dissolved in DMAc. GPC analysis of this powder revealed multimodal peaks. Considering these as a single distribution gave a M_n of 30,400 Da and an improved but still high dispersity (Đ = 8.54). However, on separating this distribution into distinct peaks, various individual distributions were identified (**i** M_n = 1,208,600 Da, Đ = 1.49; **ii** M_n = 26,900 Da, Đ = 3.56; and, **iii** M_n = 3,600 Da, Đ = 1.05) (for a full range of GPC traces arising from the present study see **Figures S1-S12** in the Supporting Information).

While environmentally problematic, dichloromethane is a classic polar, aprotic solvent that was expected to enhance the polymerisation of LGO over that seen in acetone. Indeed, in all experiments, dichloromethane gave improved dispersities and, on average, higher molecular weights when compared to the corresponding processes carried out in acetone. In test conditions identical to those described above in dichloromethane (*viz*. 9.5 M LGO, 8 mol% DBU, sealed tube, 90 °C, 21 h) resulted in quantitative polymer formation (M_n = 277,900 Da) and, when considering the multimodal distribution as a single peak, significantly improved dispersity (Đ = 3.93). Given these results, the remaining experiments associated with the present study were conducted in anhydrous dichloromethane. Notably, provided dry solvents were employed, it was found that there was no measurable difference in product characteristics or yield when these reactions were carried out either under an inert atmosphere (using nitrogen or argon) or in the presence of air.

Characterisation of the "Poly-Cyrene" Product

In addition to analysing the "poly-Cyrene"-type product **7** by ^{1}H and $^{13}C\{^{1}H\}$NMR spectroscopies (see **Figure 3** and **Figures S13-S16**), Fourier transform infrared (FT-IR) techniques were also used. As shown in **Figure 4a** (also see **Figure S19**), the C=O stretching bands in monomer **1** (shown in black) appear at 1716 and 1694 cm^{-1} while their counterparts in "poly-Cyrene" (**7**) appear, as shown in blue, at 1734 and 1697 cm^{-1}. These splittings of the carbonyl absorptions are attributed to the distinct dipole-dipole interactions between the ketone carbonyl moiety and the conformationally locked equatorially- and axially-oriented C-O bonds of the adjacent, internal acetal. This increase in wavenumber is consistent with the loss, on polymerisation of **1**, of the α,β-alkene unit and matches our prior observations of the conversion of LGO into dimer **4**.[9]

Thermogravimetric analysis (TGA) of "poly-Cyrene" revealed it possesses excellent thermal stability with a mere 5% weight loss ($T_{D5\%}$) occurring at 249 °C and with the $T_{D50\%}$ value being above 400 °C (**Figure 4b**). Differential scanning calorimetry (DSC) revealed an exotherm at 235 °C [this being the inflection point as determined by taking the first derivative of the associated curve (**Figure 4c**)]. This closely matches the TGA result, as does the second inflection point observed in the DSC study. "Poly-Cyrene" (**7**) did not appear to exhibit a glass transition below the decomposition temperature. GPC analysis of the material obtained when the polymerisation reaction was performed in dichloromethane at 90 °C for 30 h with an 8 mol% DBU loading reveals a multi-modal distribution (**Figure 4d**). When analysed as a single peak, this gave a M_n of 246,000 Da and a dispersity of 4.18 (**Figure S4**) Attempts to separate the polymeric chains of individual distributions by fractional precipitation were unsuccessful.

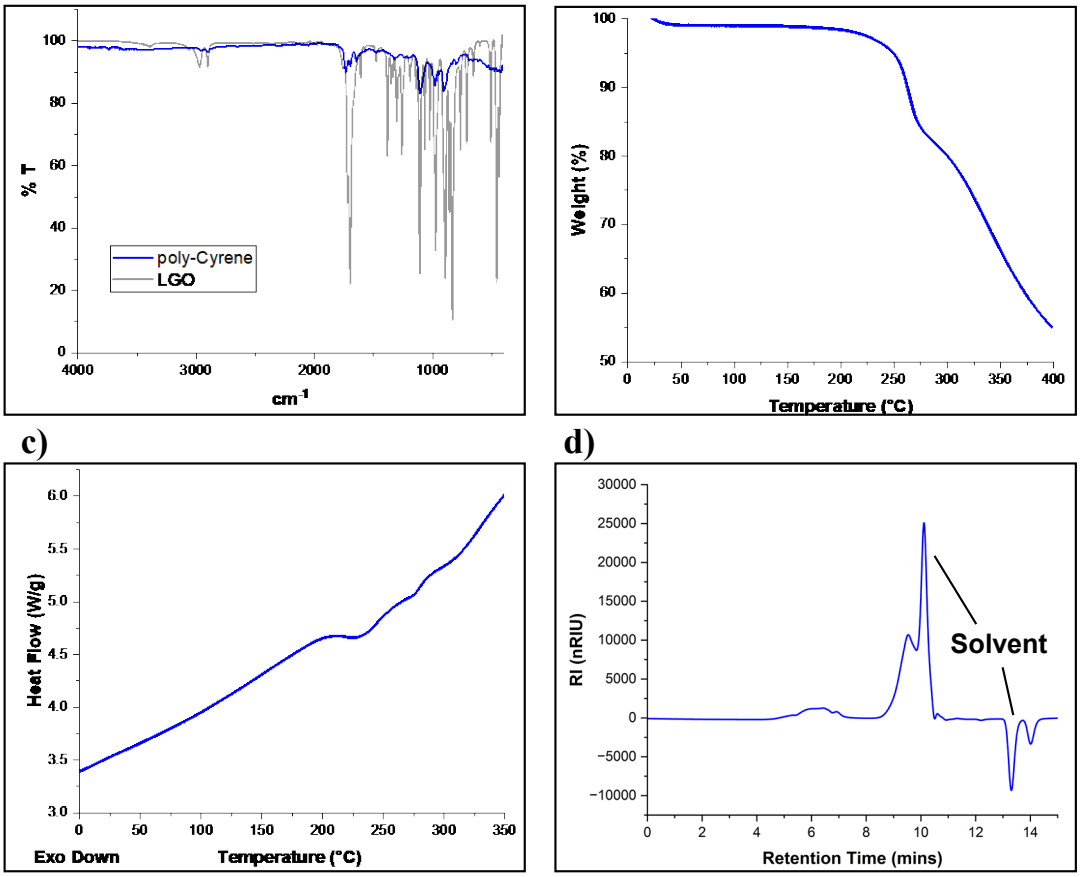

Figure 4: a) Superimposed FT-IR spectra of "poly-Cyrene" (**7**) (blue) and LGO (**1**) (black), **b)** TGA curve recorded for "poly-Cyrene" showing a $T_{D5\%}$ of 249 °C, **c)** DSC curve obtained for "poly-Cyrene", **d)** Exemplar GPC trace for the precipitated poly-Cyrene sample obtained under the following conditions: [LGO] = 9.5 M, CH_2Cl_2, 0.08 mol% DBU, 30 h, 90 °C. On interpretation as a single peak this gives M_n = 246 kDa, Đ = 4.18.

"Poly-Cyrene" (**7**) is freely soluble in dimethyl sulfoxide (DMSO) at room temperature (450 g/L, 22 °C) and when the resulting solutions are dried (at *ca.* 60 °C) then reflective/glassy but brittle films are obtained (**Figure 5**). These proved too fragile for any meaningful mechanical analyses.

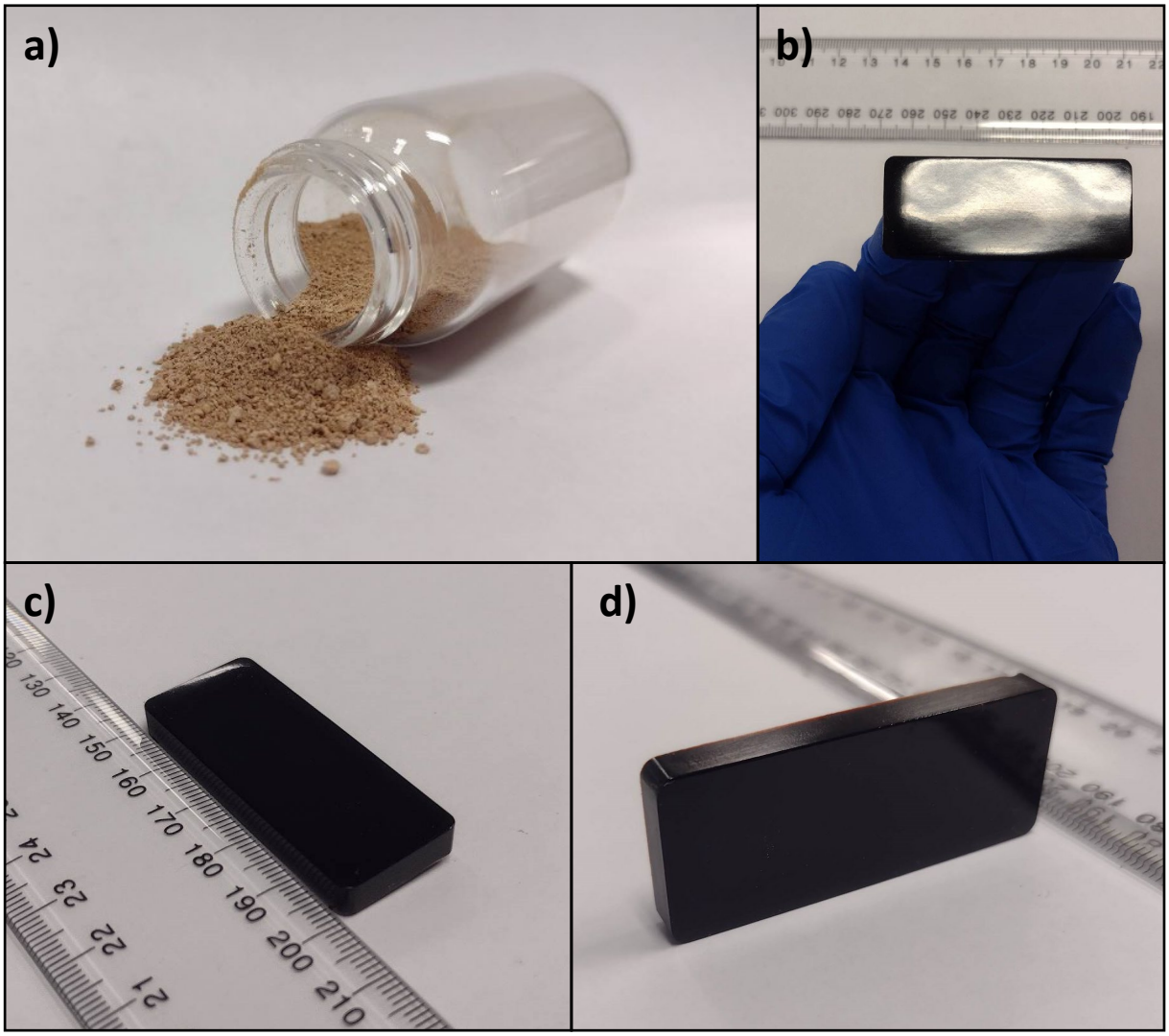

Figure 5: "Poly-Cyrene" films afforded by dissolving the material in DMSO then evaporating the resulting solution at 60 °C: **a)** powdered "poly-Cyrene" obtained by precipitation, filtration and drying, **b)** a film of "poly-Cyrene" showing the reflective surface, **c)**, **d)** two distinct views of the same poly-Cyrene "film" – dimensions: 50 × 20 mm, mass = 3.60 g.

Effect of Reaction Time and Catalyst Loading on the Polymerisation of LGO

While keeping all other reaction conditions constant (*viz*. using a *ca*. 9.5 M solution of LGO in dichloromethane contained in a sealed tube, a DBU loading of 8 mol% and heating at 90 °C) variations in reaction time were explored while all workups were conducted under the same conditions as defined previously, namely precipitating the product using chilled, poor solvent (in this case methanol) then collecting the solid product by filtration and thoroughly drying this. The outcomes of the relevant series of experiments are shown in **Table 1**. After 4 h (Entry **a**) a

lower conversion (85%) was observed and affording a lower molecular weight (M_n = 61,600) but higher dispersity (Đ = 9.91) product (**Figure S2**) as compared to the outcome obtained after 21 h (Entry **b**) (100% conversion, M_n = 277,900 Da, Đ = 3.93) (**Figure S3**). A longer reaction time (30 h, Entry **c**) afforded higher molecular weight material (M_n = 246,000 Da, Đ = 4.18) at a similar (84%) conversion (**Figure S4**). On employing a reaction time of 69 h (Entry **d**) a notable reduction in product recovery (73%) was observed, lower molecular weight material (82,600 Da) was obtained and this was of significantly higher dispersity (Đ = 8.43) (**Figure S5**).

Table 1: Impacts of reaction time and catalyst loading on average molecular weight (M_n), dispersity and yield of polymeric product.[A]

Entry	Reaction Time (h)	Catalyst Loading (mol%)	Recovery/Conversion (%)	M_n (Da) [B]	Dispersity (Đ) [B]
a	4	8	85	61,600	9.91
b	21	8	100	277,900	3.93
c	30	8	84	246,100	4.18
d	69	8	73	82,600	8.43
e	21	4	100	139,900	3.32
f	21	2	83	235,500	2.41
g	21	1	81	166,600	2.96

[A] All reactions were performed at 9.5 M concentration of LGO in dichloromethane in a sealed tube heated to 90 °C; [B] average molecular weight (M_n) and dispersity (Đ) were calculated using standard gel permeation chromatographic techniques.

Contrary to expectations, it is clear that the quality of the polymeric product diminishes with increased reaction time as evident by the sharp decrease in M_n and elevated dispersity of the product obtained after 69 h. Such an outcome could be due to the *in situ* precipitation of higher molecular weight products, these proving to be extremely difficult to transfer and so reducing the overall yield as well as preventing the higher molecular weight products being accessible to GPC analysis.

It was anticipated that reducing the catalyst loading would result in fewer propagating chains and so, theoretically, both increasing the molecular weight and decreasing the dispersity of the

resulting polymer, albeit at the expense of a reduced rate of reaction. However, as the results shown in latter parts of **Table 1** reveal, there is no clear trend observed in either molecular weight or dispersity over the catalyst loading range of 1 – 8 mol% (Entries **b**, **e – g**). The lowest measured M_n value derives from material generated using a 1 mol% catalyst loading (Entry **g**), an outcome attributed to the generation of longer, ultimately insoluble chains that are excluded (by filtration) from the GPC analysis (see **Figure S8**). This may influence the conversion rate as well, which fell from 100% at 4 and 8 mol% loadings (Entries **b**, **e**) to 81 – 83% at 1 and 2 mol% loadings (**f**, **g**), respectively.

Manipulation of the "poly-Cyrene" Scaffold: Baeyer-Villiger Oxidation

To enhance the utility of the above-reported polymerisation process, the product "poly-Cyrene" was oxidised under Baeyer-Villiger conditions similar to those described, as shown in **Scheme 2**, by Diot-Néant *et al*[17] for the conversion of dimer **2** into 2*H*-HBO-HBO (**10**).

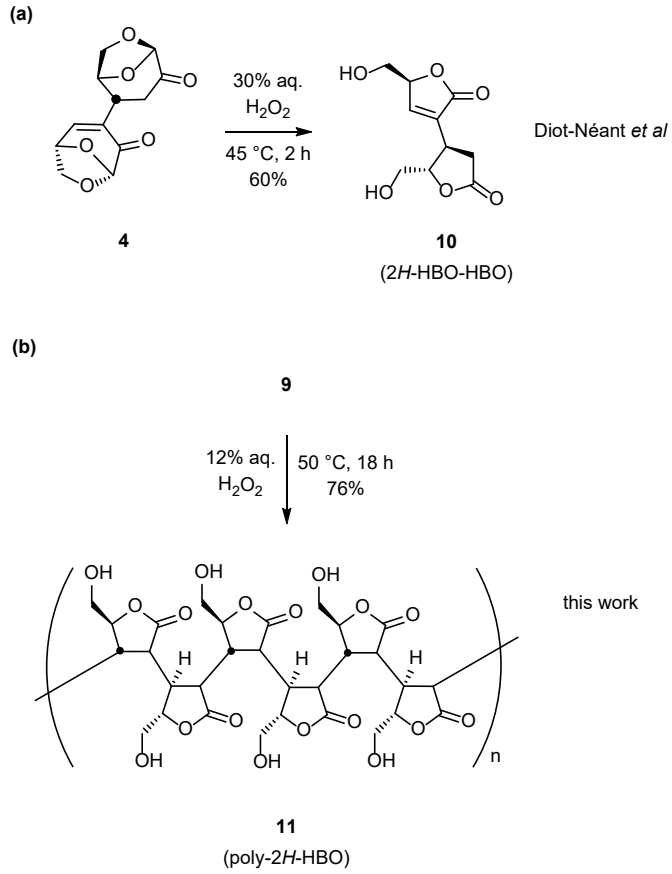

Scheme 2: (a) The reported conversion of dimer **2** into 2*H*-HBO-HBO (**10**) under Baeyer-Villiger conditions and, **(b)**, the analogous conversion of "poly-Cyrene" (**7**) into poly-2*H*-HBO (**11**) (possible capping groups not shown).

Despite "poly-Cyrene" being very hydrophobic and insoluble in water, when it was added to a magnetically stirred solution of 12% *v/v* aqueous hydrogen peroxide solution that was then heated at 50 °C, the initial suspension of the tan-coloured substrate was rapidly bleached prior to its dissolution that delivered a clear, yellow solution (**Figure 6a to 6c**). After workup (see Experimental Section for details), an off-white and porous product was formed and this proved to be highly water soluble (*ca.* 850 mg/mL) but insoluble in methanol, acetone or ethyl acetate. This product is believed, based on various studies of it as detailed below, to be a hydroxymethylated polylactone or "poly-2*H*-HBO", possibly of the form **11**.

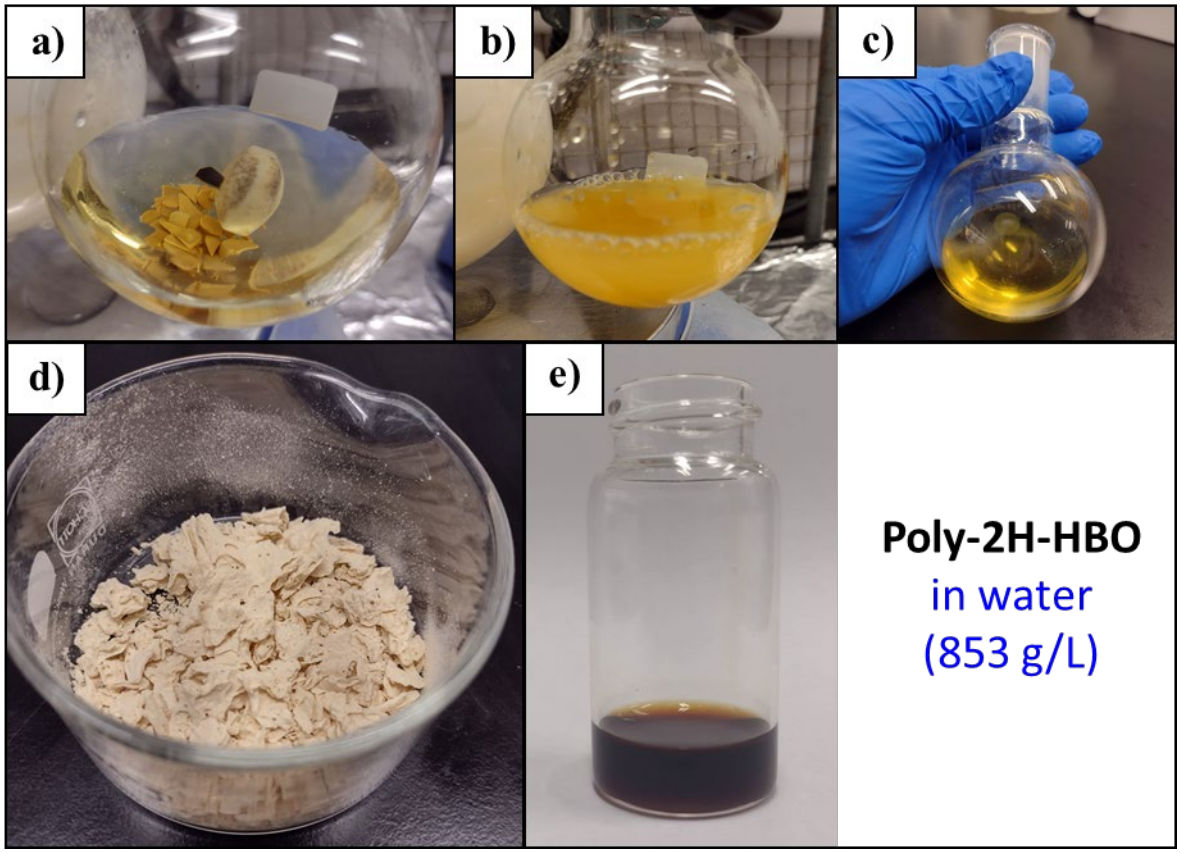

Figure 6: The Baeyer-Villiger oxidation of "poly-Cyrene": **(a)** the suspension of "poly-Cyrene" in 12% *v/v* aqueous hydrogen peroxide after heating at 50 °C for 0.5 h and showing the bleaching of starting material; **(b)** the reaction mixture after 4 h and during which time with some gas evolution was observed; **(c)** after 18 h at which time a clear, light-yellow solution was obtained; **(d)** the porous product obtained after workup and drying, and; **(e)** a saturated solution of poly-2*H*-HBO comprising 1.80 g of this material in 2.11 mL of water.

FT-IR spectroscopic analysis of poly-2*H*-HBO revealed (**Figure 7a** and **Figure S20**) a strong and broad –OH stretching band at 3357 cm^{-1} while carbonyl stretching bands are now observed at 1753 and 1711 (shoulder) cm^{-1}, the former being indicative of a γ-lactone.

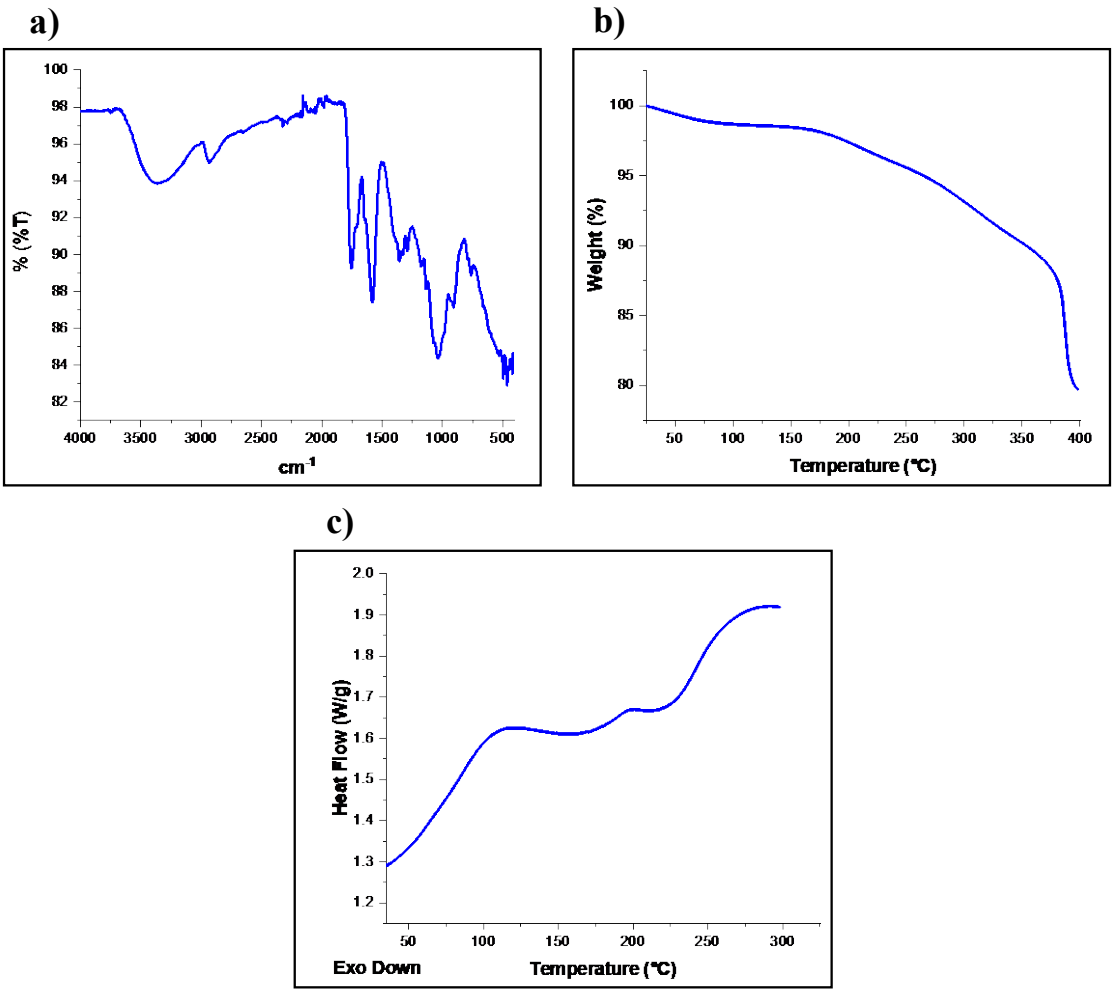

Figure 7: Characterisation of the poly-2*H*-HBO material **11** prepared by Baeyer-Villiger oxidation of poly-Cyrene (**9**): **(a)** FT-IR spectrum of poly-2*H*-HBO; (**b)** TGA curve derived from the thermal decomposition of poly-2*H*-HBO showing $T_{D5\%}$ = 265 °C; (**c)** DSC trace acquired on poly-2*H*-HBO showing exotherms.

As was the case with the precursor "poly-Cyrene" (**9**), TGA studies conducted on the derived poly-2*H*-HBO (**Figure 7b**) revealed that it, too, displayed good thermal stability. Indeed polymer **11** was marginally better with a $T_{D5\%}$ value of 265 °C and a $T_{D50\%}$ value again exceeding 400 °C. DSC analysis (**Figure 7c**) revealed two exotherms, the first with an inflection point at 114 °C and the second at 200 °C. As with "poly-Cyrene", no distinctive glass transition temperature was observed below the decomposition temperature, this being consistent with the crystalline nature of the material. Attempts to analyse poly-2*H*-HBO using

GPC techniques proved unsuccessful, an outcome attributed to the high degree of hydrogen bonding present in the polymer and so significantly skewing the data and providing inconsistent results.

The 400 MHz ^{1}H NMR spectrum of poly-2*H*-HBO (**11**) (**Figure S17**) embodied a series of very broad and overlapping resonances within the 5.50 – 3.00 ppm chemical shift range and so making specific assignments challenging. Nevertheless, a comparison of these data with those derived from the previously reported 2*H*-HBO-HBO dimer was informative.[18] In particular, and consistent with expectations and the literature, the intense signal centred at δ 3.51 is assigned to those protons associated with the new linkages formed by the oxidation reaction while the very weak one centred at δ 6.76 is attributed to the olefinic proton associated with an end-group alkene moiety.

Conclusions

A novel, facile, one-step, atom-economic and high-yielding conversion of the biomass-derived and homochiral levoglucosenone (**1**) into a high molecular weight and chemically modifiable "poly-Cyrene" scaffold is described. Furthermore, this polymer, which displays excellent thermal stability, is itself efficiently transformed into a poly-2*H*-HBO scaffold *via* a Baeyer-Villiger oxidation conducted in water under catalyst-free conditions. This second polymer is, unlike its precursor, water-soluble and offers the potential for further manipulation. Such highly efficient polymerisations of sustainably-produced platform molecules offer excellent substitutes or replacements for their petrochemically-derived counterparts and so providing direct access to a family of new and distinctly "green" materials.

Experimental Section

Chemicals and Reagents: Starting materials and reagents were generally available from Sigma-Aldrich, Merck, TCI, Strem or Lancaster Chemical Companies and were used as supplied. Drying agents and other inorganic salts were purchased from the AJAX, BDH, Chemsupply or Unilab Chemical Companies. Methanol and dichloromethane were dried using a Glass Contour solvent purification system that is based upon a technology originally described by Grubbs *et al.*[19] *iso*-Levoglucosenone (**2**) and the LGO-Cyrene dimer (**4**) were prepared as previously reported. [9,20] Where necessary, reactions were performed under an inert atmosphere.

Characterisation: Unless otherwise specified, proton (^{1}H) and carbon (^{13}C) NMR spectra were recorded at 22 °C in $(CD_3)_2SO$ on a Varian spectrometer operating at 400 MHz for proton and 100 MHz for carbon nuclei. For ^{1}H NMR spectra, signals arising from the residual protio-forms of the solvent were used as the internal standards. The signal due to residual DMSO appearing at δ_H 2.50 and the central resonance of the DMSO 'triplet' appearing at δ_C 39.5 were used to reference ^{1}H and ^{13} C NMR spectra, respectively. Infrared spectra (ν_{max}) were recorded on a Perkin-Elmer 1800 Series FTIR Spectrometer. Samples were analysed as thin films on KBr plates. The thermal stabilities of polymers were determined by performing thermogravimetric analyses (TGA) using a Thermal Instruments Q500 machine operating under a nitrogen atmosphere (flow rate of 40 mL/min) and at a heating rate of 3 °C/min. Gel permeation chromatography (GPC) was conducted on an Agilent 1260 Infinity GPC System fitted with a refractive index detector and a PLgel 5 μm MIXED-C 7.5 x 300 mm PL1110-6500 column maintained at 30 °C. *N,N*-dimethylacetamide (DMAc) was employed as the eluting solvent at a flow rate of 1.0 mL/min. The injection volume was 80 μL and molecular weight calibrations were performed with polyethylene oxide/glycol EasiVials® (Agilent Technologies, U.K.) standards that covered an average molecular mass range from 1,576,000 to 106 g/mol.

Differential scanning calorimetry (DSC) was performed using a TA Instruments Q20 machine operating at a heating rate of 3 °C/min. The sample (~8 mg) was pre-treated by being heated at a rapid rate to 120 °C so as to remove any solvent then slowly cooled to room temperature. The data were recorded between –30 °C and 350 °C. Dichloromethane (5.0 mL) then LGO (**1**, 6.00 g, 47.6 mmol) were added to an ACE-glass 15 mL pressure tube [24.5 (o.d.) x 10.2 cm] fitted with a magnetic stirrer bar. The vigorously stirred solution was then treated, dropwise at ambient temperatures (*ca*. 22 °C), with DBU (580 mg, 3.8 mmol, 8 mol%) and thereafter the reaction tube was tightly sealed (using a Teflon screwcap and associated rubber O-ring). The tube and its contents were then immersed in an oil bath maintained at 90 °C (CAUTION: USE BLAST SHIELD). After the relevant time (*e.g.* 21 h) the tube and its contents were removed from the oil bath and cooled to ambient temperatures. Thereafter, the tube was opened and the contents added, with vigorous stirring, to chilled (*ca*. 0 °C) methanol, ethanol or water (300 mL). The resulting tan precipitate was collected by gravity filtration then washed liberally with further volumes of the precipitating medium before being air-dried at *ca*. 22 °C to afford "poly-Cyrene" (**7**, 6.00 g, 100%) as a fine, tan powder. This material could be dissolved in DMSO (*ca.* 450 mg/mL) and the resulting solution allowed to evaporate to dryness at 60 °C and so forming homogenous films. The tan powder had no distinct melting point and was observed to decompose above 250 °C. IR ν_{max} 1716, 1694, 1605, 1474, 1378, 1299, 1255, 1103, 969, 888, 853, 828, 760, 706 cm^{-1} (recorded on the tan powder).

*Synthesis of poly-2*H-*HBO (**11**):* A magnetically stirred suspension of "poly-Cyrene" (**7**, 4.20 g) in water (30 mL purified by reverse osmosis) and maintained at ambient temperatures was treated with hydrogen peroxide (20 mL of a 30% aq. solution). The ensuing mixture was, while left open to the atmosphere, heated at 50 °C (oil bath). Gradually, the tan solid began to dissolve

with the accompanying formation of a clear, light-yellow solution. After 18 h the reaction mixture was cooled, first to ambient temperatures and then to *ca*. 0 °C (ice-bath) before being carefully treated, preferably at 0 °C, with either solid sodium sulfite (stoichiometric quantities) or solid manganese dioxide (100 mg). The ensuing mixture was subjected to gravity filtration and the filtrate then concentrated under reduced pressure (rotary evaporator) to afford poly-2*H*-HBO (**11**) (2.15 g, 84%) as an off-white, porous solid. No distinct m.p., decomposition above 265 °C. ^{1}H NMR [400 MHz, $(CD_3)_2SO$] see **Figure S17**; IR ν_{max} 3356, 2933, 1753, 1711, 1579, 1359, 1323, 1290, 1171, 1133, 1036, 908, 758 cm^{-1}.

Traces Derived from GPC Studies

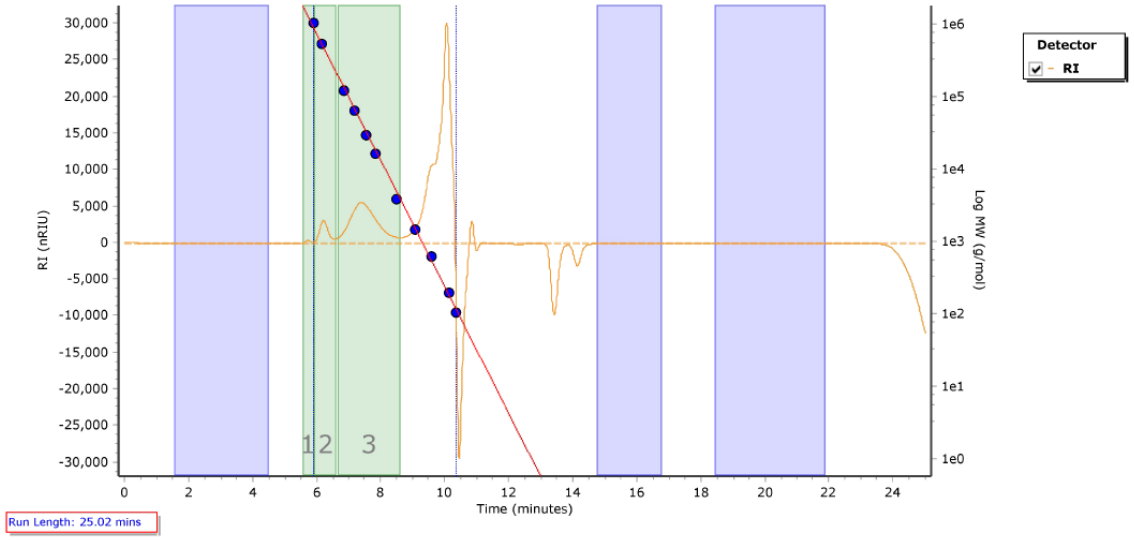

Molecular Weight Averages

Peak	Mp (g/mol)	Mn (g/mol)	Mw (g/mol)	Mz (g/mol)	Mz+1 (g/mol)	Mv (g/mol)	PD
Peak 1	1292927	1169655	1210836	1250137	1286683	1244483	1.035
Peak 2	464551	409937	447558	482342	513788	477459	1.092
Peak 3	42875	22630	45853	73978	100221	70031	2.026

Figure S1: GPC Trace Derived from the Reaction Mixture Obtained on Treating Neat LGO (**1**) with DBU (1 mol %) at 22 °C (*N,N*-dimethylacetamide used as eluting medium).

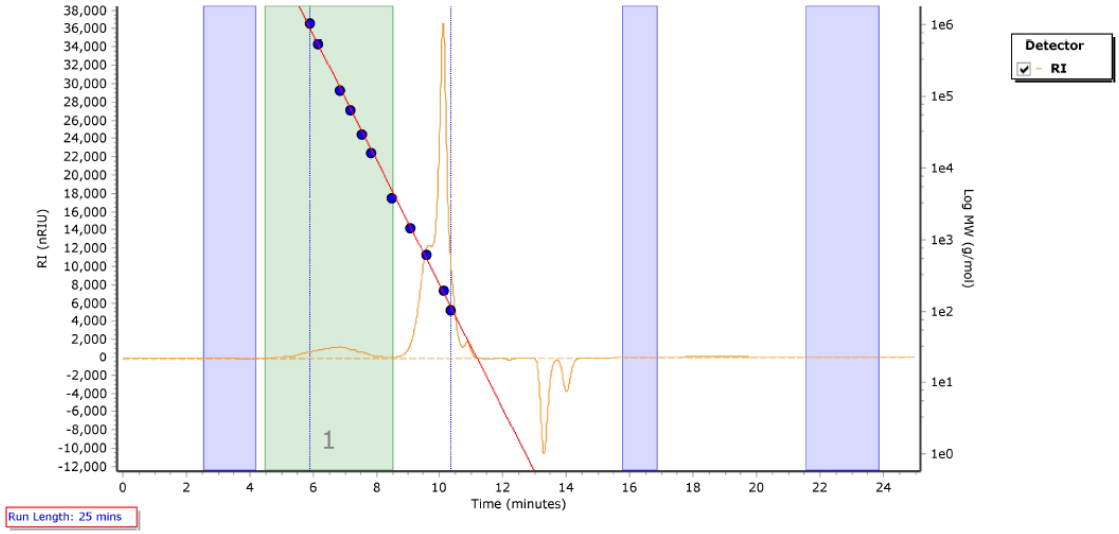

Molecular Weight Averages

Peak	Mp (g/mol)	Mn (g/mol)	Mw (g/mol)	Mz (g/mol)	Mz+1 (g/mol)	Mv (g/mol)	PD
Peak 1	131967	61604	610681	3229289	6211158	2793807	9.913

Figure S2: GPC Trace Derived from the Reaction Mixture Obtained on Treating a 4.5 M Solution of LGO in CH_2Cl_2 with DBU (8 mol %) at 90 °C for 4 h (*N,N*-dimethylacetamide used as eluting medium).

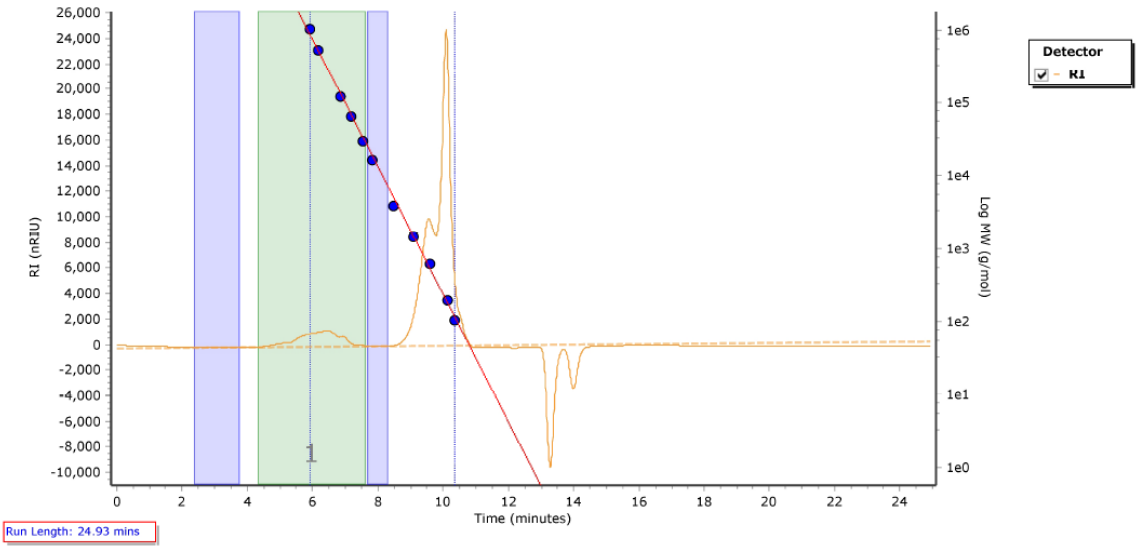

Molecular Weight Averages

Peak	Mp (g/mol)	Mn (g/mol)	Mw (g/mol)	Mz (g/mol)	Mz+1 (g/mol)	Mv (g/mol)	PD
Peak 1	285558	277932	1092721	3895753	7325520	3412497	3.932

Figure S3: GPC Trace Derived from the Reaction Mixture Obtained on Treating a 4.5 M Solution of LGO in CH_2Cl_2 with DBU (8 mol %) at 90 °C for 21 h (*N,N*-dimethylacetamide used as eluting medium).

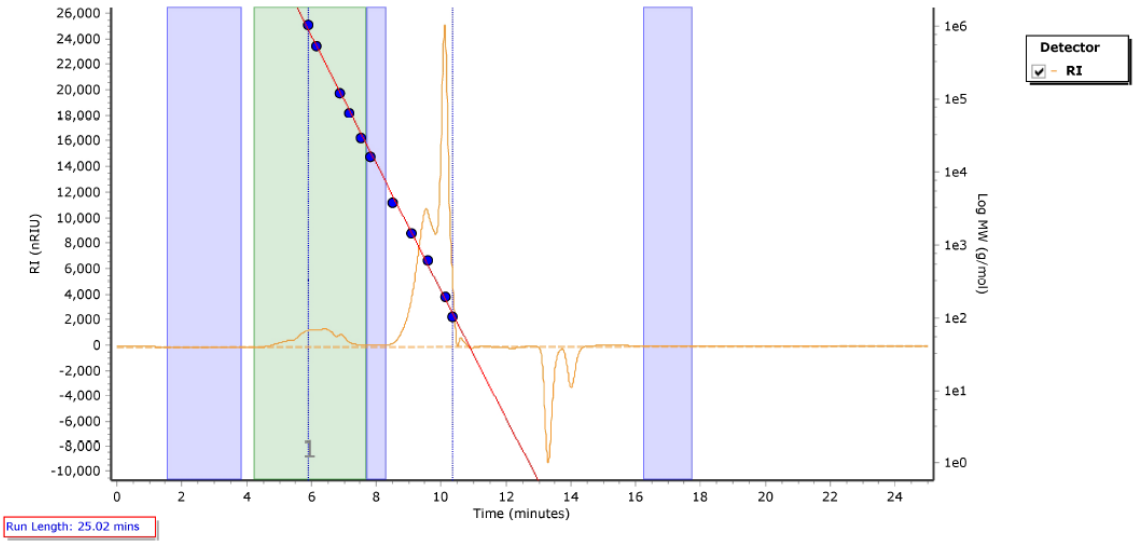

Molecular Weight Averages

Peak	Mp (g/mol)	Mn (g/mol)	Mw (g/mol)	Mz (g/mol)	Mz+1 (g/mol)	Mv (g/mol)	PD
Peak 1	305382	246074	1028208	3303099	5885326	2930978	4.178

Figure S4: GPC Trace Derived from the Reaction Mixture Obtained on Treating a 4.5 M Solution of LGO in CH_2Cl_2 with DBU (8 mol %) at 90 °C for 30 h (*N,N*-dimethylacetamide used as eluting medium).

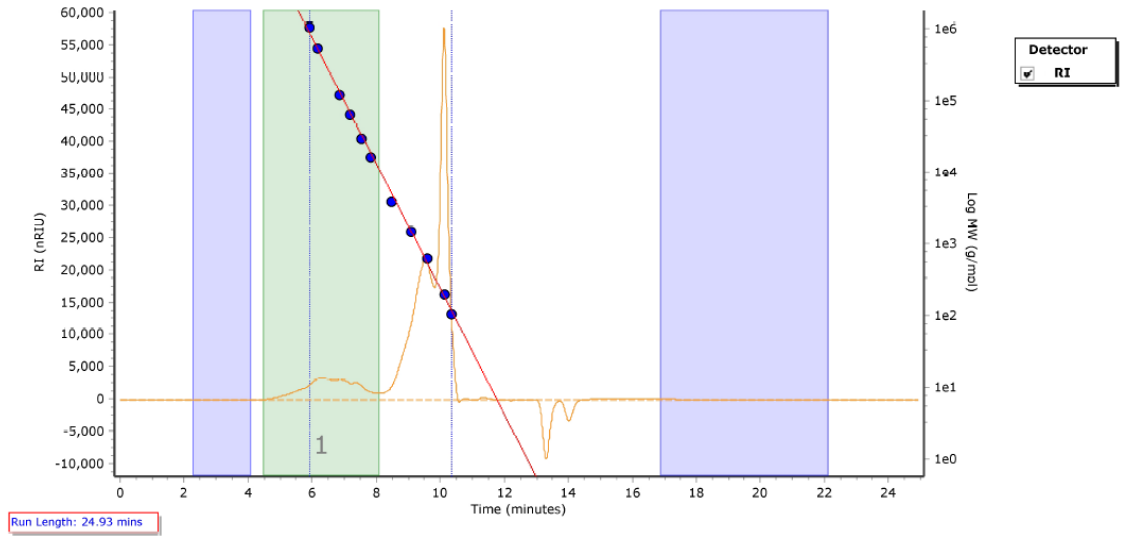

Molecular Weight Averages

Peak	Mp (g/mol)	Mn (g/mol)	Mw (g/mol)	Mz (g/mol)	Mz+1 (g/mol)	Mv (g/mol)	PD
Peak 1	392787	82573	696164	3467432	6815156	3001921	8.431

Figure S5: GPC Trace Derived from the Reaction Mixture Obtained on Treating a 4.5 M Solution of LGO in CH_2Cl_2 with DBU (8 mol %) at 90 °C for 69 h (*N,N*-dimethylacetamide used as eluting medium).

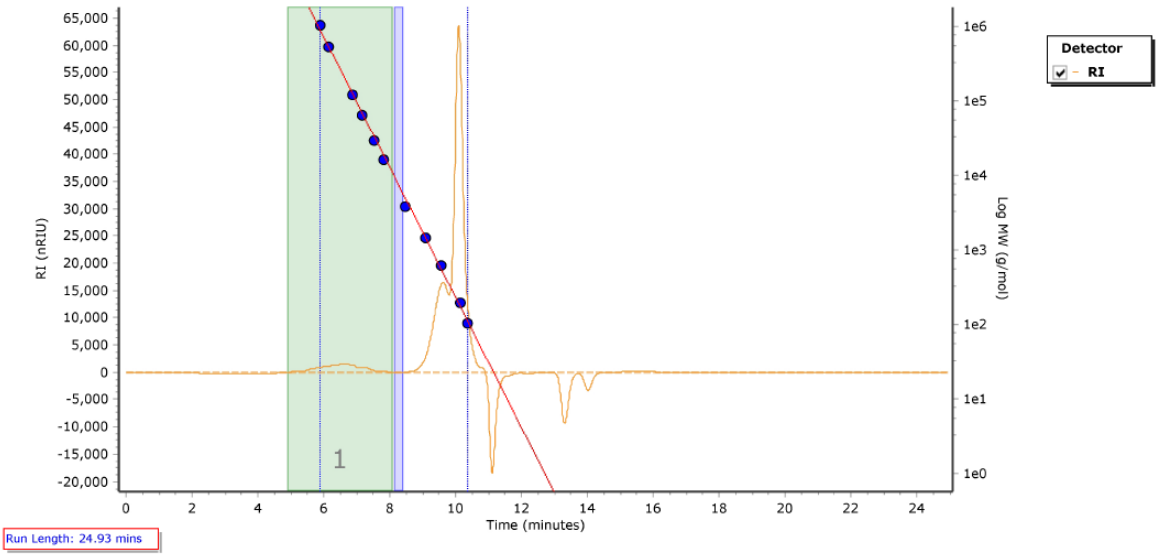

Molecular Weight Averages

Peak	Mp (g/mol)	Mn (g/mol)	Mw (g/mol)	Mz (g/mol)	Mz+1 (g/mol)	Mv (g/mol)	PD
Peak 1	181522	139867	464649	1262891	2293302	1128044	3.322

Figure S6: GPC Trace Derived from the Reaction Mixture Obtained on Treating a 4.5 M Solution of LGO in CH_2Cl_2 with DBU (4 mol %) at 90 °C for 21 h (*N,N*-dimethylacetamide used as eluting medium).

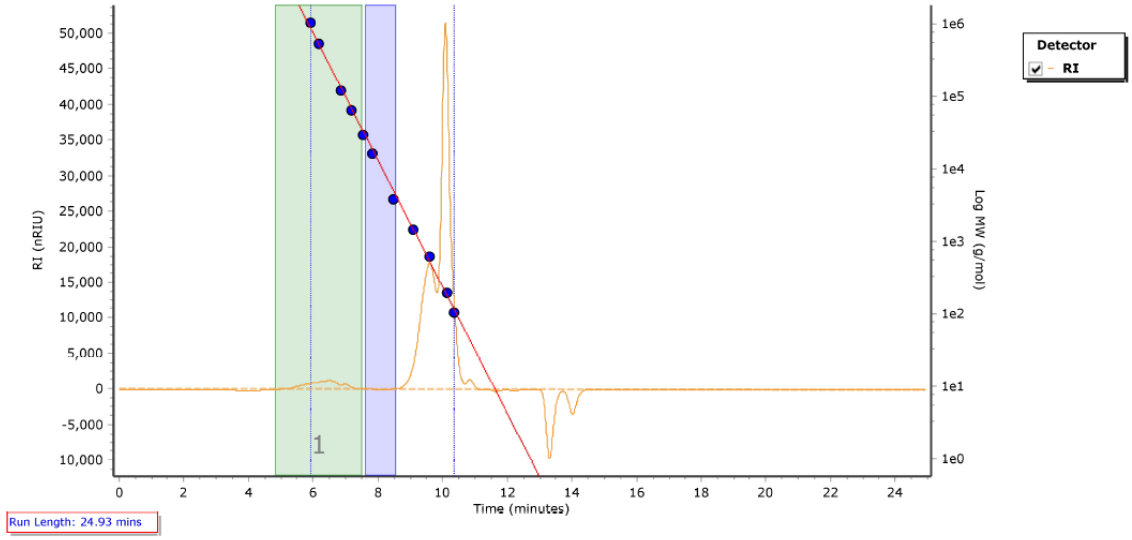

Molecular Weight Averages

Peak	Mp (g/mol)	Mn (g/mol)	Mw (g/mol)	Mz (g/mol)	Mz+1 (g/mol)	Mv (g/mol)	PD
Peak 1	262577	235501	568893	1141884	1680426	1059089	2.416

Figure S7: GPC Trace Derived from the Reaction Mixture Obtained on Treating a 4.5 M Solution of LGO in CH_2Cl_2 with DBU (2 mol %) at 90 °C for 21 h (*N,N*-dimethylacetamide used as eluting medium).

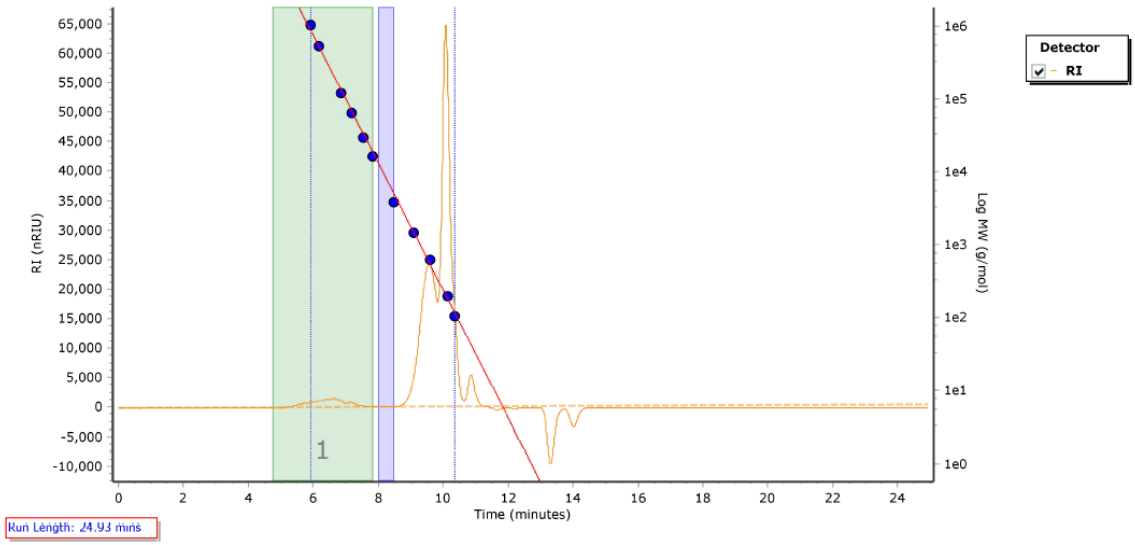

Molecular Weight Averages

Peak	Mp (g/mol)	Mn (g/mol)	Mw (g/mol)	Mz (g/mol)	Mz+1 (g/mol)	Mv (g/mol)	PD
Peak 1	200750	166565	493697	1123378	1717053	1032246	2.964

Figure S8: GPC Trace Derived from the Reaction Mixture Obtained on Treating a 4.5 M Solution of LGO in CH_2Cl_2 with DBU (1 mol %) at 90 °C for 21 h (*N,N*-dimethylacetamide used as eluting medium).

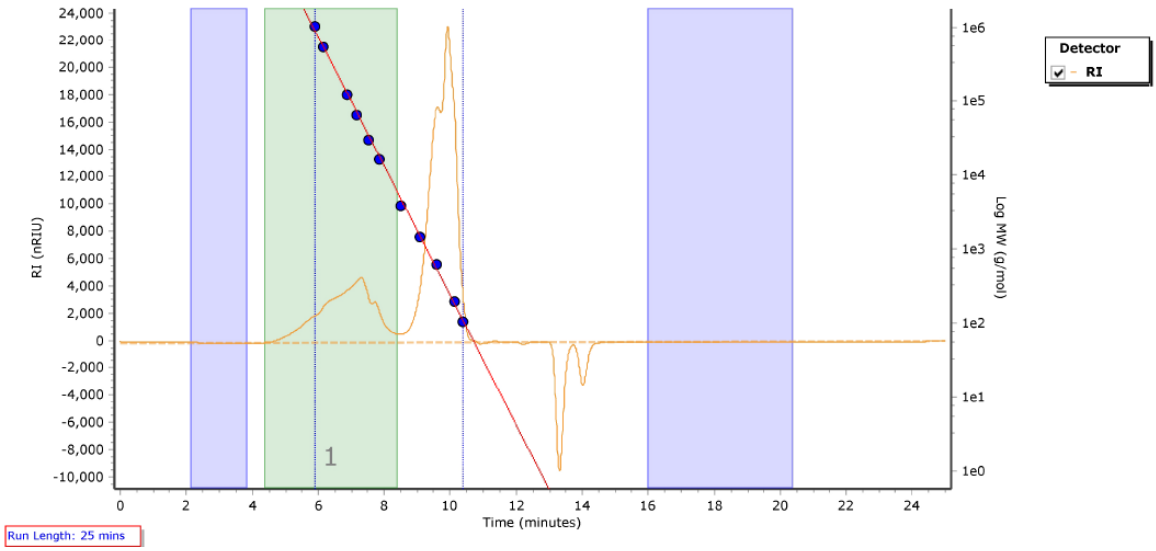

Molecular Weight Averages

Peak	Mp (g/mol)	Mn (g/mol)	Mw (g/mol)	Mz (g/mol)	Mz+1 (g/mol)	Mv (g/mol)	PD
Peak 1	52439	53976	498983	3159943	6675799	2695052	9.245

Figure S9: GPC Trace Derived from the Reaction Mixture Obtained on Treating a 4.5 M Solution of LGO in Acetone with DBU (8 mol %) at 90 °C for 21 h (*N,N*-dimethylacetamide used as eluting medium).

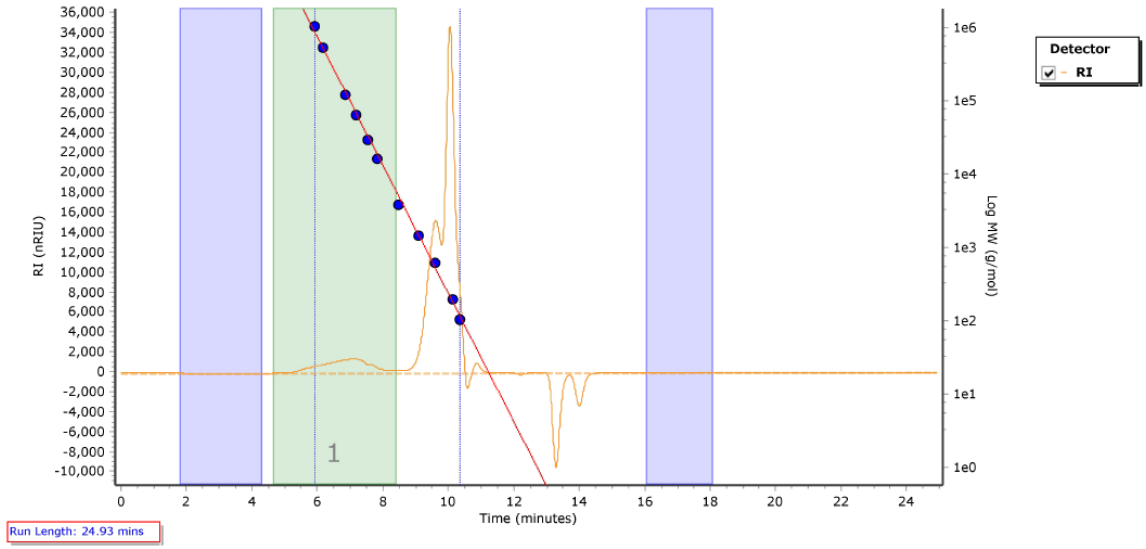

Molecular Weight Averages

Peak	Mp (g/mol)	Mn (g/mol)	Mw (g/mol)	Mz (g/mol)	Mz+1 (g/mol)	Mv (g/mol)	PD
Peak 1	75854	55776	417529	2379173	5207455	2005739	7.486

Figure S10: GPC Trace Derived from the Reaction Mixture Obtained on Treating a 4.5 M Solution of LGO in Acetone with DBU (1 mol %) at 90 °C for 21 h (*N,N*-dimethylacetamide used as eluting medium).

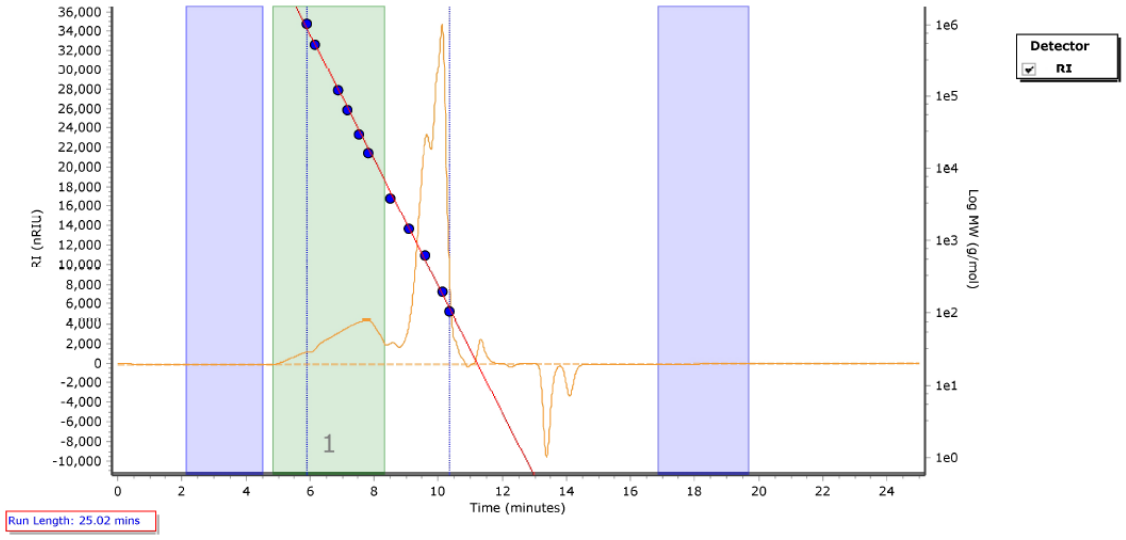

Molecular Weight Averages

Peak	Mp (g/mol)	Mn (g/mol)	Mw (g/mol)	Mz (g/mol)	Mz+1 (g/mol)	Mv (g/mol)	PD
Peak 1	20490	30440	260074	1622240	3058861	1409847	8.544

Figure S11: GPC Trace Derived from the Reaction Mixture Obtained on Treating a 4.5 M Solution of LGO in Acetone with DBU (8 mol %) at 90 °C for 72 h (*N,N*-dimethylacetamide used as eluting medium).

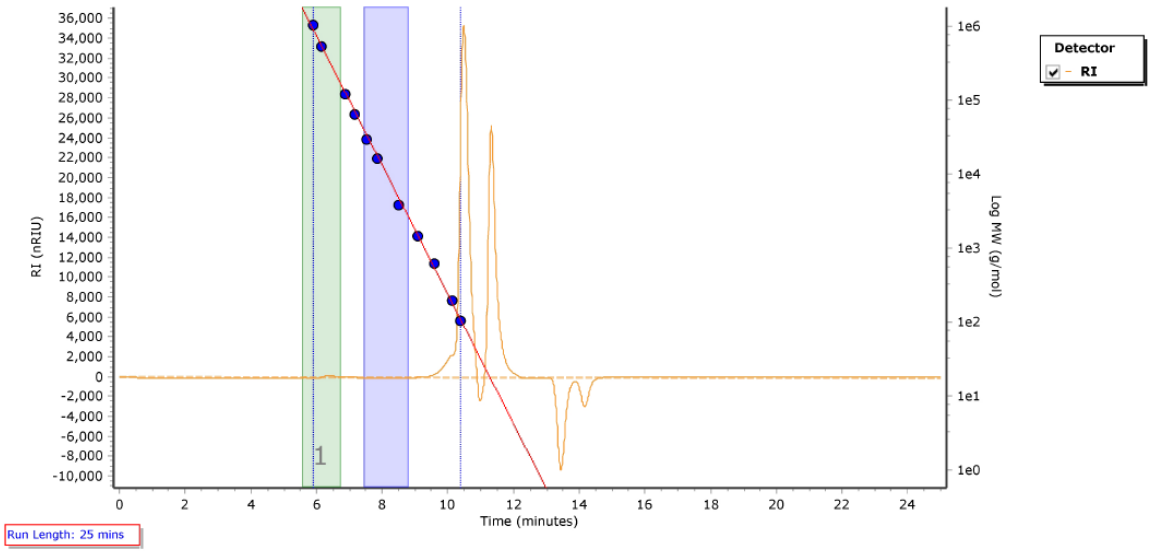

Molecular Weight Averages

Peak	Mp (g/mol)	Mn (g/mol)	Mw (g/mol)	Mz (g/mol)	Mz+1 (g/mol)	Mv (g/mol)	PD
Peak 1	332110	289893	329475	406921	594799	389181	1.137

Figure S12: GPC Trace Derived from the Reaction Mixture Obtained on Treating a 4.5 M Solution of LGO in CH_2Cl_2 with PBu_3 (4 mol %) at 90 °C for 72 h (*N,N*-dimethylacetamide used as eluting medium).

^{1}H and $^{13}C\{^{1}H\}$NMR Spectra

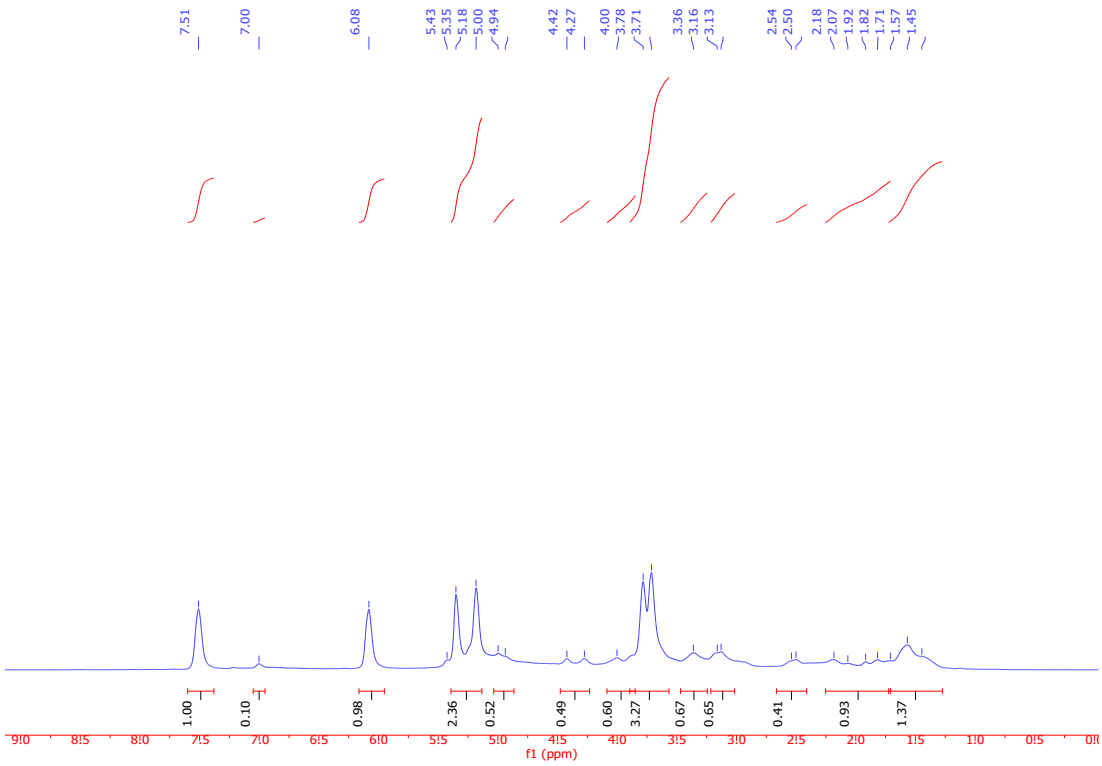

Figure S13: 400 MHz ^{1}H NMR Spectrum [recorded in $(CD_3)_2SO$] of the "poly-Cyrene"-Forming Reaction After 20 min [a 4.5 M solution of LGO in $(CD_3)_2SO$ maintained at 22 °C was treated with 8 mol% DBU].

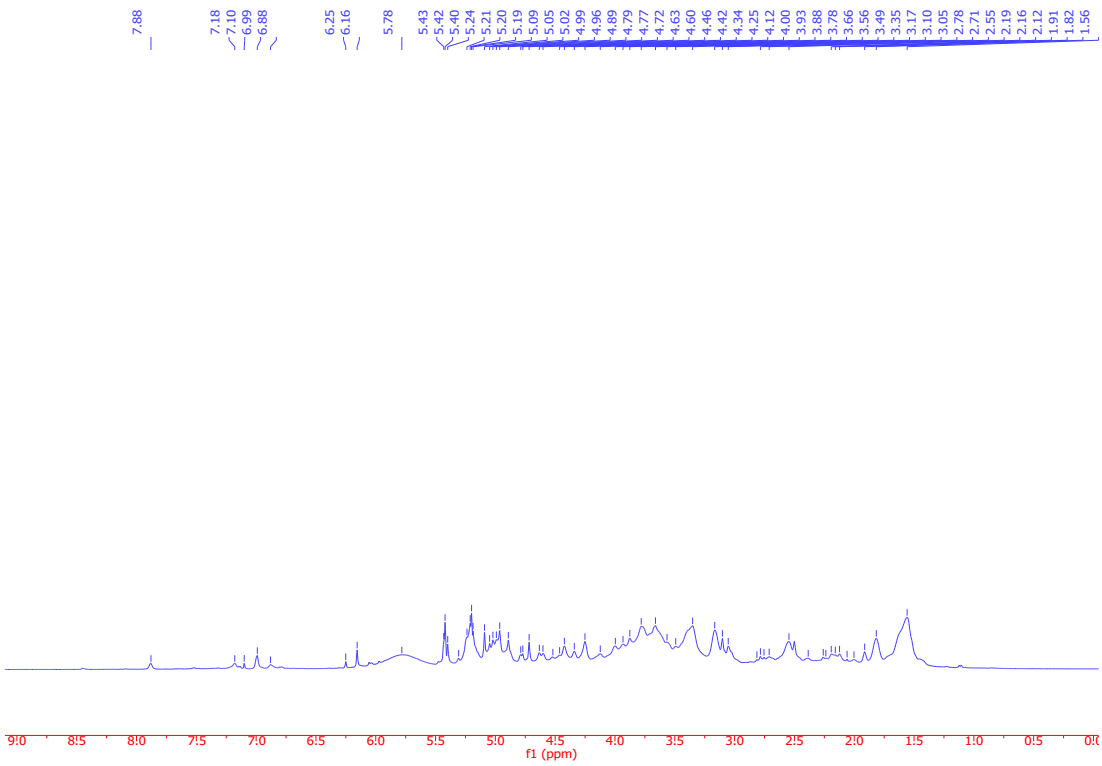

Figure S14: 400 MHz ^{1}H NMR Spectrum [recorded in $(CD_3)_2SO$] of the “poly-Cyrene”-forming Reaction After 340 min [a 4.5 M solution of LGO in $(CD_3)_2SO$ maintained at 22 °C was treated with 8 mol% DBU].

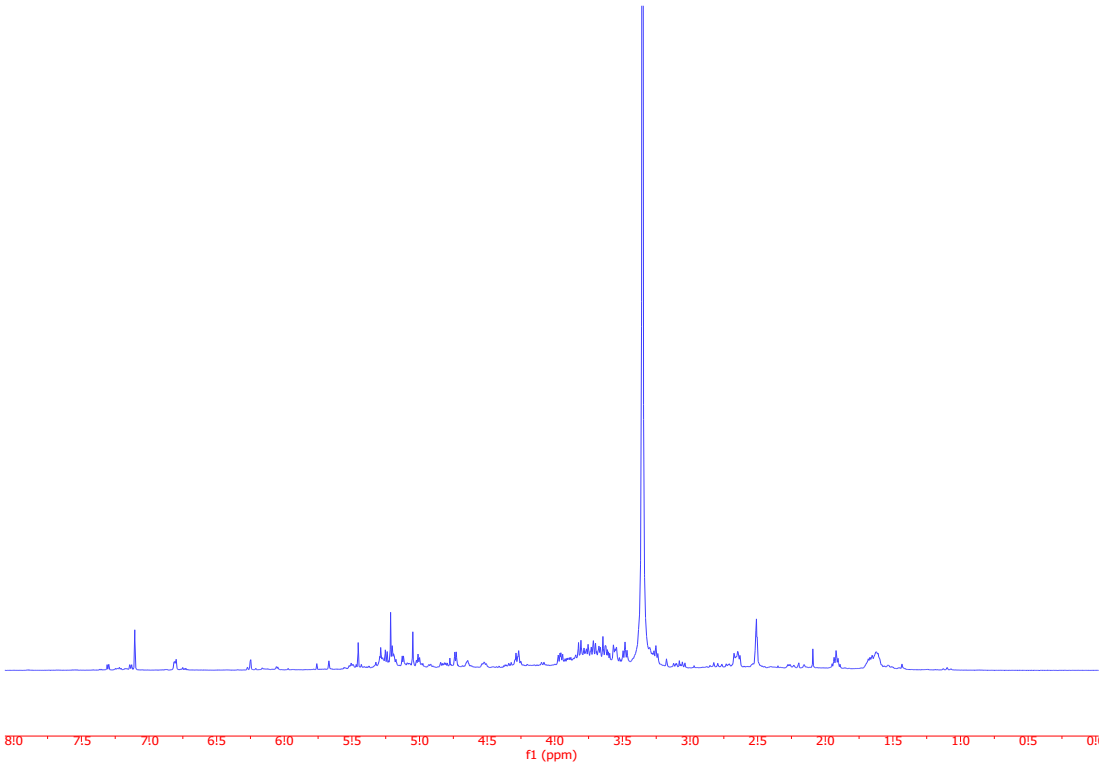

Figure S15: 400 MHz ^{1}H NMR Spectrum [recorded in $(CD_3)_2SO$] of "poly-Cyrene" (**7**) (after purification by precipitation).

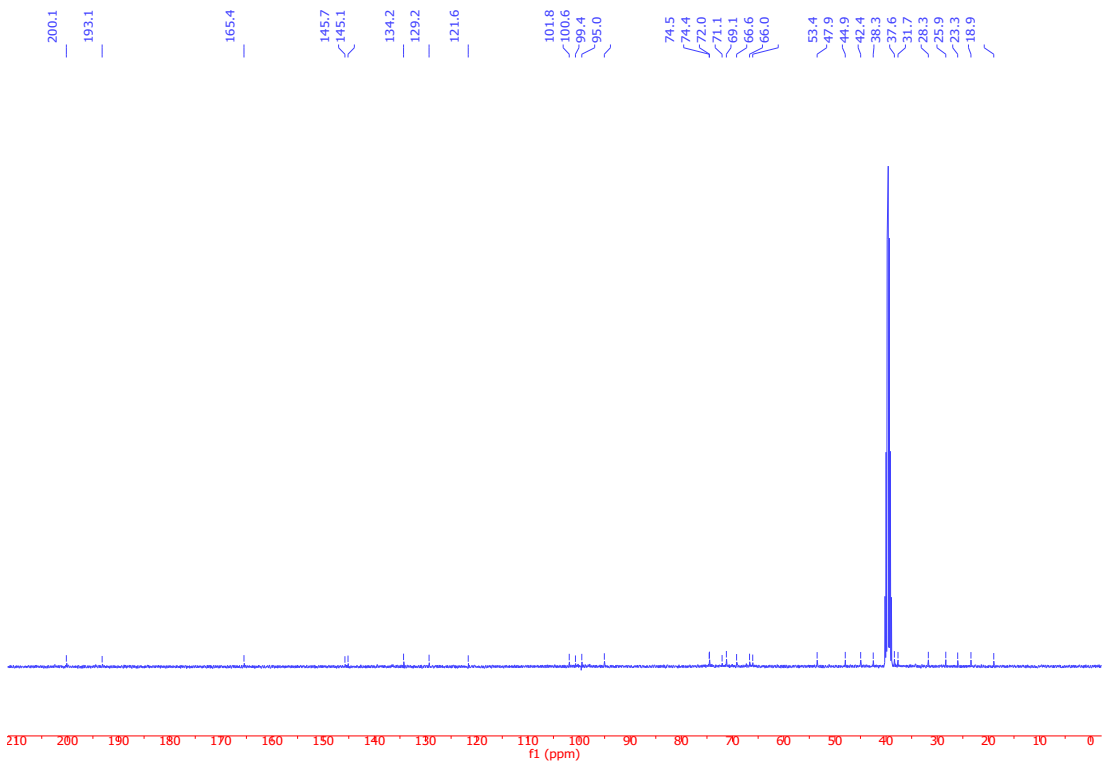

Figure S16: 100 MHz $^{13}C\{^{1}H\}$ NMR Spectrum [recorded in $(CD_3)_2SO$] of “poly-Cyrene” (**7**) (after purification by precipitation).

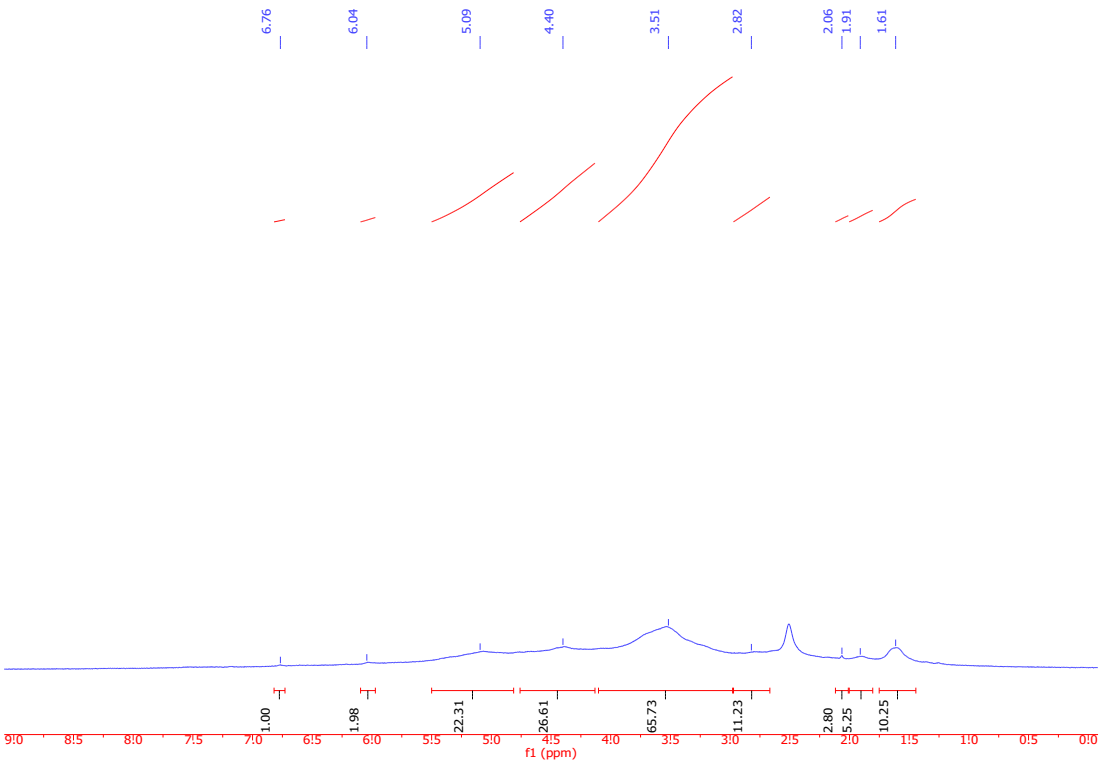

Figure S17: 400 MHz ^{1}H NMR Spectrum [recorded in $(CD_3)_2SO$] of poly-2*H*-HBO (**11**) (after isolation).

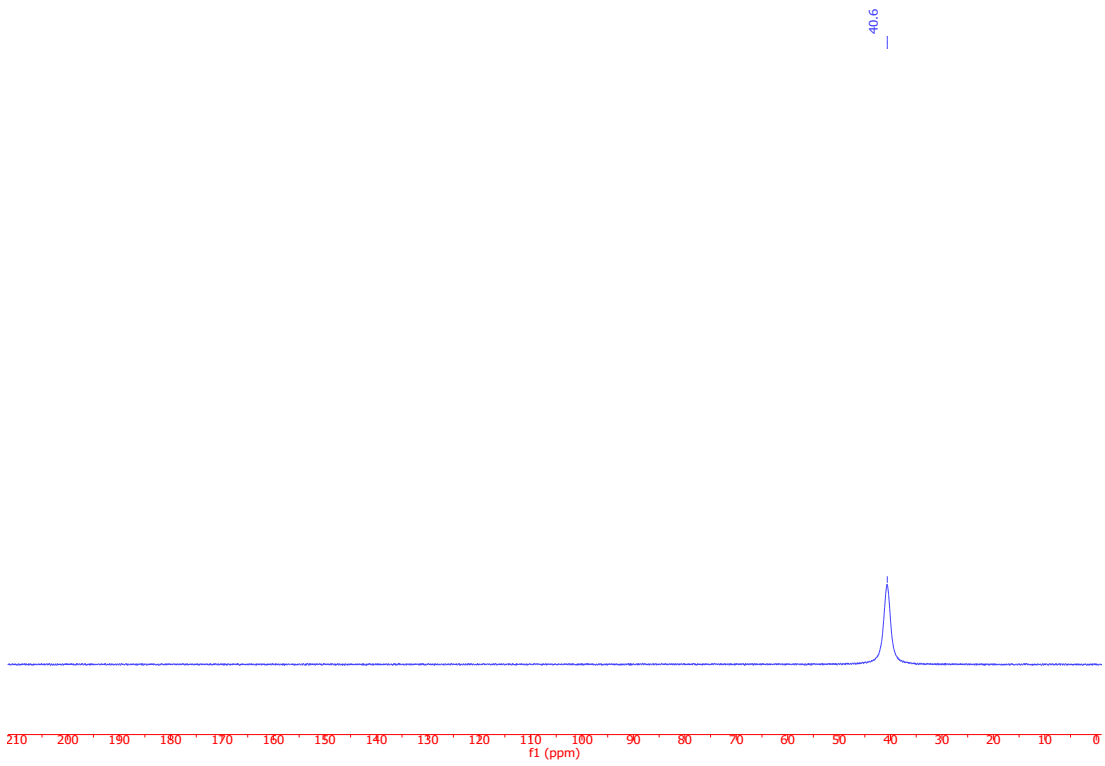

Figure S18: 100 MHz $^{13}C\{^{1}H\}$ NMR Spectrum [recorded in $(CD_3)_2SO$] of poly-2*H*-HBO (**11**) (after isolation).

FT-IR Spectra

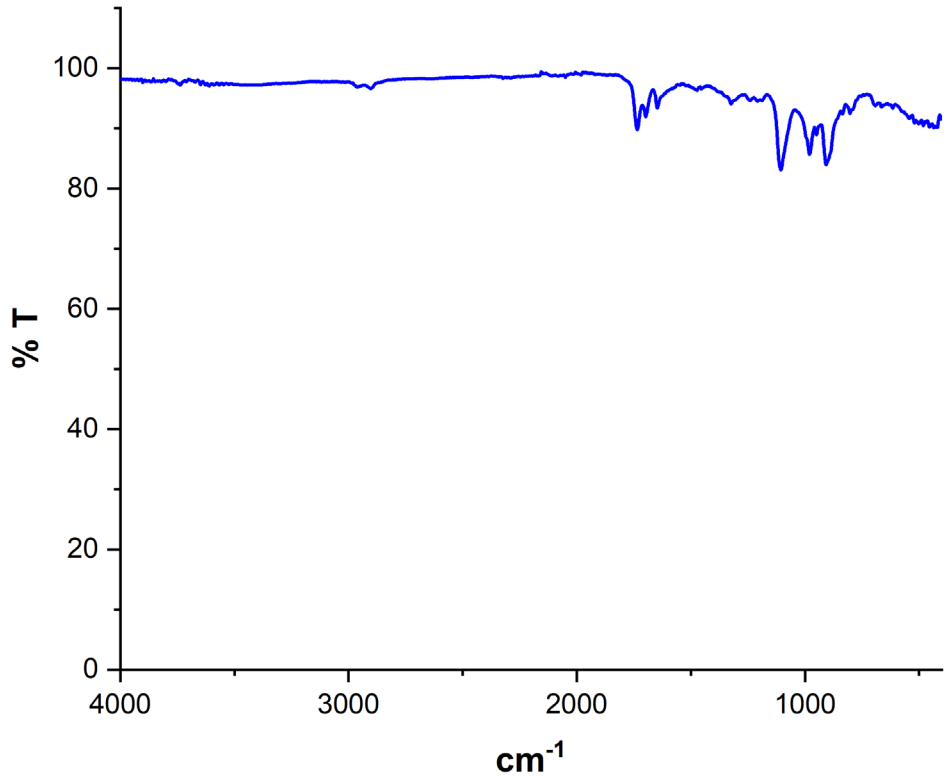

Figure S19: FT-IR Spectrum of "poly-Cyrene" (**7**) (after purification by precipitation).

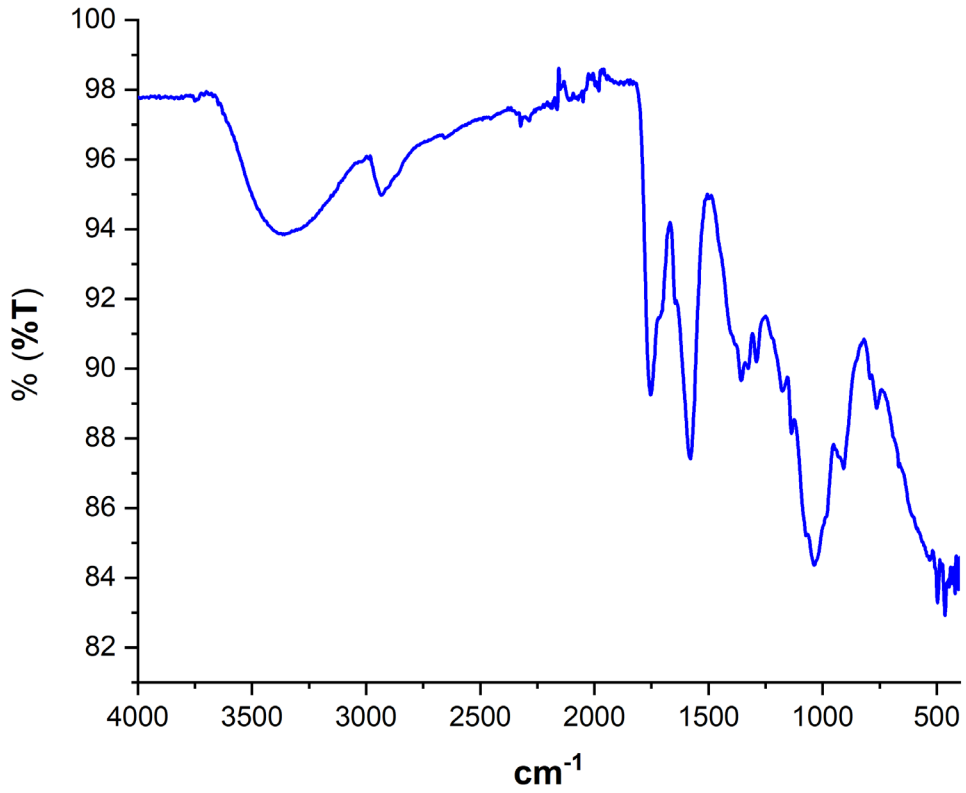

Figure S20: FT-IR Spectrum of poly-2*H*-HBO (**11**) (after isolation).

Formulae Used to Calculate E-Factors and Atom Economies

E-Factor

$$E - Factor = \frac{Mass\ of\ waste\ (g)(ignoring\ water, assuming\ catalyst\ not\ recovered)}{Mass\ of\ product\ (g)}$$

$$E - Factor = \frac{0.07\ g}{6.00\ g}$$

$$E - Factor = 0.012$$

Atom Economy

$$Atom\ Economy = \frac{Mass\ of\ atoms\ in\ desired\ product\ (g)}{Mass\ of\ atoms\ of\ all\ products\ (g)} \times 100\%$$

$$Atom\ Economy = \frac{6.00\ g}{6.07\ g} \times 100\%$$

$$Atom\ Economy = \frac{6.00\ g}{6.07\ g} \times 100\%$$

$$Atom\ Economy = 99\%$$

References

1. M. G. Banwell, B. Pollard, X. Liu, L. A. Connal, *Chemistry: An Asian Journal,* **2021**, *16*, 604-620.
2. See https://circa-group.com/products/cyrene/ (accessed 25/07/23)
3. M. B. Comba, Y.-h. Tsai, A. M. Sarotti, M. I. Mangione, A. G. Suárez, R. A. Spanevello, *European Journal of Organic Chemistry,* **2018**, *2018*, 590-604.
4. J. E. Camp, B. W. Greatrex, *Frontiers in Chemistry,* **2022**, *10*, 902239.
5. M. G. Banwell, X. Liu, L. A. Connal, M. G. Gardiner, *Macromolecules,* **2020**, *53*, 5308-5314.
6. J. Sherwood, M. De bruyn, A. Constantinou, L. Moity, C. R. McElroy, T. J. Farmer, T. Duncan, W. Raverty, A. J. Hunt, J. H. Clark, *Chemical Communications,* **2014**, *50*, 9650-9652.
7. F. Shafizadeh, R. H. Furneaux, D. Pang, T. T. Stevenson, *Carbohydr. Res.* **1982**, *100*, 303-313.
8. T.T. Stevenson, R.E. Stenkamp, L.H. Jensen, F. Shafizadeh, R.H. Furneaux, *Carbohydrate Research*, **1982**, *104(1),* 11-19.
9. X. Liu, B. Pollard, M. G. Banwell, L. J. Yu, M. L. Coote, M. G. Gardiner, B. M. A. Van Vugt-Lussenburg, B. Van der Burg, F. L. Grasset, E. Campillo, J. Sherwood, F. P. Byrne, T. J. Farmer, *Australian Journal of Chemistry,* **2022**, *75*, 331-344.
10. F. Diot-Neant, L. Mouterde, S. Fadlallah, S. A. Miller, F. Allais, *Chemistry Sustainable Chemistry,* **2020**, *13*, 2613-2620.
11. C. E. Aroyan, A. Dermenci, S. J. Miller, *Tetrahedron,* **2009**, *65*, 4069-4084.
12. E. Ciganek, *Organic Reactions,* **2004**, 201-350.
13. V. K. Aggarwal, A. Mereu, *Chemical Communications,* **1999**, 2311-2312.
14. M. De Bruyn, V. L. Budarin, A. Misefari, S. Shimizu, H. Fish, M. Cockett, A. J. Hunt, H. Hofstetter, B. M. Weckhuysen, J. H. Clark, D. J. Macquarrie, *ACS Sustainable Chemical Engineering,* **2019**, *7*, 7878-7883.
15. L. Hughes, C. R. McElroy, A. C. Whitwood, A. J. Hunt, *Green Chemistry,* **2018**, *20*, 4423-4427.
16. C. Capello, U. Fischer, K. Hungerbühler, *Green Chemistry,* **2007**, *9*, 927-934.
17. G. Bonneau, A. A. M. Peru, A. L. Flourat, F. Allais, *Green Chemistry,* **2018**, *20*, 2455-2458.
18. S. Fadlallah, A. L. Flourat, L. M. M. Mouterde, M. Annatelli, A. A. M. Peru, A. Gallos, F. Arico, F. Allais, *Macromolecular. Rapid Communications,* **2021**, *42*, e2100284.
19. A. B. Pangborn, M. A. Giardello, R. H. Grubbs, R. K. Rosen, F. J. Timmers, *Organometallics* **1996**, *15*, 1518-1520.
20. X. Liu, P. Carr, M. G. Gardiner, M. G. Banwell, A. H. Elbanna, Z. G. Khalil, R. J. Capon, *ACS Omega* **2020**, *5*, 13926-13939.

Conclusions & Future Work

Developments in the use of biomass-derived platform molecules as substitutes for fossil-derived feedstocks will be invaluable to the maintenance of the modern lifestyle and growing human population. In **Chapter Two**, an overview of our current 'toolbox' for biomass-derived platform molecules in chemistry was provided, including a background on levoglucosenone chemistry performed at the Research School of Chemistry. **Chapter Three** described a more efficient and simplified preparation of the quasi-enantiomer of levoglucosenone, *iso*-levoglucosenone. This material was then hydrogenated to provide "*iso*-Cyrene", a potential solvent which was characterised and its properties compared to the existing solvent Cyrene®. Further assessment of the role of *iso*-Cyrene as a solvent in specific transformations, particularly those to which Cyrene® is not amenable (for example, under basic conditions), would be a relevant avenue for future study. In **Chapter Four**, novel manipulations of Diels-Alder adducts prepared from levoglucosenone and *iso*-levoglucosenone revealed distinct rearrangements and caged structures available for further manipulation. In the future, assessing the ability for these novel structures to undergo polymerisation (and the properties of these products) would prove the most salient direction for research. In **Chapter Five**, an extremely efficient and atom economical synthesis of a novel polymer scaffold prepared from levoglucosenone using DBU as a catalyst was reported, alongside a functional and hydrophilic derivative arrived at through aqueous Baeyer-Villiger rearrangement. Further modification of these polymer scaffolds offers an exciting scope for future work, with their efficient and green synthesis offering a direct route to novel and functional materials. As a compilation, these publications demonstrate the diverse utility of just one biomass-derived platform molecule. I believe that the ethical and sustainable valorisation of the chemical gifts which nature has bestowed on us will be critical in transitioning away from our current unsustainable chemical reservoirs, and I hope that many more chemists will help carry the torch to this goal.